# Agronomy Research

Established in 2003 by the Faculty of Agronomy, Estonian Agricultural University

**Aims and Scope:**
*Agronomy Research* is a peer-reviewed international Journal intended for publication of broad-spectrum original articles, reviews and short communications on actual problems of modern biosystems engineering incl. crop and animal science, genetics, economics, farm- and production engineering, environmental aspects, agro-ecology, renewable energy and bioenergy etc. in the temperate regions of the world.

**Copyright & Licensing:**
This is an open access journal distributed under the Creative Commons Attribution-NonCommercial-NoDerivatives 4.0 International (CC BY-NC-ND 4.0).
Authors keep copyright and publishing rights without restrictions.

***Agronomy Research* online:**
*Agronomy Research* is available online at: https://agronomy.emu.ee/

**Acknowledgement to Referees:**
The Editors of *Agronomy Research* would like to thank the many scientists who gave so generously of their time and expertise to referee papers submitted to the Journal.

**Abstracted and indexed:**
SCOPUS, EBSCO, DOAJ, CABI Full Paper and Clarivate Analytics database: (Zoological Records, Biological Abstracts and Biosis Previews, AGRIS, ISPI, CAB Abstracts, AGRICOLA (NAL; USA), VINITI, INIST-PASCAL.)

**Subscription information:**
Institute of Technology, EMU
Fr.R. Kreutzwaldi 56,
51006 Tartu,
ESTONIA
e-mail: timo.kikas@emu.ee

**Journal Policies:**
Estonian University of Life Sciences, Latvia University of Life Sciences and Technologies, Vytautas Magnus University Agriculture Academy, Lithuanian Research Centre for Agriculture and Forestry, and Editors of *Agronomy Research* assume no responsibility for views, statements and opinions expressed by contributors. Any reference to a pesticide, fertiliser, cultivar or other commercial or proprietary product does not constitute a recommendation or an endorsement of its use by the author(s), their institution or any person connected with preparation, publication or distribution of this Journal.

**ISSN 1406-894X**

# CONTENTS

*Agronomy Research* **20**(1), 5–15, 2022
https://doi.org/10.15159/AR.22.003

# Possibilities of cucumber powdery mildew detection by visible and near-infrared spectroscopy

I. Alsiņa[1,*], G. Bimšteine[1], L. Dubova[1], J. Kaņeps[1], K. Kviesis[2], B. Bankina[1], M. Dūma[3] and A. Avotiņš[2]

[1]Latvia University of Life Sciences and Technology, Faculty of Agriculture, Institute of Plant and Soil Science, Liela street 2, LV-3001 Jelgava, Latvia
[2]Riga Technical University, Faculty of Power and Electrical Engineering, Kaļķu street 1, LV-1658 Riga, Latvia
[3]Latvia University of Life Sciences and Technology, Faculty of Food Technology, Department of Chemistry, Liela street 2, LV-3001 Jelgava, Latvia
[*]Correspondence: Ina.Alsina@llu.lv

Received: July 16th, 2021; Accepted: November 6th, 2021; Published: February 1st, 2022

**Abstract.** Cucumbers are one of the most demanded and widely grown greenhouse vegetables. Important factors that influence quality and quantity of yield are diseases. Powdery mildew (caused by *Podosphaera xanthii* and/or *Golovinomyces cichoracearum),* is one of the most harmful cucumber diseases. Early detection of mildew via non-destructive methods can optimize schemes of fungicide application. The study aimed to find regularities in the reflected light spectra, indices described in the literature, and severity of mildew. Plants were grown in the polycarbonate greenhouse under artificial lighting in a 16 h photoperiod with PAR at the tips of plants 200 ± 30 µmol $m^{-2}$ $s^{-1}$. Leaf reflection spectra were obtained using spectroradiometer RS-3500 (Ltd. Spectral Evolution). Spectral range 350–2,500 nm, bandwidth 1 nm. The severity of cucumber mildew was evaluated using 10 point scale (0- no symptoms, … 9 - the plant is dead). The vegetation indices found in the literature have been calculated. The obtained results show that the calculated indices have different sensitivities. The strongest correlation between the degree of cucumbers infection with powdery mildew and the light reflectance spectrum was found in the green range of visible light around 550 nm. Disease-Water Stress Index-2 (DSWI-2), Structure Intensive Pigment Index (SIPI), and Normalized Difference Vegetation Index (NDVI) are the most suitable indices for determining powdery mildew in cucumbers. New indices for detection of powdery mildew have been created. None of the studied indices allows determining the powdery mildew at the early stages of disease development when powdery mildew severity is below 10%.

**Key words:** *Cucumis sativus*, NDVI, SIPI, DSWI, *Podosphaera xanthii, Golovinomyces cichoracearum.*

## INTRODUCTION

Cucumber (*Cucumis sativus L.*) is one of the most demanded and widely produced greenhouse-grown vegetables. In 2010, a total area of greenhouses in Latvia was 84.0 ha with an average cucumber harvest of 76.5 t $ha^{-1}$. Throughout the following years, a steady decline in the total greenhouse area was observed. In 2019, the total greenhouse area decreased by 35.5% to 54.2 ha compared to 2010. At the same time, greenhouse productivity increased by 48.4% up to 113.5 t $ha^{-1}$ (Central Statistical Bureau of Latvia, 2019).

Cucumber is a thermophilic crop, temperature above 20 °C is optimal for growing. Greenhouse-grown cucumbers have high requirements for irradiance, air humidity, soil moisture, temperature, and fertilizers (Singh et al., 2017).

Diseases are an important factor that influences the quality and quantity of yield. Powdery mildew (caused by *Podosphaera xanthii* and/or *Golovinomyces cichoracearum*), is one of the most harmful cucumber diseases in greenhouses. The powdery mildew can decrease yield potential and reduce fruit quality if it is not controlled during the early infection phases. Visual diagnostic of diseases in early infection stages is problematic, due to the presence of symptoms on lower, more matured leaves, which often are covered by other leaves. Early disease detection is beneficial for optimal powdery mildew management strategy (i.e fungicide application) (Abdulridha et al., 2020).

Conventional scouting for foliar diseases relies primarily on the visual inspection of leaves (color, pattern, crown structures). Laboratory test approaches, such as polymerase chain reactions, an enzyme like immunosorbent assays, etc. are highly specific and sensitive to identify diseases, but these methods are destructive and labor-consuming and require specialized skills (Lu et al., 2018). Hyperspectral imaging is one of the most efficient and fast-developing non-destructive techniques for obtaining detailed information about plants (Golhani et al., 2018). Recent studies have attempted to explain the role of spectral bands in differentiation between healthy and diseased plants. Any disease that affect chlorophyll and/or water content in the plant leaves, that damage plant cells would affect leaf spectral reflectance (Semeraro et al., 2019). For accurate disease detection it is crucial to identify the most significant wavelengths and find or create vegetation indices for early diagnosis of diseases (Abdulridha et al., 2020). Despite the strong focus on powdery mildew research, further research is needed to diagnose the disease before the symptoms become apparent (Fernández et al., 2021).

The study aimed to find regularities in the reflected light spectra, indices described in the literature, and severity of mildew.

## MATERIALS AND METHODS

The experiments were carried out in a polycarbonate greenhouse of Latvia University of Life Sciences and Technologies during the autumn season of 2020. Plants were grown under artificial lighting with a 16 h photoperiod with PAR at the tips $200 \pm 30$ µmol $m^{-2}$ $s^{-1}$.

Cucumber variety ‘Atos F1’ was chosen for the experiments. Plants were grown in plastic pots; the volume of pots was adapted to plant size throughout cucumber vegetation. During the production of cucumbers, the pot volume was 12 L. Peat substratum KKS-S from Laflora ($pH_{KCl}$ 5.8–6.6, EC 0.25 mS $cm^{-1}$, PG Mix (NPK 15-10-20) 1 kg $m^{-3}$, Ca 1.78%, Mg 0.21%). Plants were fertilized once a week with 1% solution of Kristalon Green (NPK 18-18-18) with Mg, S and microelements during the vegetative phase of plant growth and with Kristalon Red (NPK 12-12-36) with microelements during the reproductive phase; in proportion $v:v_{pot}$ = 1:50.

Cucumbers were analyzed between 27 October and 22 December 2020, totally 4 times. Number of analyzed plants 15. Three leaves were selected for each plant, where the severity of infection was assessed for each leaf, then the leaf was torn off and the reflection spectrum of the leaf was determined immediately. Totally 180 leaves were visually evaluated.

Powdery mildew (caused by *Podosphaera xanthii* and/or *Golovinomyces cichoracearum*), was observed at a three week interval. The severity was assessed for individual leaves according to the same 10-point scale:

0 point – leaf without powdery mildew symptoms (Fig. 1, a);
1 point – 1–5% of leaf with powdery mildew symptoms;
2 points – 6–10% of leaf with powdery mildew symptoms;
3 points – 11–15% leaf with powdery mildew symptoms;
4 points – 16–25% of leaf with powdery mildew symptoms;
5 points – 26–40% of leaf with powdery mildew symptoms (Fig. 1, b);
6 points – 41–55% of leaf with powdery mildew symptoms;
7 points – 56–70% of leaf with powdery mildew symptoms;
8 points – 71–85% of leaf with powdery mildew symptoms;
9 points – more than 86% of leaf with powdery mildew symptoms (Fig. 1, c).

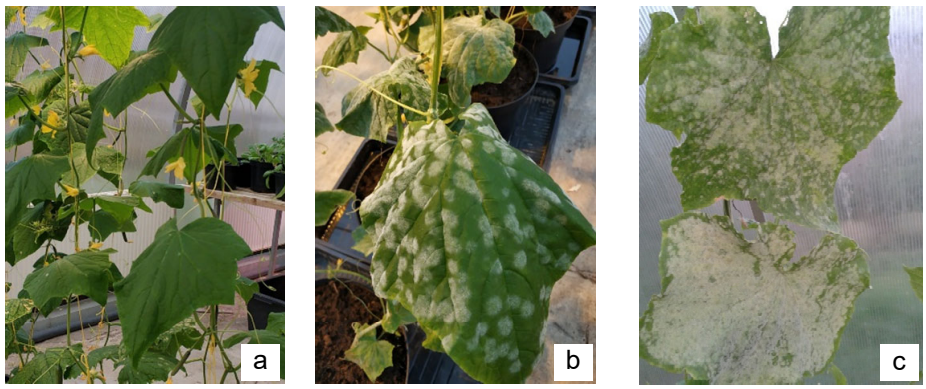


**Figure 1.** The severity of powdery mildew: a – healthy leaves; b – rated 5 points; c – rated 9 points.

Each leaf reflectance was measured with spectroradiometer RS-3500 (Ltd. Spectral evolution) in 10 replicates. Spectral range 350–2,500 nm, sampling bandwidth was 1 nm.

Indices used for the evaluation of cucumbers vitality and diseases detection are shown in Table 1.

**Table 1.** Vegetation indices (VI) calculated from leaf reflectance

| Vegetation index | Abbreviation | Equation | Reference |
|---|---|---|---|
| Carotenoids | CRI1 | $\frac{1}{W510} - \frac{1}{W550}$ | Gitelson et al., 2001 |
| Greenness Index | GI | $\frac{W554}{W677}$ | Zarco-Tejada et al., 2001 |
| Lichtenthaler index 1 | LIC1 (NDVI) | $\frac{W800 - W680}{W800 + W680}$ | Lichtenthaler, 1996 |
| Lichtenthaler index2 | LIC2 | $\frac{W440}{W690}$ | Lichtenthaler, 1996 |
| Normalized Difference Vegetation Index | NDVI (1) | $\frac{W760 - W670}{W760 + W670}$ | Padilla, 2017 |
| Plant Senescence Reflectance Index | PSRI | $\frac{W678 - W500}{W750}$ | Merzlyak et al., 1999 |
| Structure Intensive Pigment Index | SIPI | $\frac{W800 - W445}{W800 - W680}$ | Peñuelas & Filella, 1998, Zarco-Tejada et al., 2001 |
| Simple Ratio Pigment Index | SRPI | $\frac{W430}{W680}$ | Peñuelas et al., 1994 |
| Water use efficiency | WBI3 | $\frac{W950}{W900}$ | Peñuelas et al., 1993 |
| Water Index | WI | $\frac{W900}{W970}$ | Peñuelas et al., 1997 |
| Flavonoid reflectance Index | FRI | $\left(\frac{1}{W410} - \frac{1}{W460}\right) W800$ | Skoczowski et al., 2021 |
| Normalized Difference Index | CNDVI | $\frac{W750 - W705}{W750 + W705}$ | Lu et al.,2018 |
| Red Edge Index | REI | $\frac{W760}{W730}$ | Padilla, 2017 |
| Healthy index | HI | $\frac{W534 - W698}{W534 + W698} - 0.5W704$ | Mahlein et al., 2013 |
| Powdery Mildew Index | PMI | $\frac{W520 - W584}{W520 + W584} + W724$ | Mahlein et al., 2013 |
| Disease-Water Stress Index 1 | DSWI-1 | $\frac{W800}{W1660}$ | Apan et al., 2004 |
| Disease-Water Stress Index 2 | DSWI-2 | $\frac{W1660}{W550}$ | Apan et al., 2004 |
| Disease-Water Stress Index 3 | DSWI-3 | $\frac{W1600}{W680}$ | Apan et al., 2004 |
| Disease-Water Stress Index 4 | DSWI-4 | $\frac{W550}{W680}$ | Apan et al., 2004 |
| Disease-Water Stress Index 5 | DSWI-5 | $\frac{W800 - W550}{W1660 + W680}$ | Apan et al., 2004 |

Wn – reflectance at a given wavelength.

To evaluate the difference between values of vegetation indices of healthy and infected plants the M value is used (Abdulridha et al., 2020). It is considered as a significant discriminant between different vegetation indices. As the M value increases better reparability is observed.

$$M = \frac{Mean_{healthy} - Mean_{infected(1\ point)}}{\sigma_{healthy} + \sigma_{infected\ (1\ point)}}$$ where $\sigma$- standard deviation (1)

The critical value of vegetative index ($VI_{crit}$) was calculated by equation

$$VI_{crit} = Mean_{healthy} \text{-} \sigma_{healthy} - \sigma_{infected\ (1\ point)} \quad (2)$$

Using the obtained critical value of the vegetative index ($VI_{crit}$) and the corresponding line equation (Fig. 3), the identifiable powdery mildew threshold (PMT) was calculated.

## RESULTS AND DISCUSSION

During the cucumber growing season, only symptoms of powdery mildew (caused by *Podosphaera xanthii* and/or *Golovinomyces cichoracearum*) were observed. The development of the disease was relatively intensive. The severity varied from 1 to 8 points during the observations.

Early detection of powdery mildew by using non-destructive methods can minimize direct human intervention and optimize schemes of fungicide application. Fig. 2, A shows the differences between the reflectance spectra of cucumber leaves. Different parts of the spectrum show different sensitivity. The largest differences between the leaves of different infection severity were found in the visible light part of the spectrum with a reflection maximum at 552–553 nm. (Fig. 2, B). Wavelengths around 550 nm also appear in other authors' works as a sensitive indicator of plant physiological and biochemical status (Alsiņa et al., 2016; Sytar et al., 2020; Skoczowski, et al., 2021) and health (Mahlein et al., 2012; Mahlein et al., 2013; Berdugo et al., 2014; Kuska et al., 2015; Lu et al., 2018).

The reflectance grows rapidly at the 'red edge' zone. Correlation between the severity of infection with powdery mildew and reflectance derivate is observed (Fig. 2, C). In the range from 699 nm to 712 nm, the correlation of the first derivative of reflectance spectrum with the degree of infection is less than -0.9, reaching a minimum at 703 nm ($R$ = -0.953).

Wavelengths 720–960 nm indicate the peculiarities of the plant leaf surface cell structure (Roman & Ursu, 2016), the reflection spectra are relatively stable. In this part of the spectrum, the highest reflection is observed for leaves with low and medium infection degrees. The reflection spectra of severely infected leaves and asymptomatic leaves are not significantly different.

At the wavelength corresponding to the water absorption maximum (1,460 nm), it was found that there were no significant differences between the leaves with various levels of disease severity. That is in contradiction to the work of Lu and co-authors, where at this wavelength the affected leaves had lower reflection than healthy leaves (Lu et al., 2018).

To determine the severity of powdery mildew, the 21 vegetation indices shown in Table 2 were used. Correlation analysis was performed between the calculated vegetation indices and the severity of powdery mildew. A very strong correlation ($R$ > 0.8) was found in only one case, with the calculated second Disease-Water stress index DSWI-2, coefficient of correlation $R$ = -0.84. High correlation coefficients were also found for disease severity and SIPI and DSWI-5, in both cases $R$ = -0.797. A correlation coefficient larger than 0.7 was also observed for the most widely used indices

characterizing plant physiological conditions NDVI and LIC-1 (Table 2). Analyzing the wavelengths used to obtain these vegetation indices, it was found that the most sensitive regions are 445, 550, 670, 680, 760, 800 and 1,600 nm. Similar wavelengths for the determination of plant health status are mentioned also by other authors. 540 and 660 nm are mentioned by Atanassova et al., 2019, spectrum ranges from 500–700 nm and 450 and 720 nm especially for powdery mildew by Mahlein et al., 2013; 650 and 700 nm by Berdugo et al., 2014; 500–730 nm by Abdulridha et al., 2020. Correlation coefficients for health index HI and DSWI-3 were between |0.6–0.7|: -0.674 and -0.603, respectively. Correlation coefficients above |0.5| were for the two vegetation indices used in the red edges (REI and CNDVI) and for indices that can be used to determine carotenoid and flavonoid content in plant leaves. Several authors (Lu et al., 2018; Atanassova et al., 2019; Abdulridha et al., 2020) mention changes in the water content of diseased plant leaves. In our experiment, the correlation between the indices for determining the water content and the prevalence of the disease was low ($R = \pm 0.054$).

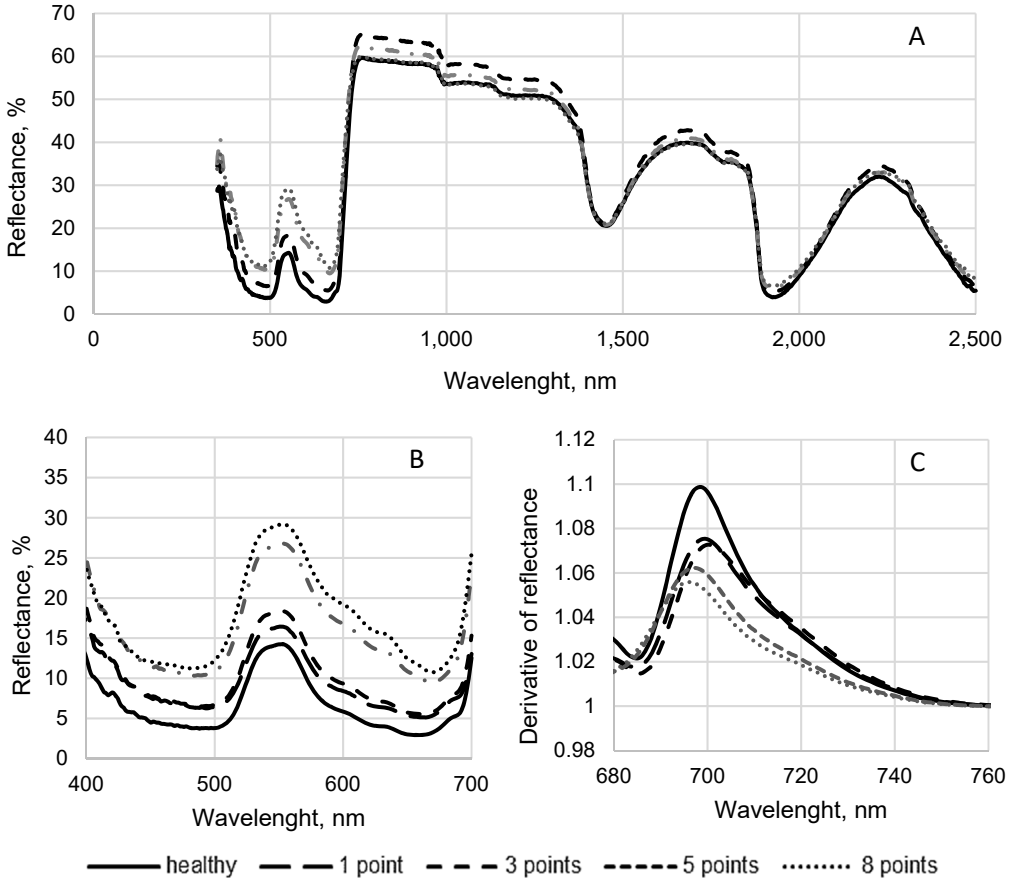


**Figure 2.** Average cucumber leaf reflectance spectra depending on the severity of mildew: A – spectral range within interval 350–2,500 nm; B – zoomed-in spectral range of 400–700 nm and C – first-order derivative zoomed in a wavelength of 680–760 nm.

The maxima (553 nm; 759 nm; 1,188 nm; 1,684 nm and 2,226 nm) and minima (1,452 nm and 1,925 nm) of the obtained reflectance spectra were used to find out whether it is possible to create indices with which would more accurately reflect the degree of mildew infection. Mentioned reflectance values were used to develop normalized difference and modified normalized difference indices. In total, 13 different indices were created, which were tested. The three best of the created indices are included at the end of the Table 2. The highest correlation coefficients (> 0.75) were obtained using the reflectance in 553 nm and 759 nm.

**Table 2.** Coefficients of correlation (R) between powdery mildew severity and calculated indices

| Parameter | Vegetation index | Abbreviation | *R* |
|---|---|---|---|
| Plant structure and pigment content | Carotenoids | CRI1 | -0.564 |
| | Greenness | GI | -0.172 |
| | Simple Ratio Pigment | SRPI | -0.070 |
| | Structure Intensive Pigment | SIPI | **-0.797** |
| | Normalized Difference Vegetation | NDVI | **-0.729** |
| | Lichtenthaler 1 | LIC-1 | **-0.701** |
| | Lichtenthaler 2 | LIC -2 | -0.033 |
| Biochemical content | Flavonoid reflectance | FRI | 0.553 |
| Plant Senescence | Plant Senescence | PSRI | -0.406 |
| Water Use efficiency | Water use efficiency | WBI | 0.054 |
| | Water Index | WBI-2 | -0.054 |
| Red Edge | Red Edge Index | REI | -0.512 |
| | Normalized Difference | CNDVI | -0.562 |
| Plant Health | Healthy | HI | -0.674 |
| | Powdery Mildew | PMI | 0.483 |
| | Disease-Water Stress | DSWI-1 | -0.018 |
| | | DSWI-2 | **-0.840** |
| | | DSWI-3 | -0.603 |
| | | DSWI-4 | -0.118 |
| | | DSWI-5 | **-0.797** |
| New generated Powdery Mildew Indices | $\frac{W759 - W553}{W759 + W553}$ | PMI-1 | **-0.859** |
| | $\frac{W759 - W553}{W1188}$ | PMI-2 | **-0.796** |
| | $\frac{W759 - W553}{W1684 - W1925}$ | PMI-3 | **-0.774** |

$R_{0.05;\,36} = 0.332$.

The best results for the identification of powdery mildew were shown by the vegetation index DSWI-2, which has the highest correlation and determination coefficient (Fig. 3, Tables 2 & 3). Wavelengths of 550 and 1,660 nm were used to calculate the index value. Unfortunately, the M value for this index is lower than for SIPI and NDVI. That suggests that DSWI-2 is less sensitive to the early detection of powdery mildew. Calculations show that infected cucumber can be distinguished from a healthy plant when the visual assessment of the degree of mildew development is 2.7 points.

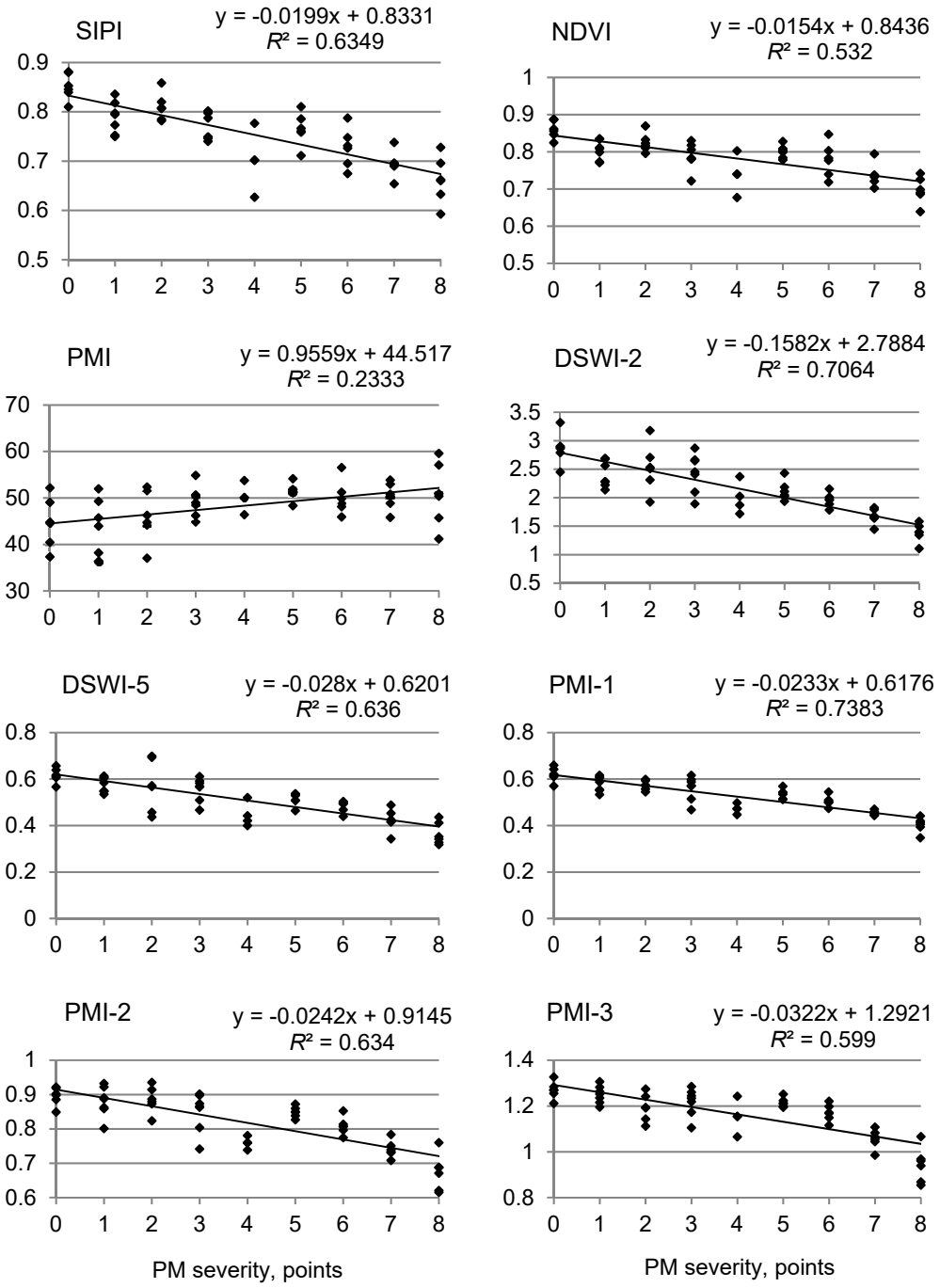


**Figure 3.** Relationship between powdery mildew (PM) severity and calculated vegetative indices (SIPI, NDVI, PMI, DSWI-2, DSWI-5), and created indices (PMI-1, PMI-2, PMI-3).

The most sensitive indices are SIPI (Structure Intensive Pigment Index) and the widely used NDVI (Normalized Difference Vegetation). The disease can be identified according to the visual assessments 2.0 and 2.2. The calculated critical values of SIPI and NDVI are 0.79 and 0.81, respectively (Table 3). Unfortunately, these indices do not have the necessary selectivity, as they are widely used (especially NDVI) to assess plant vitality, chlorophyll content, N supply (Haboudane et al., 2002; Mahlein et al., 2013; Alsiņa et al. 2016; Padilla et al., 2017; Atanassova et al., 2019; Alsiņa et al., 2020). The vegetation index PMI, specially developed for the determination of powdery mildew, in our experiments, showed low sensitivity. The critical value for identification of powdery mildew was 32.9, which corresponds to a visual assessment value of 5.5 points, making it less sensitive/effective compared to visual disease assessment. At this point, the disease has damaged nearly 50% of the plant photosynthetic area, which is too late for effective disease control.

**Table 3.** The fittingness of vegetative indices for the determination of powdery mildew on the leaves of the cucumber

| Parameter | Abbrevation of vegetative index | | | | | | | | |
|---|---|---|---|---|---|---|---|---|---|
| | SIPI | NDVI | PMI | HI | DSWI-2 | DSWI-5 | PMI-1 | PMI-2 | PMI-3 |
| M | 1.06 | 1.12 | 0.14 | 0.07 | 0.91 | 0.61 | 0.71 | 0.37 | 0.25 |
| $VI_{crit}$ | 0.79 | 0.81 | 32.9 | -12.4 | 2.36 | 0.55 | 0.56 | 0.83 | 1.19 |
| PMT | 2.0 | 2.2 | 5.5 | 5.4 | 2.7 | 2.4 | 2.7 | 3.6 | 3.2 |

The use of reflectance peaks can improve the correlation between the visual and calculated by reflectance spectrums severity of powdery mildew. The correlation coefficient for the index mentioned in literature DSWI-2 was -0.840, but the already established PMI-1 is -0.859. Unfortunately, the lowest detected powdery mildew threshold (PMT) lags behind the SIPI and NDVI mentioned in the literature.

The study demonstrates the potential of using a spectroradiometer for the identification of powdery mildew, but further research is needed to find more appropriate indices for the identification of powdery mildew at the early stages of the disease.

## CONCLUSIONS

The strongest correlation between the degree of cucumbers infection with powdery mildew and the light reflectance spectrum was found in the green range of visible light around 550 nm.

Disease-Water Stress index-2 (DSWI-2), Structure Intensive Pigment Index (SIPI), Normalized Difference Vegetation Index (NDVI) and created index for powdery mildew detection (PMI-1) are the most suitable indices for determining powdery mildew in cucumbers. None of the studied indices allows determining the powdery mildew at the early stages of disease development (powdery mildew severity is below 2 points or less than 10% of cucumber leaves are infected).

ACKNOWLEDGEMENTS. The publication is created with the support of the Latvian Rural Development Program 2014–2020 ‘Cooperation’, call 16.1 project Nr. 19-00-A01612-000010 ‘Investigation of innovative solutions and new method development for efficiency and quality increase in Latvian greenhouse sector [IRIS]’.

## REFERENCES


Abdulridha, J., Ampatzidis, Y., Roberts, P. & Kakarla, S.C. 2020. Detection powdery mildew disease in squash at different stages using UAV-based hyperspectral imaging and artificial intelligence. *Biosystemic engineering* **197**, 135–148.

Alsiņa, I., Dubova, L., Dūma, M., Erdberga, I., Augšpole, I., Sergejeva, D. & Avotiņš, A. 2020. Lighting source as cause of changes in cucumbers' physiology and morphology. *Agronomy Research* **18**, 1926–1932. doi.org/10.15159/ar.20.195

Alsiņa, I., Dūma, M., Dubova, L., Šenberga, A. & Daģis, S. 2016. Comparison of different chlorophylls determination methods for leafy vegetables. *Agronomy Research* **14**(2), 309–316.

Apan, A., Held, A., Phinn, S. & Markley, J. 2004. Detecting sugarcane 'orange rust' disease using EO-1 hyperion hyperspectral imagery. *Int J Remote Sens.* **25**(2), 489–498.

Atanassova, S., Nikolov, P., Valchev, N., Masheva, S. & Yorgov, D. 2019. Early detection of powdery mildew (Podosphaera xanthii) on cucumber leaves based on visible and near-infrared spectroscopy. *AIP Conference Proceedings* **2075**, Article No160014.

Berdugo, C.A., Zito, R., Paulus, S. & Mahlein, A.K. 2014. Fusion of sensor data for detection and diffentation of plant diseases in cucumber. *Plant Pathology* **63**, 1344–1356.

Central Statistical Bureau of Latvia. 2019. http://data1.csb.gov.lv/pxweb/lv/lauks/lauks__03Augk__ikgad/LAG100.px/table/tableViewLayout1/. Accessed 05.01.2021.

Fernández, C.I., Leblon, B., Wang, J., haddadi, A. & Wang, K. 2021 Detecting infected cucumber plants with close-range multispectral imagery. *Remote Sens.* **13**, 2948. https://doi.org/10.3390/rs13152948

Gitelson, A.A., Merzlyak, M.N., Zur, Y., Stark, R. & Gritz, U. 2001. Non-destructive and remote sensing techniques for estimation of vegetation status. **In:** *Third European Conference on Precision Agriculture* France **1**, 301–306.

Golhani, K. Balasundram, S.K., Vadamalai, G. & Pradhan, B. 2018. A review of neural networks in plant disease detection using hyperspectral data. *Inf. Process. Agr*. **5** (3), 354–371, doi.org/10.1016/j.inpa.2018.05.002

Haboudane, D., Miller, J.R., Tremblay, N., Zarco-Tejada, P.J. & Dextraze, L. 2002. Integrated narrow-band vegetation indices for prediction of crop chlorophyll content for application to precision agriculture. *Remote Sensing of Environment* **81**, 416–426, doi.org/10.1016/S0034-4257(02)00018-4

Kuska, M., Wahabzada, M., Leucker, M., Dehne, H.Z., Kersting, K., Oerke, E.C., Steiner, U. & Mahlein, A.K. 2015. Hyperspectral phenotyping on the microscopicscale: towards automated characterization of plant-pathogen interactions. *Plant methods* **11**(28). doi 10.1186/s13007-015-0073-7

Lichtenthaler, H.K. 1996. Vegetation Stress: an Introduction to the Stress Concept in Plants. *Journal of Plant Physiology* **148**, 4–14.

Lu, J., Ehsani, R., Shi, Y., de Castro, A.I. & Wang, S. 2018. Detection of multi-tomato leaf diseases (late blight, target and bacterial spots) in different stages by using a spectral-based sensor, *Scientific Reports* **8**(1), art. no. 2793.

Mahlein, A.K., Rumpf, T., Welke, P., Dehne, H.W., Plumer, L., Steiner, U. & Oerke, E.C. 2013. Development of spectral indices for detecting and identifying plant diseases. *Remote Sens. Environ* **128**, 21–30.

Mahlein, A.K., Steiner, U., Hillnhütter, C., Dehne, H.W. & Oerke, E.C. 2012. Hyperspectral imaging for small-scale analysis of symptoms caused by different sugar beet diseases. *Plant Methods* **8**(1), art.no.3. doi: 10.1186/1746-4811-8-3

Merzlyak, M.N., Gitelson, A.A., Chivkunova, O.B.& Rakitin, V.Y. 1999. Non-destructive optical detection of pigment changes during leaf senescence and fruit ripening. *Physiologia Plantarum* **106**, 135–141.

Padilla, F.M., Peña-Fleitas, M.T., Gallardo, M. & Thompson, R.B. 2017. Determination of sufficiency values of canopy reflectance vegetation indices for maximum growth and yield of cucumber. *European Journal of Agronomy* **84**, 1–15.

Peñuelas, J. & Filella, I. 1998. Visible and near-infrared reflectance techniques for diagnosing plant physiological status. *Trends in Plant Science* **3**, 151–156.

Peñuelas, J., Gamon, J.A., Fredeen, A.L., Merino, J. & Field, C.B. 1994. Reflectance indices associated with physiological changes in nitrogen- and water-limited sunflower leaves. *Remote Sensing of Environment* **48**, 135–146.

Peñuelas, J., Gamon, J.A., Griffin, K.L. & Field, C.B. 1993. Assessing community type, plant biomass, pigment composition, and photosynthetic efficiency of aquatic vegetation from spectral reflectance. *Remote Sensing of Environment* **46**(2), 110–118.

Peñuelas, J., Pinol, J., Ogaya, R. & Filella, I. 1997. Estimation of Plant Water Concentration by the Reflectance Water Index WI (R900/R970). *International Journal of Remote Sensing* **18**(13), 2869–2875.

Roman, A. & Ursu, T. 2016. Multispectral satellite imagery and airborne laser scanning techniques for the detection of archaeological vegetation marks. In book: *Landscape Archaeology on the Northern Frontier of the Roman Empire at Porolissum*. Interdisciplinary Research Project Mega Publishing House, pp. 141–152.

Semeraro, T., Mastroleo, G., Pomes, A., Luvisi, A., Gissi, E. & Aretano, R. 2019. Modelling fuzzy combination of remote sensing vegetation index for durum wheat crop analysis. *Computers and Electronics in Agriculture* **156**, 684–692.

Singh, M.C., Singh, J.P., Pandey, S.K., Mahay, D. & Shrivastva, V. 2017. Factors affecting the performance of greenhouse cucumber cultivation-A review. *International Journal of Current Microbiology and Applied Sciences* **6**(10), 2304–2323.

Skoczowski, A., Odrzywolska-Hasiec, M., Oliwa, J., Ciereszko, I. & Kornaś, A. 2021. Ecophysiological variability of Alnus viridis (Chaix) dc. green alder leaves in the bieszczady mountains (Poland). *Plants* **10**(1), 1–17.

Sytar, O., Zivcak, M., Neugart, S. & Brestic, M. 2020. Assessment of hyperspectral indicators related to the content of phenolic compounds and multispectral fluorescence records in chicory leaves exposed to various light environments. *Plant Physiology and Biochemistry* **154**, 429–438.

Zarco-Tejada, P.J., Miller, J.R., Noland, T.L., Mohammed, G.H. & Sampson, P.H. 2001. Scaling-up and model inversion methods with narrow-band optical indices for chlorophyll content estimation in closed forest canopies with hyperspectral data. *IEEE Transactions on Geoscience and Remote Sensing* **39**, 1491–1507.

*Agronomy Research* **20**(1), 16–26, 2022
https://doi.org/10.15159/AR.22.011

# An investigation of the amount of grain loss – using plant density and reel index of two popular brands of combine harvesters

S.S.A. Al-Slevani, Y.Y. Hilal* and M.H. Rafiq

University of Mosul, College of Agriculture and Forestry, Department of Agricultural Machines and Equipment, Iraq
*Correspondence: yousif.yakoub@uomosul.edu.iq

Received: January 4th, 2022; Accepted: March 8th, 2022; Published: March 18th, 2022

**Abstract.** Large wheat fields are cultivated in Iraq every year, especially in the Bazalan region. Although the grain production rate is high in Bazalan, the grain harvest loss is significant. Investigating wheat crop losses in different harvesting units is crucial to making decisions and improving working conditions. The current research was carried out to study the effect of the two popular brands of combine harvesters (New Holland TC56 and John Deere 1450 CWS) based on a relationship between the amount of loss from combine harvesters, reel indexes, and plant density. Three reel indexes (1, 1.5, and 2) and two plant densities (high-density and low-density sites) were considered. A randomised complete block split-plot design with three replications was carried out. The results showed positive superiority of the New Holland TC56 in the percentage of header losses, threshing losses, separation and cleaning losses, total harvest loss, and total loss with the highest performance efficiency of 97.725%; however, the harvester performance efficiency of the John Deere 1450 CWS remained within the acceptable loss limits. Finally, the best results were achieved with a 1.5-reel index level interacting with a high-density site; these results were statistically more significant than the differences between the New Holland TC56 and the John Deere 1450 CWS.

**Key words:** combine harvester, harvester efficiency, header losses, plant density, wheat.

## INTRODUCTION

The Bazalan-Duhok region in the northern governorate of Iraq relies heavily on agriculture for its economic existence. A large number of farmers are engaged in wheat production, and about 7,000 ha are planted with wheat (Center Statistical Organization, 2019). Presently, wheat production has become a serious issue for investors and farmers in Iraq, especially in the Bazalan region, due to climate change, different farming systems, and a shortage of skilled labour (FAO, 2021).

One of the solutions in large-scale wheat areas is that farmers and investors have increased the utilisation of combine harvesters (Kadhim, 2018). Therefore, Iraqi wheat harvesting has improved and witnesses continuous growth in harvesting patterns. In the recent past, this developed from manual labour into harvesting machines; now, a combine harvester is acceptable because of a notable change in the social structure in

rural areas. A combine harvester provides comfort, reduces labour and harvest loss, and provides a higher percentage of wheat cultivation with a decreased harvest cost and less wastage of agricultural energy; however, the loss of wheat yield is still a significant problem that seriously affects the profitability of the wheat crop (Ali & Jabara, 2021). Various critical technical parameters influence harvester performance; some are related to plants, and the others are related to harvesting machines (Šotnar et al., 2018; Derevjanko et al., 2020). Wang et al. (2021) clarified that the most important reason for this loss in harvest is the incorrect selection of the reel index while loss differences are owed to the density and type of planting. Further, Tihanov et al. (2021) found that wheat crop losses are due to improper adjustment of a harvester for different wheat crop conditions and farming systems. In fact, Bawatharan et al. (2013) and Zubko et al. (2018) stated that the amount of loss and the reasons for such loss occur as per inappropriate modifications of operating conditions, which is a result of users lacking the needed technical proficiency; consequently, the reel index, plant density, and combine harvester brand affects wheat harvest. Hence, this implies to the need to further investigate such relationships; in the Bazalan region, these factors have not been thoroughly studied.

A perfect setup of a combine harvester is the most crucial prerequisite for reducing the amount of harvest loss. Though combine harvester manufacturers provide recommended settings for each crop, these settings are based on average crop yield and average plant conditions. Therefore, the main objective is to study the effect of two popular brands of combine harvesters (New Holland TC56 and John Deere 1450 CWS) based on a relationship between levels of reel index and plant density on a percentage of header, threshing, separation and cleaning losses, total harvest loss, total loss, and harvester performance efficiency.

## MATERIALS AND METHODS

### Study area specifications

The field test was conducted at Bazalan in the Dahuk governorate of Iraq. Bazalan coordinates 36°49'14.2"N 42°53'02.0"E and monthly weather averages are shown in Fig. 1.

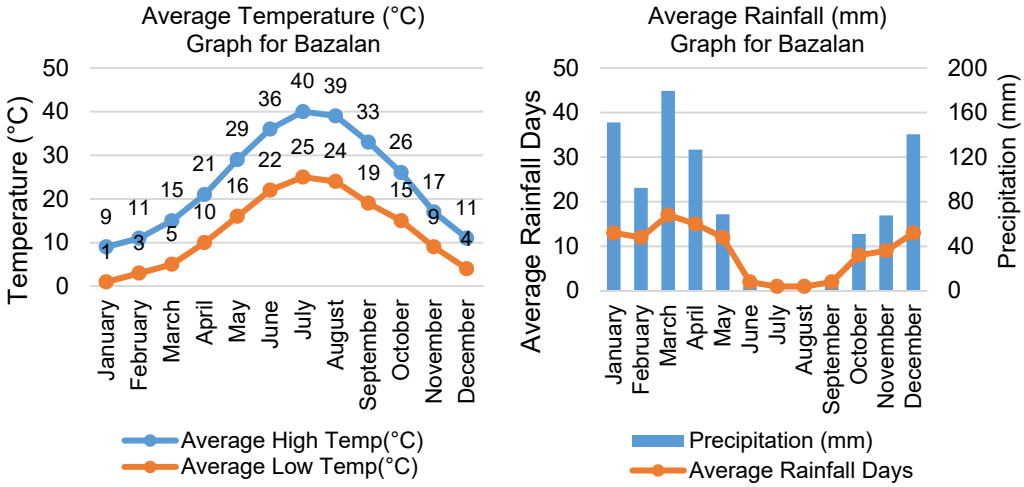


**Figure 1.** Bazalan climate weather (World weather, 2022).

**Treatments and Statistical Design**

A randomised complete block split-plot design with three replications was used to estimate the significant impact of reel index, plant density, and types of combine harvesters on wheat harvesting losses. The treatments were arranged so that the plant density was considered as the main plot factor with two plant densities. In the high-density site, the average number of spikes per square metre was 310 spikes and the average height of the crop was 50 cm; the average number of spikes in the low-density site was 186 spikes of various sizes and there was an average crop height of 30 cm. Types of combine harvesters were considered as subplot factors; the models were the New Holland TC56 combine harvester (model 2007) and the John Deere 1450 CWS combine harvester (model 2004). Table 1 presents the specifications of these combine harvesters.

**Table 1.** Specifications of combine harvesters used in the experiment (John Deere, 2007; New Holland, 2007)

| Specifications | John Deere 1450 CWS | New Holland TC56 |
|---|---|---|
| Brand | John Deere | New Holland |
| Model | 1450 CWS | TC56 |
| Years of production | 2004 | 2007 |
| Engine type (model / version) | Power TECH PVX 6068 HZ | 6.75T |
| Engine capacity | 6,788 cm3 (6.8 l.) | 7,474 cm3 (7.5 l.) |
| Cylinders, qty | 6 | 6 |
| Power | 132 kW / 180 KM | 114 kW / 155 KM |
| Header width (working) | 485 cm | 457 cm |
| Alternative widths | 365–580 cm | 366–518 cm |
| Diameter of cylinder threshing mechanism | 61 cm | 60 cm |
| Width of cylinder threshing mechanism | 130 cm | 130 cm |
| Length (with header) | 7.9 m | 9.32 m |
| Width (with header) | 4.9 m | 4.9 m |
| Width (without header) | 3.65 m | 3.37 m |
| Height (with cab) | 3.98 m | 3.8 m |
| Total weight (with cab) | 10,500 kg | 9,700 kg |

The farmer should consider the effect of the reel index value on the geometrical form of the reel tine bar trajectory and its implications on reel performance. The reel index is an often used parameter in the analysis of reel motion and performance. The reel index is denoted by equal to ωR/V or R/R0 where R0 = V/ω and the limits of R0 are $0 < R0 < R$. It should set the theoretical limits of the reel index to be $1<K<\infty$. The suitable value of this index should vary with the crop and crop conditions; the ground speed of the harvester was stable to obtain the three levels required for the reel index, which are 1, 1.5, and 2. The reel index was calculated according to the equation described in Oduori et al. (2012):

$$\text{Reel index} = \frac{\text{Reel angular velocity } (rad\ s^{-1}) \cdot \text{ radius of a reel } (m)}{\text{Header advance velocity } (m\ s^{-1})} \quad (1)$$

**Measurement of wheat crop losses**

Wheat yield losses were determined using the methods given in Eqs 2 to 6:

**1 – Percentage of pre-harvest losses (Natural loss):** The natural loss was estimated using a 65 cm × 38.5 cm frame before combine harvesters entered the field.

The frame was placed in 10 random places. Then, the percentage of pre-harvest losses was calculated from the equation proposed by Hamzah & Alsharifi (2020).

**2 – Percentage of header losses:** The header loss was estimated using three 65 cm × 38.5 cm frames at the end of each harvested row. The frames were placed at one-third of the left, middle, and right header length. Kernels and ears were finally gathered to be counted, and the method described in Jalali & Abdi (2014) was used to calculate the header loss from the following equations (2 and 3):

$$Header\ loss = (Total\ grains\ at\ the\ head - Total\ grains\ counted\ in\ the\ pre\ harvest\ losses)\text{x1,000grain weight x } 4\text{x}10^{-2} \quad (2)$$

$$Percentage\ of\ Header\ loss = \left(\frac{Header\ loss}{Total\ field\ production}\right)\text{x100} \quad (3)$$

**3 – Percentage of threshing losses:** Threshing losses are those unthreshed grain heads that escape the combine at the rear with the straw. Threshing losses can be expressed as a percentage from the equation described by Hamzah & Alsharifi (2020):

$$Percentage\ of\ threshing\ losses = \left(\frac{Mass\ of\ unthreshed\ grains}{total\ mass\ of\ grains}\right)\text{x100} \quad (4)$$

**4 – Percentage of separation and cleaning losses:** Separation and cleaning losses are lost grain with straw expressed as a percentage of total grain entering the combine (Srivastava et al., 2006).

**5 – Actual productivity:** The actual productivity was calculated via collecting the grains from the unloading auger before dropping them into the tank for a distance of 15 metres and all the experimental treatments.

**6 – Total yield:** The total yield of the crop kg/dunam was calculated by summing the following:

$$Total\ yield = \text{Net yield inside the harvester tank} + \text{Total harvest loss} + \text{pr} - \text{harvest losses} \quad (5)$$

**7 – Harvester performance efficiency:**

$$Harvester\ performance\ efficiency = \frac{Net\ yield}{Net\ yield + Total\ harvest\ loss}\text{ x100} \quad (6)$$

## RESULTS AND DISCUSSION

The natural loss percentage in the high-density site was 1.14 and 1.32% and in the low-density site was 1.39 and 1.74% for the New Holland TC56 and John Deere 1450 CWS, respectively. The difference between these values is due to a difference in the actual product to the plant density, where the productivity of the New Holland TC56 harvester was 470.58 and 272.64 kg per dunam[1] while the productivity of the John Deere 1450 CWS harvester was 408.33 and 218.27 kg dunam$^{-1}$ for the high-density and low-density sites, respectively.

[1] A dunam equals 2,500 square metres.

**Effect of plant density on wheat harvest loss and harvester efficiency**

Table 2 shows the effect of plant density on the percentage of header losses, threshing losses, separation and cleaning losses, total harvest loss, total loss, and harvester performance efficiency, respectively. The results for the effect of plant density showed statistically significant differences in all the studied traits. The header losses recorded the highest considerable loss, which was negatively reflected on the total harvester loss and the efficiency of the harvester performance. The superiority of the dense field, with the lowest percentage of loss over the low-density area, is due to the short length of the plants; meanwhile, an increase of hammering on the spikes increases the rate of loss in the low-density field, as presented in Table 2. The difference in the loss ratios between the high-density site and the low-density site was 5.62, 0.178, 0.757, 6.538, 6.871, and 5.305% for the header, threshing, and separation and cleaning losses, total harvest loss, total loss, and harvester performance efficiency, respectively. These results are consistent with the theory that a function of plant density has a significant influence on percentage losses (Kviz et al., 2015; Manzoor et al., 2021; Wang et al., 2021).

**Table 2** The impact of planting density on percentage losses in wheat harvesting and efficiency of the harvester

| Plant density | *Percentage of header losses, % | *Percentage of threshing losses, % | *Percentage of Separation and cleaning losses, % | *Total harvest loss, % | *Total loss, % | **Harvester performance efficiency, % |
|---|---|---|---|---|---|---|
| High-density site | 3.69 b | 0.726 b | 1.598 b | 6.024 b | 7.258 b | 94.372 a |
| Low-density site | 9.31 a | 0.904 a | 2.355 a | 12.562a | 14.129a | 89.067 b |

*The lowest values are the best; **The highest values are the best, the similar letters mean that there is no significant difference at the level of 5%.

**Effect of combine harvester types on wheat harvest loss and harvester efficiency**

The percentage of losses showed a significant difference between the two types of combine harvesters in the harvesting operation. The use of the New Holland TC56 harvester provided the lowest loss value and the best performance among harvesters, with a percentage of 3.928, 0.416, 1.096, 5.44, 6.71, and 94.893% of header losses, threshing losses, separation and cleaning losses, total harvest loss, total loss, and harvester performance efficiency, respectively (Table 3). Header losses, threshing losses, separation and cleaning losses were significantly influenced by the John Deere 1450 CWS harvester (Table 3). The cutting unit of the John Deere 1450 CWS harvester was associated with a possible deficiency in cutting height control. It generated a nonhomogeneous cut, causing the most significant wheat harvest loss, especially for the header losses of 9.075%. It was reflected in the total harvester loss and then in the efficiency of the harvester performance. According to Xavier et al. (2020), studies on the types of combine harvesters promote operation improvements and reduce costs; it has a greater influence on the percentage losses due to the reduced collection capacity and higher losses of the product in the field.

**Table 3.** The impact of combine harvesters on percentage losses in wheat harvesting and efficiency of the harvester

| Types of combine harvesters | *Percentage of header losses, % | *Percentage of threshing losses, % | *Percentage of Separation and cleaning losses, % | *Total harvest loss, % | *Total loss, % | **Harvester performance efficiency, % |
|---|---|---|---|---|---|---|
| New Holland TC56 | 3.928 b | 0.416 b | 1.096 b | 5.44 b | 6.71 b | 94.893 a |
| John Deere 1450 CWS | 9.075 a | 1.214 a | 2.857 a | 13.146a | 14.678a | 88.546 b |

*The lowest values are the best; **The highest values are the best, the similar letters mean that there is no significant difference at the level of 5%.

**Effect of reel index on wheat harvest loss and harvester efficiency**

The results showed that the effect of the reel index has statistically significant differences in the percentage of header losses, threshing losses, separation and cleaning losses, total harvest loss, total loss, and harvester performance efficiency (Table 4). The percentage of header losses recorded the highest significant loss.

A reel index level of 1.5 is superior in having the lowest rate of loss when compared to a reel index level of 1 or 2. In the reel index of 1 (lower values), the losses were 6.929, 0.931, 2.091, 9.951, 11.352, and 91.189%. In comparison, in the reel index of 2 (higher values), there were increased losses, which were 7.287, 0.777, 2.174, 10.238, 11.639, and 90.894% of header losses, threshing losses, separation and cleaning losses, total harvest loss, total loss, and harvester performance efficiency, respectively, as presented in Table 4.

**Table 4.** The impact of reel index on percentage losses in wheat harvesting and efficiency of the harvester

| Reel index | *Percentage of header losses, % | *Percentage of threshing losses, % | *Percentage of Separation and cleaning losses, % | *Total harvest loss, % | *Total loss, % | **Harvester performance efficiency, % |
|---|---|---|---|---|---|---|
| 1 | 6.929 b | 0.931a | 2.091 b | 9.951 a | 11.352a | 91.189 b |
| 1.5 | 5.289 c | 0.737 b | 1.664c | 7.69b | 9.091b | 93.074 a |
| 2 | 7.287 a | 0.777 b | 2.174 a | 10.238a | 11.639a | 90.894 c |

* The lowest values are the best; **The highest values are the best, the similar letters mean that there is no significant difference at the level of 5%.

In a reel index value of 1, due to the low speed of the reel in relation to the ground speed of the harvester, the spikes are pushed forward and break in front of the cutting knife. A 2-reel index means a high speed of the reel in relation to the ground speed of the harvester; this causes the fans to hammer more on the spikes and break or loosen them, leading to an increase in the quantitative loss of the yield. These results are consistent with Fadavi et al. (2017) and Chaab et al. (2020).

**Effect of the interaction between the planting density and the combine harvesters on wheat harvest loss and harvester efficiency**

Table 5 shows statistically significant differences in the effect of the interaction between crop density and type of combine harvester in percentage losses in wheat

harvesting and harvester performance efficiency. The high-density site showed the lowest loss ratio for both harvesters, outperforming the low-density site. The increase of the plant density led to the decrease of the total harvest loss for the New Holland TC56 and John Deere 1450 CWS; the results were 3.642 and 8.406% in high-density sites and 7.237 and 7.237% in low-density sites, respectively. Because of the density and length of the plant, the engineering design of the machine matched the plant density.

**Table 5.** The impact of the interaction between the planting density and the combine harvesters on percentage losses in wheat harvesting and efficiency of the harvester

| Plant density | Types of combine harvesters | *Percentage of header losses, % | *Percentage of threshing losses, % | *Percentage of Separation and cleaning losses, % | *Total harvest loss, % | *Total loss, % | **Harvester performance efficiency, % |
|---|---|---|---|---|---|---|---|
| High-density site | New Holland TC56 | 2.523 d | 0.273c | 0.846 d | 3.642 d | 4.79 d | 96.495a |
| | John Deere 1450 CWS | 4.877 c | 1.179a | 2.349 b | 8.406 b | 9.728 b | 92.249c |
| Low-density site | New Holland TC56 | 5.333 b | 0.558b | 1.346 c | 7.237 c | 8.631 c | 93.291b |
| | John Deere 1450 CWS | 13.274a | 1.249a | 3.363 a | c | 19.627a | 84.843d |

*The lowest values are the best; **The highest values are the best, the similar letters mean that there is no significant difference at the level of 5%.

The results showed significant superiority of the New Holland TC56 over the John Deere 1450 CWS. It is clear that the New Holland TC56 harvester was significantly better than the John Deere 1450 CWS with efficiencies of 96.495 and 93.291% in high-density sites and low-density sites, respectively. Furthermore, due to the adjustment efficiency and engineering design of the New Holland TC56, harvest was completed in a shorter time.

**Effect of the interaction between the planting density and the reel index on wheat harvest loss and harvester efficiency**

The harvester level reel index 1.5 in high-density site had the lowest harvester losses of 2.977, 0.646, 1.419, 5.042, and 6.277% for header losses, threshing losses, separation, and cleaning losses, total harvest loss, total loss with higher harvester performance efficiency of 95.264%, as presented in Table 6. However, the highest total harvest loss of 13.938% was at a reel index of 2 in a low-density site. It indicates that the rotates of a reel with less advancement into the yield and increased tines hit the spikes harshly, resulting in increased losses; these observations agree with the results obtained by Bawatharani et al. (2013).

The results showed that the influence of planting density was different for each reel index. The dense field outperformed the less dense area with the lowest percentage of quantitative crop loss, especially in the cutting unit that caused more than two-thirds of the total harvest loss, where the values were (3.977, 2.977, 4.145) % (9.881, 7.601, 10.429) % for both fields with a reel index of 1,1.5 and 2, respectively.

**Table 6.** The impact of the interaction between the planting density and the level of reel index on percentage losses in wheat harvesting and efficiency of the harvester

| Plant density | Reel index | *Percentage of header losses, % | *Percentage of threshing losses, % | *Percentage of Separation and cleaning losses, % | *Total harvest loss, % | *Total loss, % | **Harvester performance efficiency, % |
|---|---|---|---|---|---|---|---|
| High-density site | 1 | 3.977 d | 0.793b | 1.722d | 6.492 d | 7.727d | 93.955b |
| | 1.5 | 2.977 e | 0.646 c | 1.419e | 5.042 e | 6.277 e | 95.264a |
| | 2 | 4.145 d | 0.74 b | 1.653d | 6.538d | 7.773d | 93.897b |
| Low-density site | 1 | 9.881 b | 1.069a | 2.46 b | 13.41 b | 14.977b | 88.424d |
| | 1.5 | 7.601 c | 0.828b | 1.909 c | 10.337c | 11.905c | 90.885c |
| | 2 | 10.429 a | 0.815b | 2.695a | 13.938a | 15.505a | 87.892e |

*The lowest values are the best; **The highest values are the best, the similar letters mean that there is no significant difference at the level of 5%.

**Effect of the interaction between the reel index and the types of combine harvesters on wheat harvest loss and harvester efficiency**

Wheat harvest loss and harvester efficiency were significantly affected by the combine harvester type and the reel index (Table 7). The harvest losses were significantly different ($P < 0.05$) between the levels of reel indexes in New Holland TC56 and John Deere 1450 CWS, while the losses at New Holland TC56 were significantly lower than that of John Deere 1450 CWS. In contrast, the total harvest loss was higher at level 1 of the reel index in John Deere 1450 CWS due to increasing both percentage of header losses and the percentage of threshing losses. The percentage of losses at level 1.5 of the reel index was lower than that of the reel index 1 and 2, the header losses were higher at level 1 of the reel index in John Deere 1450 CWS, while at the levels of reel indexes 1.5 and 2, there are no statistically significant differences concerning the percentage of threshing losses (Table 7). The harvester performance efficiency was significantly higher at the reel index of 1.5 and a significant difference between 1 and 2 reel indexes on New Holland TC56 and John Deere 1450 CWS. However, the harvester performance efficiency was higher at all the three levels of reel index in New Holland TC56 than that of John Deere 1450 CWS combine harvesters.

**Table 7.** The impact of the interaction between the types of combine harvesters and the reel index on percentage losses in wheat harvesting and efficiency of the harvester

| Types of combine harvesters | Reel index | *Percentage of header losses, % | *Percentage of threshing losses, % | *Percentage of Separation and cleaning losses, % | *Total harvest loss, % | *Total loss, % | **Harvester performance efficiency, % |
|---|---|---|---|---|---|---|---|
| New Holland TC56 | 1 | 3.972 f | 0.45 c | 1.339d | 5.76 e | 7.03e | 94.582b |
| | 1.5 | 2.219 g | 0.329 d | 0.882 f | 3.43 f | 4.701f | 96.696a |
| | 2 | 5.594 e | 0.468 c | 1.067e | 7.129 d | 8.4 d | 93.401c |
| John Deere 1450 CWS | 1 | 9.886 a | 1.412 a | 2.843b | 14.142a | 15.674a | 87.797f |
| | 1.5 | 8.359 c | 1.144 b | 2.446c | 11.949c | 13.481c | 89.453d |
| | 2 | 8.979 b | 1.087b | 3.28 a | 13.347b | 14.878b | 88.388e |

*The lowest values are the best; **The highest values are the best, the similar letters mean that there is no significant difference at the level of 5%.

These results indicate that at the reel index of 1.5 in both combine harvesters, grain loss was statistically significant ($P < 0.05$) at a minimum compared to the other two levels of the reel index. Thus, the influence of the reel index and harvesters type on losses has significantly influenced.

**Effect of the interaction between the planting density, types of combine harvesters, and the reel index on wheat harvest loss and harvester efficiency**

Table 8 shows the influence of planting density, types of combine harvesters, and the reel index on the harvest losses and harvester efficiency. The results indicated that losses were influenced by the combine harvester type and the reel index in both Plant density sites. The header losses differed significantly ($P < 0.05$) between the reel index levels in New Holland TC56 and the high-density area. The losses at the reel index of 1.5 were considerably lower than that of 1 and 2. Otherwise, the header losses were not significantly at the three levels of reel index in John Deere 1450 CWS and high-density site. The wheat harvest losses at New Holland TC56 were considerably lower than John Deere 1450 CWS in high-density and low-density sites. The header losses, threshing losses, total harvest loss, and total loss were significantly higher at the reel index of 1 in John Deere 1450 CWS in low-density sites. In contrast, the separation and cleaning losses were considerably higher at the reel index of 2 in John Deere 1450 CWS in a low-density area (Table 8).

**Table 8.** The impact of the interaction between the planting density, types of combine harvesters, and the reel index on percentage losses in wheat harvesting and efficiency of the harvester

| Plant density | Types of combine harvesters | Reel index | *Percentage of header losses, % | *Percentage of threshing losses, % | *Percentage of Separation and cleaning losses, % | *Total harvest loss, % | *Total loss, % | **Harvester performance efficiency, % |
|---|---|---|---|---|---|---|---|---|
| High-density site | New Holland TC56 | 1 | 2.639g | 0.289 gf | 1.101i | 4.029g | 5.177h | 96.127b |
| | | 1.5 | 1.336 h | 0.222 g | 0.77k | 2.328h | 3.476i | 97.725a |
| | | 2 | 3.595 f | 0.308 fe | 0.666 l | 4.569g | 5.716ih | 95.631b |
| | John Deere 1450 CWS | 1 | 5.315 e | 1.297 b | 2.342e | 8.954e | 10.277e | 91.782d |
| | | 1.5 | 4.619 e | 1.069 dc | 2.069f | 7.756f | 9.078f | 92.803c |
| | | 2 | 4.696 e | 1.171 cb | 2.639d | 8.506e | 9.829e | 92.162d |
| Low-density site | New Holland TC56 | 1 | 5.305 e | 0.61 e | 1.576g | 7.491f | 8.885f | 93.037c |
| | | 1.5 | 3.102gf | 0.436 f | 0.994j | 4.532g | 5.926g | 95.666b |
| | | 2 | 7.594 d | 0.627 e | 1.468h | 9.689d | 11.083 d | 91.17e |
| | John Deere 1450 CWS | 1 | 14.458a | 1.527 a | 3.344b | 19.329a | 21.07a | 83.811h |
| | | 1.5 | 12.1 c | 1.219 cb | 2.824c | 16.142c | 17.883c | 86.103f |
| | | 2 | 13.263b | 1.002 d | 3.922a | 18.187b | 19.928b | 84.614g |

*The lowest values are the best; **The highest values are the best, the similar letters mean that there is no significant difference at the level of 5%.

The results showed statistically significant differences between the levels of reel indexes 1 and 2 in New Holland TC56 and John Deere 1450 CWS in both sites. The harvester performance was higher at reel index 1.5. However, the harvester performance was significantly higher at reel index 1.5 in New Holland TC56 and high-density site than that of all other interactions, and its highest performance efficiency reached

97.725%, as a result of achieving the lowest loss ratios in its units, especially the cutting unit and the total loss due to the high cutting efficiency. At the same time, the reel index 1 in John Deere 1450 CWS and low-density site recorded the lowest efficiency, which was 83.81%.

## CONCLUSION

The current study aimed to investigate the effect of the New Holland TC56 and John Deere 1450 CWS combine harvesters based on a relationship between levels of reel index and plant density on a percentage of losses in harvest units, total harvest loss, total loss, and harvester performance efficiency. The data revealed that the best results were achieved with a 1.5-reel index level interacting with a high-density site; these results were statistically more significant than the differences between the New Holland TC56 and the John Deere 1450 CWS. It was observed that a reel index value of 1 or 2 results in a negative effect on all of the traits. In addition, the results showed positive superiority of the New Holland TC56 in the percentage of header, threshing, separation and cleaning losses, total harvest loss, and total loss with the highest performance efficiency of 97.725%; meanwhile, the John Deere 1450 CWS showed harvester performance efficiency of up to 92.80% and remained within the acceptable loss limits. A perfect setup of the combine harvesters is the most crucial prerequisite for reducing the number of harvest losses; therefore, it is recommended to expand the use of these modern harvesters by conducting more experiments and research in better conditions for wheat crops and combine harvesters.

ACKNOWLEDGMENTS. The authors express their thanks to the University of Mosul for providing coordination of equipment and technical support.

## REFERENCES

Ali, S.H. & Jabara, O.K. 2021. An economic study of post-harvest losses for wheat farmers in iraq baghdad governorate–case study. *Iraqi Journal of Agricultural Sciences* **52**(5), 1267–1275.

Bawatharani, R., Jayatissa, D.N., Dharmasena, D.A.N. & Bandara, M.H.M.A. 2013. Impact of reel index on header losses of paddy and performance of combine harvesters. *Tropical Agricultural Research* **25**(1), 1–13.

Central Statistical Organization CSO. 2019. Wheat and barley production in 2018 (in Arabic).

Chaab, R.K., Karparvarfard, S.H., Rahmanian-Koushkaki, H., Mortezaei, A. & Mohammadi, M. 2020. Predicting header wheat loss in a combine harvester, a new approach. *Journal of the Saudi Society of Agricultural Sciences* **19**(2), 179–184.

Derevjanko, D., Holovach, I., Bulgakov, V., Kuvachev, V. & Olt, J. 2020. Theoretical and experimental research into impact of threshing tools in combine grain harvesters on quality of cereal crop seeds. *Agronomy Research* **18**(2), 393–403. https://doi.org/10.15159/AR.20.056

FAO (Food and Agriculture Organization of the United Nation). 2021. Agricultural value chain study in Iraq Dates, grapes, tomatoes and wheat. Retrieved online: https://reliefweb.int/report/iraq/agricultural-value-chain-study-iraq-dates-grapes-tomatoes-and-wheat-2021-enarku

Fadavi, R., Abdollahpour, S. & Moghaddam, M. 2017. Design, construction and evaluation of grain harvester combine's header loss based on statistical analysis and modeling the optimal factors. *Journal of Experimental Biology* **5**(4),537–544.

Hamzah, I.J. & Alsharifi, S.K.A. 2020. Innovative harvesting methods about the harvest losses for two machines. *Bulgarian Journal of Agricultural Science* **26**(4), 913–918.

Jalali, A. & Abdi, R. 2014. The effect of ground speed, reel rotational speed and reel height in harvester losses. *Journal of Agriculture and Sustainability* **5**(2),221–231.

John Deere. 2007. *1450CWS/ WTS 1550CWS /WTS Combines Parts Catalog Manual*. Deere & Company European Edition, Brasil, 188 pp.

Kadhim, Z.R. 2018. An investigation of current status of agricultural mechanization services in Iraq and future suggestions. *ARPN Journal of Agricultural and Biological Science* **13**(12), 149–164.

Kviz, Z., Kumhala, F. & Masek, J. 2015. Plant remains distribution quality of different combine harvesters in connection with conservation tillage technologies. *Agronomy Research* **13**(1), 115–123.

Manzoor, A., Bashir, M. A., Naveed, M. S., Cheema, K. L. & Cardarelli, M. 2021. Role of Different Abiotic Factors in Inducing Pre-Harvest Physiological Disorders in Radish (Raphanus sativus). *Plants* **10**(10), 2003.

New Holland. 2007. TC54 TC56 AL59 Combines Service Repair Manual 87595929. New Holland Company,164 pp.

Oduori, M.F., Mbuya, T.O., Sakai, J. & Inoue, E. 2012. Kinematics of the tined combine harvester reel. *Agricultural Engineering International: CIGR Journal* **14**(3), 53–60.

Šotnar, M., Pospíšil, J., Mareček, J., Dokukilová, T. & Novotný, V. 2018. Influence of the combine harvester parameter settings on harvest losses. *Acta technologica agriculturae* **21**(3), 105–108.

Srivastava, A.K., Goering, C.E., Rohrbach, R.P. & Buckmaster, D.R. 2006. *Engineering Principles of Agricultural Machines*. American Society of Agricultural and Biological Engineers. ST Josef, Michigan, USA, 559 pp.

Tihanov, G., Dallev, M., Hristova, G. & Mitkov, I. 2021. Loss of grain at harvesting wheat with a combine harvester. *Series. A. Agronomy* **LXIV**(1), 577–582. http://agronomyjournal.usamv.ro/pdf/2021/issue_1/Art76.pdf.

Wang, K., Xie, R., Ming, B., Hou, P., Xue, J. & Li, S. 2021. Review of combine harvester losses for maize and influencing factors. *International Journal of Agricultural and Biological Engineering* **14**(1), 1–10.

World weather. 2022. Bazalan Climate Weather Averages. Retrieved online: https://www.worldweatheronline.com/bazalan-weather-averages/dahuk/iq.aspx

Xavier, W.D., Silva, D.C., da Costa, R.B., Ribeiro, D.O., Sousa, V.S. & de S Silva, J.V. 2020. Losses in the mechanized harvesting of sugarcane as of speed function of two harvester models in tropical savanna environment. *Australian Journal of Crop Science* **14**(4), 675–682.

Zubko, V., Roubík, H., Zamora, O. & Khvorost, T. 2018. Analysis and forecast of performance characteristics of combine harvesters. *Agronomy Research* **16**(5), 2282–2302. https://doi.org/10.15159/AR.18.212

*Agronomy Research* **20**(1), 27–39, 2022
https://doi.org/10.15159/AR.22.013

# Evolution of productive and biodiversity features in lucerne fields of different ages

G. Argenti*, S. Parrini, N. Staglianò and R. Bozzi

University of Florence, School of Agriculture, DAGRI, P.le delle Cascine 18, 50144 Firenze, Italy
*Correspondence: giovanni.argenti@unifi.it

Received: January 10th, 2022; Accepted: February 23rd, 2022; Published: April 1st, 2022

**Abstract.** *Medicago sativa* is a legume forage crop characterized by high production of forage, with a notable nutritive value, but in mountain areas duration of the crop could be remarkably affected by severe environmental conditions. To assess the vegetation evolution of lucerne crops in relation to crop age, data from fields of lucerne of different ages were collected. The aim is the evaluation of lucerne productive performances, evolution of forage quality and assessment of recovery by autochthonous species that naturally recolonize the studied areas in relation to age of the cropped species. With increasing years, lucerne population was significantly decreased and replaced by different functional types of plants, such as perennial graminoids and short-lived forbs. Biodiversity increased significantly along time, and evolution of similarity indices demonstrated an evolution of vegetation toward that represented by reference grassland of the area. Productive characteristics of forage, in terms of aboveground biomass and quality, were negatively affected by age. Results permitted to assess the evolution of different features of lucerne for a mountain environment and to hypothesize the appropriate management for this resource, that could contemplate also the evolution towards the reconstitution of the reference habitat for the studied area.

**Key words:** aboveground biomass, botanical composition, *Medicago sativa*, sown meadows, succession.

## INTRODUCTION

Lucerne (*Medicago sativa*) is one of the most important forage crops in temperate environments, for its productivity and nutritive value (Hakl et al., 2021) and it has been used in different environments for thousands of years (Sheaffer et al., 2020). Its role inside agricultural systems is not only to provide good quality forage (Pacchioli & Fattori, 2014), but also to be included in crop rotations as an improving crop that covers the ground for several years while providing fodder production and other ecosystem services such as increasing chemical soil fertility (Głąb & Gondek, 2013) or reduction of weed invasion for following crops (Meiss et al., 2010).

Its high capacity for protein synthesis, resulting from nitrogen-fixing capacity due to symbiosis with rhizobia (Jáuregui et al., 2019), makes lucerne one of the most interesting forage species for its nutritional value when feeding dairy cows especially in

intensive dairy farms (Giustini et al., 2007; Tabacco et al., 2018). In Italy, it is currently cultivated on about 700,000 ha (ISTAT, 2021), one third of which is in the Emilia-Romagna region alone, as this is the production area of Parmigiano-Reggiano, one of the best known Italian agri-food products in the world (Lovarelli et al., 2019). The origin area of this PDO (Protected Designation of Origin) is restricted to only a few very specific areas of the region, often in very extensive plains or hills (Mancini et al., 2019). Nevertheless, there is a production district corresponding to some mountainous areas in which lucerne plays an important and irreplaceable role in the provision of quality fodder coupled with grass-legumes mixtures (Argenti et al., 2021). Under these conditions, however, given its considerable sensitivity to cold (Bertrand et al., 2017), lucerne undergoes severe thinning and can reduce its duration in sown meadows sown with this legume (Belanger et al., 2006). Forage resources are actually encroached along time by various types of weeds species (mainly grasses but also species belonging to other families) and this vegetation development can reduce the productive capacity of a grassland (Ponzetta et al., 2010), the quality of the forage and the profitable longevity of the crop (Chataigner et al., 2010).

Based on the above considerations, the aim of the following research was to investigate, on lucerne fields characterized by different ages, both the level and the speediness of recolonization by spontaneous vegetation. Furthermore, the study is aimed to identify production and quality trends according to the age of the crop, to define appropriate forms of management and duration of the meadows sown with lucerne for the studied area.

## MATERIALS AND METHODS

Study area comprises fields cropped with *Medicago sativa* of different ages inside the district of 'Terre di Montagna', a Consortium that assembles mountain farms that produce Parmesan cheese over 600 m a.s.l., in Emilia-Romagna Region (north Italy). In the area, climate is temperate, with an annual average temperature of 10.1 °C and a rainfall of about 930 mm (Fig. 1). Climatic information is referred to the meteorological station of Montese, the main town approximately occurring in the centre of the district (Regione Emilia-Romagna, 2021). Soils range from acidic to calcareous and developed on different kind of rocks (sandstone, limestone and marl).

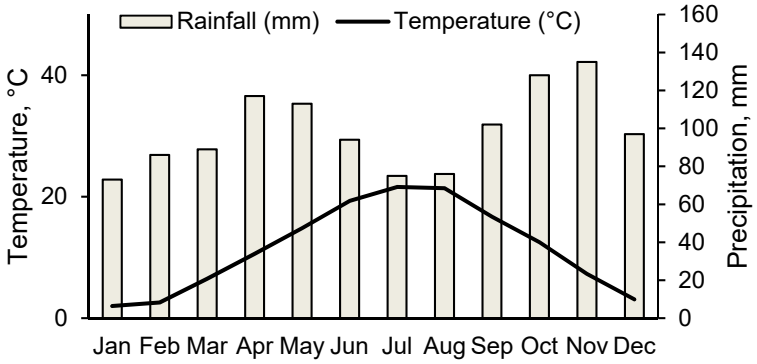


**Figure 1.** Average monthly data for temperature and precipitation for the studied area.

Main forage crops of the area are temporary meadows of lucerne and grass-legumes mixture, both binary than complex, utilized for hay production by means of 2 or 3 cuts per year (Argenti et al., 2021). Duration of the crops varies a lot according to forage species involved and farmer options, but, even if meadows are generally cropped for 4–5 years since sowing, it is common to find also lucerne fields older than the ordinary duration. Concerning fertilization management, only organic manure at sowing is performed and no further additional fertilization is generally added during crop cultivation. In this research, 4 different fields of 2, 4, 8 and 12 years has been selected, included at an altitude of about 700–800 m a.s.l., on flat or poorly sloped areas. Fields were within a radius of 5 km from the centre of the area (N 44° 16', E 10° 58') and with similar environmental and climatic characteristics. Soils of the four study sites (Table 1) are quite homogeneous, with a clay-loam texture and an average pH of 6.7 in water (Soilgrids, 2022).

**Table 1.** Main soil properties for the investigated sites

| Parameter | Value |
|---|---|
| Sand (%) | 25.4 |
| Clay (%) | 33.5 |
| Silt (%) | 41.1 |
| Type | Clay Loam |
| pH (water) | 6.7 |
| Bulk density (g $cm^{-3}$) | 1.31 |

For each survey point, data collection was performed on three different subplots where many productive and botanical parameters were recorded. All the samplings reported refer to the early vegetative stage(end of May), before the first mowing as performed in previous similar research (Török et al., 2011).

Aboveground biomass was clipped from a square of 0.5×0.5 m, as reported by Mikhailova et al. (2000). Fresh biomass was stored in sealable bags and then was dried in a forced air oven at 80 °C to constant weight for dry matter determination as usually performed in forage science (Wang et al., 2019). On the same area, Leaf Area Index (LAI, $m^2 \cdot m^{-2}$), a variable related to the complex structure of the canopy and to its biomass allocation (Francone et al., 2014), was collected by means of a ceptometer (LI-COR, USA). Each dried forage sample was grounded through a mill (Brabender OHG, Germany) to pass 1 mm and analysed for the following parameters: crude protein (CP) and Acid Detergent Fibre (ADF) as main drivers of quality (Lemaire & Belanger, 2020) according to standard laboratory procedures (AOAC, 2012).

Vegetation was monitored on the same sample areas. Cover of all vascular plants was recorded by means of visual estimation (Boob et al., 2019a). In the following data elaboration, species were grouped to the following functional types: *Medicago sativa* (sown crop), perennial forbs (excluding lucerne), perennial graminoids, short lived forbs and short lived graminoids according to the classification adopted by Török et al. (2011).

Species diversity was assessed by means of parameters such the number of species observed in each sample, Shannon diversity index (H') calculated by Eq. 1:

$$H' = - \Sigma(p_i \times \ln p_i) \quad (1)$$

and by Pielou evenness index (J', Eq. 2):

$$J' = H'/\ln S \quad (2)$$

where '$p_i$' is the percentage proportion (expressed as decimal fraction) of the *i*-species in the canopy and 'S' is the total number of species in each sample, or richness (Pruchniewicz, 2017).

Finally, to evaluate the level of naturalization reached by lucerne fields as a function of age, the list of species from each sample was compared to the list of characteristic species of a given reference habitat (Raduła et al., 2020), *i.e.* those species native and

typical of a particular community occurring in a specific area (Helm et al., 2015). In our case the list of characteristic species was derived from Habitat 6510 (Lowland hay meadows), considered as the reference habitat of the area, as reported in a Guide to habitat of community interest for the Emilia-Romagna Region (Bassi et al., 2015). Comparison between lucerne fields and the reference habitat was performed by means of two of the most used similarity indices (Eqs 3 and 4, Magurran, 2004):

$$\text{Sørensen Index } (S_S): 2a/(2a + b + c) \quad (3)$$

$$\text{Jaccard Index } (J_S): a/(a + b + c) \quad (4)$$

where 'a' is the number of species shared by the two lists (lucerne fields and reference habitat), and 'b' and 'c' are the number of species unique to the two lists. Thus, calculation of these parameters needs only presence/absence of the species and not their percentage of occurrence. Both indices range from 0 (no similarity) to 1 (identity).

To compare data from different field age, ANOVA was performed adopting Tukey test or LSD as post hoc tests. Results were used to assess possible relationships among monitored parameters and evolution of a specific parameters along time. Analyses were performed with the SPSS statistical software (release 27, IBM, 2020).

## RESULTS AND DISCUSSION

Table 2 reports evolution of percentage presence of identified functional groups of species in the lucerne fields of different age. Ground cover of cropped species differs significantly along time, with a highly decreased cover in oldest fields (5.7% and 6.3% for 8 and 12 years old areas respectively). The functional group that benefitted mostly from this evolution was that of perennial graminoids (such as *Lolium perenne*, *Dactylis glomerata* or *Arrhenatherum elatius*), that increased from 6.0 to more than 50% in oldest samples. Other functional groups differed in a less relevant way or did not show any significant difference along time.

**Table 2.** Percentage cover of species belonging to different functional groups in relation to age of fields. Values are means ± standard error

| | Age (years) of lucerne fields | | | |
|---|---|---|---|---|
| | 2 | 4 | 8 | 12 |
| *Medicago sativa* | $77.3 \pm 4.3^{a}$ | $34.3 \pm 2.7^{b}$ | $5.7 \pm 2.3^{c}$ | $6.3 \pm 2.1^{c}$ |
| Perennial forbs | $4.7 \pm 0.6^{ns}$ | $7.7 \pm 1.6^{ns}$ | $9.0 \pm 4.7^{ns}$ | $19.7 \pm 1.6^{ns}$ |
| Perennial graminoids | $6.0 \pm 2.0^{b}$ | $36.6 \pm 1.3^{ab}$ | $58.6 \pm 8.5^{a}$ | $53.0 \pm 12.1^{a}$ |
| Short lived forbs | $1.7 \pm 0.3^{b}$ | $6.7 \pm .7^{a}$ | $8.0 \pm 1.9^{a}$ | $7.7 \pm 1.3^{a}$ |
| Short lived graminoids | $10.3 \pm 3.2^{ns}$ | $14.7 \pm 1.2^{ns}$ | $18.7 \pm 3.3^{ns}$ | $13.3 \pm 5.9^{ns}$ |

Values with the same letters are not significantly different according to Tukey test ($P < 0.05$); ns = not significant.

Development of vegetation along years interested also forage production, with an aboveground biomass that decreased significantly from recent to old fields (Fig. 2). Simultaneously to this evolution, a reduction in the average quality of the forage has been recorded, with a significant decrease in crude protein content and an increase in the fibrous components, evidenced by increasing ADF values. Decrease of crude protein content (from 22.3% to 12.5%) was more rapid than reduction of above ground biomass.

Concerning LAI, a general reduction of this parameter was recorded along time with a less remarkable relation to years since sowing.

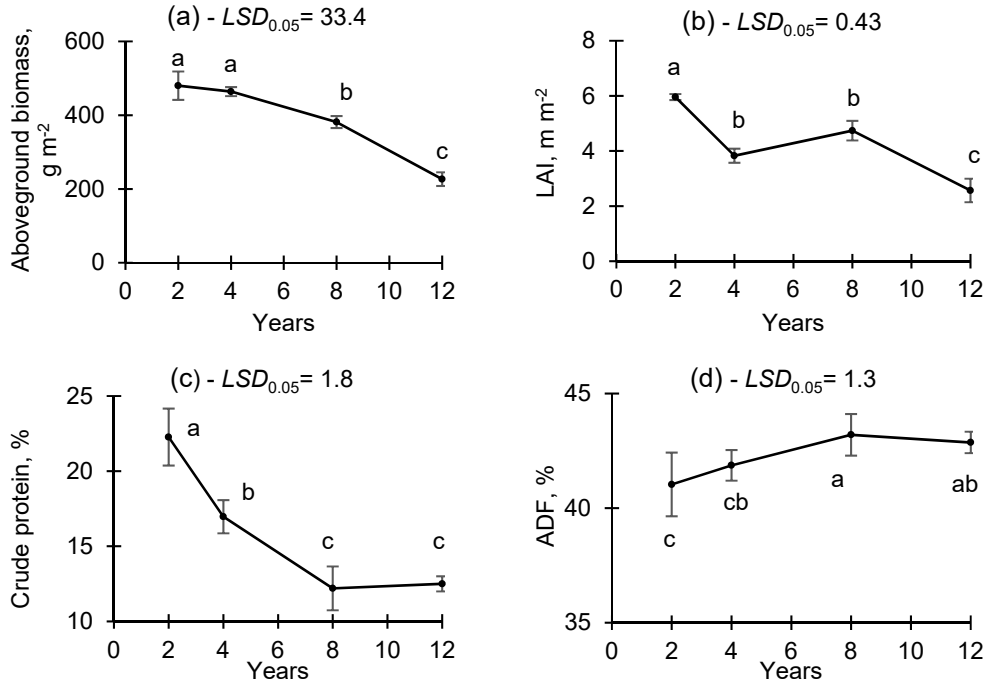


**Figure 2.** Evolution of aboveground biomass (AGB) (a), Leaf Area Index (LAI) (b), crude protein content (c) and ADF (d) in lucerne according to different age fields. Bars represent standard errors. *LSD* is the least significant difference ($P$ = 0.05) for each analysed variable.

Evolution along time of botanical composition and forage quality is significantly related to age of fields (Fig. 3). Presence of weeds increases constantly in relation to age with a very accurate logarithmic curve ($R^2$ = 0.91). Infestation by weeds is faster at the beginning of naturalization process. At the same time crude protein content decreases along time with a similar pattern but with a lower accuracy ($R^2$ = 0.77).

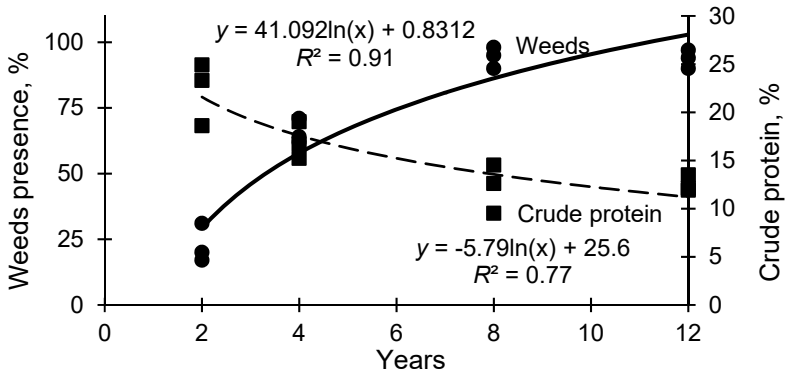


**Figure 3.** Regressions of presence of weeds and crude protein content with age of lucerne fields.

Evolution recorded did not differ from that observed in other studies related to mowed grasslands. Utilization itself can improve recovery of native species inside sown forage crops, as mowing is acknowledged to introduce seeds from other fields into grasslands or favour some kinds of species according to time and frequency of cutting (Gaujour et al., 2012). Reduction of lucerne cover in relation to age observed in this survey is similar to that reported by Török et al. (2011) that analysed lucerne fields from 1 to 10 years of age. Native species recolonization is limited in the first years by high density of the seeded plant as reported by Li et al. (2008). High presence of standing biomass can also explain suppression of species belonging to native flora that develop more remarkably in older stage of evolution, according to Güsewell & Edwards (1999). Perennial species are the most represented category in older stage of evolution (Štolcová, 2002) and especially perennial grasses are the most frequent in secondary succession (Török et al., 2008) and our results are consistent to previous studies concerning this aspect (Feng et al., 2007).

Reduction of productive and qualitative features in lucerne as consequence of age is reported by many authors (Teixeira et al., 2007) and this behaviour is due to different causes, such as self-thinning for competition, specific environmental conditions (such as acid pH or waterlogging), presence of pests or diseases (Burnett et al., 2020). Especially in mountain areas, also climatic conditions can affect development and diffusion of grassland resources (Dibari et al., 2015) and this is particularly true for lucerne which is acknowledged to be very sensitive to cold (Ta et al., 2020). Our results are in line with what is commonly performed in many hilly areas of Italy where a duration of 3–4 years is envisaged, since after this period a strong decline is observed with impact on productive features (Parrini & Bonari, 2002), while some authors report a reduction in yield of lucerne that starts earlier, with a third year aboveground biomass higher in grass/legumes mixtures than in monoculture of lucerne (Dhakal & Anowarul Islam, 2018). Decrease of aboveground biomass with increasing fields age recorded in our trial follows almost the same pattern reported by Török et al. (2011). In our case, yield reduction is due to the replacement of lucerne by grasses that are not adequately supported by fertilization due to the very extensive management, as it is known that grasses have high requirements of N for maintaining a high productive level (Helgadóttir et al., 2018).

Evolution of forage quality in sown meadows is closely related to their botanical composition and high presence of weeds, that present lower nutritive value than sown species, produces a decrease of protein content (Reiné et al., 2020). Thus, changes in cover of lucerne or, in general, legumes along time affects nutritive value of the forage biomass (Movedi et al., 2019). Assessing pure stands of *Medicago sativa* with different proportion of grasses, Pacchioli & Ligabue (2013) found a reduction of 34% of crude protein and an increase of 15% of ADF in lucerne fields highly encroached by grasses compared to pure stands. These results are consistent with our findings and demonstrate the higher variation along time of crude protein content respect to fibre components, in particular cellulose and lignin included in ADF parameters. Anyway, presence of grasses inside a pure stand of lucerne can also play a positive role, for instance to reduce productive decline of this legume, due to higher persistency of grasses (Berzins et al., 2011) and to protect lucerne from low temperature (Aponte et al., 2019). Due to the different nutritional value of lucerne hay available over the years (Boob et al., 2019b), the different chemical composition, especially the lower content of crude protein and the

higher content of fibre fraction, should be properly evaluated, at least with rapid tools, in order to balance the diet intended for dairy cows (Parrini et al., 2022).

**Table 3.** Diversity indices in relation to age of fields. Values are means ± standard error

| | Age (years) of lucerne fields | | | |
|---|---|---|---|---|
| | 2 | 4 | 8 | 12 |
| Number of perennial species | $4.7 \pm 0.3^{b}$ | $5.3 \pm 0.3^{b}$ | $6.3 \pm 0.9^{b}$ | $10.0 \pm 1.1^{a}$ |
| Number of short lived species | $3.0 \pm 0.5^{ns}$ | $5.0 \pm 1.1^{ns}$ | $4.7 \pm 0.4^{ns}$ | $4.1 \pm 1.5^{ns}$ |
| Total richness | $7.7 \pm 0.6^{b}$ | $10.3 \pm 0.8^{ab}$ | $11.0 \pm 0.6^{ab}$ | $14.1 \pm 2.1^{a}$ |
| H' | $0.86 \pm 0.07^{b}$ | $1.60 \pm 0.07^{a}$ | $1.79 \pm 0.08^{a}$ | $1.89 \pm 0.22^{a}$ |
| Pielou index | $0.42 \pm 0.04^{b}$ | $0.69 \pm 0.01^{a}$ | $0.75 \pm 0.02^{a}$ | $0.72 \pm 0.07^{a}$ |

Values with the same letters are not significantly different according to Tukey test ($P < 0.05$); ns = not significant.

Studied diversity indices are reported in Table 3 in order to analyse the evolution of biodiversity as affected by naturalization development. Number of species in botanical samples increased significantly along time, ranging from an average of 7.7 species in two year old fields to 14.1 in oldest meadows. Notably, only the first value is significantly different from the last one. Species that perform natural recolonisation of lucerne fields are mainly perennial, with an average value of 10 species per sample at last data collection significantly different from previous ages. On the contrary, species number per sample of short lived species (*i.e.* annual or biennial) are not significantly different for all fields age. Concerning biodiversity, Shannon index is significantly lower in the youngest fields (2 years old) with respect to oldest and the same trend is observed for Pielou index. Thus, a constant naturalization of old lucerne fields can be recorded, with a very high rapidity of this process in the first years of development, confirming what was observed in terms of ground cover.

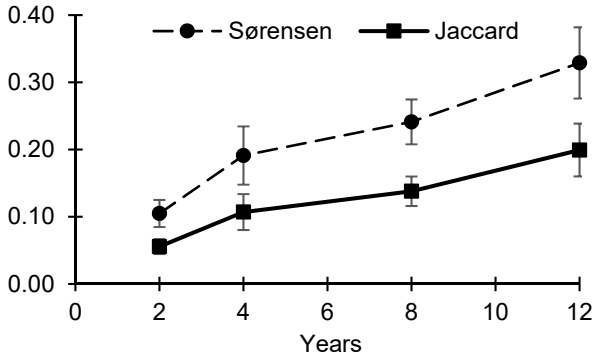


**Figure 4.** Evolution of similarity indices (Sørensen and Jaccard) of lucerne fields with reference grassland habitat (6510) according to different age. Bars represent standard errors.

Some characteristic species of the chosen reference grasslands were found in all different fields. Assessment of evolution of similarity among lucerne fields and reference plant community was performed by two different indices (Fig. 4). Both represented in the same way and with the same pattern the evolution towards the reference habitat composition, with a very reduced similarity in most recent fields (0.10 and 0.06 for

Sørensen and Jaccard respectively) with respect to oldest one (0.33 and 0.20). Also these parameters point out, by means of analysis of the slope of the regression line, a higher velocity of recovery in the first years of naturalisation.

Results are generally consistent with previous studies. Colonisation of native species are mainly represented, in terms of number, by perennial species as pointed out by Török et al. (2011). These authors state a possible recovery in roughly 10 years, even if other studies pointed out very different time to reach an almost stable vegetation composition (Fonseca & Ganade, 2001). Kelemen et al. (2017) observed that recent field are dominated by the sown crop (*Medicago sativa*) for its competitiveness in using available resources, and the other species are able to use other kind of resources occupying different ecological niches. Different factors are involved in the naturalization process, such as ordinary management of the grasslands or specific restoration techniques (Kiehl et al., 2010). Also, absence of soil tillage for many years, as occur in lucerne crop, can favor diversity and richness along time, mainly represented by development of perennial species that profited of absence of this kind of disturbance (Meiss et al., 2010). In absence of specific active intervention, anyway, secondary succession can lead in the long term to seminatural vegetation (Csecserits & Rédei, 2001), even if a factor that enhances naturalization process is the presence of spontaneous grasslands in the surroundings of the managed fields (Öster et al., 2009).

Comparison of species composition in different age fields and in the reference grassland by means of similarity indices allowed to evaluate that dissimilarity tends to reduce with increasing age. Török et al. (2010) found the same results in restoration interventions on previous lucerne fields ant this tendency was mainly due to changes in life forms (shift from short lived to perennials as reported before). It is anyway possible to have lower similarity performances in lucerne fields from 5 to 10 years old compared to reference grasslands (Török et al., 2011). Increasing biodiversity in old lucerne field along time, measured by means of Shannon index, was assessed by Kelemen et al. (2012), which considered this as a promising evolution towards a stable vegetation typical of seminatural grasslands for that investigated area. Yuan et al. (2015), on lucerne-rich stands in an arid environment, stated that time is the most important environmental factor affecting evolution of vegetation in these conditions.

## CONCLUSIONS

The study make available data concerning development of lucerne fields as consequence of age since sowing. Production and nutritive value were strongly affected by age, and this was mainly due to two different and contrasting processes: the lucerne innate self-thinning that produces a sharp decline of presence along time, and a natural recolonization of space left by sown crop that is occupied by native species, mainly represented by perennial species. This evolution is responsible of the naturalization process described that can recover, in the long time, the natural plant communities of the area. This development, pointed out also in several previous studies, can produce two distinct outcomes. In some conditions, it is possible to produce a lucerne renovation, at least with a one-year cereal species before a new lucerne stand, to enhance the productive services provided by this crop. In this case, a maximum duration of 4–5 years should be envisaged, in order to face productive and qualitative decline of lucerne fields. Eventual intensification with fertilization to maintain a high level of productive and qualitative

features in meadows enriched of grasses could be an option to prolong the duration of these sown resources. In other situations, where the agricultural activity is abandoned or highly reduced and where provision of other ecosystem services by grasslands is a priority, a recovery of local plant communities is possible through the naturalisation of the old fields left to colonization by autochthonous species of the surroundings. The destiny of this process is able to recover a stable plants community, even if the time of a definitive naturalisation is not certain, as it depends on many variables, such as environmental characteristics, mowing frequency and boundary management, and at least 10 years seem necessary. The development towards these reference habitats can anyway be improved and favoured by extensive management (reduced number of cutting, release of mulch biomass from mowing, etc.) or direct improvement utilising seeds from donor sites rich in target species, as suggested by some authors.

ACKNOWLEDGEMENTS. Authors acknowledge the Consortium 'Terre di Montagna' for Parmesan cheese production in mountain areas which funded the research. Our acknowledgements also to farmers that allowed our experimental activities.

## REFERENCES

AOAC, 2012. Official methods and analysis. Association of Official Analytical Chemists, 19th edition. Gaithersburg.

Aponte, A., Samarappuli, D. & Berti, M.T. 2019. Alfalfa–grass mixtures in comparison to grass and alfalfa monocultures. *Agronomy Journal* **111**(2), 628–638. doi: 10.2134/agronj2017.12.0753

Argenti, G., Parrini, S., Staglianò, N. & Bozzi, R. 2021. Evolution of production and forage quality in sown meadows of a mountain area inside Parmesan cheese consortium. *Agronomy Research* **19**(2), 344–356, 2021. doi: 10.15159/AR.21.061

Bassi, S., Bolpagni, R., Pezzi, G. & Pattuelli, M. 2015. *Habitat di interesse comunitario in Emilia-Romagna*. Regione Emilia-Romagna, Bologna, 292 pp.

Belanger, G., Castonguay, Y., Bertrand, A., Dhont, C., Rochette, P., Couture, L., Drapeau, R., Mongrain, D., Chalifour, F.P. & Michaud, R. 2006. Winter damage to perennial forage crops in eastern Canada: causes, mitigation, and prediction. *Canadian Journal of Plant Science* **86**, 33–47. doi:10.4141/P04-171

Bertrand, A., Bipfubusa, M., Claessens, A., Rocher, S. & Castonguay, Y. 2017. Effect of photoperiod prior to cold acclimation on freezing tolerance and carbohydrate metabolism in alfalfa (*Medicago sativa* L.). *Plant Science* **264**, 122–128. doi: 10.1016/j.plantsci.2017.09.003

Berzins, P., Rancane, S. & Svarta, A. 2011. The productive longevity of perennial grasses swards depending on the NPK fertilizer rates. In: *Proceedings of the 8th International Scientific and Practical Conference. Volume 11,* Rēzekne, pp. 244–251.

Boob, M., Truckses, B., Seither, M., Elsäßer, M., Thumm, U. & Lewandowski, I. 2019a. Management effects on botanical composition of species-rich meadows within the Natura 2000 network. *Biodiversity and Conservation* **28**(3), 729–750. doi: 10.1007/s10531-018-01689-1

Boob, M., Elsaesser, M., Thumm, U., Hartung, J. & Lewandowski, I. 2019b. Harvest time determines quality and usability of biomass from lowland hay meadows. *Agriculture* **9**(9), 198. doi: 10.3390/agriculture9090198

Burnett, V.F., Butler, K.L., Hirth, J.R., Mitchell, M.L., Clark, S.G. & Nie, Z. 2020. Lucerne (*Medicago sativa* L.) persistence remains unchanged under variable cutting regimes. *Agronomy* **10**(6), 844. doi: 10.3390/agronomy10060844

Chataigner, F., Surault, F., Huyghe, C. & Julier, B. 2010. Determination of botanical composition in multispecies forage mixtures by Near Infrared Reflectance Spectroscopy. In: Huyghe, C. (ed.): *Sustainable use of Genetic Diversity in Forage and Turf Breeding*. Springer, Dordrecht, 199–203. doi: 10.1007/978-90-481-8706-5-28

Csecserits, A. & Rédei, T. 2001. Secondary succession on sandy old-fields in Hungary. *Applied Vegetation Science* **4**(1), 63–74. doi: 10.1111/j.1654-109X.2001.tb00235.x

Dhakal, D. & Anowarul Islam, M. 2018. Grass-legume mixtures for improved soil health in cultivated agroecosystem. *Sustainability* **10**, 2718. doi: 10.3390/su10082718

Dibari, C., Argenti, G., Catolfi, F., Moriondo, M., Staglianò, N. & Bindi, M. 2015. Pastoral suitability driven by future climate change along the Apennines. *Italian Journal of Agronomy* **10**(3), 109–116. doi: 10.4081/ija.2015.659

Feng, D., Zongsuo, L., Xuexuan, X., Lun, S. & Xingchang, Z. 2007. Community biomass of abandoned farmland and its effects on soil nutrition in the Loess hilly region of Northern Shaanxi, China. *Acta Ecologica Sinica* **27**(5), 1673–1683. doi: 10.1016/S1872-2032(07)60038-9

Fonseca, C.R. & Ganade, G. 2001. Species functional redundancy, random extinctions and the stability of ecosystems. *Journal of Ecology* **89**, 118–125. doi: 10.1046/j.1365-45.2001.00528.x

Francone, C., Pagani, V., Foi, M., Cappelli, G. & Confalonieri, R. 2014. Comparison of leaf area index estimates by ceptometer and PocketLAI smart app in canopies with different structures. *Field Crops Research* **155**, 38–41. doi: 10.1016/j.fcr.2013.09.024

Gaujour, E., Amiaud, B., Mignolet, C. & Plantureux, S. 2012. Factors and processes affecting plant biodiversity in permanent grasslands. A review. *Agronomy for sustainable development* **32**(1), 133–160. doi: 10.1007/s13593-011-0015-3

Giustini, L., Acciaioli, A. & Argenti, G. 2007. Apparent balance of nitrogen and phosphorus in dairy farms in Mugello (Italy). *Italian Journal of Animal Science* **6**(2), 175–185. doi: 10.4081/ijas.2007.175

Głąb, T. & Gondek, K. 2013. The influence of soil compaction on chemical properties of mollic fluvisol soil under lucerne (*Medicago sativa* L.). *Polish Journal of Environmental Studies* **22**(1), 107–113.

Güsewell, S. & Edwards, P. 1999. Shading by *Phragmites australis*: a threat for species-rich fen meadows? *Applied Vegetation Science* **2**, 61–70. doi: 10.2307/1478882

Hakl, J., Kunzová, E., Tocauerová, Š., Menšík, L., Mrázková, M. & Pozdíšek, J. 2021. Impact of long-term manure and mineral fertilization on yield and nutritive value of lucerne (*Medicago sativa*) in relation to changes in canopy structure. *European Journal of Agronomy* **123**, 126219. doi: 10.1016/j.eja.2020.126219

Helgadóttir, Á., Suter, M., Gylfadóttir, T.Ó., Kristjánsdóttir, T.A. & Lüscher, A. 2018. Grass–legume mixtures sustain strong yield advantage over monocultures under cool maritime growing conditions over a period of 5 years, *Annals of Botany* **122**, 337–348. doi: 10.1093/aob/mcy074

Helm, A., Zobel, M., Moles, A.T., Szava-Kovats, R. & Pärtel, M. 2015. Characteristic and derived diversity: implementing the species pool concept to quantify conservation condition of habitats. *Diversity and Distributions* **21**(6), 711–721. doi: 10.1111/ddi.12285

IBM, 2020. IBM SPSS Statistics for Windows, Version 27.0. IBM Corp., Armonk, NY.

ISTAT, 2021. https://www.istat.it. Istituto Nazionale di Statistica. Accessed 16.11.2021.

Jáuregui, J.M., Mills, A., Black, D.B., Wigley, K., Ridgway, H.J. & Moot, D.J. 2019. Yield components of lucerne were affected by sowing dates and inoculation treatments. *European Journal of Agronomy* **103**, 1–12. doi: 10.1016/j.eja.2018.10.005

Kelemen, A., Török, P., Valkó, O., Albert, Á. & Tóthmérész, B. 2012. Spontaneous grassland recovery in extensively managed alfalfa fields. In: *8th European Conference on Ecological Restoration*. České Budějovice, pp. 1–4.

Kelemen, A., Tóthmérész, B., Valkó, O., Miglécz, T., Deák, B. & Török, P. 2017. New aspects of grassland recovery in old-fields revealed by trait-based analyses of perennial-crop-mediated succession. *Ecology and Evolution* **7**(7), 2432–2440. doi: 10.1002/ece3.2869

Kiehl, K., Kirmer, A., Donath, T.W., Rasranm, L. & Hölzel, N. 2010. Species introduction in restoration projects – evaluation of different techniques for the establishment of semi-natural grasslands in Central and Northwestern Europe. *Basic and Applied Ecology* **11**, 285–299. doi: 10.1016/j.baae.2009.09.002.

Lemaire, G. & Belanger, G. 2020. Allometries in plants as drivers of forage nutritive value: A review. *Agriculture* **10**(1), 5. doi: 10.3390/agriculture10010005.

Li, J.-H., Xu, D.-H. & Wang, G. 2008. Weed inhibition by sowing legume species in early succession of abandoned fields on Loess Plateau, China. *Acta Oecologica* **33**, 10–14. doi: 10.1016/j.actao.2007.07.001

Lovarelli, D., Bava, L., Zucali, M., D'Imporzano, G., Adani, F., Tamburini, A. & Sandrucci, A. 2019. Improvements to dairy farms for environmental sustainability in Grana Padano and Parmigiano Reggiano production systems. *Italian Journal of Animal Science* **18**(1), 1035–1048. doi: 0.1080/1828051X.2019.1611389

Magurran, A.E. 2004. *Measuring biological diversity*. Blackwell Publishing Company, Oxford, 266 pp.

Mancini, M. C., Arfini, F. & Guareschi, M. 2019. Innovation and typicality in localised agri-food systems: the case of PDO Parmigiano Reggiano. *British Food Journal* **121**(12), 3043–3061. doi: 0.1108/BFJ-10-2018-0662

Meiss, H., Mediene, S., Waldhardt, R., Caneill, J., Bretagnolle, V., Reboud, X. & Munier-Jolain, N. 2010. Perennial lucerne affects weed community trajectories in grain crop rotations. *Weed Research* **50**(4), 331–340. doi: 10.1111/j.1365-3180.2010.00784.x

Mikhailova, E.A., Bryant, R.B., Cherney, D.J.R., Post, C.J. & Vassenev, I.I. 2000. Botanical composition, soil and forage quality under different management regimes in Russian grasslands. *Agriculture, Ecosystems & Environment* **80**(3), 213–226. doi: 10.1016/S0167-8809(00)00148-1

Movedi, E., Bellocchi, G., Argenti, G., Paleari, L., Vesely, F., Staglianò, N., Dibari, C. & Confalonieri, R. 2019. Development of generic crop models for simulation of multi-species plant communities in mown grasslands. *Ecological Modelling* **401**, 111–128. doi: 10.1016/j.ecolmodel.2019.03.001

Öster, M., Ask, K., Römermann, C., Tackenberg, O. & Eriksson, O. 2009. Plant colonization of ex-arable fields from adjacent species-rich grasslands: the importance of dispersal vs. recruitment ability. *Agriculture, Ecosystems & Environment* **130**(3–4), 93–99. doi: 10.1016/j.agee.2008.12.005

Pacchioli, M.T. & Fattori, G. 2014. *Feed for dairy cows. Forage crops*. C.R.P.A., Reggio Emilia, 84 pp. (in Italian).

Pacchioli, M.T. & Ligabue, M. 2013. The most important aim for alfalfa is quality. *Informatore Agrario* **1**, 34–37 (in Italian).

Parrini, P. & Bonari, E. 2002. Erba medica (*Medicago sativa* L.). In: R. Baldoni & L. Giardini (eds) *Foraggere e tappeti erbosi*. Patron ed., Bologna, 83–118 (in Italian).

Parrini, S., Staglianò, N., Bozzi, R. & Argenti, G. 2022. Can Grassland Chemical Quality Be Quantified Using Transform Near-Infrared Spectroscopy? *Animals* **12**(1), 86. doi: 10.3390/ani1201008

Ponzetta, M.P., Cervasio, F., Crocetti, C., Messeri, A. & Argenti, G. 2010. Habitat improvements with wildlife purposes in a grazed area on the Apennine mountains. *Italian Journal of Agronomy* **5**, 233–238. doi: 10.4081/ija.2010.233

Pruchniewicz, D. 2017. Abandonment of traditionally managed mesic mountain meadows affects plant species composition and diversity. *Basic and Applied Ecology* **20**, 10–18. doi: 10.1016/j.baae.2017.01.006

Raduła, M.W., Szymura, T.H., Szymura, M., Swacha, G. & Kącki, Z. 2020. Effect of environmental gradients, habitat continuity and spatial structure on vascular plant species richness in semi-natural grasslands. *Agriculture, Ecosystems & Environment* **300**, 106974. doi: 10.1016/j.agee.2020.106974

Regione Emilia-Romagna, 2021. https://ambiente.regione.emilia-romagna.it. Accessed 25.11.2021.

Reiné, R., Ascaso, J. & Barrantes, O. 2020. Nutritional quality of plant species in Pyrenean hay meadows of high diversity. *Agronomy* **10**(6), 883. doi: 1 0.3390/agronomy10060883

Sheaffer, C.C., Evers, G.W. & Jungers, J.M. 2020. Cool-Season Legumes for Humid Areas. In: K. J. Moore et al. (eds). *Forage. The science of grassland agriculture*. 7th edition. John Wiley & Sons Ltd, Chichester, 263–296.

Soilgrids, 2022. https://soilgrids.org. Accessed 3.2.2022.

Štolcová, J. 2002. Secondary succession on an early abandoned field: vegetation composition and production of biomass. *Plant Protection Science* **38**, 149–154.

Ta, H.T., Teixeira, E.I., Brown, H.E. & Moot, D.J. 2020. Yield and quality changes in lucerne of different fall dormancy ratings under three defoliation regimes. *European Journal of Agronomy* **115**, 126012. doi: 10.1016/j.eja.2020.126012

Tabacco, E., Comino, L. & Borreani, G. 2018. Production efficiency, costs and environmental impacts of conventional and dynamic forage systems for dairy farms in Italy. *European Journal of Agronomy* **99**, 1–12. doi: 10.1016/j.eja.2018.06.004

Teixeira, E.I., Moot, D.J., Brown, H.E. & Fletcher, A.L. 2007. The dynamics of lucerne (Medicago sativa L.) yield components in response to defoliation frequency. *European Journal of Agronomy* **26**(4), 394–400. doi: 10.1016/j.eja.2006.12.00

Török, P., Deák, B., Vida, E., Valkó, O., Lengyel, S. & Tóthmérész, B. 2010. Restoring grassland biodiversity: sowing low-diversity seed mixtures can lead to rapid favourable changes. *Biological Conservation* **143**(3), 806–812. doi: 10.1016/j.biocon.2009.12.024

Török, P., Kelemen, A., Valko, O., Deak, B., Lukacs, B. & Tothmeresz, B. 2011. Lucerne-dominated fields recover native grass diversity without intensive management actions. *Journal of Applied Ecology* **48**(1), 257–264. doi: 10.1111/j.1365-2664.2010.01903.x

Török, P., Matus, G., Papp, M. & Tothmeresz, B. 2008. Secondary succession of overgrazed Pannonian sandy grasslands. *Preslia* **80**(1), 73–85.

Yuan, Z.Q., Yu, K.L., Wang, B.X., Zhang, W.Y., Zhang, X.L., Siddique, K.H., Stefanova, K., Turner, N.C. & Li, F.M. 2015. Cutting improves the productivity of lucerne-rich stands used in the revegetation of degraded arable land in a semi-arid environment. *Scientific reports* **5**(1), 12130. doi: 10.1038/srep12130

Wang, G., Liu, S., Liu, T., Fu, Z., Yu, J. & Xue, B. 2019. Modelling above-ground biomass based on vegetation indexes: a modified approach for biomass estimation in semi-arid grasslands. *International Journal of Remote Sensing* **40**(10), 3835–3854. doi: 10.1080/01431161.2018.1553319

*Supplementary material*

**Table A1.** ANOVA results for investigated parameters presented in Table 1 and 2

| Variable | Source of variation | DF | MS | F test value | *p*-value |
|---|---|---|---|---|---|
| *Medicago sativa* | Age | 3 | 3408.08 | 129.41 | < 0.001 |
| Perennial forbs | Age | 3 | 128.09 | 1.23 | 0.362 |
| Perennial graminoids | Age | 3 | 1676.52 | 9.96 | 0.004 |
| Short lived forbs | Age | 3 | 26.00 | 5.78 | 0.021 |
| Short lived graminoids | Age | 3 | 35.86 | 0.83 | 0.515 |
| Number of perennial species | Age | 3 | 16.97 | 9.69 | 0.005 |
| Number of short lived species | Age | 3 | 2.33 | 0.76 | 0.549 |
| Total richness | Age | 3 | 20.31 | 4.59 | 0.038 |
| H' | Age | 3 | 0.66 | 13.19 | 0.002 |
| Pielou index | Age | 3 | 0.67 | 10.13 | 0.004 |

*Agronomy Research* **20**(1), 40–55, 2022
https://doi.org/10.15159/AR.21.163

# Phosphate solubilization potential of indigenous rhizosphere fungi and their biofertilizer formulations

D.A. Balogun[1,2], M.A. Oke[3], L. Rocha-Meneses[4,5], OB. Fawole[6] and P.F. Omojasola[1,*]

[1]University of Ilorin, Faculty of Life Sciences, Department of Microbiology, 1515 Ilorin, Nigeria
[2]Nigerian Stored Products Research Institute, 1489 Ibadan, Nigeria
[3]Independent Researcher, Edmonton, AB, Canada. T5X 0H2.
[4]University of Sharjah, Research Institute of Sciences and Engineering, Center for Sustainable Energy and Power Systems Research, Biomass & Bioenergy Research Group, 27272 Sharjah, United Arab Emirates
[5]Estonian University of Life Sciences, Institute of Technology, Chair of Biosystems Engineering, Kreutzwaldi 56, EE51006 Tartu, Estonia
[6]University of Ilorin, Faculty of Agriculture, Department of Agronomy, 1515 Ilorin, Nigeria
[*]Correspondence: jasola@unilorin.edu.ng

Received: September 28th, 2021; Accepted: December 13th, 2021; Published: December 16th, 2021

**Abstract.** The harmful effects of chemical fertilizers on soil, plants, and eco-systems have stimulated the growth of the global biofertilizer market. However, biofertilizer use remains limited in developing countries due to inadequate research and poor technology. The use of readily available materials for biofertilizer production can be a good starting point. This study aimed to investigate phosphate-solubilizing potentials of soil fungi and the shelf-life of their biofertilizer formulations using sawdust and charcoal as carriers. Soil samples from the rhizosphere were cultured on Pikovskaya (PVK) agar, and the best phosphate solubilizers (*Aspergillus niger, Aspergillus fumigatus* and *A. flavus*) were screened for their phosphate-solubilization potentials on solid medium. Results obtained showed that *A. niger* had the highest solubilization index of 1.72, followed by *A. fumigatus,* and *A. flavus* with a solubilization index of 1.01 and 0.95, respectively. Optimization studies showed that after 5 days of incubation, *A. niger, A. flavus* and *A. fumigatus* solubilized 149, 112 and 126 mg $L^{-1}$ of phosphate, respectively. These values increased to 549 mg $L^{-1}$ on day 11 for *A. niger*, 379 mg $L^{-1}$ on day 9 for *A. flavus* and 430 mg $L^{-1}$ on day 9 for *A. fumigatus*. Furthermore, *A. fumigatus* and *A. flavus* proved to be better inoculants than *A. niger* as they maintained higher CFU $g^{-1}$ counts throughout the experiment. Also, sawdust supported higher counts of the three inoculants than charcoal and was thus the best carrier. The findings demonstrated that these aspergilli can be harnessed for improving soil fertility and plant development.

**Key words:** *A. niger, A. flavus, A. fumigatus,* biofertilizer, optimization, phosphate solubilization, shelf-life.

## INTRODUCTION

Phosphorus is the most vital element for the growth and development of plants after nitrogen. It carries out key roles in the growth of plants, and it is also the major plant growth limiting nutrient (Azubuike et al., 2016)). Plants naturally have abilities to obtain nutrients through the formation of beneficial relationships with microbes (Lema et al., 2012). However, they encounter different growth limiting factors throughout their lifecycle. They overcome these conditions through different natural processes such as development of ability to adapt to changes in their immediate environments, and by adopting alternative metabolic pathways. Plants face many obstacles during development and growth; one of such is their inefficient uptake of phosphate from soil due to the complex nature of phosphates present in the soil (Jones & Oburger, 2011). In addition to that, the low levels of phosphorus in the Earth crust further limit absorption. Hence, improving the absorption rate of phosphorus in the soil is a key issue in agriculture (Cordell et al., 2009).

Recently, there has been a significant rise in the use of fertilizers formulated using microorganisms (Nosheen et al., 2021). This has aided the race to minimize the deleterious effects of synthetic fertilizers on the environment and soil. Many studies revealed the potential role of microorganisms to solubilize phosphates. This includes mediating the bioavailability of soil phosphorus (Cong et al., 2020), aiding the mineralization of organic phosphates (Tate, 1984; Tamburini et al., 2012), solubilizing inorganic phosphate minerals into absorbable forms (Fixen & Johnston, 2012) and storing large amounts of phosphorous in biomass. Chen et al. (2006) reported that phosphorus-solubilizing microorganisms (PSMs) can secrete acids, which are of organic structure. These compounds then acidify the cellular components of microorganisms, leading to the solubilization of inorganically bound phosphates ($PO_4^-$ or $PO_4^{2-}$) by dissociating them from any metallic element they are bound to. Many microorganisms with phosphate- solubilization potential have been isolated from soil. The most common groups of organisms are those of fungal (*Penicillium* and *Aspergillus*) and bacterial origin (*Pseudomonas* and *Bacillus*) (Wakelin et al., 2004). Inoculation of soil with microbes to improve soil fertility began in the late 19$^{th}$ century when microbes were sold for the purpose of producing fertilizers (Kilian et al., 2000).

Dittmar et al. (2009) described fertilizers as naturally occurring or synthetically formulated substances, which when incorporated into plants or soil, provide vital nutrients for plant growth and development. The two main forms of fertilizers are synthetically- (chemical fertilizers) and non-synthetically (biofertilizers) formulated fertilizers. The continuous use of inorganic synthetic fertilizers over the years has helped to improve soil fertility and crop yield. However, the adverse effects that these fertilizers have posed on the ecosystem, plants, and soil is getting alarming in these past few years (Islam et al., 2017). Due to the degrading effects of chemical fertilizers on the environment, scientists have sought for safe alternatives, which are not lethal, non-synthetic, and cheap. This search led to the discovery of biofertilizers. One of the merits of using chemical fertilizers, particularly those of nitrogen and phosphorus origin, is their direct and swift action when applied to the soil. Also, chemical fertilizers are quite cheap, hence affordable to farmers of all kinds. However, overdependence on these chemicals

has led to deterioration in soil fertility, destruction of useful organisms in the soil (e.g., microbes and earthworms) and eutrophication, which has exposed plants to different diseases (Majumdar, 2015). More so, increased acidity due to the prolonged use of chemical fertilizers can cause accumulation of heavy metals in the soil (Dai et al., 2021). This can consequently limit the replication of beneficial bacteria and fungi.

Microorganisms are very important components of biofertilizers as their use can improve soil fertility and proliferation of beneficial bacteria and fungi. They are used as $N_2$ fixers (*Rhizobium, Bradyrhizobium, Azospirillum* and *Azotobacter*), phosphate solubilizers (*Bacillus, Pseudomonas, Aspergillus*, *Penicillium*, *Fusarium, Trichoderma*, *Mucor*, *Ovularopsis*, *Tritirachium* and *Candida*), and phosphate mobilizers (*Mycorrhiza*) are some of the biofertilizer inoculants commonly used (Pal et al., 2015). Besides the microbial inoculants, the inert carriers are also an important component of biofertilizers. They serve as protectants for the microbes, especially when the immediate environment (soil) is hostile, which helps the living inoculants to remain viable for a longer period in the soil (Chaudhary et al., 2020). Materials that have been employed as bioinoculant carriers include peat, clay, wood ash, grain protective coverings (brans and husks), natural and synthetic polymers, compost and alginate (Mitter et al., 2021; Sakpirom et al., 2021). In recent times, the use of nanoparticles has also gained increased attention (Chuen et al., 2021). However, considering the abundance of sawdust and the practice of charcoal production in developing countries where farmers depend on less advanced technologies, the use of these materials as bioinoculant carriers is an attractive option.

This study analyzed the phosphate-solubilizing potentials of three different fungi (*Aspergillus niger, Aspergillus fumigatus* and *A. flavus*) were analyzed. Soil samples from the rhizosphere were isolated, characterized, and cultured on growth medium in order to quantify the amount of phosphorus that they are capable of dissolving in both solid and liquid medium. In addition, optimization of incubation conditions was carried out to investigate the best conditions for phosphate solubilization in fungi. Finally, the phosphate-solubilizing isolates were incorporated into biofertilizers as living inoculants, then packed and stored to ascertain their viability using sawdust and charcoal as carriers.

## MATERIALS AND METHODS

### Sampling site and soil collection

Soil samples were taken from the University of Ilorin, Ilorin, Kwara State, Nigeria (Lat. 8.492819, Long. 4.596161) and from the Nigerian Stored Product Research Institute, Ilorin, Nigeria (Lat. 8.454472, Long. 4555397). The samples were obtained from the rhizosphere of palm tree, banana tree, mango tree, *Moringa* tree. The sample collection was carried out based on the method described by Xiao et al. (2008). For this, 20 g of soil was collected at 0–5 cm around the root of the plants. The soil was then bagged into separate sterile Ziploc bags and kept in the refrigerator (4 °C) until use. Granulated rock phosphate (30 g) was obtained from the laboratory of the Department of Agronomy, University of Ilorin, Ilorin, Nigeria. One hundred grams of fine powder of calcium phosphate used throughout the course of this study was also obtained from the same laboratory.

**Preparation of media**

The two media used for this study were Pikovskaya (PVK) agar and Potato Dextrose (PD) Agar. PVK medium was formulated using the method described by Elias et al. (2016). For this, 0.5 g of $(NH_4)_2SO_4$, 0.5 g of $MgSO_4.7H_2O$, 0.3 g of NaCl, 0.3 g of KCl, 0.03 g $FeSO_4.7H_2O$, 0.02 g of $MnSO_4.H_2O$, 10.0 g of $Ca_3(PO_4)_2$, 10 g glucose and 15 g agar were used. The PD agar was prepared based on the description provided by the manufacturer. The medium was homogenized using a magnetic stirrer and further autoclaved at 121 °C for 15 minutes. Pikovskaya agar was prepared by weighing its constituents into a 1,000 mL conical flask, then adding 1,000 mL of distilled water into the mixture, this was then gently shaken and heated on a magnetic stirrer for 20 minutes until the mixture is well homogenized and all the calcium deposits are completely dissolved, the mixture was then autoclaved at 121 °C for 15 minutes. Pikovskaya broth was prepared using the same method above but without adding agar.

**Isolation of rhizosphere fungi**

This was done using the pour plate method as described by Nelofer et al. (2016). Separate serial dilutions of each soil sample were prepared. One gram of soil sample was introduced into 9 mL of sterile distilled water shaken vigorously and serial dilutions of the resulting suspension were prepared in separate tubes containing similar amount of sterile distilled water. Aliquots (1 mL) of appropriate dilutions were then dispensed into molten PVK agar (at 45 °C) and swirled for even homogenisation. The plates were incubated at 27 °C for 3–5 days.

All the distinct colonies that grew on PVK agar and that had zone of clearance (halo) around them were aseptically subcultured and incubated at 27 °C for 3–4 days. This method was repeated until a pure isolate of each isolate was obtained. The pure cultures were then transferred into a sterile solid agar slant (PDA) and kept at 4 °C until use.

**Identification of isolates**

Identification of the isolates was using a combination of colonial-microscopic characteristics (Fawole & Oso, 2004) and molecular identification. Molecular identification was done by sequencing of the ITS gene of the best three isolates from the screening process. Extraction of the genomic DNA of the isolates was done using fungal DNA isolation kit 26200 (Norgen Biotek Corp., Canada). Amplification of the ITS region of the genome was done using PCR with the primers ITS4: 5–TCCTCCGCTTATTGATATGC-3 and ITS5: 5-GGAAGTAAAAGTCGTAACAAGG-3. The PCR mix contained 10× PCR buffer (1.0 µL), 25 mM $MgCl_2$ (1.0 µL), 5 pmol of forward and reverse primers (0.5 µL each), DMSO (1.0 µL), 2.5 mM DNTPs (0.8µL), Taq 5U $uL^{-1}$ (0.1 µL), 10 ng $\mu L^{-1}$ DNA (2.0 µL), and $H_2O$ (3.1 µL). The PCR reaction was run under the following conditions: initial denaturation was done for 5 min at 94 °C, followed by 30 sec denaturation at 94 °C; annealing was done at 54 °C for 35 sec, extension was at 72 °C for 45 sec (36 cycles), and final extension was at 72 °C for 7 min. Finally, the reaction was held under holding temperature of 10 C (∞). The PCR amplicon was then loaded on 1.5 % agarose gel using a 1 kbp plus ladder (Invitrogen). the estimated size of the amplicon was 850 bp. The product was purified and sequenced using the ABI genetic analyzer model 3500 automated sequencer (Applied Biosystems, USA). Obtained sequences were identified based on homology with the highest similarity using the BLASTN tool (www.ncbi.nlm.nih.gov:80/BLASTN/).

**Screening for phosphate solubilization potentials on agar medium (PVK agar)**

The isolates previously grown on PVK agar were screened to quantify the amount of phosphate solubilized in the solid medium. This was done by aseptically transferring fungal isolates from stock cultures into PVK agar. The samples were then incubated at 28 °C for 4 to 7 days. The diameter of halo formed was measured using a ruler and used to calculate the solubilization index (Equation 1), as described by Saxena et al. (2013):

$$\text{Solubilization Index (SI)} = \frac{\text{Colony diameter + Halo zone diameter}}{\text{Colony diameter}} \quad (1)$$

**Preparation of fungal inocula**

The isolates were cultivated on PD agar and incubated at a temperature of 27 °C for 7 days. An aliquot of 10 mL of sterile distilled water was then measured into each of the culture plates. The plates were swirled gently to dislodge conidia from the culture surface. The dislodged conidia suspensions were then collected in 250 mL conical flasks and filtered through a few layers of cheesecloth and then centrifuged. The resulting pellet was re-suspended in sterile distilled water and the concentration of conidia was adjusted to $1.0\times10^8$ CFU $mL^{-1}$ using a Neuber haemocytometer (Niranjana et al., 2009; Mahadevamurthy et al., 2016).

**Estimation and quantification of solubilized phosphate in liquid medium**

Sterile PVK medium of 100 mL volume was prepared in 250 mL flask and was supplemented with either 0.5% calcium phosphate (CaP) or rock phosphate (RP). The pH of the medium was adjusted to 7.0 with 2 M NaOH or $H_2SO_4$. The sterilized PVK medium was inoculated with a $1.010^8$ CFU $mL^{-1}$ spore suspension of each isolate and incubated in a shaker at 150 rpm and 27 °C. The incubation was done in triplicate for each isolate and their results were recorded as average values (Elias et al., 2016). The amount of solubilized phosphorous and the decrease in pH were measured every 24 hours for 4 days. This was done by aseptically collecting 5 mL of culture broth and centrifuging it at 5,000 rpm for 10 minutes to separate suspended solids and mycelial fragments. The pH of the supernatant was then measured, and the amount of solubilized phosphate was quantified. Aliquots of the medium were taken every 24 hours and quantified for dissolved phosphate using the chlorostannous acid reduced molybdophosphoric blue colour method (Naik et al., 2013).

**Determination of pH in the liquid medium**

Changes in pH of the medium were measured with a pHep® Hanna pH meter using 5 mL samples collected every 24 hours.

**Optimization of phosphate solubilization**

The optimization of the growth conditions for phosphate solubilizing fungi was done by the method described by Yadav & Tarafdar (2003). A spore concentration of $1.0\times10^8$ cells per mL was inoculated into sterile PVK broth medium. The pH of the medium (before inoculation) was adjusted to 7 using 2 M NaOH or $H_2SO_4$. Incubation was carried out in a shaker at 150 rpm and 27 °C. Aliquots of the medium were taken every 24 hours and assayed for dissolved phosphate using the chlorostannous acid

reduced molybdophosphoric blue colour method. This was done continuously until a decline in phosphate levels was observed.

The phosphate solubilization capacity of the fungal isolates at varying concentrations of metallic phosphate was analyzed by incubating each isolate in Pikovskaya Broth medium which was supplemented with two phosphates sources *viz*. CaP or RP at the following concentrations: 1.5, 2.5, 5.0, 7.5, and 10 g $L^{-1}$. This was done by replacing the original CaP used in the formulation of PVK medium with varying quantities of CaP or RP.

Phosphate solubilization capacity at different initial medium pH was investigated by varying the pH of the Pikovskaya broth medium between 5 and 9 t. The flasks were incubated at 27 °C for 96 hours and changes in pH were recorded accordingly.

The effect of inoculum size on phosphate solubilization was studied by using varying concentrations of the spore suspension ranging from 0.5–2.0×$10^6$ spores $mL^{-1}$ (Niranjana et al., 2009 and Mahadevamurthy et al., 2016).

**Biofertilizer Formulations**

The biofertilizer formulations were prepared based on the method described by Bhattacharjee & Dey (2014). Here, fungal isolates were grown on PDA and when sporulation was noticed (after 7 days) 9 mL of sterile distilled water was added to the agar plates and shaken until the spores became dislodged. The displaced spores were collected in a sterile conical flask, filtered through cheesecloth, and then centrifuged. The recovered spores were adjusted to 1.0×$10^8$ CFU $mL^{-1}$ with the aid of a haemocytometer as described by Niranjana et al. (2009) and Mahadevamurthy et al. (2016). Fungal spores (9 mL) were then inoculated into 300 mL of sterile potato dextrose broth. A mass of 1 kg of sterilized carrier material (charcoal or sawdust) was then introduced into the mixture and blended. The mixture was allowed to dry at 27 °C. After drying, it was packed in Ziplock bags and saved at room temperature until use.

**Statistical Analysis**

Statistical significance was determined using one-way and two-way analysis of variance (ANOVA), while multiple comparisons between means were determined by Tukey's multiple comparisons test. All data were expressed as means of triplicates ± standard deviation, and values of $p < 0.05$ were considered significant.

## RESULTS AND DISCUSSION

**Characterization of the phosphate-solubilizing fungi (PSF)**

Three fungal isolates (*A. niger, A. flavus*, and *A. fumigatus)* were used in this study to investigate the potential of solubilizing phosphate in both solid and liquid medium. Fig. 1 shows the microscopic view of the three isolates utilized in this study. Hefnawy et al. (2009) reported that these fungal isolates are capable of solubilizing high quantities of phosphate even under low nutrient conditions.

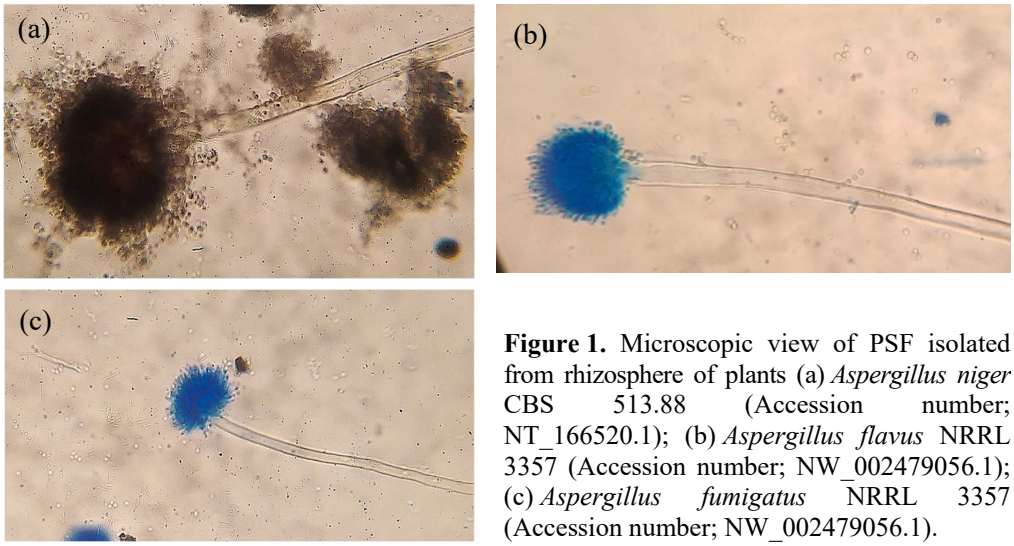


**Figure 1.** Microscopic view of PSF isolated from rhizosphere of plants (a) *Aspergillus niger* CBS 513.88 (Accession number; NT_166520.1); (b) *Aspergillus flavus* NRRL 3357 (Accession number; NW_002479056.1); (c) *Aspergillus fumigatus* NRRL 3357 (Accession number; NW_002479056.1).

**Solubilization index of the phosphate solubilizing fungi**

The amount of phosphate solubilized by *A. niger, A. flavus* and *A. fumigatus* on a solid medium (PVK agar) supplemented with calcium phosphate is reported in Fig. 2. As it can be seen from the figure, *A. niger* had the highest solubilization index (1.72 SI), followed by *A. fumigatus* (1.01 SI), and *A. flavus* (0.95 SI).

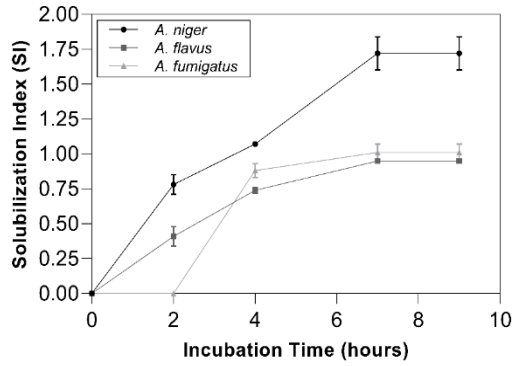


**Figure 2.** Solubilization Index of the three isolates on PVK agar after 9 days of incubation. Values are means of 3 replicates and error bars represent standard deviation.

The high performance of *A. niger* can be explained by the fact that this isolate produces organic acids that are highly ionizable and that can cause the solubilization of calcium phosphate compounds (Pradhan & Sukla, 2005). Additional studies performed by Yasser et al. (2014) and Seshadri et al. (2004) showed that *A. niger* solubilizes high quantities of phosphates from calcium phosphate supplements. These results can also be explained by the halo zone. A study performed by Hefnawy et al. (2009) has shown that *A. niger* formed a wider halo zone on Pikovskaya agar when supplemented with calcium phosphate than *A. flavus and A. fumigatus*. However, the same study reported that *A. fumigatus* had a higher phosphate solubilization index than *A. flavus*.

**Effect of different pH levels on solubilized phosphate**

The effect of different pH values (pH 5 to pH9) on the phosphate solubilization potential of the fungal isolates is shown in Fig. 3. The effects of different pH values (pH

to pH 9) on the solubilized phosphate 5quantities by the isolated fungi is shown in Fig. 3. From the results, overall, the pH of the liquid medium plays a vital role in the amount of phosphate solubilized, it was observed that pH 7 proved to be the best for phosphate solubilization, followed by acidic pH, while alkaline pH caused the least phosphate solubilization among all the 3 isolates. Ordinarily, an acidic pH should cause more phosphate solubilization because of the presence acids that could help ionize locked phosphates, however, fungi species of the *Aspergillus* genera grow best under neutral pH conditions than under low or high pH hence tends to solubilize more phosphate under neutral conditions.

Overall, the pH of the incubation process plays a vital role in the amount of solubilized phosphate generated. All the isolates had the maximum solubilized phosphate at pH 7, and the minimum at pH 9, except for *A. fumigatus*. These results can be explained by the fact that the *Aspergillus* genera can grow in a wide pH range, but the optimum growth is found at pH 7 (Wheeler et al., 1991). Other studies performed by Wu et al. (2012) and Anitha & Padma (2016) also reported pH 7 as the most favorable for solubilized phosphate production by fungal isolates.

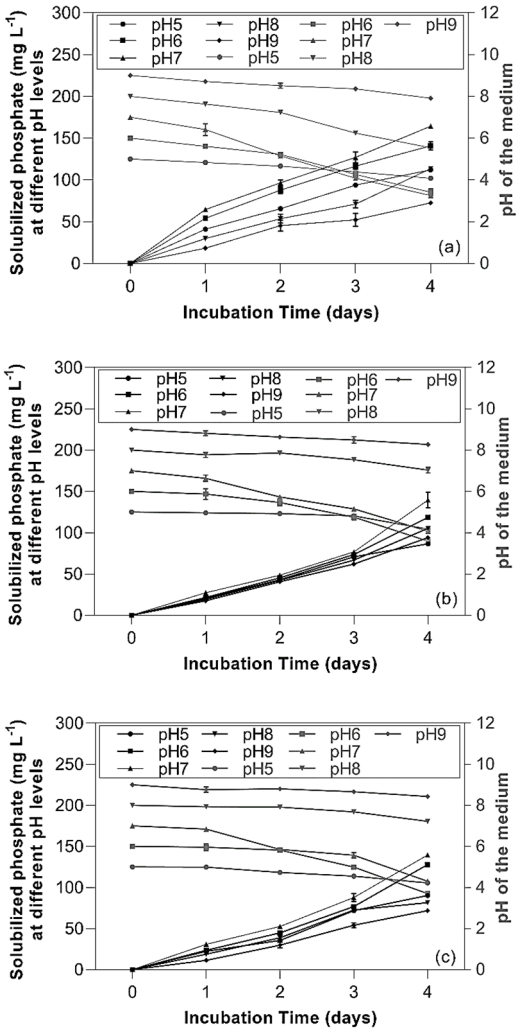


**Figure 3.** Effect of different pH levels on solubilized phosphate (a) *A. niger;* (b) *A. flavus*; (c) *A. fumigatus.* Values are means of 3 replicates and error bars represent standard deviation.

**Effect of different phosphate sources on phosphate solubilization**

The effect of different calcium phosphate concentrations on solubilized phosphate are reported in Fig. 4. For *A. niger*, the phosphate solubilization was higher for samples with a calcium phosphate concentration of 7.5 g $L^{-1}$, followed by samples with a concentration of 5.0 g $L^{-1}$, 2.5 g $L^{-1}$, 1.45 g $L^{-1}$, and 10 g $L^{-1}$. When it comes to *A. flavus* and *A. fumigatus,* both organisms had a similar performance. Samples with calcium phosphate concentration of 5 g $L^{-1}$ had the highest amount of solubilized phosphate (between 148 and 152 mg $L^{-1}$), and samples with calcium phosphate concentration of 10 g $L^{-1}$ had the lowest *amount* of solubilized phosphate (between 54 and 82 mg $L^{-1}$).

The effect of different rock phosphate concentration on the amount of solubilized phosphate is shown in Fig. 5. For *A. niger*, the highest (178 mg $L^{-1}$) and lowest (94 mg $L^{-1}$) amount of solubilized phosphate was achieved when the rock phosphate concentration was 5 g $L^{-1}$, and 10 g $L^{-1}$, respectively. For *A. flavus* and *A. fumigatus*, the maximum amount of solubilized phosphate (158–169 mg $L^{-1}$) was reported when the rock phosphate concentration was 7.5 g $L^{-1}$, and the minimum amount (34–60 mg $L^{-1}$) when the rock phosphate was 2.5 g $L^{-1}$.

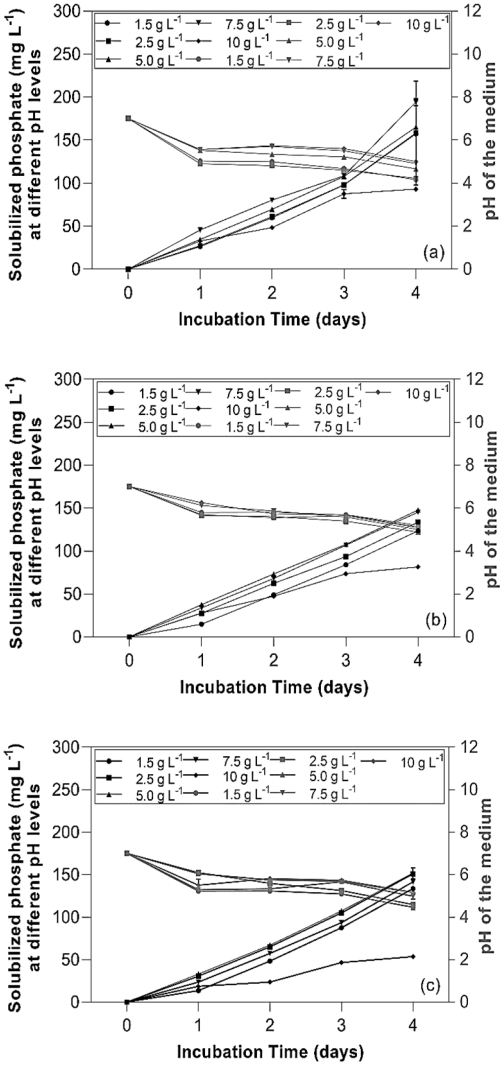


**Figure 4.** Effect of different concentrations of calcium phosphate on solubilized phosphate (a) *A. niger;* (b) *A. flavus;* (c) *A. fumigatus.* Error bars represent standard deviation of triplicate samples.

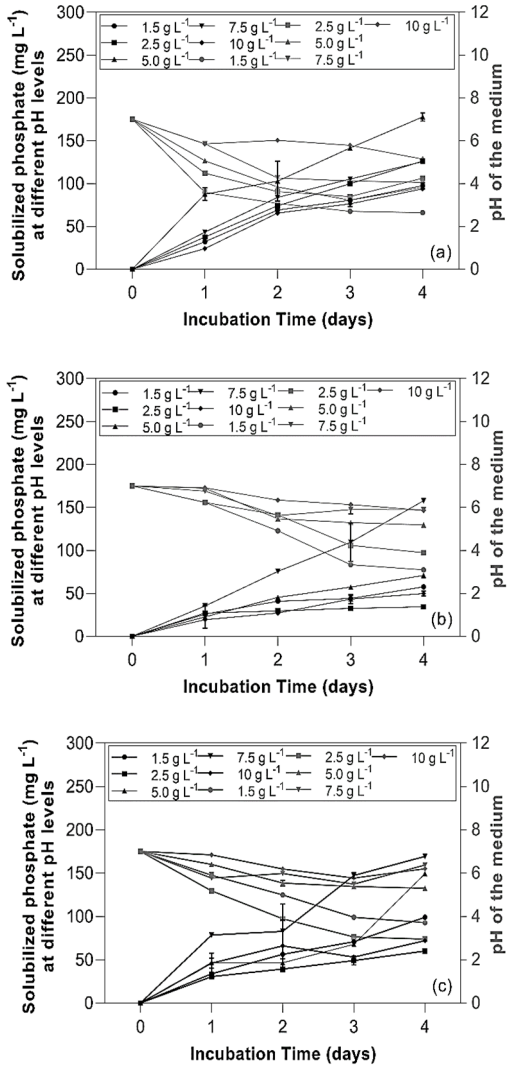


**Figure 5.** Effect of different concentrations of rock phosphate on solubilized phosphate (a) *A. niger;* (b) *A. flavus;* (c) *A. fumigatus.* Error bars represent standard deviation of triplicate samples.

In this section, two different sources of phosphate (calcium and rock phosphate) were used to investigate changes in the amounts of solubilized phosphate. Overall, the utilization of calcium phosphate has led to the highest solubilized phosphate yield, when compared to rock phosphate. This may be due to the complex nature of the atoms and compounds that comprise rock phosphate (Moawad et al. 1996 and Mahamuni et al., 2012). Pradhan & Sukla (2005) and Mahamuni et al. (2012) reported that one of the reasons why rock phosphate does not solubilize easily is because of the presence of strong apatite bonds in its molecules. These bonds make it hard for other compounds to bond to rock phosphate. Also, from our observations, *A. niger* solubilized phosphates more efficiently than *A. flavus* when calcium phosphate was used to supplement the growth medium. Similar findings were reported by Das et al., 2013.

**Effect of inoculum size on phosphate solubilization**

The effect of inoculum size on solubilized phosphate is presented in Fig. 6. For all the isolates (*A. niger, A. flavus,* and *A. fumigatus*) the highest amount of solubilized phosphate (188–234 mg $L^{-1}$) was obtained for samples with an inoculum size of $2.0\times10^6$ CFU $mL^{-1}$, while the lowest amount of solubilized phosphate (122–128 mg $L^{-1}$) was achieved for samples with an inoculum size of $0.5\times10^6$ CFU $mL^{-1}$.

These results show that the inoculum size of the isolates affects the amount of solubilized phosphate. Higher inoculum sizes shorten the time required for the phosphate solubilization, and also led to a high rate of phosphate solubilization. This is due to the higher proliferation of mycelia and increased activity of the associated enzymes at higher spore concentrations of the inoculum. The best inoculum size was at $2.0\times10^6$ CFU $mL^{-1}$ for all the isolates and the trend for phosphate solubilization efficiency was *A. niger*, followed by *A. flavus*, and *A. fumigatus*.

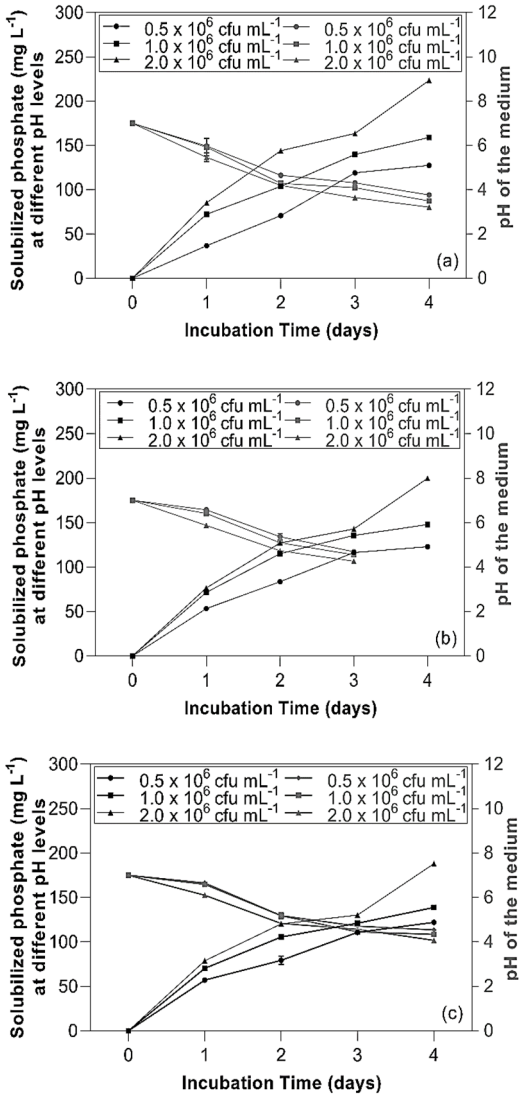


**Figure 6.** Effects of different inoculum size on the solubilized phosphate of (a) *A. niger;* (b) *A. flavus* (c) *A. fumigatus.* Error bars represent standard deviation of triplicate samples.

**Effect of optimization on phosphate solubilization and fungal count**

A pre-optimization study was carried out to quantify the phosphate solubilized by the three fungal isolates under normal conditions. The results obtained from the pre-optimization process were further compared with those obtained under optimized conditions. The results from the optimization process were then applied during the cultivation of the strain.

Fig. 7 (a) shows the effect of the optimization of incubation conditions on the (phosphate solubilization potential) PSP of PSF. Overall, unoptimized samples had the lowest amount of solubilized phosphate (78–100 mg $L^{-1}$), while optimized samples had the highest amounts (293–517 mg $L^{-1}$). For pre-optimized samples after 24 hours of incubation, *A. flavus* had solubilized 25 mg $L^{-1}$, *A. fumigatus* 32 mg $L^{-1}$, and *A. niger* 62 mg $L^{-1}$, while for optimized samples after 24 hours of incubation, *A. flavus* had solubilized 9 mg $L^{-1}$, *A. fumigatus* 84 mg $L^{-1}$, and *A. niger* 77 mg $L^{-1}$. For *A. niger*, the results obtained from the optimization studies showed that phosphate solubilization continued incrementally until the 11$^{th}$ day of incubation. When *A. flavus* and *A. fumigatus* were used, there was also an increase in the phosphate solubilization, but only until day 9. There was a wide gap in the amount of phosphate solubilized by the three isolates at pre-optimization and optimization stages, with significantly higher solubilization being recorded under optimized conditions. This underscores the importance of using optimal growth and culture conditions for phosphate solubilization. Previous studies similarly demonstrated that the use of optimal levels of pH, temperature, agitation and nutrients promoted maximum phosphate solubilization (Behera et al., 2017a; Behera et al., 2017b).

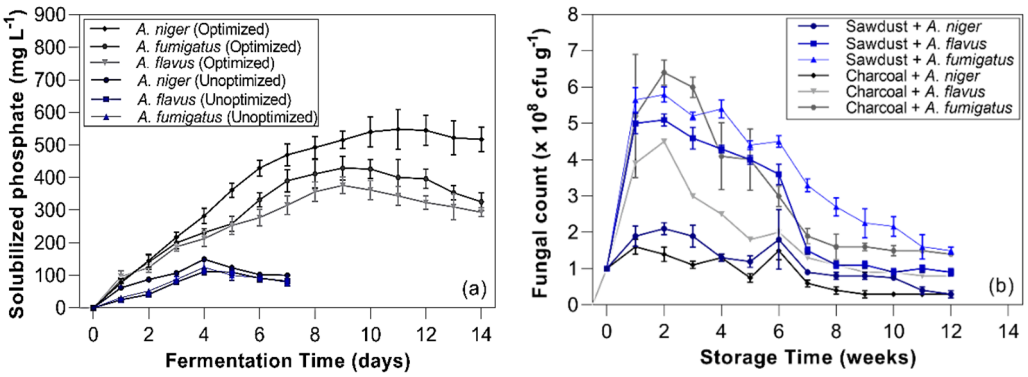


**Figure 7.** Effects of (a) optimization of incubation conditions on phosphate solubilization; (b) storage time on the viability of phosphate solubilizing fungi. Error bars represent standard deviation of triplicate samples.

The influence of storage time on the viability of fungal isolates of phosphate solubilizing potentials is reported in Fig. 7(b). As it can be seen from the figure, after 12 weeks of storage *A. fumigatus* had the highest fungal count with $1.0\times10^8$ CFU $g^{-1}$ on sawdust and $1.4\times10^8$ CFU $g^{-1}$ on charcoal. Next was *A. flavus* with $0.9\times10^8$ CFU $g^{-1}$ on sawdust and $0.8\times10^8$ CFU $g^{-1}$ on charcoal. The least count was recorded for *A. niger* with a count of $0.3\times10^8$ CFU $g^{-1}$ on both charcoal and sawdust.

Similar results on the phosphate solubilization of *A. niger*, *A. fumigatus,* and *A. flavus* were reported by Kooliyottil et al. (2013). The authors concluded that *A. niger* solubilized higher amounts of phosphate when compared to *A. fumigatus* and *A. flavus.* In the same study, the authors showed that *A. fumigatus* has a higher solubilization potential when compared to *A. flavus.* However, this observation was not in line with the results obtained in our study since *A. flavus* solubilized more phosphate than *A. fumigatus*. Chang & Yang (2009) reported that *A. fumigatus* had a phosphate solubilizing potential of 113 mg $L^{-1}$ after 7 days of incubation. In our study, the same isolate solubilized 125 mg $L^{-1}$ of phosphate only after 4 days of incubation under unoptimized conditions, and 429 mg $L^{-1}$ after 9 days of incubation under optimized conditions. A study by Das et al. (2013) found that *A. niger* and *A. flavus* solubilized 121 mg $L^{-1}$ and 91 mg $L^{-1}$ of phosphate, respectively after 14 days of incubation. However, in our study both isolates solubilized higher quantities in the same time interval. These differences can be explained by the natural tendency of strains of the same species originating from different sources to behave differently. Furthermore, the soils used in these studies were obtained from different climates, which may have different effects on the metabolism of these strains (Jain et al., 2014).

**Effect of storage time and carrier material on the viability of biofertilizer inoculants**

The influence of storage time on the viability of biofertilizer inoculants is reported in Table 1. After 8 weeks of storage, A. *fumigatus* stored with sawdust carrier had the highest fungal count ($2.4\times10^8$ CFU $g^{-1}$) and *A. niger* stored with charcoal carrier had the least fungal count ($0.4\times10^8$ CFU $g^{-1}$). Generally, it was observed that the best and most stable biofertilizer inoculant was *A. fumigatus* as it maintained relatively higher counts in both carrier materials throughout the study period compared to the other inoculants. On the other hand, *A. niger* appeared to be the least favourable as it had the least counts throughout. This may be due to the relatively higher growth rate of the other two strains.

**Table 1.** Total fungal counts ($\times10^8$ CFU $g^{-1}$) of biofertilizers formulated with different carriers during storage at 27 °C

| Time | *A. niger* | | *A. flavus* | | *A. fumigatus* | |
|---|---|---|---|---|---|---|
| (weeks) | sawdust | charcoal | sawdust | charcoal | sawdust | charcoal |
| 1 | $1.9 \pm 0.2^a$ | $1.6 \pm 0.5^a$ | $5.0 \pm 0.4^a$ | $3.7 \pm 0.8^a$ | $5.5 \pm 0.4^a$ | $5.0 \pm 0.6^a$ |
| 2 | $2.1 \pm 0.4^a$ | $1.4 \pm 0.2^b$ | $5.0 \pm 0.1^a$ | $4.3 \pm 0.5^a$ | $5.7 \pm 0.8^a$ | $6.2 \pm 0.3^a$ |
| 3 | $1.9 \pm 0.2^a$ | $1.1 \pm 0.2^b$ | $4.9 \pm 0.3^a$ | $3.3 \pm 0.7^b$ | $5.2 \pm 0.5^a$ | $5.9 \pm 0.2^a$ |
| 4 | $1.3 \pm 0.2^a$ | $1.3 \pm 0.4^a$ | $4.5 \pm 0.4^a$ | $2.3 \pm 0.4^b$ | $5.4 \pm 0.6^a$ | $4.4 \pm 0.3^b$ |
| 5 | $1.2 \pm 0.2^a$ | $0.8 \pm 0.3^a$ | $4.1 \pm 0.2^a$ | $1.8 \pm 0.2^b$ | $4.6 \pm 0.4^a$ | $4.2 \pm 0.6^a$ |
| 6 | $1.7 \pm 0.4^a$ | $1.3 \pm 0.7^a$ | $3.6 \pm 0.6^a$ | $1.7 \pm 0.4^b$ | $4.8 \pm 0.2^a$ | $3.3 \pm 0.7^b$ |
| 7 | $0.9 \pm 0.3^a$ | $0.6 \pm 0.1^a$ | $1.8 \pm 0.2^a$ | $1.3 \pm 0.1^b$ | $3.4 \pm 0.6^a$ | $1.9 \pm 0.3^b$ |
| 8 | $0.9 \pm 0.2^a$ | $0.4 \pm 0.2^b$ | $1.2 \pm 0.2^a$ | $1.1 \pm 0.1^a$ | $2.8 \pm 0.2^a$ | $1.4 \pm 0.3^b$ |

[a,b] Fungal counts of the same bioinoculant on the same row having the same subscripts are not significantly different (*t*-test, $p > 0.05$).

Also, it was observed that the sawdust carrier supported the fungal inoculants better than charcoal as the fungal counts of inoculants in the sawdust carrier were higher than those in charcoal carrier, especially in the final weeks of storage where the difference in counts between the two carriers was significant ($p < 0.05$) (Table 1). This can be

attributed to the fact that sawdust is a cellulolytic material, which serves as a nutrient source for the fungal inoculants. Furthermore, it can help improve porosity and help retain water (Lin et al., 2021). On the contrary, charcoal that contains low or no nutrient. Mahdi et al. (2010) reported that biofertilizer inoculants can only be viable for 6 months. However, the result from this showed that all the isolates started to lose viability after the eighth week of storage. This variation may be due to the different carriers, available nutrients, soil moisture levels and the microbial strains used in this study.

## CONCLUSION

This study investigated the phosphate solubilizing potentials of three fungi from the genus *Aspergillus* (*A. niger, A. flavus,* and *A. fumigatus*). The results obtained show that *A. niger* had the highest solubilization index while *A. flavus* had the lowest. Optimization experiments showed that after 5 days of incubation *A. niger* was able to solubilize the highest amount of phosphate, while *A. flavus* solubilized the lowest. Overall, *A. niger, A. flavus,* and *A. fumigatus* have great potential for phosphate solubilization. Sawdust performed better as a carrier for all the inoculants and is thus recommended as a carrier of choice. These fungal isolates can be further converted into biofertilizers and used as a replacement for conventional chemical fertilizers. This will help to reduce environmental impacts and load caused by synthetic fertilizers in the soil, plants, and water bodies. Since phosphorus is an essential source of nutrients and is the least mobile nutrient available to plants, phosphate solubilizing fungi (*A. niger, A. fumigatus* and *A. flavus*) are recommended to be inoculated into the soil using sawdust as the carrier. This will help to dissolve phosphates that are locked up in the soil by converting them into soluble forms that can be utilized and absorbed by the plant roots.

## REFERENCES


Anitha, S. & Devi, S.N. 2016. Efficiency of Aspergillus terreus to solubilize insoluble form of phosphorus into soluble form under various cultural conditions. *International Journal of Pharma and Bio Sciences* **7**(1), 120–126.

Azubuike, C.C., Chikere, C.B. & Okpokwasili, G.C. 2016. Bioremediation techniques-classification based on site of application: principles, advantages, limitations and prospects. *World Journal of Microbiology and Biotechnology* **32**(11), 180. doi: 10.1007/s11274-016-2137-x

Behera, B.C., Yadav, H., Singh, S.K., Mishra, R.R., Sethi, B.K., Dutta, S.K. & Thatoi, H.N. 2017a. Phosphate solubilization and acid phosphatase activity of Serratia sp. isolated from mangrove soil of Mahanadi river delta, Odisha, India. *Journal of Genetic Engineering and Biotechnology* **15**(1), 169–178. doi: https://doi.org/10.1016/j.jgeb.2017.01.003

Behera, B.C., Yadav, H., Singh, S.K., Sethi, B.K., Mishra, R.R., Kumari, S. & Thatoi, H. 2017. Alkaline phosphatase activity of a phosphate solubilizing Alcaligenes faecalis, isolated from mangrove soil. *Biotechnology Research and Innovation* **1**(1), 101–111. doi: https://doi.org/10.1016/j.biori.2017.01.003

Bhattacharjee, R. & Dey, U.K. 2014. Biofertilizer, a way towards organic agriculture: A review. *African Journal of Microbiology Research* **8**, 2332–2343.

Chang, C.H. & Yang, S.S. 2009. Thermo-tolerant phosphate-solubilizing microbes for multi-functional biofertilizer preparation. *Bioresource Technology* **100**(4), 1648–1658. doi: 10.1016/j.biortech.2008.09.009

Chaudhary, T., Dixit, M., Gera, R., Shukla, A.K., Prakash, A., Gupta, G. & Shukla, P. 2020. Techniques for improving formulations of bioinoculants. *3 Biotech* **10**(5), 199. doi: 10.1007/s13205-020-02182-9

Chen, Y.P., Rekha, P.D., Arun, A.B., Shen, F.T., Lai, W.A. & Young, C.C. 2006. Phosphate solubilizing bacteria from subtropical soil and their tricalcium phosphate solubilizing abilities. *Applied Soil Ecology* **34**(1), 33–41. doi: https://doi.org/10.1016/j.apsoil.2005.12.002

Chuen, N.L., Ghazali, M.S.M., Hassim, M.F.N., Bhat, R. & Ahmad, A. 2021. Chapter 43 - Agro-waste-derived silica nanoparticles (Si-NPs) as biofertilizer. In Bhat, R. (eds), *Valorization of Agri-Food Wastes and By-Products*. Academic Press, London, 881–897. doi:https://doi.org/10.1016/B978-0-12-824044-1.00029-5

Cong, W.-F., Suriyagoda, L.D.B. & Lambers, H. 2020. Tightening the phosphorus cycle through phosphorus-efficient crop genotypes. *Trends in Plant Science* **25**(10), 967–975. doi: https://doi.org/10.1016/j.tplants.2020.04.013

Cordell, D., Drangert, J.-O. & White, S. 2009. The story of phosphorus: Global food security and food for thought. *Global Environmental Change* **19**(2), 292–305. doi: https://doi.org/10.1016/j.gloenvcha.2008.10.009

Dai, P., Cong, P., Wang, P., Dong, J., Dong, Z. & Song, W. 2021. Alleviating soil acidification and increasing the organic carbon pool by long-term organic fertilizer on tobacco planting soil. *Agronomy* **11**(11), 2135. doi: https://doi.org/10.3390/agronomy11112135

Das, A., Dutta, B.K. & Barooah, A.K.. 2013. In vitro solubilization of inorganic phosphate by phosphate solubilizing fungi isolated from tea agroecosystem soil of Barak Valley, Southern Assam. *International Journal of Microbiological Research,* **4**(3), 336–341.

Dittmar, H., Drach, M., Vosskamp, R., Trenkel, M.E., Gutser, R. & Steffens, G. 2009. Fertilizers, 2. Types. In Ullmann, F. (eds), *Ullmann's Encyclopedia of Industrial Chemistry*. Wiley-VCH, New York. doi:https://doi.org/10.1002/14356007.n10_n01

Elias, F., Muleta, D. & Woyessa, D. 2016. Effects of phosphate solubilizing fungi on growth and yield of haricot bean (phaseolus vulgaris l.) Plants. *Journal of Agricultural Science* **8**, 204. doi: 10.5539/jas.v8n10p204

Fawole, M.O. & Oso, B.A. 2004. *Laboratory Manual of Microbiology* (4th ed.). Spectrum Books Ltd, Ibadan. Owerri, pp. 71–81.

Fixen, P.E. & Johnston, A.M. 2012. World fertilizer nutrient reserves: a view to the future. *J. Sci. Food Agric.* **92**(5), 1001–1005. doi: 10.1002/jsfa.4532

Hefnawy, M.A., Gharieb, M.M., Eissa, O.A. & Ammar., A.M. 2009. Evaluation and optimization of rock phosphate and tri-calcium phosphate solublization by some soil fungi. *Egypt. J. Exp. Biol. (Bot.)* **5**(0), 75–84.

Islam, M., Islam, S., Akter, A., Rahman, M. & Nandwani, D. 2017. Effect of organic and inorganic fertilizers on soil properties and the growth, yield and quality of tomato in Mymensingh, Bangladesh. *Agriculture* **7**, 18. doi: 10.3390/agriculture7030018

Jain, R., Saxena, J. & Sharma, V. 2014. Differential effects of immobilized and free forms of phosphate-solubilizing fungal strains on the growth and phosphorus uptake of mung bean plants. *Annals of Microbiology* **64**(4), 1523–1534. doi: 10.1007/s13213-013-0795-6

Jones, D.L. & Oburger, E. 2011. Solubilization of phosphorus by soil microorganisms. In Bünemann, E., Oberson, A. & Frossard, E. (eds). *Phosphorus in Action: Biological Processes in Soil Phosphorus Cycling*. Springer Berlin Heidelberg, Berlin, Heidelberg, 169–198. doi:10.1007/978-3-642-15271-9_7

Kilian, M., Steiner, U., Krebs, B., Junge, H., Schmiedeknecht, G. & Hain, R. 2000. FZB24 Bacillus subtilis - mode of action of a microbial agent enhancing plant vitality. *Pflanzenschutz-Nachrichten Bayer* **1**, 72–93.

Kooliyottil, R., Malviya, M., Sati, P., Tiwari, S. & Pandey, A. 2013. Response of cold-tolerant Aspergillus spp. to Solubilization of Fe and Al phosphate in presence of different nutritional sources. *ISRN Soil Science.* doi: 10.1155/2013/598541

Lema, K.A., Willis, B.L. & Bourne, D.G. 2012. Corals form characteristic associations with symbiotic nitrogen-fixing bacteria. *Applied and Environmental Microbiology* **78**(9), 3136–3144. doi: 10.1128/aem.07800-11

Lin, S., Gunupuru, L.R., Ofoe, R., Saleh, R., Asiedu, S.K., Thomas, R.H. & Abbey, L. 2021. Mineralization and nutrient release pattern of vermicast-sawdust mixed media with or without addition of Trichoderma viride. *PLoS One* **16**(7), e0254188. doi: 10.1371/journal.pone.0254188

Mahadevamurthy, M., Channappa, TM., Sidappa, M., Mythrashree, SR. & Nagaraj, AK. 2016. Isolation of phosphate solubilizing fungi from rhizosphere soil and its effect on seed growth parameters of different crop plants. *Journal of Applied Biology & Biotechnology* **4**(6), 022–026. DOI:10.7324/JABB.2016.40604

Mahamuni, S., Wani, P. & Patil, A. 2012. Isolation of phosphate solubilizing fungi from rhizosphere of sugarcane & sugar beet using TCP & RP solubilization. *Asian Journal of Biochemical and Pharmaceutical Research ISSN: 2231-2560,* **2**, 237–244.

Mahdi, S., Hassan, G., Samoon, S., Rather, H., Dar, S. & Zehra, B. 2010. Bio-fertilizers in organic agriculture. *Journal of Phytology* **2**, 42–54.

Majumdar, K. 2015. Bio-fertilizer use in Indian agriculture. *Indian Journal of Research* **4**(6), 377–381.

Mitter, E.K., Tosi, M., Obregón, D., Dunfield, K.E. & Germida, J.J. 2021. Rethinking crop nutrition in times of modern microbiology: Innovative biofertilizer technologies. *Frontiers in Sustainable Food Systems* **5**(29), 606815. doi: 10.3389/fsufs.2021.606815

Moawad, A., Premono, M.E. & Vlek, P. 1996. Effect of phosphate-solubilizing Pseudomonas putida on the growth of maize and its survival in the rhizosphere. *Indonesian Journal of Crop Science* **11**(1), 13–23.

Naik, S.K., Maurya, S., Kumar, R., Sadhna, K., Gagrai, S., Das, B., Kumar, S. & Bhatt, B.P. 2013. Inorganic phosphate solubilization by phosphate solubilizing fungi isolated from acidic soils. *African Journal of Microbiology Research* **7**(34), 4310–4316. doi: 10.5897/AJMR2013.5947

Nelofer, R., Syed, Q., Nadeem, M., Bashir, F., Mazhar, S. & Hassan, A. 2016. Isolation of phosphorus-solubilizing fungus from soil to supplement biofertilizer. *Arabian Journal for Science and Engineering* **41**(6), 2131–2138. doi: 10.1007/s13369-015-1916-2

Niranjana, S.R., Lalitha, S. & Hariprasad, P. 2009. Mass multiplication and formulations of biocontrol agents for use against fusarium wilt of pigeonpea through seed treatment. *International Journal of Pest Management* **55**(4), 317–324. doi: 10.1080/09670870902919147

Nosheen, S., Ajmal, I. & Song, Y. 2021. Microbes as biofertilizers, a potential approach for sustainable crop production. *Sustainability* **13**(4), 1868. doi: https://doi.org/10.3390/su13041868

Pal, S., Singh, H.B., Farooqui, A. & Rakshit, A. 2015. Fungal biofertilizers in Indian agriculture: Perception, demand and promotion. *Journal of Eco-friendly Agriculture* **10**(2), 101–113.

Pradhan, N. & Sukla, L. 2005. Solubilization of inorganic phosphates by fungi isolated from agriculture soil. *Arfrican Journal of Biotechnology* **5**(10), 850–854.

Sakpirom, J., Nunkaew, T., Khan, E. & Kantachote, D. 2021. Optimization of carriers and packaging for effective biofertilizers to enhance Oryza sativa L. growth in paddy soil. *Rhizosphere* **19**, 100383. doi: https://doi.org/10.1016/j.rhisph.2021.100383

Saxena, J. 2013. Phosphate solubilization by a few fungal strains belonging to the genera Aspergillus and Penicillium. *African Journal of Microbiology Research* **7**, 4862–4869. doi: 10.5897/AJMR2013.5991

Seshadri, S., Ignacimuthu, S. & Lakshminarasimhan, C. 2004. Effect of nitrogen and carbon sources on the inorganic phosphate solubilization by different Aspergillus niger strains. *Chemical Engineering Communications* **191**(8), 1043–1052. doi: 10.1080/00986440490276308

Singh, T., Ghosh, T.K., Tyagi, M.K. & Duhan, J. 1999. Survival of rhizobia and level of contamination in charcoal and lignite. *Annals of biology* **15**(2), 155–158.

Tamburini, F., Pfahler, V., Bünemann, E.K., Guelland, K., Bernasconi, S.M. & Frossard, E. 2012. Oxygen isotopes unravel the role of microorganisms in phosphate cycling in soils. *Environmental Science & Technology* **46**(11), 5956–5962. doi: 10.1021/es300311h

Tate, K.R. 1984. The biological transformation of P in soil. *Plant and Soil* **76**(1), 245–256. doi: 10.1007/BF02205584

Wakelin, S.A., Warren, R.A., Harvey, P.R. & Ryder, M.H. 2004. Phosphate solubilization by Penicillium spp. closely associated with wheat roots. *Biology and Fertility of Soils* **40**(1), 36–43. doi: http://dx.doi.org/10.1007/s00374-004-0750-6

Wheeler, K.A., Hurdman, B.F. & Pitt, J.I. 1991. Influence of pH on the growth of some toxigenic species of Aspergillus, Penicillium and Fusarium. *International Journal of Food Microbiology* **12**(2), 141–149. doi: https://doi.org/10.1016/0168-1605(91)90063-U

Wu, Y., He, Y., Yin, H., Chen, W., Wang, Z., Xu, L. & Zhang, A. 2012. Isolation of phosphate-solubilizing fungus and its application in solubilization of rock phosphates. *Pak J Biol Sci.* **15**(23), 1144–1151. doi: 10.3923/pjbs.2012.1144.1151

Xiao, C.Q., Chi, R.A., Huang, X.H., Zhang, W.X., Qiu, G.Z. & Wang, D.Z. 2008. Optimization for rock phosphate solubilization by phosphate-solubilizing fungi isolated from phosphate mines. *Ecological Engineering* **33**, 187–193.

Yadav, R.S. & Tarafdar, J.C. 2003. Phytase and phosphatase producing fungi in arid and semi-arid soils and their efficiency in hydrolyzing different organic P compounds. *Soil Biology & Biochemistry* **35**, 745–751.

Yasser, M.M., Mousa, A.S.M., Massoud, O.N. & Nasr, S.H. 2014. Solubilization of inorganic phosphate by phosphate solubilizing fungi isolated from Egyptian soils. *Journal of Biology and Earth Sciences* **4**(1), B83–B90.

*Agronomy Research* **20**(1), 56–64, 2022
https://doi.org/10.15159/AR.21.161

# Potential of multivariate analyses of X-ray fluorescence spectra for characterisation of the microchemical composition of plant materials

A. Brangule[1,3*], M. Bērtiņš[2], A. Vīksna[2] and D. Bandere[1]

[1]Riga Stradins University, Department of Pharmaceutical Chemistry, Dzirciema 16, LV-1007 Riga, Latvia
[2]University of Latvia, Faculty of Chemistry, Jelgavas 1, LV-1004 Riga, Latvia
[3]Baltic Biomaterials Centre of Excellence, Headquarters at Riga Technical University, Kalku street 1, LV-1658 Riga, Latvia
[*]Correspondence: agnese.brangule@rsu.lv

Received: February 1st, 2021; Accepted: November 23th, 2021; Published: December 6th, 2021

**Abstract.** This work describes a method for the rapid element analysis of plant material using ED-XRF in conjunction with chemometrics. An effective analysis method is developed by measuring certified reference materials (CRM) of plant materials (algae, cabbage, lichen) covering major chemical elements with ED-XRF, to overcome the matrix effect. All samples have been measured additionally by ICP-MS. The ICP-MS analysis was used for missing information on the concentration of some elements in certificated standards. In addition, ICP-MS with CRM has been used to determine sample related element sensitivity for microelements for ED-XRF analyses.
The ED-XRF spectral patterns were used for multivariate principal component analyses by SIMCA strategy instead of each element concentration calculation. The model allows quickly analyse samples for similarity and differentiate them based on a little difference in spectral pattern, which corresponds to a minor difference in element concentration pattern. Samples with specific chemical composition could be easily spotted for in-depth analysis.
The proposed strategy for plant material sample chemical composition screening allows the quick method to improve laboratory work efficiency, reduce unnecessary analysis and rapid method for control reliability of results of more complex chemical methods, such as ICP-MS.

**Key words:** chemometrics, ED-XRF, ICP-MS, multivariate analysis, plants, screening analysis, SIMCA.

## INTRODUCTION

Research on plants and medicinal herbs has a long tradition. However, plants' complex composition is a challenge for their analysis because plants contain both organic and inorganic constituents (Elzain et al., 2016; Pohl et al., 2018; Winkler et al., 2020). The main challenges in plant's multi-element analysis using analytical techniques are concentration variation (macro, micro and trace), content of water, spatial variation

of the composition, matrix effect (mainly organic substances), difficulties in sample preparation, digestion, extraction procedures (Bharti et al., 2017; Bharti et al., 2021).

The chemical composition of plants is affected by several factors: soil composition, climatic and environmental conditions, water quality, fertilisation and plant protection agents, and their ability to assimilate, accumulate and transfer elements (Laursen et al., 2011; Pytlakowska et al., 2012; Pohl et al., 2018; georgieva et al., 2020).

Previous studies have shown that plants are a link between soil quality and human and animal organisms. Therefore, they can be used as powerful indicators (Queralt et al., 2005; Malizia et al., 2010; Laursen, et al., 2011; Pytlakowska, et al., 2012; Remon et al., 2013).

Essential and trace elements play a significant role in plants (Vatansever, 2016). Several techniques, such as atomic absorption spectroscopy (AAS), inductively coupled plasma-mass spectrometry (ICP-MS), inductively coupled plasma-atomic emission spectroscopy (ICP-AES), neutron activation analysis (NAA), X-ray fluorescence (XRF) spectroscopy, energy dispersive X-ray fluorescence (ED-XRF) spectroscopy, synchrotron radiation X-ray fluorescence (SR ED-XRF) spectroscopy, laser-induced breakdown spectroscopy (LIBS), particle-induced X-ray emission (PIXE), etc. are g enerally used for the trace element analysis in plants and medicinal herbs (Başgel & Erdemoğlu, 2006; Babu et al., 2015; Elzain et al., 2016; Bharti et al., 2019; Lázaro et al., 2020; Winkler et al., 2020). The drawback of AAS, ICP-MS, ICP-AES techniques is the requirement of sample digestion and dissolution. These techniques are time-consuming and destructive. Non-destructive plant sample multi-elemental analysis techniques are LIBS, NAA and XRF (ED-XRF and SR ED-XRF). However, these methods also have some limitations and drawbacks. For example, the LIBS can be limited by sensitivity and reproducibility (Sharma et al., 2018; Lázaro et al., 2020). A serious concern related to NAA and SR ED-XRF techniques is synchrotron and nuclear reactor availability and cost for routine analysis and quality control of plants and medicinal herbs.

The present study describes a method for the rapid element analysis and profiling (fingerprinting) plant material using energy dispersive X-ray fluorescence spectroscopy (ED-XRF). The ED-XRF method is non-destructive, has minimal sample preparation, simple spectra, and is applicable as a multi-element method over a wide range of concentrations, and the equipment cost is low. This technique has been used for the micro-elemental qualitative and quantitative analysis (Ekinci et al., 2003; Mbaye et al., 2015). In this work, the ED-XRF patterns combined with multivariate principal component analysis (PCA) were used for fingerprinting, which implies the determination of combinations of elements (Djingova et al., 2004). A fingerprint is defined as a specific profile that visualises the chemical composition of a particular sample. Several studies suggest that the fingerprinting technique can be effectively used to construct a specific pattern of recognition. Fingerprints can be used for organic and inorganic matter characterisation in plants, such as ICP and XRF methods for inorganic, but FTIR and chromatography for organic composition. The ED-XRF fingerprinting technique combined with a multivariate statistical procedure is used to extract information from these fingerprinting profiles about the origin, quality and to compare fingerprinting profiles of different herbs (Laursen et al., 2011; Custers et al., 2016; Torres Astorga et al., 2018; Brangule et al., 2020).

The XRF method is strongly influenced by matrix effects (Guild & Stangoulis, 2016). In addition, light elements comprising water and organic matter also negatively affect measurements due to X-ray scattering and attenuation (Ravansari, 2020). To minimise the plants' matrix effect, four matrix-matched reference materials were used, covering a wide range of elements and strict reference values.

The objective of the present work is to evaluate: (i) the use of the ED-XRF method for fingerprinting medicinal herbs in combination with PCA and (ii) the effect of matrix-matched standards on result interpretation.

## MATERIALS AND METHODS

### Samples

The same certified reference materials and medicinal herbal samples were used for ICP-MS and for ED-XRF analysis.

Certified reference materials (CRM): *IAEA 336 Lichen*, *IAEA 392 Algae*, *IAEA 413 Algae*, *BCR 679 Algae* were used to standardise methods for the following elements: Al, As, Ba, Br, Ca, Cd, Cl, Co, Cr, Cu, Fe, Hg, K, Mg, Mn, Mo, Na, Ni, P, Pb, Rb, Sb, Se, Sr, V, Zn.

Plant Material – medicinal herbs (MH): 13 different Chamomile (*Matricariae flos*), 6 small-leaved Linden (*Tiliae flos*), 4 Calendula (*Calendulae flos*) and Hibiscus (*Hibisci sabdariffae flos*) commercial tea samples available in Latvia.

### Sample preparation

All medicinal herb samples were ground to powder and sifted through a 2 mm sieve. Powders were stored at room temperature for further analysis.

For the XRF method samples were pressed in pellets using a manual hydraulic press. The diameter of the pellet disc was 10 mm and mass 0.2 g. The pellets reduce scattering, show a higher signal-to-noise ratio, and this allows the light elements to be detected above the background.

For the ICP method samples were prepared using the microwave-assisted acid digestion method. Samples were ground with a laboratory mill (*JI3M, Russia*) and then sieved through a 0.2 mm sieve (*Rotilabo*). Approximately 0.2 g of each sample was weighed into Teflon vessel, then 6 mL of concentrated $HNO_3$ (TraceMetal grade, 69%, Fischer) and 2 mL of concentrated $H_2O_2$ (For Trace Analysis, 30%, Fischer) were added, and the vessel was tightly closed. Samples were heated in a microwave oven (Milestone Start E) under pressure conditions. The heating program was set as heating for 15 min to 160 °C and holding at 160 °C for 30 min. After heating, vessels were cooled to room temperature and deionized water (< 0.055 μS $cm^{-1}$, Adrona) was used to dilute samples to 50 mL.

### Analytical methods

ED-XRF. Shimadzu EDX-8000 (furnished with a Rh anode, max power 50 kV, vacuum, no filter, 10 mm collimator, 600 s measurement time).

ICP-MS. Inductively Coupled Plasma Mass Spectrometer (Agilent 8900 ICP-MS QQQ) equipped with a micro-mist nebuliser and He collision cell was applied to determine the following elements: Na, Mg, Al, P, K, Ca, V, Cr, Mn, Fe, Co, Ni, Cu, Zn, g a, g e, As, Se, Rb, Sr, Y, Cd, Ba, La, Ce, W, and Pb.

The following instrumental parameters of ICP-MS were set: RF power (1.550 W); sampling depth (8 mm); nebulizer gas flow rate (0.90 mL $min^{-1}$); plasma gas flow (15 L $min^{-1}$); He cell gas flow (5 mL $min^{-1}$); extraction 1 lens (-5.0 V); extraction 2 lens (7.0 V); omega lens 7.0 (-200 V); omega bias lens (-110 V); octupole bias (-3.0 V); cell gas flow rate (20% of full scale); axial acceleration (1.0 V).

The calibration g raph was made using six standard solutions in the concentration range from 0.1 μg $L^{-1}$ to 500.0 μg $L^{-1}$. Analytical standard stock solutions were prepared from Certified Reference Material (HPS, ICP-MS-68A, 10 mg$L^{-1}$, traceable to NIST SRM 3100). Element concentrations in samples were calculated using the external calibration graph method, and the blank correction was applied. Internal standard solution (10 μg $L^{-1}$, Agilent) was used for system stability control during measurements. Two standard solutions (10 μg $L^{-1}$) were used between every ten samples to verify system stability.

**Analysis of the spectra**

The ED-XRF spectra were evaluated in order to select emission lines. Spectra were investigated, and normalisation was performed with the academic freeware software *SpectraGryph 1.2.14*. The spectra were normalised to the Rh tube emitted Rh $K_\alpha$ line.

The ICP-MS data procession, collection, and calculation of results were made by a *MassHunter* workstation program, including its subprograms - Instrument control and Offline data analysis.

**Chemometrics**

The principal component and hierarchical cluster analysis were performed using *SIMCA 14* software. Spectra were smoothed and denoised by a Savitzky - golay filter (polynomial order 5 and points 10), the second derivative of the samples was recorded. The component analysis was used to identify the dominant clusters in the data set. For the HCA, Ward's algorithm was used.

## RESULTS AND DISCUSSION

Since the ICP-MS is suitable for a wide range of concentrations and elements, the ICP-MS method was chosen to fill the missing dates in creating a fingerprinting model. Theoretically, the ED-XRF method can measure a wide range of elements, from sodium Na (11) through uranium U (92). In practice, ED-XRF sensitivity is not sufficient for light elements such as sodium, magnesium, aluminium and silicon. The same certified reference materials (*IAEA 336 Lichen*, *IAEA 392 Algae*, *IAEA 413 Algae*, *BCR 679 Algae*) and medicinal herbal samples were used for both methods ICP-MS and ED-XRF.

Standard materials are usually certified for specific elements (10–15) with a specific concentration. Concentrations can vary significantly from one certified material to another. The ICP-MS method was chosen, to obtain information about the standards of uncertified components and their concentrations with high probability.

Analysing the ED-XRF spectra (Fig. 1) together with the quantitative results obtained by ICP-MS, the information about the sensitivity of the ED-XRF method and the detection limits of elements was obtained. For example, in certified standards, elements in very different concentration intervals were detected. For *K–elements*: magnesium Mg minimal concentration 4,000 mg $kg^{-1}$; aluminium Al and silicon Si – 600 mg $kg^{-1}$;

phosphorus P and sulphur S – 200 mg kg$^{-1}$; titanium Ti to molybdenum Mo–10 mg kg$^{-1}$ and *L–elements* such as led Pb and mercury Hg at least 50 mg kg$^{-1}$.

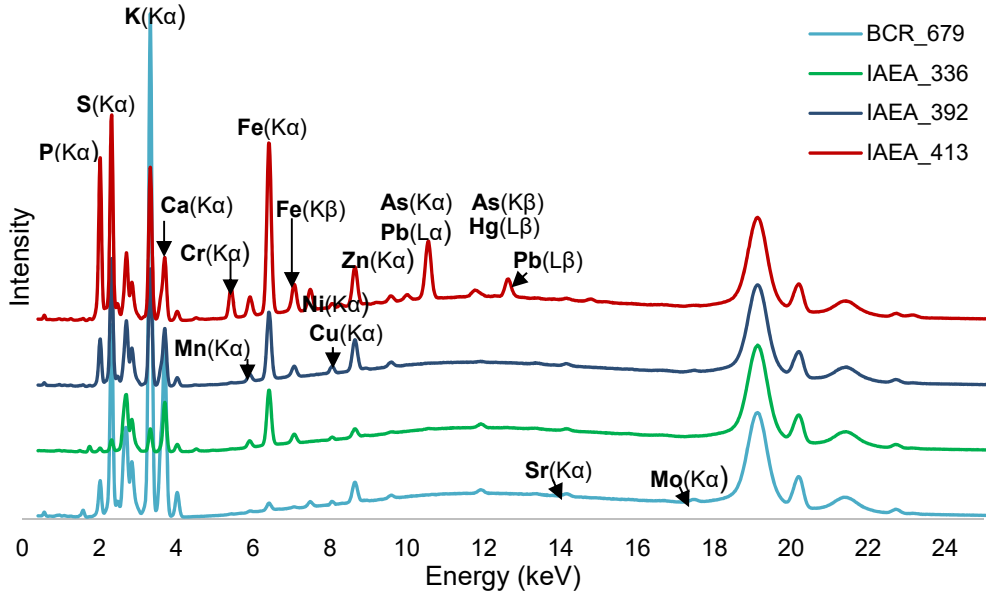


**Figure 1.** The ED-XRF patterns for certified reference standards (CRM).

It can be concluded that analysing different samples must consider that a high concentration of an element in a sample does not g uarantee that these elements will have visible peaks in the spectrum. For example, magnesium - a small peak can be observed only in a sample with a concentration above 4,000 mg kg$^{-1}$. However, the peak is not visible in the sample with a magnesium concentration above 1,000 mg kg$^{-1}$.

Analysis of the data obtained by the ICP-MS and ED-XRF method shows that the intensity of spectral lines depends on the combination of elements in the samples. For example, a high concentration of potassium K in CRM 679 affects the sensitivity of aluminium Al. High concentration potassium reduces the possibility to identify aluminium as escape peaks partly overlap the spectral line of aluminium. Nevertheless, in CRM 336, potassium concentration is significantly lower, and aluminium is detectable at 680 mg kg$^{-1}$.

Fig. 2 shows an example of two elements Cu and Zn, with high sensitivity. Copper is detectable at low concentration ~ 3 mg kg$^{-1}$, but zinc makes intensity patterns proportionally to CRM certified concentrations.

The obtained data showed that very significant in the fingerprinting is the interference effect - the overlapping of spectral lines distorting results for one or more elements. For example, overlapping spectral lines for: led Pb Lα and arsenic As Kα (10.55 keV); arsenic As Kβ and mercury Hg Lβ (11.80 keV) and chlorine Cl Kα and rhodium Rh lamp Lα and Lβ spectral lines (Fig. 3) were detected.

Literature shows that it is possible to build a fingerprinting model even if there are overlapping peaks. This is because the overlapping peak g ives the spectrum a particular shape, making the spectrum unique for each sample.

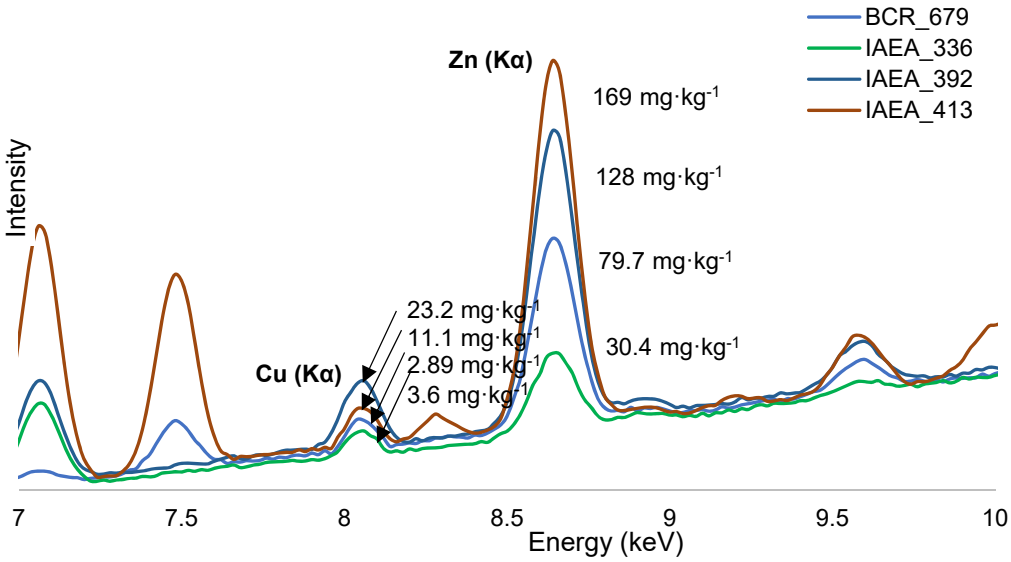


**Figure 2.** ED-XRF pattern intensities of Cu and Zn affected by the concentration in the certified reference material.

The next point of interest was to differentiate ED-XRF fingerprints of medicinal herbs MH and verify compliance with certificated reference materials. The conclusions about the fingerprinting method's effect were obtained by combining the ED-XRF and ICP-MS methods with unsupervised multidimensional statistical analysis.

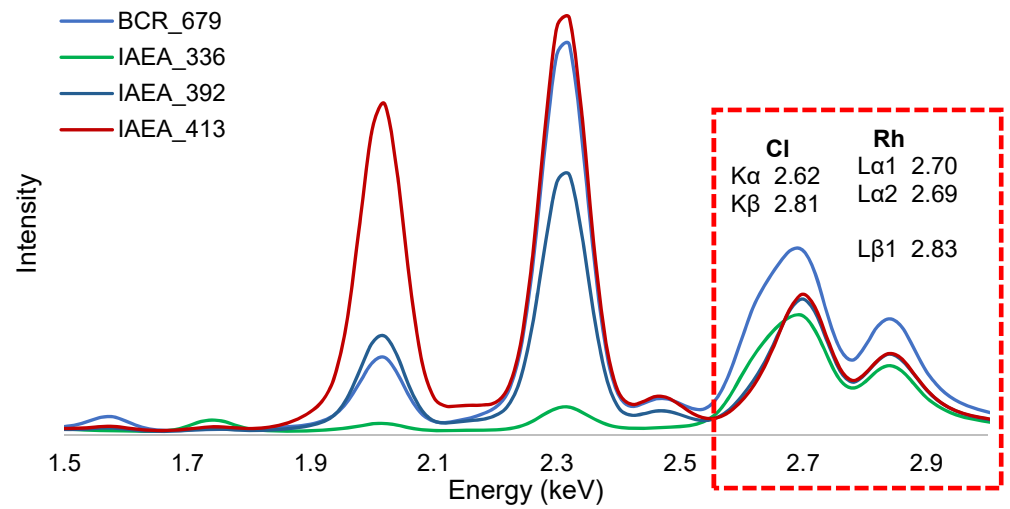


**Figure 3.** Overlapping element peaks for chlorine Cl and rhodium Rh.

The formation of clusters was depicted in diagrams and dendrograms. Four major clusters in PCA can be identified (Fig. 4): linden, chamomile, calendula and separate cluster for three reference materials – *IAEA 336 Lichen*, *IAEA 392 Algae*, *IAEA 413 Algae*.

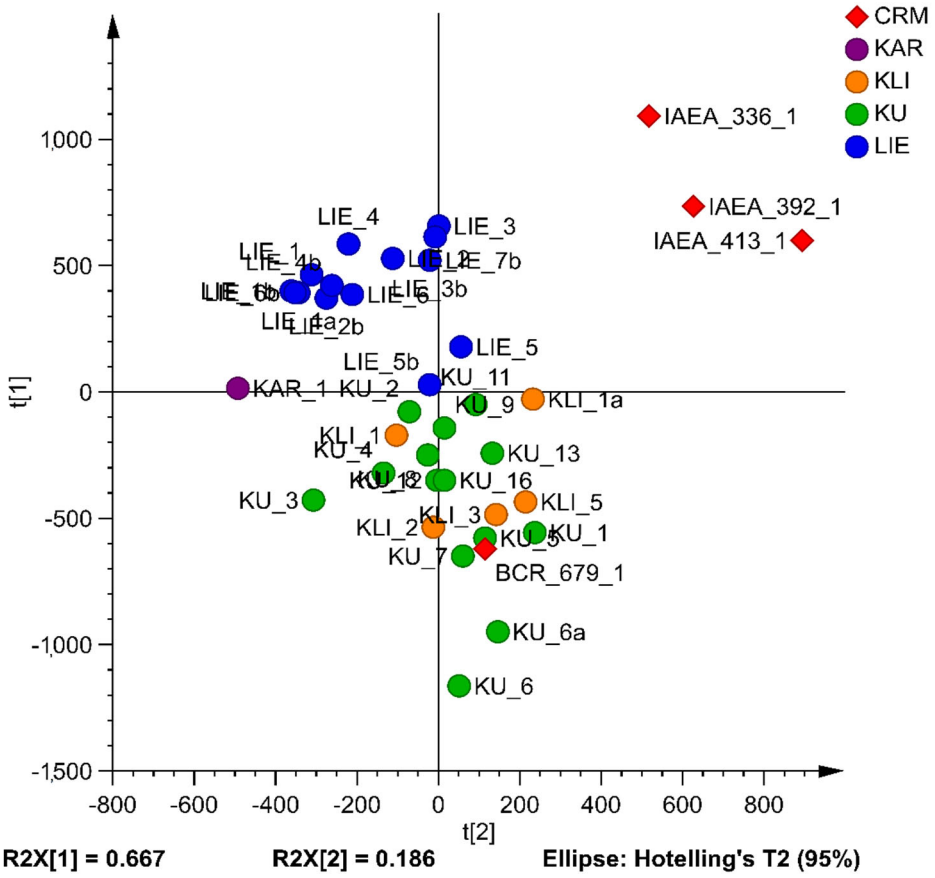


**Figure 4.** The PCA clusters for certified reference standards (CRM) and medicinal herbs. Red diamonds – CRM; blue – linden; green – chamomile; orange – calendula; violet – hibiscus.

PCA1 describes 67%, but PCA2 19%, forming 86% of spectral information. Loadings of PCA show a clear difference between PCA1 and PCA2: the potassium concentration describes dispersion across the PCA1 axis in samples, but across the PCA2 axis - by the ratio between calcium and iron concentration - dominant increase in calcium concentration and decrease in iron concentration. A combination of the first two components describes 85% of the composition of detectable elements. Cluster component PCA3 forms only 7% of the information, showing a dominant increase in iron concentration.

The PCA diagram shows that only one standard fits into the herbal cluster. The other three CRMs form a separate cluster. This leads to the conclusion that the matrix effect is essential using the fingerprint method and should be taken into account when choosing standards.

## CONCLUSIONS

This work demonstrates the potential of the ED-XRF spectra fingerprinting method in combination with statistical analysis as a sensitive, rapid and non-destructive method for quality control in order to check trace element contents on this type of matrix.

The XRF method has improved during recent years by enhancing SDD detector resolution and increasing count rates. The current technical capabilities of XRF systems provide researchers with valuable information about major micro and macro elements. However, the use of XRF for the control of trace concentration of heavy elements is limited by current sensitivity, and more sensitive methods should be used.

ACKNOWLEDGEMENTS. The research received funding from the ERAF Post-doctoral Research Support Program project Nr. 1.1.1.2/16/I/001 Research application 'Development of screening methods by innovative spectroscopy techniques and chemometrics in the research of herbal medicine', Nr. 1.1.1.2/VIAA/2/18/273.
This project has received funding from the European Union's Horizon 2020 research and innovation programme under the g rant agreement No 857287.

## REFERENCES

Babu, N.G., Srinivasu, Ch.Ch., Raju, T.P. & Lakshmana Das, N. 2015. Estimation of Trace Element Concentrations in Anti-Epileptic Medicinal Plants by Using EDXRF. 2015. *Int. J. Eng. Res*. **4**(2), 211–216.

Başgel, S. & Erdemoğlu, S.B. 2006. Determination of mineral and trace elements in some medicinal herbs and their infusions consumed in Turkey. *Sci. Total. Environ*. **15**(359), 82–9.

Brangule, A., Šukele, R. & Bandere, D. 2020. Herbal medicine characterization perspectives using advanced FTIR sample techniques – diffuse reflectance (DRIFT) and photoacoustic spectroscopy (PAS). *Front. Plant Sci.* **11**, 356.

Bharti, A.S., Sharma, S., Shukla, N., Tiwari, M.K. & Uttam, K.N. 2017. Elemental investigation of the leaf and seed of coriander plant by synchrotron radiation X-ray fluorescence spectroscopy. *Natl. Acad. Sci. Lett.* **40**(5), 373–377.

Bharti, A.S., Sharma, S., Singh, A.K., Tiwari, M.K. & Uttam, K.N. 2021. Assessment of the elemental profile of leafy vegetables by synchrotron-radiation-induced energy dispersive X-ray fluorescence spectroscopy. *J. Appl. Spectrosc.* **88**(3), 653–661.

Bharti, A.S. Sharma, S. & Uttam, K.N. 2019. Elemental assessment of the leaf and seed of Rauwolfia serpentina (Sarpagandha) by direct current arc optical emission spectroscopy. *Natl. Acad. Sci. Lett*. **43**(4), 361–365.

Custers, D., Courselle, P., Apers, S. & Deconinck, E. 2016. Chemometrical analysis of fingerprints for the detection of counterfeit and falsified medicines. *Reviews in Analytical Chemistry*, **35**(4), 145–168.

Djingova, R., Kuleff, I. & Market, B. 2004. Chemical fingerprinting of plants. *Ecol. Res.* **19**, 3–11.

Ekinci, N., Ekinci, R., Polat, R. & Budak, G. 2003. Analysis of trace elements in medicinal plants with energy dispersive X-ray fluorescence. *J. Radioanal. Nucl. Chem*. **260**, 127–131.

Elzain, A.H., Ebrahim, A.M. & Ali Eltoum, M.S. 2016. Comparison between XRF, PIXE and ICP-OES techniques applied for analysis of some medicinal plants. *IOSR-JAC* **9**(4), 06–12.

Georgieva, S.K., Georgieva, A., Peteva, Z. & Dimova, D. 2020. Trace elements in commonly used medicinal plants from Varna region, Bulgaria. *Environ. Sci. Pollut. Res*. 1–7.

Guild, G.E. & Stangoulis, J.C. 2016. Non-matrix matched glass disk calibration standards improve XRF micronutrient analysis of wheat grain across five laboratories in India. 2016. *Front Plant Sci*. **7**.

Laursen, K.H., Schjoerring, J.K., Olesen, J.E., Askegaard, M., Halekoh, U. & Husted, S. 2011. Multielemental fingerprinting as a tool for authentication of organic wheat, barley, faba bean, and potato. *J. Agric. Food Chem.* **59**, 4385–4396.

Lázaro, M.C., Morais, C.P., Silva, T.V., Senesi, G.S., Junior, D.S., Neto, J.A.G., Ferreira, E.C. 2020. Dry ashing for signal enhancement in laser-induced breakdown spectroscopy (LIBS). *Anal. Lett.*, **54**(12), 2009–2021.

Malizia, D., Giuliano, A., Ortaggi, G. & Masotti, A. 2012 Common plants as alternative analytical tools to monitor heavy metals in soil. *Chem. Cent. J*. **6**(2), S6.

Mbaye, M., Traore, A., Ndao, A.S. & Wague, A. Multivariate statistical techniques to determine essential and toxic elements in biological samples by X-ray fluorescence. 2015. *Instrum. Sci. Technol.* **43**(3), 369–378.

Pohl, P., Bielawska-Pohl, A., Dzimitrowicz, A., Greda, K., Jamroz, P., Lesniewicz, A., Szymczycha-Madeja, A. & Welna, M. 2018. Understanding element composition of medicinal plants used in herbalism – a case study by analytical atomic spectrometry. *J. Pharm. Biomed.* **10**(159), 262–271.

Pytlakowska, K., Kita, A., Janoska, P., Połowniak, M. & Kozik, V. 2012. Multi-element analysis of mineral and trace elements in medicinal herbs and their infusions. *Food Chem*. **135**(2), 494–501.

Queralt, I., Ovejero, M., Carvalho, M.L., Marques, A.F. & Labres, J.M. 2005. Quantitative determination of essential and trace element content of medicinal plants and their infusions by XRF and ICP techniques. *X-Ray Spectrom*. **34**(3), 213–217.

Ravansari, R., Wilson, S.C. & Tighe, M. 2020. Portable X-ray fluorescence for environmental assessment of soils: Not just a point and shoot method. *Environ Int*. **134**.

Remon, E., Bouchardon, J.C., Le Guédard, M., Bessoule, J. & Conord, C. 2013. Are plants useful as accumulation indicators of metal bioavailability? *Environ. Pollut*. **175**, 1–7.

Sharma, S., Bharti, A.S., Tiwari, M.K. & Uttam, K.N. 2018. Effect of manganese stress on the mineral content of the leaves of wheat seedlings by use of X-ray fluorescence excited by synchrotron radiation. *Spectrosc. Lett.* 1–9.

Torres Astorga, R., de Los Santos Villalobos, S., Velasco, H., Domínguez-Quintero, O., Pereira Cardoso, R., Meigikos Dos Anjos, R., Diawara, Y., Dercon, G. & Mabit, L. 2018. Exploring innovative techniques for identifying geochemical elements as fingerprints of sediment sources in an agricultural catchment of Argentina affected by soil erosion. 2018. *Environ. Sci. Pollut. Res*. **25**, 20868–20879.

Vatansever, R., Ozyigit, I.I. & Filiz, E. 2016. Essential and beneficial trace elements in plants, and their transport in roots: a review. *Appl. Biochem. Biotechnol*. **181**, 464–482.

Winkler, A., Rauwolf, M., Sterba, J.H., Wobrauschek, P., Streli, C. & Turyanskaya, A. 2020. Total reflection X-ray fluorescence analysis of elemental composition of herbal infusion and teas. *J. Sci. Food Agric*. **100**(11), 4226–4236.

*Agronomy Research* **20**(1), 65–72, 2022
https://doi.org/10.15159/AR.22.015

# Implementation of simultaneous performance of two technological operations with different machine-and-tractor units

V. Bulgakov[1], J. Olt[2,*], S. Pascuzzi[3], V. Nadykto[4], V. Kyurchev[4], V. Mitkov[4] and F. Santoro[3]

[1]National University of Life and Environmental Sciences of Ukraine, 15 Heroyiv Oborony Str., UA 03041 Kyiv, Ukraine
[2]Estonian University of Life Sciences, Institute of Forestry and Engineering, 56 Kreutzwaldi Str., EE 51006 Tartu, Estonia
[3]University of Bari Aldo Moro, Department of Agricultural and Environmental Science, Via Amendola, 165/A, IT 70125 Bari, Italy
[4]Dmytro Motornyi Tavria State Agrotechnological University, 18[B] Khmelnytsky Ave, UA 72310 Melitopol, Zaporozhye Region, Ukraine
[*]Correspondence: jyri.olt@emu.ee

Received: January 25th, 2022; Accepted: April 6th, 2022; Published: April 18thd, 2022

**Abstract.** The gap between two technological operations should be minimal in the production environment. For this, special combined (multi-operational) machine-and-tractor units (MTU) are used. Their agricultural machines have sequentially installed working devices for various technological purposes. In the absence of such MTUs, single-operation units are used. Such units more often have different working widths. For their simultaneous operation in the same field, the first unit (for example, a sowing unit) must have a wider width than the second one (for example, a rolling one). In practice, the opposite case occurs more often when the first unit's working width is less than the second unit's working width. As a result, the first machine-and-tractor unit delays the work of the second one. This article aims to develop the algorithm for the simultaneous operation of two machine-and-tractor units of different field performance. The first of them (a sowing unit) has a working width of 3.6 m, and the second (a rolling one) is 6.1 m. As a result, the following has been established using the example of processing a field of 80 hectares: the second unit should start its work (i.e., rolling the crops) when the first one (sowing) has sown a certain area. According to the formula proposed in the article, the size of this area is 44 hectares. Under natural working conditions, the second unit (rolling) started its work after the first (sowing) unit has sown 44 hectares of the field area. As a result, both units have completed the entire area with a half-hour gap, i.e., practically simultaneously and without delay from each other.

**Key words:** operating speed, sowing, rolling, technological operation, working width.

## INTRODUCTION

The execution time of technological operations in the agricultural crop growing has a significant impact on its yield. From factory farming, for example, it is known that the shorter the technological operation time for:

i) soil preparation and sowing;

ii) sowing and rolling crops, etc., the less moisture loss, the more efficient its use.

First of all, use wide-cut, which means high-performance machine-and-tractor units (MTU). They consist of both one and several machines (units) (Ivanovs et al., 2018; Bulgakov et al., 2018; Bulgakov et al., 2021).

Combined MTUs are best suited to shorten the time between adjacent technological operations (e.g., soil preparation and sowing, sowing, and rolling). The most typical of them is the unit considered in work (Bulgakov et al., 2017). It is a series-connected machine for applying mineral fertilizers and a grain seeder. A characteristic feature of this MTU is the same working width of used machines. Its primary disadvantage is its sizeable kinematic length.

A combined unit for harrowing soil and crops and grain crops sowing with the synchronous application of the main, starting fertilizer, and rolling the crops with a spiral-screwed roller (Jebur et al., 2013; Maslov et al., 2019), is more complicated. Combining the listed operations in one pass is based on working bodies such as applicators for the main application of mineral fertilizers, conventional double-disk furrow openers for sowing seeds of grain crops, and a starting fertilizer dose. A spiral-screwed roller is used to roll the sown seeds to a given depth into the soil layer with an optimal density in series with them.

Bertollo et al. (2018) investigated two technological operations that are performed sequentially. The first operation consists of preparing the soil with a chisel plow, and the second involves sowing an agricultural crop. The difference between the combination of these technological operations is that they can be performed asynchronously. This fact means that the operating mode of each unit does not depend on each other.

The appearance of tractors equipped with a front linkage and a front power take-off shaft makes it possible to create combined units according to the ‘push-pull’ scheme (Yaroshenko, 2015; Bulgakov et al., 2016). In this variant, the rear agricultural machine operates in the traction mode and the front one in the pushing mode. The machines are spaced apart in the longitudinal direction at a distance approximately equal to the tractor's overall length. However, the cut width of the front and rear machines in such a unit is equal. And since they are used with the same tractor, they also work in the same way.

Recently, the Controlled Traffic Farming (CTF) system has been increasingly used in many countries (Tullberg et al., 2007; Antille et al., 2015; Chamen, 2015; Galambošová et al., 2017). In this system, machine and tractor units' movement occurs along permanent traffic lines (PTL). The working cut width of the used machine and tractor units is equal to or a multiple of the PTL pitch (Talarczyk et al., 2016; Antille et al., 2019). All technological operations are generally performed sequentially. And if some machine and tractor units work simultaneously, their movement modes depend on each other. This circumstance is predetermined by the system's essence, which provides aggregate movements in strictly defined field zones.

From the above analysis, the following remains unclear: how to organize the operation of machine-and-tractor units in one field under the following conditions:

i) MTU operation should occur with a minimum time gap;

ii) the unit's performance executing the first operation is more significant than the MTU performance performing the second technological operation.

In the absence of such units' work, the first one, i.e., less productive of them, can disrupt the mode of operation of another. In practice, this will manifest itself in the latter's periodic downtime, which is an undesirable result.

To avoid this, the goal of this work is to develop an algorithm for operating two MTUs in one field, in which the performance of the first unit is lower than that of the second one.

## THEORETICAL PREMISES

The basis of the developed algorithm for operating two MTUs of different performances is as follows: the first unit, less productive starts working first; the second unit is included in the technological process at a particular time and then works simultaneously with the first unit until the entire work volume is completed.

First, one should answer the question: what area of the field (let us label it by $S_o$) the first unit should process for the second one to work right after it until the very end without stopping.

According to the condition, the performance of the first MTU $W_1$ is less than the performance of the second unit $W_2$. Then:

$$\left.\begin{aligned} &W_1 < W_2; \\ &W_1 = 0.1B_1 \cdot V_1 \cdot \tau_1; \\ &W_2 = 0.1B_2 \cdot V_2 \cdot \tau_2, \end{aligned}\right\} \quad (1)$$

where $B_1, V_1, \tau_1$; $B_2, V_2, \tau_2$ = the working width, the travel speed, and the working time's utilization factor for the first and second MTU, respectively.

The duration of the first unit operation is labeled $T_1$, and the second one is $T_2$. And since the performance of the latter is higher, then the time of its operation over the entire field of $S$ area will not be less than some $\Delta T$ value, that is:

$$T_2 = T_1 - \Delta T.$$

Because of this, we can write that:

$$\left.\begin{aligned} S &= W_1 \cdot T_1; \\ S &= W_2 \cdot T_2 = W_2(T_1 - \Delta T). \end{aligned}\right\} \quad (2)$$

Equating the right-hand sides of the equations of system (2) and taking into account the second and third equations of system (1), after transformations, we obtain:

$$\Delta T = \frac{S}{0.1B_1 \cdot V_1 \cdot \tau_1} \cdot \left(1 - \frac{B_1 \cdot V_1 \cdot \tau_1}{B_2 \cdot V_2 \cdot \tau_2}\right). \quad (3)$$

The $\Delta T$ value is the time it takes for the first unit to process the field with the $S_0$ area and after which the second unit starts working, i.e.:

$$S_o = W_1 \cdot \Delta T. \quad (4)$$

Taking into account the Eq. (3), the expression (4) will take the following final form:

$$S_o = S \cdot \left(1 - \frac{B_1 \cdot V_1 \cdot \tau_1}{B_2 \cdot V_2 \cdot \tau_2}\right). \quad (5)$$

It should be noted that under the condition of both units' same performance, i.e., when $B_1 \cdot V_1 \cdot \tau_1 = B_2 \cdot V_2 \cdot \tau_2$ from Eqs (3) and (5), we obtain $\Delta T = S_o = 0$, which is quite a logical result.

## MATERIALS AND METHODS

For checking the developed theoretical prerequisites, experimental studies of two machine-and-tractor units based on the MTZ-890 (Belarus) tractor have been carried out. The first has sown winter wheat (Fig. 1), and the second unit has carried out rolling crops (Fig. 2). In the south of Ukraine's arid conditions, such a technological method as rolling is essential.

**Figure 1.** Sowing machine-and-tractor unit.

**Figure 2.** Rolling machine-and-tractor unit.

Brief technical description of both MTUs is presented in Table 1. Both units have worked in the field with an area is equal to $S = 80$ ha. This field size is typical for the south of Ukraine. In the process of experimental studies, the speed of movement $V$ and the working width $B$ of each MTU have been determined.

**Table 1.** Brief technical description of sowing and rolling units

| Index | Sowing MTU | Rolling MTU |
|---|---|---|
| Tractor | MTZ-890 (Belarus) | MTZ-890 (Belarus) |
| Tractor weight (kg) | 3,900 | 3,915 |
| and engine power (kW) | 65 | 65 |
| Machine | SZ-3.6 | KZK-6 |
| Manufacturer | Elvorti | Vostok |
| Constructive width (m) | 3.6 | 6.1 |
| Working device | Disk furrow opener | Single packer roller |
| Number of working devices | 24 | 51 |
| Connection to the tractor | Trailed | Trailed |
| Minimum turning radius ($R_{min}$, m) | 4.1 | 4.1 |
| Length of straight movement on the headland ($L_o$, m) | 6.3 | 7.0 |
| Weight (kg) | 1,300 | 2,400 |

For this, the field has been divided into sections $L_a = 250$ m long each. The time $t_a$ of the unit passing the test section in two replicates has been recorded using an FS-8200 electronic stopwatch with a measurement accuracy of 0.1 s.

The speed of movement of the machine-and-tractor unit has been calculated using the formula:

$$V = \frac{L_a}{t_a}.$$

The method for determining the working width of the machine-and-tractor unit has been as follows. The passage of each of them has been determined by the visible edge of the processed field strip. At the given $L$ distance from it, 50 pegs have been set with 1 m steps. Then the machine-and-tractor unit has made a working stroke, the visibility of which has been determined by the new edge of the field's processed strip. After that, the shortest $h_i$ distance from this edge to each installed peg has been measured (Fig. 3).

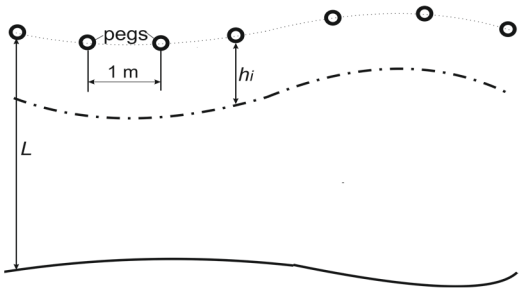


**Figure 3.** The measuring scheme of the MTU working width:
——— – edge of the MTU previous pass;
– · – · – edge of the MTU last working pass.

The working width $B$ of the machine-and-tractor unit has been calculated from the following equation:

$$B = L - h_i.$$

In this case, the $L$ index value has been equal to 5 m for the sowing unit and 8 m for the rolling one.

To measure the $L$ distance with an accuracy of 1 cm, a Tolsen tape measure with a measurement limit of up to 10 m has been used.

The seeding and rolling machine-and-tractor units' quality of work have been assessed by the statistical parameters of fluctuations in their working width. The latter ones have been taken as:

i) average squared deviations;
ii) coefficients of variation;
iii) normalized correlation functions. As known (Nadykto, 2017), the latter characterizes the degree of interaction (correlation) between the random process values at different points in its course time. That is, they estimate the frequency of the oscillatory process.

## RESULTS AND DISCUSSION

Experimental studies have established that, according to its potential capabilities, the seeding machine-and-tractor unit could move at a speed of 2.28 m $s^{-1}$ (8.2 km $h^{-1}$). The average value of its effective working width has been 3.5 m (Table 2).

**Table 2.** Research results of sowing and rolling units

| MTU | $B$, m | $V$, km $h^{-1}$ | $\tau$ | $W$, ha $h^{-1}$ | $S_0$, ha | $\Delta T$, h |
|---|---|---|---|---|---|---|
| Sowing | 3.5 | 8.2 | 0.70 | 2.0 | 44.0 | 22.0 |
| Rolling | 6.0 | 8.9 | 0.85 | 4.5 | | |

Studies of such units in Ukraine have established that the efficiency factor ($\tau$) averages 0.70. Then, taking into account the second equation of

system (1), the calculated performance of the sowing machine-and-tractor unit is $W_1 = 2.0$ ha h$^{-1}$.

The maximum possible movement speed of the second, i.e., the rolling unit, has been 2.47 m s$^{-1}$ (8.9 km h$^{-1}$), as follows from experimental studies. Its average effective width has been 6.0 m. The efficiency factor in time for such units, as practice shows, is higher and is, on average, 0.85.

Using the third equation of system (1), it has been established that the estimated performance of such a machine-and-tractor unit should be equal to $W_2 = 4.5$ ha h$^{-1}$. It is 2.25 times more than the seeding unit performance (Table 2).

The width of the headland has been calculated for both machine-and-tractor units. The latter is known to have two meanings:

i) minimum ($E_{min}$);

ii) valid ($E_r$).

On the headland, both units have performed a pear-shaped turn. In this maneuver, $E_{min}$ is calculated using the following formula:

$$E_{min} = 2.8 \cdot R_{min} + L_o + 0.5 \cdot B.$$

The actual value of the swath width $E_r$ is known to be either equal or a multiple of the machine working width:

$$E_r = \text{Integer}\left(\frac{2.8 \cdot R_{min} + L_o + 0.5 \cdot B}{B}\right) \cdot B.$$

Numerical values for determining $E_{min}$ and $E_r$ parameters are presented in Table 1 below. The calculations have established the following:

– for sowing MTU: $E_{min} = 19.58$ m; $E_r = 21.6$ m;

– for rolling MTU: $E_{min} = 21.48$ m; $E_r = 24.4$ m.

As can be seen, the effective width of the headland of the sowing machine-and-tractor unit $E_r$ is equal to 6 values of its working width $B$. For the rolling MTU, the value of the parameter $E_r$ is equal to 4 values of the value $B$.

The calculation according to the formula (5) has shown that for the simultaneous completion of the work of both units in the same field, the first of them (i.e., sowing one) must be the first process (sow) 44 hectares. For this, it will need 22 hours (Table 1).

After that, the second (i.e., rolling) machine-and-tractor unit is connected to work. In the future, both units must operate in the same field until both operations are completed (Fig. 4).

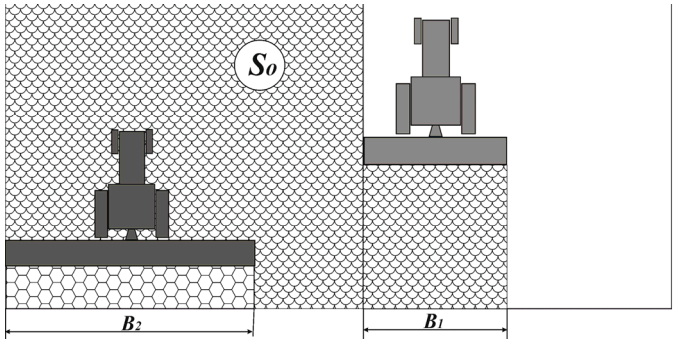


**Figure 4.** Operating scheme of sowing and rolling machine-and-tractor units.

According to the calculations, the sowing machine-and-tractor unit has worked in the field for 22 hours in the considered machine-and-tractor units' actual operation. Then the second machine-and-tractor unit started to perform its technological process. Later, both units finished processing the entire field with a gap of 0.5 hours. That is, almost simultaneously.

The unit's work quality was satisfactory. It is evidenced by the normalized correlation functions of each working width oscillations (Fig. 5).

An essential characteristic of each function is the point where they cross the zero threshold. In practice, this abscissa means the length of the correlation between adjacent dimensions of the process under study. The greater the location of this point from the vertical coordinate axis, the more low-frequency process is the random oscillatory process.

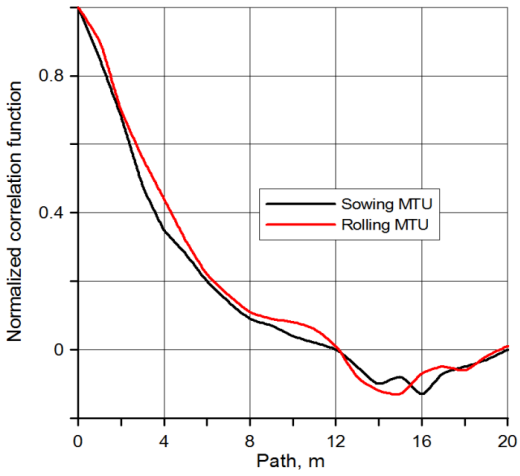


**Figure 5.** Normalized correlation functions of MTU width oscillations.

In this case, both units' correlation length has turned out to be practically the same and approximately equal to 12 m (Fig. 5).

In principle, this means that for a sowing unit moving at a speed of 2.28 m $s^{-1}$, the tightness of the connection between two adjacent measurements of the working width has disappeared only after 12 m / 2.28 m $s^{-1}$ = 5.3 s. For the rolling unit, this figure has been 4.9 s.

The root-mean-square deviation of fluctuations in the sowing unit's working width is ± 3.4 cm, and the rolling one is ± 3.6 cm. The variation coefficients of the oscillations of the parameters $B_1$ and $B_2$ have not exceeded 1%. Together, this data indicates a fairly rectilinear movement of the studied units, which, in the end, is a positive fact.

## CONCLUSIONS

A methodology has been developed to organize two technological operations of sequential execution by machine-and-tractor units. The first performance is less than the performance of the second one. It has been established that the latter must begin its work after the first machine-and-tractor unit completes its technological process in a particular area ($S_o$). This parameter's value can be determined from Eq. (5), which links the entire field ($S$) with both units' performance.

The theoretical dependencies' reliability has been proven by the practical work of the seeding and rolling machine-and-tractor units. The performance of the second has been 2.25 times higher than the performance of the second one. Using the proposed methodology for organizing their joint work has allowed both units almost simultaneously and with satisfactory quality to complete the sowing and rolling of winter wheat crops in a field of 80 hectares.

The proposed technique can be successfully applied to organize the conduct of two technological operations of sequential execution by any other machine-and-tractor units, in which the performance of the first is less than the performance of the second one.

## REFERENCES


Antille, D.L., Chamen, W.C.T., Tullberg, J.N. & Lal, R. 2015. The potential of controlled traffic farming to mitigate greenhouse gas emissions and enhance carbon sequestration in arable land: A critical review. *Transactions of the ASABE* **58**(3), 707–731. doi: 10.13031/trans.58.11049

Antille, D.L., Peets, S., Galambošová, J., Botta, G.F., Rataj, V., Macak, M., Tullberg, J.N., Chamen, W.C.T., White, D.R., Misiewicz, P.A., Hargreaves, P.R., Bienvenido, J.F. & Godwin, R.J. 2019. Review: Soil compaction and controlled traffic farming in arable and grass cropping systems. *Agronomy Research* **17**(3), 653–682.

Bertollo, G.M., Schlosser, J.F., Bertinatto, R., Martini, A.T. & Rudell, I.Y.P. 2018. Tractor performance in sowing with furrower configurations in areas with controlled traffic of machines. *Engenharia Agrícola* **38**(5), 665–672. doi: 10.1590/1809-4430-Eng.Agric.v28n5p665-672/2018

Bulgakov, V., Adamchuk, V., Arak, M., Petrychenko, I. & Olt, J. 2017. Theoretical research into the motion of combined fertilising and sowing tractor-implement unit. *Agronomy Research* **15**(4), 1498–1516, doi: 10.15159/AR.17.059

Bulgakov, V., Ivanovs, S., Nadykto, V., Kuvachov, V. & Masalabov, V. 2018. Research on the turning ability of a two-machine aggregate. *INMATEH-Agricultural Engineering* **54**(1), 139–146.

Bulgakov, V., Adamchuk, V., Arak, M., Nadykto, V., Kyurchev, V. & Olt, J. 2016. Theory of vertical oscillations and dynamic stability of combined tractor-implement unit. *Agronomy Research* **14**(3), 689–710.

Bulgakov, V., Olt, J., Ivanovs, S., Kuvachov, V. & Lillerand, T. 2021. Research into Dynamics of Motion Performed by Modular Power Unit as Part of Ploughing Tractor-Implement Unit. *Proceedings of the 32nd DAAAM International Symposium*, 0576–0585, B. Katalinic (Ed.), Published by DAAAM International, ISBN 978-3-902734-33-4, ISSN 1726-9679, Vienna, Austria. doi: 10.2507/32nd.daaam.proceedings.082.

Chamen, T. 2015. Controlled traffic farming – From worldwide research to adoption in Europe and its future prospects. *Acta Technologica Agriculturae* **18**(3), 64–73. doi: 10.1515/ata-2015-0014

Galambošová, J., Macák, M., Rataj, V., Antille, D.L., Godwin, R.J., Chamen, W.C.T., Žitnak, M., Vitazkova, B., Dudaak, J. & Chlpik, J. 2017. Field evaluation of controlled traffic farming in Central Europe using commercially available machinery. *Transactions of the ASABE* **60**(3), 657–669. doi: 10.13031/trans.11833

Ivanovs, S., Bulgakov, V., Nadykto, V. & Kuvachov, V. 2018. Theoretical investigation of turning ability of two-machine sowing aggregate. *Engineering for rural development* **17**, 314–322.

Jebur, H.A., Mostafa, M.M., Elnono, M.A. 2013. Performance evaluation of farm tractor using variable weights on rear wheels during ploughing and sowing operations. *Farm Machinery and Power* **30**(3), 645–660.

Maslov, G.G., Lavrentev, V.P., Yudina, E.M. & Taran, A.D. 2019. Improving the process of harrowing and sowing crops. *American Journal of Pharmaceutical Sciences* **6**, 7060–7064.

Nadykto, V. 2017. Fundamentals of scientific research. Kherson: OLDI-PLUS, 268 pp. (in Ukrainian).

Talarczyk, W., Szulc, T., Szczepaniak, J. & Lowinski, L. 2016. Functional verification of unit for strip tillage, fertilization and corn sowing. *Journal of Research and Applications in Agricultural Engineering* **61**(2), 110–113.

Tullberg, J.N., Yule, D.F. & McGarry, D. 2007. Controlled traffic farming - From research to adoption in Australia. *Soil and Tillage Research* **97**(2), 272–281. doi: 10.1016/j.still.2007.09.007

Yaroshenko, P.M. 2015. Grounding of the combined unit chart for the presowing cultivation and simultaneous sowing of the row crop cultures. *Technology Audit and Production Reserves* **5/1**(25), 25–29.

*Agronomy Research* **20**(1), 73–90, 2022
https://doi.org/10.15159/AR.22.018

# Mechanical weed control strategies for grain amaranth (*Amaranthus cruentus* L.)

P. Casini*, G. Biancofiore and E. Palchetti

University of Florence, Department of Agriculture, Food, Environment and Forestry (DAGRI) 18 P. le delle Cascine, IT50144 Firenze, Italy
*Correspondence: paolo.casini@unifi.it

Received: January 25th, 2022; Accepted: April 5th, 2022; Published: April 19th, 2022

**Abstract.** Currently, no herbicide is registered for grain amaranth in Europe, the United States and South America. Hence, weed control must be addressed with alternative methods. Field trials were conducted in 2018 and 2019 in Central Italy by comparing some mechanical weed control treatments in grain amaranth (*Amaranthus cruentus* L.). In 2018, the five treatments were: untreated control ($T1_{18}$), cutter hoeing ($T2_{18}$), flat share cuts and one central duck foot tine ($T3_{18}$), flat share cuts and two central duck foot tines ($T4_{18}$), and three duck foot tines ($T5_{18}$). In 2019, the five treatments were: untreated control ($T1_{19}$), three duck foot tines ($T2_{19}$), flex tine harrowing ($T3_{19}$), flex tine harrowing plus finger weeding with red fingers ($T4_{19}$), and finger weeding with red fingers ($T5_{20}$). In 2018, amaranth was a successful competitor against weeds from 40 days after emergence (10 true leaf stage, corresponding to BBCH code 15). The competitive ability was showed by excellent seed yields averaging 1.2 t $ha^{-1}$, for all treatments. This feature was also confirmed to some degree in 2019. However, seed yield in 2019 was more strongly influenced by treatment as well as by the lower emergence of plants. All the mechanical methods employed can be effectively used for weed control in grain amaranth. Treatments with the flex tine harrower and finger weeder negatively affected the plant density at harvest, necessitating further optimization. However, combined mechanical strategies proved the most effective, especially in controlling dicot weeds. There is a need to optimize strategies, with mechanical equipment, to anticipate and improve the ground cover of amaranth. These strategies include selecting optimal plant density and the correct distancing between the rows for easier mechanical control.

**Key words:** pseudocereal, grain amaranth competition, weed control.

## INTRODUCTION

The rediscovery and the improvement of various pseudocereals (including exotic types) for European environments has led to the valorization of species that have remained neglected for a long time. Buckwheat (*Fagopyrum esculentum* Moench.) and quinoa (*Chenopodium quinoa* Willd.) have contributed to the establishment of new markets in both food and non-food sectors. Another species that has managed to occupy a good market segment is amaranth (*Amaranthus* spp.), native to Mexico and Central America which, together with corn, beans and various pumpkin species, represented one of the main foods of the Maya and/or Aztecs (Sauer, 1950; Turchi, 1987).

The rediscovery of this plant as a precious food resource dates back to the 1970s with studies published by Downton (1973), highlighting the remarkable nutritional properties of the most widespread species: *Amaranthus cruentus* L., *A. hypochondriacus* L., *A. caudatus* L. and *A. edulis* Speg. Regarding the former two species, research has developed to such an extent that important markets both within and outside the areas of origin have been established (Tucker, 1986; Granados & Lòpez, 1990).

The main characteristic of this species is related to the nutritional content of the seeds, that are rich in protein (15–18%), and with averages of 5.2 and 0.37 $g^{-1}$ 100 $g^{-1}$ dry matter in lysine and calcium, respectively (Saunders & Becker, 1984; Petr et al., 2003). Moreover, amaranth is characterized by the absence of gluten and is therefore, suitable for celiac nutrition (Ballabio et al., 2011). These characteristics provides this species with high market potential, especially where up until now, it has been confined almost exclusively to the health sector (Hackman & Mayers, 2003). In addition to being the basis of a large number of food preparations, amaranth is also used for the formulation of bars, snacks, muesli, puffed seeds, extruded materials and other products such as cooked vegetable (Mulandana et al., 2009).

Equally interesting, is the use of amaranth in the non-food sector, although this aspect has not been well investigated. The cosmetic and pharmacological sectors benefit mostly from the high content of squalene, a triterpene with an average content of 4.2% (ranging from trace levels to 7.3%) in amaranth seed oil, which is the most plentiful plant source of squalene (Han-Ping & Corke, 2003). The oil content of the seeds is on average 6.0%, from which both tocopherol and squalene are used in the cosmetic industry, especially in the skin and hair care sectors and, more generally, in hypoallergenic formulations.

Although the potential of this pseudocereal has been established even beyond the areas of origin (Carlsson, 1980; Gimplinger et al., 2007), amaranth has not received much attention in Italy, despite promising agronomic trials conducted over multiple years. Based on good yields of *Amaranthus cruentus* L. and *A. hypochondriacus* L. (Alba et al., 1997; Lovelli et al., 2005; Rivelli et al., 2008; Ercoli et al., 1987; Massantini et al., 1987; El Gendy et al., 2018), the possibility of introducing this species was highlighted despite the fact that studies reporting agronomic techniques are as yet still limited (Ercoli et al., 1987; Casini & La Rocca, 2014; Pulvento et al., 2015; Casini & Biancofiore, 2020a; Casini & Biancofiore, 2020b; Gresta et al., 2020; Pulvento et al., 2021).

Amaranth is a C4 plant that is characterized by a very slow initial growth for the first 3–5 weeks after emergence, a period during which it is very susceptible to weed competition (Sooby et al., 1998; Bavec & Mlakar, 2002; Kudsk et al., 2012; Brust et al., 2014). However, the critical period may vary considerably according to both the cultivation environment and the variety used (Nurse et al., 2016). The variability in the duration of the reproductive cycle of amaranth, and the potential seed production, can be attributed to various causes. The presence of weeds is considered the most important. The extent to which weed competition reduces amaranth yield varies considerably, and is dependent on both the density and the prevalent species of weed (Chaudhari et al., 2019). An uncontrolled infestation of amaranth also leads to a decrease in the quality of the grain and an increase in production costs.

Amaranth is very susceptible to broadleaf weed herbicides. Previous studies have shown that colazone, clopyralid, phenmdipham and triflusulfuron are tolerated by amaranth (Kudsk et al., 2012). However, problems with the use of herbicides were reported, such as loss of seeds at harvest and the presence of volunteer amaranth plants in the following

cop (Kudsk et al., 2012). Although the application of 50 g $ha^{-1}$ oxyfluorfen 40 days after sowing of amaranth has been demonstrated to be useful in the control of weeds (Chaudari et al., 2019), currently no herbicide is registered for this species in Europe, the United States and South America. Hence, weed control must be addressed with integrated management and cultural practices which have been found to be effective in controlling weeds (Ojo, 1997). These methods should include the selection of seeding density and distances between the rows, as well as the use of different types of inter-row cultivators. Peiretti & Gesumaria (1998) observed that single rows with plants spaced at 0.30 and 0.45 m are the most appropriate in terms of the rate of inter-row coverage, which offers advantages for weed control by competition. However, amaranth yield is only slightly affected with an increase in density from 47 to 100 plants $m^{-2}$. Similar results were reported previously (Casini & La Rocca, 2014; Casini & Biancofiore, 2020b). It was shown that the use of double rows permitted taking advantage of a better ground cover than single rows. Moreover, together with the possibility of mechanical intervention for weed control, the double rows also provided a higher yield.

Under many environmental conditions, the use of inter-row cultivation is the only weed control method available to organic farmers (Gélinas & Sequin, 2008; Nurse et al., 2016). However, mechanical methods may only be performed within a limited time period as the development of the crop can hinder the passage of equipment causing damage to the crop. These methods require that amaranth is sown at row distances based on the available equipment in the farm, to permit an easy inter-row cultivation.

After the first weeks of emergence, starting from the 10 true leaf stage, ground cover is almost complete, thereby permitting the crop to compete with weeds for light, water and nutrients (Casini & La Rocca, 2014).

The need for effective weed control is driven, not only by the negative effects on seed yield, but by the presence of wild relatives, such as *Amaranthus retroflexus* L. (redroot pigweed) and the survival of grain amaranth seeds in the soil. Contamination with black seeds of the wild relatives in grain amaranth makes seed cleaning and processing difficult (Ojo, 1997). Although the hybridization between cropped and weedy *Amaranthus* spp., has not yet been ascertained (Brenner et al., 2000, 2013; Nurse et al., 2016), and has thus far only been detected between *A. hypochondriacus* L. and *A. hybridus* L. (Kauffman & Weber, 1990), the possibility of hybridization may represent a serious problem for crops intended for the multiplication of certified seed. Regarding the survival of amaranth seeds in the soil and their potential to be a weed problem for subsequent crops, it must be taken into consideration that amaranth seeds are very small (1,000 seed weight 0.5–0.8 g) and that their ripening is uneven. Furthermore, the loss of seed at the time of harvest can be significant (Kauffmann & Weber, 1990). The few studies that have been conducted relating to the survival of the seed of cultivated amaranth in the soil, report that it is significantly shorter than weed relatives and that it highly unlikely constitute a rotational problem, although seed loss can be abundant (Omani et al., 1999; Kudsk et al., 2012).

Reducing weed competition for the first 4–6 weeks after sowing, results in increased biomass, seed proteins and yield (Ojo, 1997). Although it is not feasible to use residual herbicides, this scenario does not present a problem in grain amaranth cultivation as cultural and mechanical methods can serve as excellent alternatives to guarantee a qualitatively and economically sustainable production (Russell, 1977; Coolman & Hoyt, 1993; Morse, 1993).

Given that there is little research available on weed control in grain amaranth, the present research was initiated to evaluate the effectiveness of some mechanical methods in field experiments.

## MATERIALS AND METHODS

Two field experiments were carried out in 2018 and 2019 in Tuscany, Central Italy at 'Tenuta di Cesa' agricultural research station (43° 18' north; 11° 47' east, 246 m asl) on a neutral, loamy-sandy soil. The physical and chemical characteristics of the soil (depth of 20 cm) were as follows: sand 36.2%, loam 37.9%, clay 25.9%, total N 0.121% and P (Olsen) 13 ppm. Exchangeable Ca, Mg and K, were 4180, 641 and 142 ppm, respectively. Meteorological data was recorded using SIAP automatic equipment, controlled and validated by the Regional Hydrological and Geological Sector.

Initially, the research envisaged identical treatments over both years. However, the prolonged rainy period that occurred during the first year, did not permit mechanical weeding at the appropriate times with both flex-tine harrowing and the finger weeder. Therefore, the treatments were different over the two-year trial and are detailed in Table 1.

**Table 1.** Details of mechanical weed control treatments and application dates according to amaranth BBCH codes (Martínez-Núñez et al., 2019)

| Experiment 1 – 2018 | | | | Experiment 2 – 2019 | | | |
|---|---|---|---|---|---|---|---|
| Treatment Code | Treatment detail | Date | BBCH growth stage* | Treatment Code | Treatment detail | Date | BBCH growth stage* |
| $T1_{18}$ | Untreated Control | - | - | $T1_{19}$ | Untreated Control | - | - |
| $T2_{18}$ | Cutter Hoeing | June 5 (37 DAE) | 15 | $T2_{19}$ | Three duck foot tines | June 18 (34 DAE) | 13 |
| $T3_{18}$ | Flat share cuts and one central duck foot tine | June 5 (37 DAE) | 15 | $T3_{19}$ | Flex tine harrowing | June 6 (22 DAE) | 12 |
| $T4_{18}$ | Flat share cuts and one central duck foot tines with second operator | June 5 (37 DAE) | 15 | $T4_{19}$ | Flex tine harrowing + Finger weeding with red fingers | June 6 (22 DAE) June 18 (34 DAE) | 12 13 |
| $T5_{18}$ | Three duck foot tines | June 5 (37 DAE) | 15 | $T5_{19}$ | Finger weeding with red fingers | June 18 (34 DAE) | 13 |

*BBCH codes corresponding to the following amaranth growth stages: 12 – (3–4 true leaves); 13 – (6–7 true leaves); 15 – (8–10 true leaves). Weed growth stage at time of weeding: 2018: from 4 to 8 true leaves; 2019: from 2 to 4 true leaves. Meteorological data occurred at the time of the treatments: 2018; clear sky, air temperature 20.0 °C, wind speed 2.4 m $s^{-1}$. 2019 T3 and T4: clear sky, air temperature 21.2 °C, wind speed 2.3 m $s^{-1}$; T2 and T5: clear sky, air temperature 24.5 °C, wind speed 1.7 m $s^{-1}$.

The cutter hoeing treatment ($T2_{18}$) was performed with 0.5 m wide units equipped with 15 cm cutters at a cultivation depth of 7–10 cm and driving speed of 2.5 km $h^{-1}$. $T3_{18}$ was carried out with two 20 cm flat share cuts and one 15 cm duck foot tine at a cultivation depth of 5–7 cm and driving speed of 3.0 km $h^{-1}$. Equipment used for $T4_{18}$ was equipped with 20 cm flat cuts and 15 cm duck foot tines at a cultivation depth of 5–7 cm and driving speed of 3.0 km $h^{-1}$. $T5_{18}$ and $T2_{19}$ treatments were performed

with 20 cm duck foot tines at a cultivation depth of 5–7 cm and driving speed of 3.5 km $h^{-1}$. $T3_{19}$ and $T4_{19}$ were equipped with 0.7 cm diameter flexible tines inclined by -35°at a cultivation depth of 2–3 cm and a driving speed of 6.5 km $h^{-1}$. Finger weeding for $T4_{19}$ and $T5_{19}$was carried out at a cultivation depth of 3–4 cm and a driving speed of 3.5 km $h^{-1}$. Details of the equipment are reported in Fig. 1 while agronomic techniques are reported in Table 2.


**Figure 1.** Equipment utilized in the experiments: a) $T2_{18}$ – 'Breviglieri' equipment, M21-2 model; b) $T5_{18}$ and $T2_{19}$ – 'Gaspardo' equipment, HL-6R model; c) $T4_{18}$ – 'Spapperi' equipment without crop guard between horizontal knives; d) $T3_{18}$ – 'Badalini' equipment. Due to the amaranth growth stage, flex tine harrows were not used; e) $T3_{19}$ and $T5_{19}$ – Equipment without brand name (handcrafted design); f) $T4_{19}$ and $T5_{19}$ – 'Sfoggia' equipment, Kress model.

The experiments were carried out under rainfed conditions according to a Randomized Complete Block (RCB) design with four replicates. In order to carry out treatments with open field equipment, plots were 30 m long consisting of 8 rows spaced 0.6 m apart (surface area of 144 $m^{-2}$). Within each plot, a test area (the 4 central rows for a length of 5 m) was permanently allocated for all phenological, morphological and productive data, as well as weed community analysis. Seeding rate was 0.120 kg $plot^{-1}$ corresponding to an expected plant density of 60 $m^{-2}$. UNIFI6161, a new line of *Amaranthus cruentus* L., obtained by the University of Florence, was used.

**Table 2.** Agronomic techniques during the field trials

| | 2018 | 2019 |
|---|---|---|
| Preceding crop | Protein pea | Sunflower |
| Soil preparation | 0.3 m plowing, August 2017<br>Disc harrowing, October 12, 2017<br>Rotary harrowing, April 20, 2018 | 0.3 m plowing, August 2018<br>Disc harrowing, January 11, 2019<br>Rotary harrowing, May 7, 2019 |
| Pre-sowing fertilization | N 55.2 kg $ha^{-1}$ (Urea)<br>P 78.0 kg $ha^{-1}$ (Triple superphosphate + Mineral superphosphate | N 55.2 kg $ha^{-1}$ (Urea)<br>P 78.0 kg $ha^{-1}$ (Triple superphosphate + Mineral superphosphate) |
| Insecticide treatment | Deltametrine<br>250 g $100^{-1}$ L water<br>May 29 | Deltametrine<br>250 g $100^{-1}$ L water<br>May 25 |
| Date of sowing | April 20 | May 8 |
| Date of emergence | April 29 | May 15 |
| Date of harvesting | September 13 | September 19 |

The effectiveness of the treatment was evaluated by counting weeds and visually estimating the ground cover of the latter both immediately before the treatment and before the harvest of the crop, using the Braun-Blanquet cover-abundance scale (Maabel, 1979). A quadrat (0.5×0.5 m) was randomly positioned in each sampling area and three replicate analyses were performed. An average of the three samples was utilized for the statistical analysis. Both the average weed counts performed in all test areas and the percentage composition of the dominant species were considered as part of the weed community typical of the experimental area. Immediately following the pre-harvest counting, the weeds were removed manually and the total fresh and dry weight estimated. With regard to the main weed species, the effectiveness of the treatments was calculated and expressed as a percentage reduction in the number of plants compared to those present in the T1 control.

Visual ground cover of the crop as well as the dates of the different phenological stages were recorded. These stages, according to the specific BBCH codes (Martínez-Núñez et al., 2019) were as follows: 12 (four true leaves), 13 and 15 (six and ten true leaves, respectively), 50 (full panicle appearance), 65 (full flowering), 75 and 85 (milky and waxy maturity, respectively) and 89 (maturation), respectively. For the maturation stage, seed consistency was taken into consideration together with complete filling (non-translucent endosperm). Morphological crop traits were evaluated by considering the average of ten plants, randomly harvested in each sample plot.

The harvest was performed by a combine harvester. Seed humidity was recorded on a 100 g sample. After drying the seeds to a standard humidity of 12% (airflow at 35 °C for 48 h), yield calculations were then performed. Treatments were considered as a factor with fixed effects in the ANOVA model. Data on the percentage composition of weed flora and visual ground cover were subjected to the angular transformation as follows:

$$Y = arcsine\sqrt{\frac{p}{100}}$$

Differences between means were tested utilizing the Tukey test at $P \leq 0.05$, $P \leq 0.01$ or $P \leq 0.001$. COSTAT 6.45 software was used for the statistical analysis.

## RESULTS AND DISCUSSION

### Meteorological data

Fig. 2 shows the climatic trends during the field experiments. The average minimum and maximum temperatures recorded in 2018 were 12.5 and 27.5 °C, respectively, conforming to the ten-year average of the geographical area. The intense and persistent rains over March-April 2018 (110 mm) led to a slight delay in the sowing date, relative to that predicted to be most suitable for the area. Even over the May-June period, the rains were of an unusual frequency and intensity (75 mm), resulting in a change in some of treatments planned due to the excessive height of the amaranth plants.

The average minimum and maximum temperatures recorded in 2019 were 11.8 and 26.6 °C, respectively. Rainfall, that occurred in both the second and third ten day periods of April led to a delay in the sowing, that was then postponed to May. During the month of May, when the crop was at the 12–13 phenological stage, temperatures ranged from 6.5 and 18.0 °C (below average monthly levels) with a rainfall of 127 mm. These environmental conditions led to a delay in plant development and physiological parameters characterizing the species. The last 10 days of July were characterized by both heavy and abundant rainfall, attaining a level of 233 mm of the total of 552 mm recorded in April-September period.

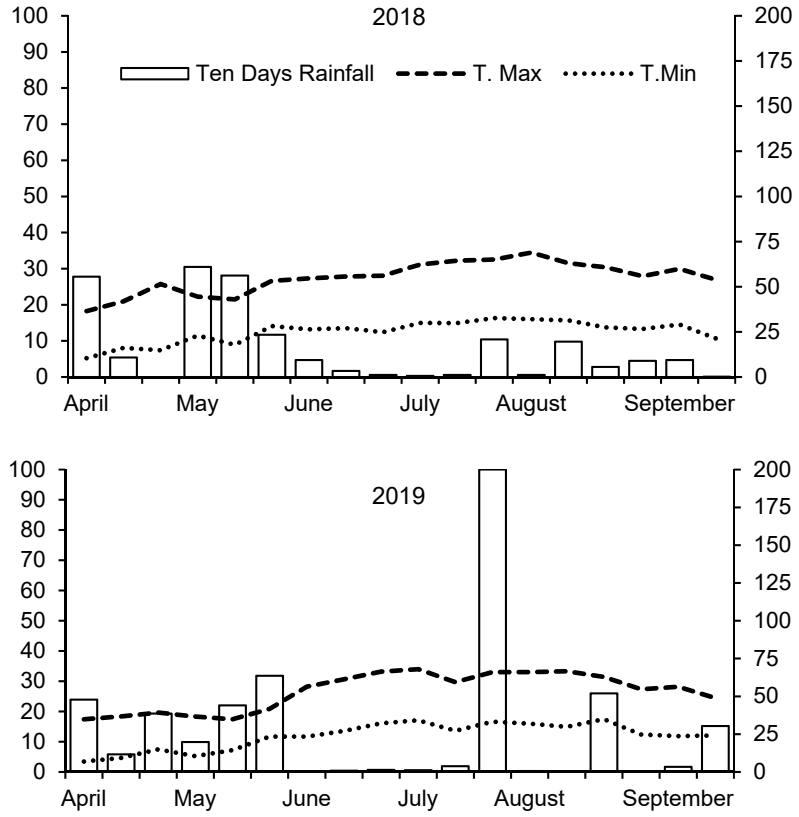


**Figure 2.** Temperature and rainfall recorded during the field experiments.

**Experiment 1 – 2018**

For experiment 1 in 2018, the time of the phenological growth stages of amaranth, together with the ground cover trend, are shown in Fig. 3. The maturation of the crop in the different treatments was completed 145 days after emergence (DAE). Growth in the earlygrowth stages, between the emergence and stage 13, was particularly slow (about 30 days), a characteristic that distinguishes this species.

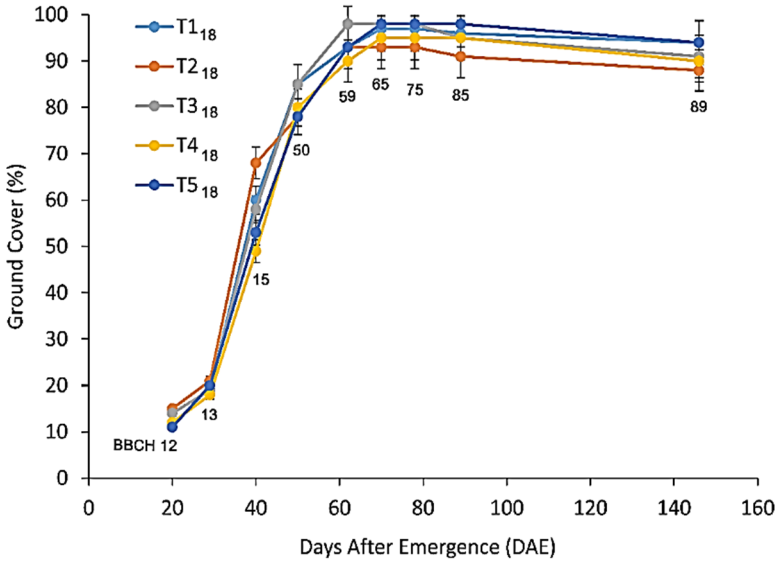


**Figure 3. Experiment 1.** Amaranth ground cover in relation to the treatments and phenological growth stages according to BBCH codes. Error bars represent the interval of the variability of the Tukey test. If the bars do not overlap, the difference between averages is significant at $P \leq 0.05$. $T1_{18}$: Untreated Control; $T2_{18}$: Cutter Hoeing; $T3_{18}$: Flat share cuts and one central duck foot tine; $T4_{18}$: Flat share cuts and one central duck foot tines with second operator; $T5_{18}$: Three duck foot tines.

The beginning of the reproductive phase, coinciding with stage 59, occurred at 63 DAE. Full flowering (stage 65) in this species is strongly scaled, with an acropetal trend on the panicle. The time interval between stages 85 and 89 was 55 DAE, which was particularly long. Fig. 3 also evidences the rapid growth of amaranth from the stage 13.

Significant differences in amaranth ground cover were observed starting from stage 15, corresponding to one week after the treatments (37 DAE). In this phase, the highest ground cover of 76.3% was found in $T2_{18}$. This was significantly different from the remaining treatments, particularly in $T4_{18}$, where the coverage was 49.1%.

Stage 15, together with stage 50, highlighted significant differences between some treatments. The rapid development of the foliage in $T2_{18}$ may have been favored by improved soil aeration and consequent reduction in water loss due to capillary rise. Thereafter, in the subsequent phenological growth stages, starting from 65 onwards, significant differences were only reported between $T1_{18}$ and $T2_{18}$.

Table 3 showed that the weed community in the area of the experimental trial was mostly composed of dicots (94.5%), with the remaining percentage composed of monocots. Of the dicots, 51.7% consisted of *Portulaca oleracea* L., followed by

*Solanum nigrum* L. (36.2%), *Convolvolus arvensis* L. (5.4%) and *Chenopodium album* L. (0.4%), respectively. Regarding the monocots, 58.0% was represented by *Echinochloa crus-galli* (L.) P. Beauv.

Hence, the weed community appeared simplified, with only two dicot species representing 87.9% of the weed community, typical for all the conventional agriculture farms within the area. Moreover, the seasonal trend may also have influenced the predominance of *P. oleracea*.

**Table 3. Experiment 1.** Mean floristic composition detected before treatments as a percentage of abundance compared to the total weed number

| Species/ Abundance | Portulaca oleracea | Solanum nigrum | Convolvulus arvensis | Chenopodium album | Other dicots | Echinochloa crus-galli | Other monocots | Total dicots | Total monocots |
|---|---|---|---|---|---|---|---|---|---|
| Abudance, % | 51.7 | 36.2 | 5.4 | 0.4 | 0.8 | 5.0 | 0.5 | 94.5 | 5.5 |
| Other minor species | *Helianthus pauciflorus* Nutt., *Fallopia convolvulus* (L.) Holub, *Abutilon teophrasti* Medik., *Amaranthus retroflexus* L.,*Cirsium arvense* (L.) Scop., *Fumaria officinalis* L., *Heliotropium europaeum* L., *Senecio vulgaris* L., *Taraxacum officinalis* Web., *Brassica nigra* L., *Phytolacca americana* L., *Mercurialis annua* L., *Sinapis arvensis* L., *Cynodon dactylon* (L.) Pers., *Avena* spp., *Lolium* spp., *Digitaria sanguinalis* (L.) Scop., *Setaria viridis* (L.) Beauv. | | | | | | | | |

The effectiveness of the treatments in reducing the number of predominant weeds is shown in Fig. 4. A drastic reduction of dicots, exceeding 85%, was observed with all mechanical treatments, with the exception of *C. arvensis*. Specifically, amaranth did not appear to compete effectively against *S. nigrum* ($T1_{18}$). There was a 8.3% reduction of the latter species compared to the remaining weeds under all treatments, of which $T4_{18}$ and $T5_{18}$ were especially effective (reduction exceeding 95%), and significantly better compared to $T2_{18}$ and $T3_{18}$.

*P. oleracea*, by far the most widespread weed in all plots, was significantly reduced by all treatments. However, the untreated amaranth $T1_{18}$ also showed an excellent competitive ability in reducing this weed by 75.8%. In contrast with the results reported for *P. oleracea*, for *C. arvensis* all treatments were practically ineffective, probably attributable to the prostrate posture and long climbing branches of the weed, and to the presence of rhizomes continuously forming new shoots. With regard to *E. crus-galli*, control was particularly effective with the $T2_{18}$ and $T5_{18}$ treatments (98.0% of reduction), while significantly smaller differences were observed with $T3_{18}$ (68.5%) and $T4_{18}$ (50.1%), respectively. The excellent effectiveness of $T2_{18}$ was attributable to the type of action performed by this equipment (rotating and cutting parts at a shallow depth) which acts on weeds that were characterized by a bundled and still superficial root system at the time of treatment. However, once again (Fig. 4), the good competitive ability of untreated amaranth ($T1_{18}$) resulted in a 98.1% reduction of *E. crus-galli*. This effect can be ascribed to two main factors. The first resides in the root system of amaranth, characterized by rapid growth, and the deep penetration of taproot by the stages 13 and 15. The second resides in the rapid epigeal growth, starting from the same phenological growth stages, resulting in a rapid and almost complete ground cover, and in so doing, exercising an excellent competitive advantage for water, nutrients and light.

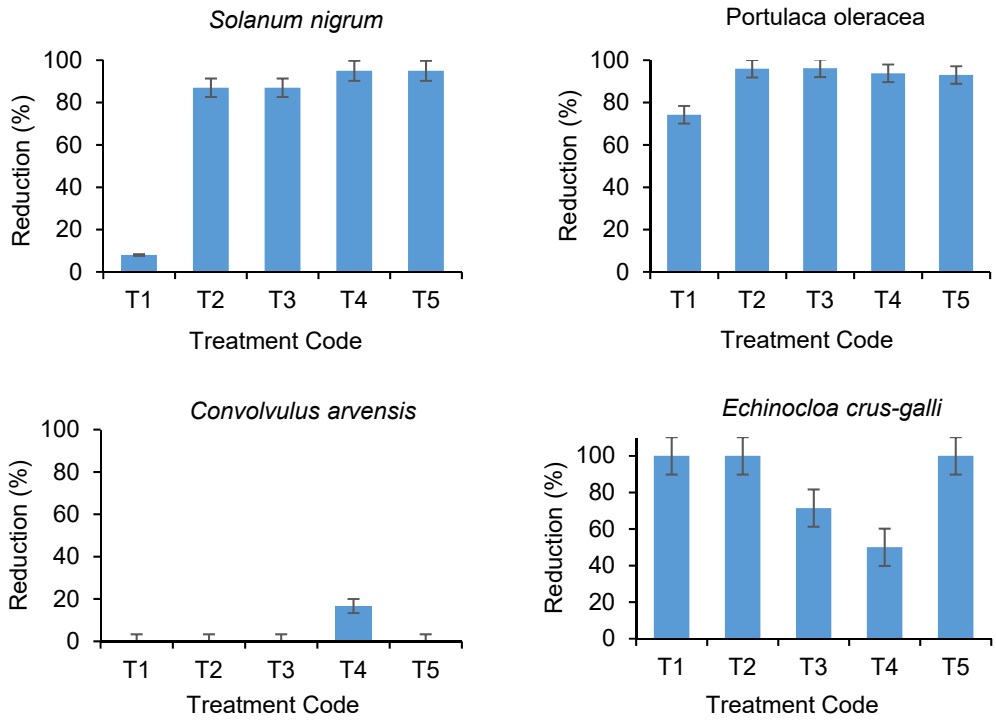


**Figure 4. Experiment 1.** Percentage reduction in the number of weeds compared to control belonging to the main species. If the bars do not overlap, the difference between averages is significant at $P \leq 0.05$. $T1_{18}$: Untreated Control; $T2_{18}$: Cutter Hoeing; $T3_{18}$: Flat share cuts and one central duck foot tine; $T4_{18}$: Flat share cuts and one central duck foot tines with second operator; $T5_{18}$: Three duck foot tines.

The data reported in Table 4 showed significant differences for all weed parameters. The ground cover data allowed the identification of two groups. The first was from $T1_{18}$ to $T3_{18}$, with an average of 52.4%, which was significantly higher than that observed in the second group comprised of $T4_{18}$ and $T5_{18}$ (8.2%). This was also confirmed in part by the number of weeds per $m^{-2}$ and by the total dry weight of the weeds per $m^{-2}$. For the latter, $T1_{18}$ was significantly higher with 150.5 g $m^{-2}$, while the lowest dry weight was recorded in $T2_{18}$ (38.7 g $m^{-2}$). For amaranth, there were no significant differences in plant height and plant density per $m^{-2}$, with respective averages of 155.9 cm and 57.8 $m^{-2}$ plants. From the present experiment, it was not possible to identify the critical weed-free period, defined by Nurse et al. (2016) and Knezevic et al. (2002). Given the rapid increase in ground cover of amaranth and associated increased growth competitiveness, the weeds were shown to spread rapidly in the first growth phases of the crop, corroborating previous work (Sooby et al., 1998; Bavec & Mlakar, 2002; Kudsk et al., 2012; Brust et al., 2014). However, despite an excess of 51.0 weeds per $m^{-2}$ observed in $T1_{18}$ (untreated control), the weeds did not affect negatively the morphological characteristics of the crop. Therefore, the present results indicate the excellent competitive ability of the crop, also confirmed by grain production. All seed yields exceeded 1.3 t $ha^{-1}$, with the exception of those found in $T5_{18}$. The only significant reduction compared to $T1_{18}$ was observed in $T5_{18}$ (1.19 t $ha^{-1}$), and was likely attributed

to the greater depth of the moving parts of the equipment used that could have damaged the more superficial roots of the plants since the mechanical intervention was performed at a fairly advanced stage of growth (37 DAE). Furthermore, no significant differences were observed in the humidity of the seeds at harvest (12.7% on average).

**Table 4. Experiment 1.** Plant height, density, seed humidity and yield of the amaranth crop recorded at harvest, as well as total weed ground cover, density and dry weight

| | Weeds | | | Grain amaranth | | | |
|---|---|---|---|---|---|---|---|
| Treatment Code | Ground cover, % | Total weed density, n $m^{-2}$ | Dry weight, g $m^{-2}$ | Plant height, cm | Plant density, n $m^{-2}$ | Seed humidity, % | Seed yield, t $ha^{-1}$ |
| $T1_{18}$ | 62.9[a] | 51.0[a] | 150.5[a] | 145.2 | 58.8 | 12.7 | 1.40[a] |
| $T2_{18}$ | 50.0[a] | 8.1[b] | 38.7[d] | 158.1 | 63.3 | 12.4 | 1.36[ab] |
| $T3_{18}$ | 44.3[a] | 12.3[b] | 63.7[c] | 160.0 | 62.2 | 12.6 | 1.34[ab] |
| $T4_{18}$ | 8.2[b] | 14.0[b] | 84.5[b] | 166.3 | 54.9 | 12.7 | 1.38[ab] |
| $T5_{18}$ | 8.3[b] | 6.4[b] | 51.6[cd] | 150.3 | 63.4 | 13.0 | 1.19[b] |
| *Significance* | ** | * | ** | *ns* | *ns* | *ns* | * |

*ns*: not significant; *: significant at $P \leq 0.01$; **: significant at $P \leq 0.05$. Means within rows followed by the same letter(s) are not different at 5% level as per Tukey's test; $T1_{18}$: Untreated Control; $T2_{18}$: Cutter Hoeing; $T3_{18}$: Flat share cuts and one central duck foot tine; $T4_{18}$: Flat share cuts and two central duck foot tines with second operator; $T5_{18}$: Three duck foot tines.

**Experiment 2 – 2019**

For experiment 2 in 2019, the general trend of the phenological growth stages of amaranth (Fig. 5) in Experiment 2, confirmed that observed in Experiment 1. There was a rapid growth starting from stage 15, approximately to 40 DAE. Moreover, an extended period of 40 days was similarly required for the seed filling (stage 85). Fig. 5, showing crop ground cover in relation to the different treatments, showed significantly different effects starting from stage 50. In this growth stage, the ground cover showed significant differences between $T2_{19}$ (72.5%) and $T4_{19}$ (87.5%), as well as between $T2_{19}$ and $T4_{19}$ and the remaining treatments. Interestingly, in $T4_{19}$ there were 13.8 fewer plants per $m^{-2}$ than in $T2_{19}$. The lower plant density in $T4_{19}$ probably led to less intraspecific competition and, therefore, a greater leaf area production and, consequently, ground cover. This dynamic is important and assumes a role of primary importance in providing a competitive advantage of amaranth against weeds, which in turn may have a positive effect on seed yield (Nurse et al., 2016). Considering the aforementioned plasticity of the amaranth sown at different densities, it is important to underline that when selecting both the plant density and the distance between the rows various aspects need to be taken into consideration. These include the type of equipment available for weeding and the behavior of the amaranth in a specific geographical area. Moreover, seeding rate flexibility depends on both the spectrum and density of weeds in the field. If thermophilic broad-leaf weeds predominate, then sowing amaranth seeds in narrow or double rows could accelerate ground cover, thereby providing a competitive advantage. As was shown previously, the rate of ground coverage is doubled using the aforementioned technique compared to that recorded with single rows (Casini & Biancofiore, 2020b). Good ground coverage by the crop also influences ground temperature and the red/far-red light ratio, which are lower below the plant canopy, resulting in a lower germination of weed seeds (Teasdale & Daughty, 1993; Batlla et al., 2000). Furthermore,

for *A. cruentus* and *A. hypochondriacus*, the release of allelopathic substances able to improve the competitive effect has also been demonstrated (Connick et al., 1989; Allemann & Denner, 2006; Tejeda-Sartorius et al., 2011).

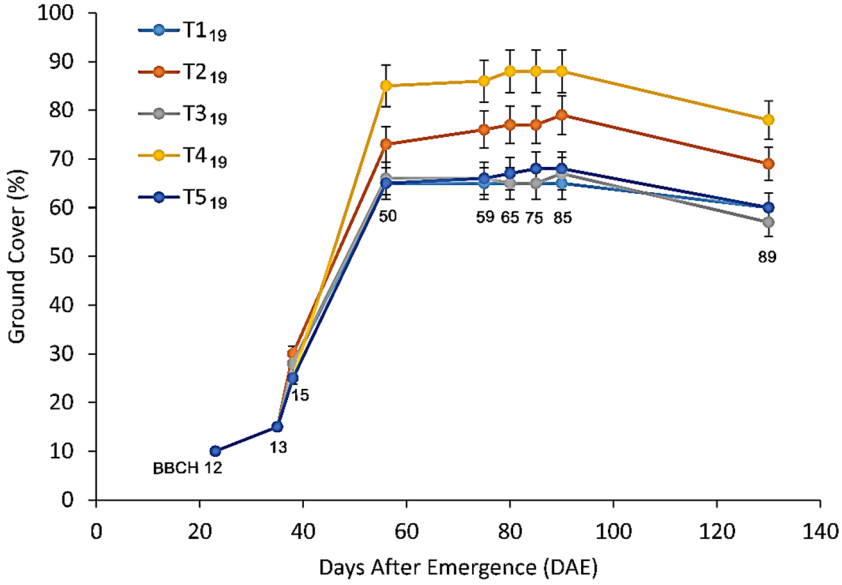


**Figure 5. Experiment 2.** Amaranth ground cover in relation to the treatments and phenological growth stages according to BBCH codes. Error bars represent the interval of the variability of the Tukey test. If the bars do not overlap, the difference between averages is significant at $P \leq 0.05$. $T1_{19}$: Untreated Control; $T2_{19}$: Three duck foot tines; $T3_{19}$: Flex tine harrowing; $T4_{19}$: Flex tine harrowing and finger weeding with red fingers; $T5_{19}$: Finger weeding with red fingers.

Additionally, in the present experiment (Table 5) the dicot weeds were undoubtedly the predominant species (95.1%), mainly represented by *S. nigrum* and *P. oleracea*.

**Table 5. Experiment 2.** Mean floristic composition detected before treatments as a percentage of abundance compared to the total weed number

| Species/ Abundance | Portulaca oleracea | Solanum nigrum | *Convolvulus arvensis* | *Amaranthus retroflexus* | Other dicots | Echinochloa crus-galli | Other monocots | Total dicots | Total monocots |
|---|---|---|---|---|---|---|---|---|---|
| Abundance, % | 48.8 | 43.8 | 0.8 | 1.0 | 0.7 | 4.3 | 0.6 | 95.1 | 4.9 |
| Other minor species | *Abutilon teophrasti* Medik., *Amaranthus retroflexus* L., *Brassica nigra* L., *Fallopia convolvulus* (L.) Holub., *Fumaria officinalis* L., *Helianthus pauciflorus* Nutt., *Heliotropium europaeum* L., *Mercurialis annua* L., *Sinapis arvensis* L., *Taraxacum officinalis* Web., *Avena* spp., *Cynodon dactylon* (L.) Pers., *Digitaria sanguinalis* (L.) Scop., *Setaria viridis* (L.) Beauv. | | | | | | | | |

By analyzing the effectiveness of the treatments against the most common weeds (Fig. 6), excellent control was shown against *S. nigrum*. The best results were obtained

in $T3_{19}$ (79.2%) and $T2_{19}$ (78.1%), followed by $T5_{19}$ (76.0%). In the $T4_{19}$, a significantly lower result of 56.6% was recorded.

Additionally, with regard to P. *oleracea*, an average reduction of 53.2% compared to the control was recorded. In $T3_{19}$, the reduction was equal to 23.5%. Given the postponement of the mechanical treatments, *P. oleracea* with its prostrate habitus and deep taproot was more difficult to eradicate under these conditions.

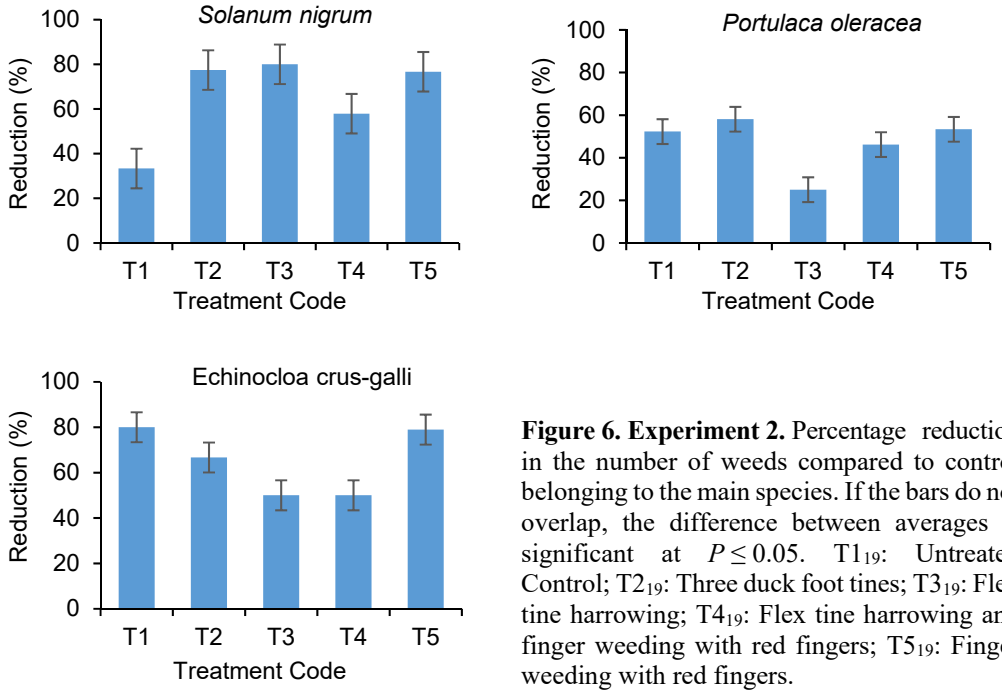


**Figure 6. Experiment 2.** Percentage reduction in the number of weeds compared to control belonging to the main species. If the bars do not overlap, the difference between averages is significant at $P \leq 0.05$. $T1_{19}$: Untreated Control; $T2_{19}$: Three duck foot tines; $T3_{19}$: Flex tine harrowing; $T4_{19}$: Flex tine harrowing and finger weeding with red fingers; $T5_{19}$: Finger weeding with red fingers.

In $T1_{19}$ amaranth demonstrated an excellent competitive effect against the most widespread monocot, *E. crus-galli*. This was attributable to the rapid and good ground coverage of the crop, starting from stage 15, and also from the limited leaf area of the weed. The most effective treatment in reducing this weed occurred in $T2_{19}$ (65.3%) and in $T5_{19}$ (79.8%).

Data on the ground cover of weeds and their density at the time of harvest (Table 6), confirm the good competitive ability of amaranth. A weed density of 55.8 $m^{-2}$ was found in T1, not significantly different from that observed in $T3_{19}$ and $T5_{19}$. This was also confirmed by the dry weight of the weeds which was 75.2 g $m^{-2}$. For this parameter, the results also highlighted how the combined $T4_{19}$ treatment was effective not only in reducing weed number, but above all in reducing weed development, significantly lowering dry weight to 39.3 g $m^{-2}$.

Table 6 also shows how some of the mechanical treatments negatively affected crop density. Compared to the average of 20.3 $m^{-2}$ plants in $T1_{19}$ and $T2_{19}$, plant number was significantly reduced to 7.9 with the flex tine harrowing associated with the finger weeder ($T4_{19}$). The negative effect of flex tine harrowing (machinery developed for cereal crops rather than dicots) was also due to the choice of the phenological phase in which to perform the treatments. This equipment should ideally be utilized as soon as

the deep taproot has formed in order to protect the plant from uprooting. However, given the unfavorable climatic conditions, treatments were performed coinciding with stage 13, evidently causing substantial damage to the hypogeal part of the crop.

**Table 6. Experiment 2.** Plant height, density, seed humidity and yield of the amaranth crop recorded at harvest, as well as total weed ground cover, density and dry weight

| | Weeds | | | Grain amaranth | | | |
|---|---|---|---|---|---|---|---|
| Treatment Code | Ground cover, % | Total weed density, n $m^{-2}$ | Dry weight, g $m^{-2}$ | Plant height, cm | Plant density, n $m^{-2}$ | Seed humidity, % | Seed yield, t $ha^{-1}$ |
| $T1_{19}$ | $67.7^{a}$ | $55.8^{a}$ | $75.2^{b}$ | 118.1 | $18.9^{ab}$ | 22.4 | $0.75^{c}$ |
| $T2_{19}$ | $51.6^{c}$ | $25.9^{b}$ | $49.5^{c}$ | 122.3 | $21.7^{a}$ | 24.8 | $0.99^{b}$ |
| $T3_{19}$ | $72.1^{a}$ | $47.2^{a}$ | $99.0^{a}$ | 119.5 | $15.7^{ab}$ | 23.1 | $0.94^{b}$ |
| $T4_{19}$ | $51.9^{c}$ | $26.9^{b}$ | $39.3^{c}$ | 133.2 | $7.9^{c}$ | 25.2 | $1.12^{a}$ |
| $T5_{19}$ | $59.7^{b}$ | $37.0^{ab}$ | $48.3^{c}$ | 124.5 | $15.5^{ab}$ | 23.0 | $0.98^{b}$ |
| *Significance* | ** | ** | ** | *ns* | * | *ns* | ** |

ns: not significant; *: significant at $p \leq 0.01$; **: significant at $p \leq 0.05$.Means within rows followed by the same letter(s) are not different at 5% level as per Tukey's test $T1_{19}$: Untreated Control; $T2_{19}$: Three duck foot tines; $T3_{19}$: Flex tine harrowing; $T4_{19}$: Flex tine harrowing and finger weeding with red fingers; $T5_{19}$: Finger weeding with red fingers.

Despite the lower plant density at harvest compared to that expected at sowing, the treatments using flex tine harrowing ($T3_{19}$) and the finger weeder ($T4_{19}$), as well as the combined equipment treatment ($T5_{19}$), did not result in significantly different yields. Seed production was on average of 1.0 t $ha^{-1}$. The lower plant density invariably stimulated side-branching with the development of secondary panicles to compensate for the lower seed production of the main panicle. This aspect resulted in a gradual maturation which was delayed over time, ensuing a higher seed humidity of 25.2% at harvest in T4, which was higher (although not significantly) than that in $T1_{19}$ and $T5_{19}$. Nonetheless, with the humidity levels in the seeds under open-field cultivation, drying is essential to attain the threshold level of 11–12% for safe storage.

Overall, the best yield of 1.12 t $ha^{-1}$ was obtained with the combined $T4_{19}$ treatment, which was significantly higher than the lowest yield of 0.75 t $ha^{-1}$ in the untreated control $T1_{19}$.

## CONCLUSIONS

Based on the seasonal trend recorded in Experiment 1, which resulted in a delay in both the sowing time and that of the mechanical treatments, it was not possible to completely assess the efficacy of the different treatments. Nonetheless, the predominant dicot weeds were effectively controlled under all treatments, contrary to that reported with interventions against monocots. Despite the fact that the various mechanical treatments were carried out over a period of time varying between 22 and 37 DAE, for the purposes of the competitive effects of the weeds on the crop, this interval selected is compatible with previous studies in another agroclimatic environment (Nurse et al., 2016). After 30 DAE, the problem shifts from the possible competitive effects to the difficulty of late mechanical intervention which is linked to the excessive development of both the crop and weeds.

Amaranth, at least in these experiments, proved to be an extremely competitive species against weeds starting from about 40 DAE at stage 15 corresponding to the 10 true leaf stage. Similar results were also obtained by Jena et al. (2009) and Shukla et al. (2014) in *Amaranthus hypochondriacus*, where the untreated control was compared with both hand weeding and the use of a herbicide in post-emergence.

The competitive ability of amaranth was also confirmed by the seed yield. Not only was the seed yield not significantly different between the treatments, but was also shown to be of a good level, exceeding 1.2 t $ha^{-1}$ on average. This characteristic was also confirmed to some degree in the second year of experimentation, even if strongly influenced by treatments and a lower plant density compared to the previous year. A plant density of less than 30 plants $m^{-2}$ was considered optimal according to Sooby et al. (1998) and Casini & La Rocca (2014). In addition, seed yield in the second year was also more strongly influenced by mechanical treatment compared to the first year.

The results of the single treatment repeated in both years (three duck foot tines; $T5_{18}$ and $T2_{19}$) confirmed the effectiveness of this equipment, even though it performed less well in controlling weeds, equivalent to 25%, in the second year.

Treatments with the flex tine harrower and finger weeder ($T3_{19}$, $T4_{19}$ and $T5_{19}$) negatively influenced the plant density at harvest, a clear sign necessitating adjustments in these interventions to achieve optimal results. However, the combined treatment ($T4_{19}$) was shown to be the best in weed control, specifically the dicot weeds. Furthermore, this treatment facilitated the rapid and extensive ground cover of the crop, providing a competitive advantage against weeds.

The present study suggests that all the mechanical methods for inter-row cultivation can be effectively used to control weeds in grain amaranth. However, there is a need to optimize strategies to anticipate and improve the ground cover of amaranth.

Single row width as a parameter does not significantly influence crop production on the experimental site. The choice of distance must be implemented according to the both type of machinery available and the soil type. Loose soils, for example, will easily permit treatment closer to the row using horizontal knives or rotating finger weeders. Instead for clay-rich soils, machinery with adequate crop guard systems would need to be used.'

Optimal plant density is a priority, as well as effectively choosing the correct distance between the rows according to easier mechanical control (Endres 1986; Jamriška 1998; Chaudhari et al. 2009; Olofintoye et al., 2011; Singh et al., 2017). According to Casini & Biancofiore (2020b), the use of double rows (18 + 60 cm) permitted taking advantage of a better ground cover than single rows, together with the possibility of mechanical treatments for weed control. Future research on the mechanical control of weeds in grain amaranth in Central Italy, should focus on the type of equipment, the false seedbed technique and the possible integration of thermal methods.

ACKNOWLEDGMENTS. A special thanks to all the staff of the 'Tenuta di Cesa (Arezzo) - Terre Regionali Toscane' for the competent and enthusiastic cooperation in conducting the experimental trail.

FUNDING. This study was supported by Tozzi Green S.p.A., Italy.

## REFERENCES


Alba, E., Polignano, G.B. & Notarnicola, L. 1997. Yield stability in a set of *Amaranthus* entries in Southern Italy. *Ital. J. Agron*. **1**, 65–71.

Allemann, J. & Denner, F.D.N. 2006. Allopathic influence of soils planted to *Amaranthus cruentus* L. on two tomato (*Lycopersicon esculentum* Mill.) cultivars. *South African J. of Plant and Soil* **23**(2), 142–143. doi 10.1080/02571862.2006.10634745

Ballabio, C., Uberti, F., Di Lorenzo, C., Brandolini, A., Penas, E. & Restani, P. 2011. Biochemical and immunochemical characterization of different varieties of Amaranth (*Amaranthus* L. ssp.) as a safe ingredient for gluten-free products. *J. Agric. Food Chem*. **59**(24), 12969–74. doi 10.1021/jf2041824

Batlla, D., Kruk, B.C. & Benech-Batlla Arnold, R.L. 2000.Very early detection of canopy presence by seeds through perception of subtle modifications in red-farred signals. *Funct. Ecol*. **14**(2), 195–202. doi 10.1046/j.1365-2435.2000.00418.x

Bavec, F. & Mlakar, S.G. 2002. Effects of soil and climatic conditions on emergence of grain amaranths. *Eur. J. Agron.***17**, 93–103. doi:10.1016/S1161-0301(01)00144-7

Brenner, D.M., Baltensperger, D.D., Kulakow, P.A., Lehmann, J.W., Myers, R.L., Slabbert, M.M. & Sleugh, B.B. 2000. Genetic resources and breeding of *Amaranthus*. *Plant. Breed. Rev*. **19**, 227–285.

Brenner, D.M., Johnson, W.G., Sprague, C.L., Tranel, P.J. & Young, B.G. 2013. Crop-weed hybrids are more frequent for the grain amaranth 'Plainsman' than for 'D136-1'. *Genet. Resour. Crop Evol*. **60**, 2201–2205. doi 10.1007/s10722-013-0043-8

Brust, J., Claupein, W. & Gerhards, R. 2014. Growth and weed suppression ability of common and new cover crops in Germany. *Crop Protection* **63**, 1–8. doi 10.1016/j.cropro.2014.04.022

Carlsson, R. 1980. Quantity and quality of *Amaranthus* grain from plants in temperate, cold and hot, and subtropical climates-A review. In *Proceedings of the Second Amaranth Conference*, p. 48. Rodale Press, Emmaus, PA.

Casini, P. & Biancofiore, G. 2020a. Optimizing sowing time for boosting productivity and nutritional quality of amaranth (*Amaranthus cruentus* L.) genotypes under Mediterranean climate. *Acta Agriculturae Slovenica* **115**(1), 183–191. doi 10.14720/aas.2020.115.1.1228

Casini, P. & Biancofiore, G. 2020b. Influence of row spacing on canopy and seed production in grain amaranth (*Amaranthus cruentus* L.). *Agron. Res*. **18**(1), 53–62. doi doi.org/10.15159/AR.20.015

Casini, P. & La Rocca, F. 2014. *Amaranthus cruentus* L. is suitable for cultivation in Central Italy: field evaluation and response to plant densities. *Ital. J. Agron*. **9**(602), 166–175. doi: 10.4081/ija.2014.602

Chaudari, D.I., Desai, L.J. & Kalal, P.H. 2019. Effect of Integrated Weed Management on Growth, Yield, Yield Attributes and Economics of Grain Amaranth (*Amaranthus hypochondriacus* L.) under South Gujarat Condition. *Int. J. Curr. Microbiol. App*. **8**(7), 2598–2604. doi: org/10.20546/ijcmas.2019.807.320

Chaudhari, J.H., Raj, V.C., Srivastava, R.K. & Ahir, M.P. 2009. Effect of varying sowing date and row spacing on yield attributes and yield of rabi grain amaranth (*Amaranthus hypochondriacus* L.) under south Gujarat conditions. *Agric. Sci. Digest* **29**(2), 65–68.

Connick, W.J., Bradow, J.M. & Legendre, M.G. 1989. Identification and Bioactivity of Volatile Allelochemicals from Amaranth Residues. *J. of Agric. and Food Chem*. **37**(3), 792–796. doi 10.1021/jf00087a049

Coolman, R.M. & Hoyt, G.D. 1993. The effect of reduce tillage on soil environment. *Hort. Technol*. **3**, l43–145.

Downton, W.J.S. 1973. *Amaranthus edulis.* A high lysine grain amaranth. *World Crops* **25**, 20.

El Gendy, A.N.G., Tavarini, S., Conte, G., Pistelli, L., Hendawy, S.F., Omer, E.A. & Angelini, L.G. 2018. Yield and qualitative characterisation of seeds of *Amaranthus hypochondriacus* L. and *Amaranthus cruentus* L. grown in Central Italy. *Ital. J. Agron*. **13**(1), 63–73. doi 10.4081/ija.2017.993

Endres, C.S. 1986. Influence of production practices on yield and morphology of *Amaranthus cruentus* and *Amaranthus hypochondriacus*. M.S. Thesis, Univ. of Arkansas, Fayetteville.

Ercoli, L., Masoni, A. & Massantini, F. 1987. Influenza della fertilizzazione azotata sulla produzione di proteine da amaranto e chenopodio attraverso il frazionamento umido. *Agric. Med*. **117**, 131–139.

Gélinas, B. & Seguin, P. 2008. Evaluation of management practices for grain Amaranth production in Eastern Canada. *Agron. J*. **100**(2), 344–350. doi: 10.2134/agronj2007.0189

Gimplinger, D.M., Dobos, G., Schonlechner, R. & Kaul, H.P. 2007. Yield and quality of grain amaranth (*Amaranthus* sp.) in Eastern Austria. *Plant Soil Environ.* **53**(3), 105–112. doi: 10.17221/2224-pse

Granados, S.D. & Lòpez, R.G.F. 1990. Chinampas: historia y etnobotanica de la 'alegria' (*Amaranthus hypocondriacus* L.). En: El amaranto *Amaranthus* spp. Su cultivo e aprovechamiento. Montecillo, Mexico.

Gresta, F., Meineri, G., Oteri, M., Santonoceto, G., Lo Presti, V., Costale, A. & Chiofalo, B. 2020. Productive and qualitative traits of *Amaranthus cruentus* L.: An unconventional healthy ingredient in animal feed. *Animals* **10**(8), 1428, 1–18. doi 10.3390/ani10081428

Hackmam, D. & Myers, R. 2003. Market opportunities for grain amaranth and buckwheat growers in Missouri. *Report to the Federal-State Marketing Improvement Program*, Washington, DC.

Han-Ping, H. & Corke, H. 2003. Oil and squalene in *Amaranthus* grain and leaf. *J. Agric. Food Chem*. **51**(27), 7913–7920. doi: 10.1021/jf030489q

Jamriška, P. 1998. The effect of variety and row spacing on seed yield of Amaranth (*Amaranthus* ssp.). *Rostlinna Vyroba* **44**(2), 71–76.

Jena, S.N., Sahu, P.K., Nayak, A. & Tripathy, S. 2009. Crop weed competition in grain amaranth (*Amaranthus hypochondriacus*). *Environ. and Ecol*. **27**(3), 1200–1201.

Kauffman, C.S. & Weber, L.E. 1990. Grain amaranth. In: Janick J, Simon J.E. (eds), *Advances in new crops*, Timber Press, Portland, Oregon, USA, pp. 127–139.

Knezevic, S.Z., Evans, S.P., Blankenship, E.E., Van Acker, R.C. & Lindquist, J.L. 2002.Critical period for weed control: the concept and data analysis. *Weed Sci.* **50**, 773–786. doi 10.1614/0043-1745(2002)050[0773:CPFWCT]2.0.CO;2.

Kudsk, P., Taberner, A., de Troiani, R.M.D., Sánchez, T.M. & Mathiassen, S.K. 2012. Herbicide tolerance and seed survival of grain amaranth (*Amaranthus* sp.). *Austr. J. of Crop Sci*. **6**(12), 1674–1680.

Lovelli, S., Pizza, S., Capolnio, T., Gherbin, P. & Perniola, M. 2005. Analisi di crescita e valutazione agronomica di alcune specie erbacee a basso tenore di glutine. In: Proceedings of 34th *Congress of the Italian Society of Agronomy*. 20–22 September, Foggia, Italy, 298–299.

Maabel, E. van der. 1979. Transformation of cover-abundance values in phytosociology and its effects on community similarity. *Vegetatio* **39**(2), 97–114. doi 10.1007/BF00052021

Martínez-Núñez, M., Ruiz-Riva, M., Vera-Hernández, P.F. & Bernal-Muńoz, R. 2019. The phenological growth stages of different amaranth species grown in restricted spaces based in BBCH code. *South African J. of Bot*. **124**, 436–443. doi.org/10.1016/j.sajb.2019.05.035

Massantini, F., Masoni, A. & Ercoli, L. 1987. Potenzialità agronomiche dell'amaranto e del chenopodio come specie adatte al frazionamento umido: prove biennali. *Agric. Med*. **117**, 31–41.

Morse, R.D. 1993. Components of sustainable production systems for vegetables conserving soil moisture. *Hort. Tech*. **3**, 211–214.

Mulandana, N.S., Mamadi, N.E., Du Plooy, C.P. & Beletse, Y.G. 2009. Effect of spacing and transplanting time on amaranth yield. *African Crop Sci. Conference Proceedings* **9**, 243–246.

Nurse, R.E., Obeid, K. & Page E.R. 2016. Optimal planting date, row width, and critical weed-free period for grain amaranth and quinoa grown in Ontario, Canada. *Can. J. Plant Sci*. **96**, 360–366. doi: Dx.doi.org/10.1139/cjps-2015-0160

Ojo, D.O. 1997. Effect of weeding frequencies on grain amaranth (*Amaranthus cruentus* L.) growth and yield. *Crop Protection* **16**(5), 463–466. doi: 10.1016/S0261-2194(97)00017-3

Olofintoye, J.A.T., Adeniyi, H.A. & Olagorite, A.A. 2011. Effects of phosphorus fertilizer and intra row spacing on the growth and yield on grain amaranth (*Amaranthus cruentus*). *Agric. J*. **6**(6), 366–368.

Omani,E.N., Haigh,A.M., Medd,R.W. & Nicol,H.I. 1999. Changes in germinability, dormancy and viability of *Amaranthus retroflexus* as affected by depth and duration of burial. *Weed Res*. **39**, 345–354.

Peiretti,E.G. & Gesumaria,J.J. 1998. Effect of interrow spacing on growth and yield of grain amaranth (*Amaranthus* spp). *Investigación Agraria, Producción y Protección Vegetales* **13**(1/2), 139–151.

Petr, J., Michalik, I., Tlaskalova, H., Capouchova, I., Famera, O., Urmiska, D., Tukova, L. & Knoblochova, H. 2003. Extension of the spectra of plant products for the diet in celiac disease. *Czech J. Food Sci*. **21**, 59–70.

Pulvento, C., Lavini, A., Riccardi, M., D'Andria, R. & Ragab, R. 2015. Assessing amaranth adaptability in a Mediterranean area of South Italy under different climatic scenarios. *Irr. and Drain.* **64**(1), 50–58. doi 10.1002/ird.1906

Pulvento, C., Sellami, M.H. & Lavini A. 2021. Yield and quality of *Amaranthus hypochondriacus* grain amaranth under drought and salinity at various phenological stages in southern Italy. *J. of the Sci. of Food and Agric*. doi: doi.org/10.1002/jsfa.11088

Rivelli, A.R., Gherbin, P., De Maria, S. & Pizza, S. 2008. Field evaluation of *Amaranthus* Species for Seed and Biomass Yields in Southern Italy. *Ital. J. Agron*. **3**(3), 225–229. doi :10.4081/ija.2008.225

Russell, R.S. 1977. Plant Root Systems: Their Function and Interaction with the Soil. Mc Graw Hill Press Company (UK) Ltd, London.

Sauer, J.D. 1950. The grain amaranths: A survey of their history and classification. *Ann. Mo. Bot. Gard.* **37**, 561–632.

Saunders, R.M. & Becker, R. 1984. *Amaranthus*: A potential food and feed resource. In: *Advances in cereal science and technology, volume VI*. American Association of Cereal Chemists, INC MN., 357–397.

Shukla, D.K., Prasad, B. & Pratap, T. 2014. Weed management strategies for better yield and economics of grain amaranth (*Amaranthus hypochondriacus*) in mountain agriculture. *J. of Hill Agric.* **5**(2), 194–197.

Singh, M.C., Phogat, B.S. & Raiger, H.L. 2017. Effect of different weed control practices on grain amaranth (*Amaranthus hypochondriacus* L.). *Int. J. of Sci. Env*. **7**(1), 849–853.

Sooby, J., Myers, R., Bettensperger, D., Brenner, D., Wilson, R. & Block, C. 1998. Amaranth. Production manual for the Central United States. A guide to growing and marketing. University of Nebraska High Plains Ag Lab, Sidney, Nebraska (USA), pp. 24.

Teasdale, J.R. & Daughtry, C.T. 1993. Weed suppression by live and desiccated hairy vetch (*Vicia villosa*). *Weed Sci.* **41**(2), 207–212. doi: 10.1017/S0043174500076074

Tejeda-Sartorius, O., Vaquera-Huerta, H. & Cadena-Iñiguez, J. 2011. Effect of amaranth residues (*Amaranthus hypochondriacus* L.) on weed control and yield of radish, onion and carrot. *Spanish J. of Agric. Res*. **9**(1), 284–295. doi: Doi.org/10.5424/sjar/20110901-040-10

Tucker, J.B. 1986. Amaranth: the once and future crop. *Bio Science* **36**(1), 9–13.

Turchi, F. 1987. L'amaranto: una coltura poco nota ricca di interessanti prospettive. *Rivista di Agricoltura Subtropicale e Tropicale* **57**(1–2), 89–116.

*Agronomy Research* **20**(1), 91–102, 2022
https://doi.org/10.15159/AR.22.016

# Breeding and genetic improvement of soft winter wheat with the use of spelt wheat

I.P. Diordiieva[1,*], L.O. Riabovol[1], Ya.S. Riabovol[2], O.P. Serzhuk[1], Iu.I. Nakloka[3], O.P. Nakloka[4] and S.P. Karychkovska[5]

[1]Uman National University of Horticulture, Faculty of Agronomy, Department of Genetics, Plant Breeding and Biotechnology, 1 Institytska Str., UA20300 Uman, Ukraine
[2]Limagrain Ukraine LLC, 55 Turgenevskaya Str., UA04050 Kiev, Ukraine
[3]Uman National University of Horticulture, Faculty of Agronomy, Department of General Agriculture, 1 Institytska Str., UA20300 Uman, Ukraine
[4]Uman National University of Horticulture, Faculty of Agronomy, Department of Vegetable growing, 1 Institytska Str., UA20300 Uman, Ukraine
[5]Uman National University of Horticulture, Faculty of Management, Department of Ukrainian and foreign languages, 1 Institytska Str., UA20300 Uman, Ukraine
[*]Correspondence: diordieva201443@gmail.com

Received: February 15th, 2022; Accepted: April 1st, 2022; Published: April 13rd, 2022

**Abstract.** In the process of carrying out studies as a result of hybridization of soft wheat with spelt wheat, a number of new forms that differ in morphobiological and economically valuable features were obtained. The aim of the research was to expand the genetic diversity of soft wheat by hybridization with spelt wheat, analysis of the heterotic effect in hybrids in order to systematize the samples and obtain valuable original forms for the breeding process of creating high-yielding varieties.

As a result of research the breeding technology of creating high-yielding forms of soft winter wheat by cross-species hybridization of *Triticum aestivum* L. × *Triticum spelta* L. has been improved. It has been determined that the plant height and ear length in hybrids are inherited by type of intermediate inheritance or negative dominance, the number of grains in the ear - by type of intermediate inheritance or positive dominance; ear grain weight - by type of superdominance or positive dominance. In $F_2$ hybrids there is a dihybrid cleavage into forms with speltoid, squarehead and typical ear with a quantitative predominance of speltoid plants, which indicates the control of the 'ear shape' indication by two non-allelic genes. The ear shape of the soft wheat original varieties in relation to speltoid varieties turned out to be a recessive trait, but at the same time it was dominant to a squarehead form. Regardless of the genotypes of soft wheat included in the combination of crossbreeding with spelt wheat, red color ear indication was determined by a monogenic type of inheritance. Varieties of soft winter wheat Artaplot, Umanska Tsarivna and Freya have been created, which are included in the State Registry of Plant Varieties Suitable for Distribution in Ukraine and recommended for cultivation in Polissia.

**Key words:** intraspecific hybridization, inheritance of characteristics, ear morphotype, grain quality, productivity, variety.

## INTRODUCTION

The main directions in wheat breeding are the creation of high-yielding varieties with excellent grain quality (Guzman et al., 2016). However, in recent years there has been a tendency to yield increase along with a marked decline in grain quality (Rybalka, 2011). That is why a number of scientific institutions are currently conducting breeding work to create high-yielding and high-quality wheat varieties resistant to adverse environmental factors.

World practice has shown that an effective method of breeding is the crossing of geographically distant forms, but the success of breeding work depends on the successful selection of hybridization components, namely the initial material (Rybalka, 2011; Xie et al., 2015). To create new varieties of wheat that would meet the requirements of modern agricultural production, it is advisable to use genetically distant forms (Peleg et al., 2011; Polyanetska, 2012). At the same time wild, semi-wild and forgotten forms are often the donors of high content of protein, gluten, lysine and resistance to diseases and pests.

In particular, spelt wheat is used as a donor of valuable characteristics as it is a donor of high protein content and contains almost all the nutrients in a harmonious and balanced state that a human body needs. The researches of domestic and foreign breeders have shown a positive effect of hybridization of soft and spelt wheat, in particular a significant expansion of existing genetic diversity and getting new forms of wheat that combine high protein and gluten content of spelled and high productivity of wheat (Polyanetska, 2012; Guzman et al., 2016). However, according to Rybalka (2011) it is undesirable to carry out such crossings as it leads to spelt quality deterioration and soft wheat inheritance of complicated grain threshing and ear fragility.

Breeders in a number of countries around the world are improving the quality of wheat by hybridizing it with spelt. In this direction, some progress has been made in Switzerland, Austria and Serbia, where spelt varieties Bauländer, Schwabenkorn, Frankenkorn (Austria), Nirvana (Serbia), Altgold Rotkorn (Sweden) have been created (Dvorak et al., 2012). In Ukraine, extensive research in this area has been conducted at Uman National University of Horticulture, Ukrainian Scientific Institute of Plant Breeding and the Plant Production Institute named after V. Ya. Yuriev.

We conducted a number of studies on the hybridization of soft wheat and spelt wheat, which made it possible to form a collection of samples from the resulting variety of breeding materials unique in morphological, biological and biochemical characteristics. They are a source of valuable genetic plasma to improve existing and create new varieties of wheat.

**The aim** of our research was to expand the genetic diversity of soft wheat by hybridization with spelt wheat, to analyse the heterosis effect in hybrids to systematize the created samples and obtain valuable original forms by involving them in the breeding process to create high-yielding varieties.

## MATERIALS AND METHODS

Research on the breeding and genetic improvement of soft winter wheat with the use of spelt wheat began in 2006 under the direction of Dr. F. M. Parii in the research field of the Department of Genetics, Plant Breeding and Biotechnology of Uman

National University of Horticulture, located in Uman, Cherkasy region, the zone of the Right Bank Forest-Steppe of Ukraine, the subzone of unstable moisture.

As an initial material for hybridization regionalized varieties of soft wheat Favorytka, Smuglianka, Podolianka, Zolotokolosa, Harus, Bila Tserkva semi-dwarf, Myrhad, Kryzhynka, Farandol, Yermak, Selianka, Panna, Krasnodarska 99 and spelt wheat Zoria Ukrainy were involved. Hybridization was performed by manual emasculation of flowers and subsequent controlled pollination by the restricted method. Emasculated spikelets of the female parent together with the male parent were placed under a parchment insulator.

To determine the nature of the quantitative trait inheritance by the dominance degree (hp), the formula of Griffing (1950) and the gradation of Beyl & Atkins (1965) were used:

$$hp = (F_1 - MP)/(P_{max} - MP), \quad (1)$$

where hp – dominance assessment; $F_1$ – arithmetic mean of first generation hybrids; $P_{max}$ – arithmetic mean of the male parent with the highest manifestation of the trait; MP – arithmetic mean of two parent forms.

The created material ranking due to the dominance degree was performed according to the following gradation: 1) $hp < -1$ – negative superdominance (negative heterosis, or depression); 2) $-1 \leq hp < -0.5$ – negative dominance; 3) $-0.5 \leq hp \leq 0.5$ – intermediate inheritance; 4) $0.5 < hp \leq 1$ – positive dominance; 5) $hp > 1$ – positive superdominance (positive heterosis).

The share of original and hypothetical heterosis was calculated by the formulas of Daskalev et al (1967):

$$\text{true heterosis: } X = (F_1 - P_{max}) \times 100 / P_{max}, \quad (2)$$

where $F_1$ – the value of the hybrid trait; $P_{max}$ – the highest trait value of one of the parents.

$$\text{hypothetical heterosis: } X = F_1 \times 100 / MP, \quad (3)$$

where $F_1$ – the value of the hybrid trait; MP – arithmetic mean of the two initial forms.

Correspondence of cleavage in $F_2$ hybrid combinations was theoretically expected using $\chi 2$ (Dospekhov, 1985).

Testing of the created materials was carried out during 2013–2020 under the conditions of Uman National University of Horticulture. All accounting and observation were carried out in accordance with the 'State qualification methodology of plant varieties expertise on definition of suitability for distribution in Ukraine (grains, grouts, and leguminous species)' (2012). Soft winter wheat Podolyanka variety was the standard. A systematic method of plots placement was used in the research. The numbers were arranged in blocks with a plant density of 400 thousand pcs per ha under four-time repetition.

Plant height was measured in the field before harvesting. Biometric indicators (ear length and plant height) were determined on 50 plants selected from each plot in two non-contiguous replicates. Wheat sample grouping by plant height was performed according to the method of Dorofeev et al. (1987). Quality indicators (gluten and protein content in grain, flour strength) were determined by infrared spectroscopy using the

Infratec™ Nova instrument (FOSS Analytical, Sweden). After accounting and measurements, grain was threshed and yield was determined.

The reliability of research, the degree of features variation and the significance of differences between indicators of laboratory tests (protein and gluten content) were determined at the level of significance of $P \leq 0.01$, for field studies - $P \leq 0.05$, for hybridological analysis - $P \leq 0.001$ using statistical analysis program (SAS) v. 9.1.3. The variation coefficient (Cv, %), standard deviation (S) and experimental error (Sx) were determined by the method of E. R. Ehrmantraut et al. (2000) and the use of MS Excel program.

Formal and qualification examination of the created varieties was carried out in 19 branches of the Ukrainian Institute for Plant Variety Examination of different regions and geographical zones of Ukraine (Steppe, Forest-Steppe, Polissia): Artaplot variety during 2016–2018, Umanska Tsarivna variety - 2018–2020, Freia variety - 2019–2021.

## RESULTS AND DISCUSSIONS

Spelt wheat is a hexaploid species of wheat with a similar to soft wheat genomic composition ($A^uBD$), so their hybridization is relatively easy, although there are some issues related to the morphological structure of plants (spelt is tall, while varieties for hybridization are mostly short and semi-dwarf) and flowering period.

In the spelt study a pollinator is usually used. However, there was a small proportion of cross combinations with positive progeny transgressions, where spelt was the female parent. In most cross-breeding combinations where soft wheat was used as the female parent, an average level of cross-compatibility was observed (25.3–35.4% of seed formation). In cross-breeding combinations where spelt wheat was the female parent, a low level of seed formation was recorded - 7.8–19.5%, indicating low cross-compatibility of spelt wheat.

**Dominance degree and analysis of heterosis effect of breeding-valuable features.** Seeds obtained as a result of hybridization were sown in a breeding nursery for splitting and grouping analysis of mixed materials due to phenotype. In some other variants, backcrossing was carried out to enrich the forms with economically valuable genes. $F_1$ progeny were evaluated for the equal decline of economically valuable features and heterosis display. Complex analysis of the inheritance patterns of a particular feature makes it possible to conduct targeted breeding in subsequent generations (Kochmarskij et al., 2012). However, heterosis amount of first-generation of wheat hybrids can vary widely, and its level does not always predict the emergence of valuable transgressive forms in fissile generations, as the first hybrid generation may have interallelic gene interactions that are not inherited by subsequent generations. Therefore, this indicator should be analyzed in a complex according to all criteria, which provides greater efficiency of breeding (Prasad et al., 1998).

In the result of the study it was found that that five of 16 singled out forms have inherited plant height by intermediate type, four hybrids showed negative dominance, two - depression (Table 1). Three crossbreeding combinations showed positive dominance and one - positive dominance of the tall-growing parent form.

**Table 1.** Degree of dominance and level of heterosis according to the main economically valuable indicators of soft winter wheat samples obtained by interspecific hybridization with spelt wheat

| Trait | Degree of dominance and level of heterosis | Sample and combination of crossing | | | | | | | | | | | | | | |
|---|---|---|---|---|---|---|---|---|---|---|---|---|---|---|---|---|
| | | 255 (Krasnodarska 99 × Zoria Ukrainy) | 268 (Farandol × Zoria Ukrainy) | 270 (Zoria Ukrainy × Farandol) | 278 (Panna × Zoria Ukrainy) | 302 (Zoria Ukrainy × Panna) | 305 (Yermak × Zoria Ukrainy) | 308 (Selianka × Zoria Ukrainy) | 313 (Smuhlianka × Zoria Ukrainy) | 340 (Zolotokolosa × Zoria Ukrainy) | 348 (Zoria Ukrainy × Zolotokolosa) | 358 (Kopylivchanka × Zoria Ukrainy) | 364 (Harus × Zoria Ukrainy) | 365 (Kryzhynka × Zoria Ukrainy) | 370 (Favorytka × Zoria Ukrainy) | 375 (Podolianka × Zoria Ukrainy) |
| Plant height | Degree of dominance, (hp) | 0.75 | -0.74 | 0.61 | 0.29 | 0.57 | -1.42 | -0.72 | -0.38 | -0.33 | 0.33 | -1.71 | -0.63 | -0.87 | 1.17 | -0.38 |
| | The nature of inheritance | PPD | PNI | PPD | II | PPD | D | PNI | II | II | II | D | PNI | PNI | PS | I I |
| | True heterosis, % | -4.6 | -31.3 | -7.0 | -11.6 | -7.00 | -33.6 | -36.0 | -20.9 | -18.6 | -18.6 | -44.1 | -36.0 | -33.6 | 2.30 | -20.9 |
| | Hypothetical heterosis, % | 112.6 | 88.6 | 109.5 | 103.9 | 107.8 | 83.7 | 86.7 | 95.1 | 96.2 | 96.2 | 76.5 | 87.6 | 86.6 | 113.5 | 95.1 |
| Ear length | Degree of dominance, (hp) | -0.86 | -0.90 | 0.05 | -0.60 | 0.28 | -0.72 | -0.68 | -0.89 | -0.54 | 0.34 | -0.64 | -0.91 | -0.63 | -0.29 | -0.27 |
| | The nature of inheritance | PNI | PNI | II | PNI | II | PNI | PNI | PNI | PNI | II | PNI | PNI | PNI | II | II |
| | True heterosis, % | -33.5 | -38.0 | -19.0 | -30.4 | -13.9 | -31.6 | -33.5 | -33.5 | -29.7 | -12.7 | -31.6 | -39.9 | -31.0 | -25.3 | -24.6 |
| | Hypothetical heterosis, % | 81.1 | 77.5 | 101.2 | 85.9 | 106.3 | 83.7 | 83.0 | 80.8 | 87.1 | 108.2 | 84.7 | 76.0 | 85.2 | 92.9 | 93.3 |
| Grain number in the ear | Degree of dominance, (hp) | 1.0 | -0.50 | 1.50 | 2.20 | 0.60 | 0.71 | 2.50 | 0.33 | 0.43 | -0.43 | 0.50 | -0.20 | 1.00 | 1.33 | 0.50 |
| | The nature of inheritance | PPD | PNI | PS | PS | PPD | PPD | PS | II | II | II | II | II | PPD | PS | II |
| | True heterosis, % | 0.00 | -6.25 | 2.08 | 6.12 | -2.04 | -1.96 | 6.25 | -4.00 | -4.00 | -9.80 | -2.08 | -6,12 | 0.00 | 2.00 | -3.85 |
| | Hypothetical heterosis, % | 106.4 | 97.8 | 106.5 | 111.8 | 103.2 | 105.3 | 110.9 | 102.1 | 102.1 | 96.8 | 102.2 | 98.9 | 106.4 | 108.5 | 104.2 |
| Grain weight of the ear | Degree of dominance, (hp) | 1.87 | 2.54 | -0.53 | 2.53 | -0.12 | 0.62 | 0.00 | 0.75 | 1.38 | 0.10 | 1.67 | 1.33 | 0.19 | 1.36 | 0.94 |
| | The nature of inheritance | PS | PS | PNI | PS | II | PPD | II | PPD | PS | II | PS | PS | II | PS | PPD |
| | True heterosis, % | 10.1 | 6.1 | -16.9 | 14.0 | -10.2 | -3.3 | -7.3 | -2.6 | 4.1 | -9.8 | 5.9 | 2.7 | -7.9 | 3.7 | -0.5 |
| | Hypothetical heterosis, % | 124.6 | 110.4 | 93.4 | 125.4 | 98.8 | 106.0 | 100.0 | 108.7 | 116.8 | 101.2 | 116. | 112.0 | 102.1 | 115.5 | 110. |

Note: * PS – heterosis (positive superdominance); PPD – partial positive dominance; II intermediate inheritance; PNI– partial negative inheritance; D – depression (negative dominance).

In general, from the $F_1$ population, plants of sample 358 (78 cm) were characterized by the lowest stem obtained with the use of soft winter wheat variety Kopylivchanka, and the highest - samples created by hybridization of Krasnodarska 99 × Zoria Ukrainy (112 cm) and Favorytka × Zoria Ukrainy (118 cm).

Negative dominance was observed in most singled out forms. Only five hybrids had intermediate inheritance. The use of spelt wheat as the female parent provided ear elongation in first-generation hybrids. Exactly such hybrids were characterized by the longest ear (12.8–13.8 cm) and trait intermediate inheritance (hp = 0.05–0.34). It should be noted that these hybrids, despite the ear elongation, had significant inferior to spelt in this indicator. Therefore, in all other selected samples there was a negative value of original heterosis at the level of - 12.7–19.0%. The number of grains in the ear in most progeny is inherited by intermediate inheritance type and partial positive dominance, while the grain weight of the ear - by type of over dominance.

**The inheritance of breeding and valuable traits.** $F_1$ hybrids were monotypic in ear morphological structure and were characterized by a speltoid shape, glume red color and awnlessness, which indicate the dominance of the speltoid inheritance. Seeds of $F_1$ hybrids were sown by the spaced planting in a breeding nursery. After the end of the growing season in $F_2$ hybrids, the phenotypic manifestation of ear morphology was assessed. In the $F_2$ progeny, 412 plants out of 546 had traits of spelt wheat, 85 - of soft wheat and 49 - of squarehead wheat (Table 2).

**Table 2.** Hybridological analysis of $F_2$ progeny segregation by phenotype

| Trait | Ear phenotype | Segregation | | | | |
|---|---|---|---|---|---|---|
| | | actual | expected | ratio | $\chi$ 2 actual | $\chi$ 2 theo |
| Ear form | spelt | 412 | 410 | 12 : 3 : 1 | 4.19* | 5.99 |
| | soft wheat | 85 | 99 | | | |
| | squarehead | 49 | 37 | | | |
| Awn availability | awnedness | 428 | 410 | 3 : 1 | 3.17* | 3.84 |
| | awnless | 118 | 136 | | | |
| Ear color | red | 424 | 410 | 3 : 1 | 1.92* | 3.84 |
| | white | 122 | 136 | | | |

Note: * – the value of $\chi$ 2 is significant at the level $P \leq 0.001$.

Thus, in $F_2$ there was a quantitative advantage of plants with speltoid ear shape over plants with of squarehead and natural shape. The typical ear shape in comparison with the speltoid shape was recessive, but at the same time it was dominant relative to the squarehead shape. The peculiarity of hybrid segregation is the dominance of the trait 'squarehead ear', which was not among the parent forms. In subsequent generations, the segregation of forms with a compact ear type (short, ultra-dense ear) was also observed.

According to a number of studies, the Q gene located in the long arm of chromosome 5A is essential in the formation of speltoid shape of wheatear. It belongs to the family of transcription factors APETALA-2, which control the flower development (de Faris et al., 2003). The change of only one pair of nucleotides in the alleles of the Q gene led to the emergence of an ear with an elastic stem and spikelets that easily peel (recessive allele) instead of long, brittle stem, which has a difficult threshing ear

(dominant allele), which was fundamental in wheat cultivation (Gil-Humanes et al., 2009). The q-5D and q-5B genes are thought to be involved in inhibition of speltoid trait. The influence of regulatory genes is not excluded, because even a single mutation in their sequence can lead to significant changes in the phenotype (Kosuge et al., 2012).

The squarehead trait may have a different genetic nature. Polysomy, aberrations or gene mutations can cause it. The latter can be monogenic recessive, monogenic dominant and dominant with a recessive epistasis manifestation (Kosuge et al., 2012). The formation of plants with a squarehead ear shape among hybrid progeny is due to the dominant gene C and a number of recessive genes expressed in the Q gene presence. Ear density is also regulated by extension genes $L_1$, $L_2$. In the presence of recessive alleles of all these genes (genotype $ccl_1l_1l_2l_2$), hexaploid wheat develops a short, dense clavate ear of 'squarhead' type. In the absence of ear extension genes, common wheat forms short and dense ear and becomes square-headed or clavate-shaped (Simonov et al., 2016).

Populations of $F_2$ hybrids were studied on the basis of awnedness of ear. Soft wheat awnedness is a recessive trait that is not seen in $F_1$ hybrids and is found in the second generation, regardless of the morphological structure of the ear. In our studies, the cleavage into awnless and awned forms was 410 : 136 ($\chi 2 = 3.17$), which is significantly consistent with the monogenic cleavage of 3 : 1. A number of studies have found that the genes of almost all wheat chromosomes can affect the display of the 'awnedness-awnlessness' trait. In addition, modifier genes, genotypic environment, and regulatory genes affect too (Sichkar et al., 2016). However, most scientists believe that awnlessness is controlled by a single dominant $B_1$ gene of chromosome 5AL. Awnlessness in $F_1$ hybrids inherited from spelt and segregation of awned forms among $F_2$ hybrids confirm the dominance of awnlessness over awnedness (Morhun & Oksom, 2011; Mukhordova, 2015).

Genetic analysis of the hybrid segregation obtained by crossing varieties with red and white ears and conducted by a number of scientists indicates the monogenic nature of this trait inheritance. Dominant allele concentration in the genome determines the intensity of coloration (Filipchenko, 1979; Nilsson-Ehle, 1909; Khlestkina et al., 2016). However, when crossing some red-eared varieties with white-eared ones Nilsson-Ehle (1909) found splitting both 3 : 1 and 15 : 1 with different red color gradations. Now three genes have been identified that determine the red color of the ear: Rg1, localized on chromosome 1BS, $Rg_2$ – on chromosome 1DS, $Rg_3$ – on chromosome 1AC (Khlestkina et al., 2009; Khlestkina et al., 2016).

Our researches have shown that when crossing soft wheat with spelt, the red color of the ear in $F_2$ hybrids has a constant tendency of permanent dominance over its white color. The experiment revealed 424 red-eared and 122 white-eared plants, which significantly corresponded to the ratio of 3 : 1 ($\chi^2 = 1.92$). Thus, regardless of the genotypes of soft wheat varieties included in the combination of crossbreeding with spelt, the trait of the red color of the ear showed a dominant monogenic nature of inheritance.

Subsequent generations of hybrids *Triticum aestivum* L. × *Triticum spelta* L. showed further cleavage by ear morphology and except spelt, squarehead and typical forms, intermediate forms were observed between soft and spelt wheat and densely

spiked samples. In order to systematize obtained progeny, we proposed a classification according to the morphological structure of the ear, due to which all the obtained material is divided into six morphotypes: spelt, speltoid, a form with a typical soft wheat ear, squarehead, subcompactoid and compactoid (Diordiieva et al., 2018).

The most valuable from a practical point of view are speltoid forms with a typical soft wheat ear and squarehead forms, because they have a well-grained ear with easy grain threshing, which provides high crop yields. Spelt is not characterized by high ear grain content, and, as a result, it has lower productivity. However, the main hindrance to its manufacturing application is the complicated grain threshing (about 60%), which complicates the process of their mechanized harvesting. Forms with a long low-density ear have a number of advantages, in particular rapid ear drying after the rain, which reduces the susceptibility of plants to disease and the formation of large grains with excellent technological properties. In such forms, high pollen fertility and yield have been observed.

**Analysis of hybrids of *Triticum aestivum* L. × *Triticum spelta* L. in terms of productivity and quality of grain.** In order to identify donors of certain economic and valuable traits, the created samples were analyzed according to the level of their display. The research analyzes newly created wheat samples and previously created stable forms that are stored in the genetic collection of the Department of Genetics, Plant Breeding, and Biotechnology. All created materials, taking into account the general plant habits and morphological structure of the ear, were divided into soft wheat, spelt and intermediate (spelt-like) forms. The group of soft wheat included samples with a medium-dense or dense ear (16–28 spikelets per 10 cm of ear) with a typical glume and easy grain threshing. The group of spelt wheat combines forms with a long low-density ear (< 16 spikelets per 10 cm of ear), coarse glume and complicated grain threshing. Spelt-like group include samples that occupied an intermediate position between the parental forms in terms of the morphological structure of the ear. The range of variability on the basis of 'plant height' trait was 52–129 cm. Created samples, according to the classification of Dorofeev (1987) were divided into tall (over 120 cm), medium (105–119 cm), short (85–104) cm), semi-dwarfs (60–84 cm) and dwarfs (< 60 cm). Low-growing and semi-dwarf groups of wheat turned out to be the most numerous and productive.

As a result of research among the progeny of $F_{4–5}$, a significant increase in productivity and quality of grain was recorded in samples 255 and 340, which had a yield of 6.65–6.67 t $ha^{-1}$, protein content of 13.9–14.4%, gluten - 30.4–30.5% (Table 3).

Among the progeny of $F_{5–10}$, samples 1809, 3872, 4075, 6274 and 6750 were singled out, which during the whole research period were characterized by a combination of high productivity (5.97–7.28 t $ha^{-1}$) with high protein (15.5–18.0%) and gluten (36.8–39.2%) content in grain and high flour strength (365–387 alveograph units).

**Table 3.** Economically valuable indicators of soft winter wheat collection samples created by hybridization *Triticum* aestivum L. × *Triticum* spelta L. (Ukraine, Cherkasy region, 2013–2020)

| Breeding material | Plant height, cm | Ear lenth, cm | Thousand grain weight, g | Flour strength (W), a.u. | Gluten content in grain, % | Protein content in grain, % | Productivity, t ha$^{-1}$ |
|---|---|---|---|---|---|---|---|
| | $F_{4–5}$ (average for 2019–2020) | | | | | | |
| Podolianka (st) | 88 | 9.5 | 50.5 | 295 | 29.3 | 13.4 | 6.21 |
| 255 | 88 | 10.1** | 51.2 | 310 | 30.4*** | 14.4*** | 6.65** |
| 278 | 95** | 10.2** | 48.1 | 328** | 31.2*** | 14.8*** | 6.35 |
| 340 | 90 | 10.4** | 51.3 | 308 | 30.5*** | 13.9*** | 6.67** |
| 348 | 115** | 12.5** | 46.7 | 352** | 36.2*** | 16.9*** | 5.62 |
| 365 | 87 | 10.4** | 46.8 | 338** | 34.1*** | 15.6*** | 5.51 |
| 375 | 98* | 11.3** | 48.2 | 335** | 32.2*** | 15.2*** | 5.75 |
| *LSD** | 4* | 0.4* | 1.8* | 15* | 0.2* | 0.1* | 0.25* |
| $x \pm S_x$ | 95.2 ± 8 | 10.5 ± 0.7 | 46.2 ± 1.5 | 342 ± 18 | 33.2 ± 1.6 | 15.3 ± 0.8 | 5.87 ± 0.24 |
| *Cv,* % | 30.1 | 14.5 | 17.1 | 12.5 | 27.6 | 13.8 | 6.11 |
| $S_x$, % | 4.2 | 3.78 | 1.6 | 3.8 | 2.5 | 2.5 | 3.51 |
| | $F_{5–10}$ (average for 2013–2018) | | | | | | |
| Podolianka (st) | 86 | 9.7 | 52.5 | 302 | 29.5 | 13.7 | 6.77 |
| 1692 | 100** | 8.6 | 55.3** | 312 | 30.2*** | 14.1*** | 7.03** |
| 1686 | 78 | 8.8 | 50.2 | 325** | 31.8*** | 15.3*** | 6.41 |
| 1675 | 61 | 9.6 | 48.8 | 335** | 33.5*** | 16.2*** | 5.81 |
| 1678 | 59 | 8.7 | 46.9 | 330** | 32.3*** | 16.1*** | 6.31 |
| 1809 | 79 | 14.1** | 45.6 | 387** | 39.2*** | 18.0*** | 5.97 |
| 3872 | 93** | 10.7** | 50.7 | 368** | 36.8*** | 15.8*** | 7.03** |
| 4075 | 94** | 10.2** | 50.2 | 365** | 36.8*** | 15.9*** | 7.08** |
| 6274 | 95** | 11.8** | 51.8 | 372** | 37.1*** | 15.5*** | 7.12** |
| 6750 | 98** | 10.1** | 51.7 | 375** | 37.2*** | 16.0*** | 7.28** |
| *LSD** | 3* | 0.3* | 1.7* | 18* | 0.2* | 0.1* | 0.22* |
| $x \pm S_x$ | 79.0 ± 9 | 8.8 ± 0.6 | 50.1 ± 1.7 | 347 ± 21 | 32.3 ± 1.8 | 15.3 ± 0.8 | 6.27 ± 0.32 |
| *Cv,* % | 31.1 | 13.7 | 17.1 | 18.5 | 28.6 | 14.2 | 5.09 |
| $S_x$, % | 5.4 | 3.4 | 1.6 | 4.1 | 2.5 | 2.5 | 2.41 |

Note: * – significance of differences between indicators of laboratory tests (protein and gluten content) were determined at the level of significance of $P \leq 0.01$, for other indicators – $P \leq 0.05$; ** – the difference is significant at the level $P \leq 0.05$; *** – the difference is significant at the level $P \leq 0.01$.

**The results of winter wheat breeding.** As a result of a number of studies on interspecific hybridization, individual and kin selection and sample analysis, high-yielding genotypes 1809, 6274 and 3872 were identified, which were transferred to the Ukrainian Institute of Plant Variety Examination under the names Artaplot, Umanska Tsarivna and Freia.

Formal and qualification examination was conducted in 19 branches of the Ukrainian Institute for Plant Variety Examination, located in different regions and geographical zones (Steppe, Forest-Steppe, Polissia) of Ukraine. During the approbation period, Artaplot, Umanska Tsarivna and Freia exceeded the average yield of varieties

that passed the State Registration in the previous five years in Polissia and were characterized by high grain quality indicators (Table 4).

**Table 4.** Field research results of indicators of economic suitability of soft winter wheat varieties Artaplot, Umanska Tsarivna, Freia

| Trait | | Value | | | | | | | |
|---|---|---|---|---|---|---|---|---|---|
| | | Artaplot (2016–2018) | | Umanska Tsarivna (2018–2020) | | | Freia (2019–2021) | | |
| | | F* | P* | S* | F* | P* | S* | F* | P* |
| Average all varieties yield that have passed the State registration for the previous five years, t ha$^{-1}$ | | 6.38 | 5.66 | 5.28 | 6.71 | 5.87 | 5.19 | 6.69 | 5.99 |
| Variety yield at standard humidity (14%), t ha$^{-1}$ | | 6.15 | 6.19 | 4.79 | 6.59 | 5.87 | 4.87 | 6.29 | 6.52 |
| ± to average yield | | -0.23 | +0.53 | -0.49 | -0.12 | 0.0 | -0.32 | -0.40 | +0.53 |
| Growing season duration, days | | 285 | 290 | 268 | 259 | 273 | 273 | 260 | 283 |
| Plant height, cm | | 849 | 86 | 86 | 93 | 98 | 104 | 101 | 108 |
| Thousand grain weight, g | | 43.7 | 45.2 | 40.4 | 44.1 | 40.5 | 45.2 | 46.0 | 42.1 |
| Protein content, % | | 14.8 | 14.3 | 14.5 | 14.0 | 13.3 | 14.4 | 14.7 | 14.1 |
| Gluten content, % | | 31.2 | 30.6 | 28.8 | 28.1 | 26.7 | 29.2 | 30.3 | 27.7 |
| Flour strength, a.u. | | 280 | 285 | 253 | 244 | 182 | 214 | 237 | 131 |
| Bread volume from 100 g of flour, mL | | 900 | 880 | 840 | 970 | 900 | 970 | 940 | 860 |
| Immunity to, score | lodging | 9 | 9 | 9 | 7 | 6 | 9 | 6 | 6 |
| | shedding | 9 | 9 | 8 | 9 | 9 | 9 | 8 | 9 |
| | drought | 8 | 9 | 7 | 7 | 7 | 5 | 7 | 7 |
| | powdery mildew | 8 | 8 | 8 | 7 | 7 | 7 | 8 | 8 |
| | brown rust | 8 | 8 | 9 | 9 | 8 | 7 | 7 | 8 |
| | fusarium head blight | 7 | 8 | 9 | 8 | 6 | 9 | 8 | 6 |
| | frit fly | 9 | 9 | 8 | 9 | 8 | 7 | 9 | 9 |
| | corn bug | 9 | 9 | 8 | 8 | 9 | 9 | 9 | 9 |
| Winter resistance, score | | 8 | 8 | 8 | 7 | 8 | 9 | 9 | 9 |
| Freezing resistance (according to Plant Production Institute named after V. Ya. Yuriev) | | 7.2 | | 6.7 | | | 6.5 | | |

Note: *S – Steppe; F – Forest steppe; P – Polissia.

According to the results of the qualification expertise, the varieties Artaplot (in 2018), Umanska Tsarivna (in 2020) and Freia (in 2021) are included in the State Registry of Plant Varieties Suitable for Distribution in Ukraine (2021) and recommended for cultivation in Polissia.

## CONCLUSIONS

1 Breeding technologies for creating highly productive forms of soft winter wheat by interspecific hybridization of *Triticum aestivum* L. × *Triticum spelta* L. have been improved.

2 Studies have shown that plant height and ear length in hybrids of *Triticum aestivum* L. × *Triticum spelta* L. are inherited by the type of intermediate inheritance or partial negative inheritance; the grain number in the ear - by type of intermediate inheritance or partial positive dominance; grain weight of the ear - by type of superdominance or partial positive dominance.

3 In $F_2$ hybrids there is a dihybrid cleavage into forms with speltoid, squarehead and normal ears, with a quantitative predominance of speltoid plants, which indicates the control of the trait 'ear shape' by two non-allelic genes. The ear shape of the soft wheat original varieties in relation to speltoid wheat varieties turned out to be recessive, but at the same time it was dominant to the squarehead form. Regardless of the genotypes of soft wheat included in the combination of crossbreeding with spelt wheat, red color ear indication was determined by a monogenic type of inheritance.

4 Varieties of soft winter wheat Artaplot, Umanska Tsarivna and Freia were created, which is included in the State Registry of Plant Varieties Suitable for Distribution in Ukraine and recommended for cultivation in Polesia.

## REFERENCES


Beyl, G.M. & Atkinsk, R.E. 1965. In heritance of quantitative characters in grain sorgum. *Jowa. J. Sci*. **77**(3), 345–358.

Daskalev, H., Iordanom, A. & Ognyanova, A. 1967. Heterosis with domastitis. Bulgarian academy of sciences, Sofia, pp. 179.

de Faris, J., Fellers, J.P., Brooks, S.A. & Gill, B.S. 2003. Bacterial artificial chromosome contig spanning the major domestication locus Q in wheat and identification of a candidate gene. *Genetics*. **164**, 311–321.

Diordiieva, I., Riabovol, L., Riabovol, Ia., Serzhuk, O., Novak, A. & Kotsiuba, S. 2018. The characteristic of wheat collection created by *Triticum aestivum* L. / *Triticum spelta* L. hybridization. *Agronomy research* **16**(4), 2005–2015. doi: 10.15159/AR.18.181

Dorofeev, V.F., Ydachin, R.A. & Semenova, L.V. 1987. *World wheats*. Agropromizdat, Moscow, 560 pp. (in Russian).

Dospekhov, B.A. 1985. *Field experience methodology (with the basics of statistical processing of research results)*. Agropromizdat, Moskow, 351 pp. (in Russian).

Dvorak, J., Deal, K.R., Luo, M.C., You, F.M., von Borstel, K. & Dehghani, H. 2012. The origin of spelt and free-threshing hexaploid wheat. *Journal of Heredity* **103**, 426–441. doi: 10.1093/jhered/esr152

Ehrmantraut, E., Shevchenko, I. & Nenyn, P. 2000. Mathematical analysis and interpretation of research. Coll. Science. works Institute for Sugar Beet UAAS 2, 189–205. (in Ukrainian).

Filipchenko, Yu.A. 1979. *Genetics of soft wheats*. Moskow, 560 pp. (in Russian).

Gil-Humanes, J., Pistón, F., Martín, A. & Barro, F. 2009. Comparative genomic analysis and expression of the APETALA2-like genes from barley, wheat, and barley-wheat amphiploids. *BMC Plant Biology* **9**, 66. doi: 0.1186/1471-2229-9-66

Griffing, B. 1950. Analysis of quatitative gene-acrion by constant parent regression and related techniques. *Genetics* **35**, 303–321. doi: 10.1093/genetics/35.3.303

Guzman, C., Mondal, S., Govindan, V., Autrique, J.E., Posadas-Romano, G. & Cervantes, F. 2016. Use of rapid tests to predict quality traits of CIMMYT bread wheat genotypes grown under different environments. *LWT Food Sci. Technol.* **69**, 327–333. doi: 10.1016/j.lwt.2016.01.068

Khlestkina, E.K., Pshenichnikova, T.A., Röder, M.S., Salina, E.A., Arbuzova, V.S. & Börner, A. 2016. Comparative mapping of genes for glume colouration and pubescence in hexaploid wheat (*Triticum aestivum* L.). *Theor. Appl. Genet*. **113**(5), 801–807. doi: 10.1007/s00122-006-0331-1

Khlestkina, E.K., Röder, M.S. & Börner, A. 2009. Identification of glume coloration genes in synthetic hexaploid and common wheats. *Wheat Inf. Serv. (e WIS),* **108**, 1–3.

Kochmarskij, V.S., Kirilenko, V.V. & Kolomiec, L.A. 2012. The main methods and results of winter wheat breeding for productivity and adaptability in the Forest-Steppe of Ukraine. *Farming and breeding in Belarus* **48**, 345–354. (in Ukrainian).

Kosuge, K., Watanabe, N., Melnik, V.M., Laikova, L.I. & Goncharov, N.P. 2012. New sources of compact spike morphology determined by the genes on chromosome 5A in hexaploid wheat. *Genet. Resour. Crop Evol*, **59**, 1115–1124. doi: 10.1007/s10722-011-9747-9

Morhun, V.V. & Oksom, V.P. 2011. Creation of genetically improved lines of winter wheat by induction of micromutations. *Science reports of NULES of Ukraine* **24(**2), 95–104.

Mukhordova, M.E. 2015. Heritability of economically valuable traits of soft winter wheat hybrids. *Reporter of t Altai State Agricultural University* **7**, 20–24. (in Russian).

Nilsson-Ehle, H. 1909. Kreuzungsversuchungen an Hafer und Weizen. Lands. *Univ. Aersskrift N.F. Afd*. **2**(2), 122.

Peleg, Z., Fahima, T., Korol, A.B., Abbo, S. & Saranga, Y. 2011. Genetic analysis of wheat domestication and evolution under domestication. *Journal of Experimental Botany* **62**, 5051–5061. doi: 10.1093/jxb/err206

Polyanetska, I.O. 2012. Breeding-genetic improvement of *Triticum spelta* (L.) and it use breeding of *Triticum aestivum* (L.). [PhD. Thesis] Kyiv, Institute of Agriculture. (in Ukrainian).

Prasad, K.D., Haque, M.F. & Ganguli, D.K. 1998. Heterosis studies for yield and its components in bread wheat (*Triticum aestivum* L.). *Indian J. Genet* **1**, 97–100.

Rybalka, O.I. 2011. Wheat quality and its improvement. Logos, Kyiv, 496 pp. (in Ukrainian).

Sichkar, S.M., Morhun, V.V. & Dubrovna, O.V. 2016. The inheritance nature of the ear morphological traits in hybrids *Triticum spelta* × *Triticum aestivum. Factors of Experimental Evolution Of Organisms* **18**, 149–153 (in Ukrainian).

Simonov, A.V., Pshenichnikova, T.A., Lapochkina, I.F. & Vatanabe, N. 2016. Interaction of genes determining the ear shape of original wheat and located in the chromosome 5AL. *Vavilov Journal of Genetics and Breeding* **20**(1), 57–64. doi: doi.org/10.18699/VJ15.115

State qualification methodology of plant varieties expertise on definition of suitability for distribution in Ukraine (grains, grouts, and leguminous species) 2012. Kyiv, Ukraine Institute of Plant Varieties Expertise, pp. 81. (in Ukrainian).

State register of plant varieties suitable for dissemination in Ukraine 2021. Kyiv, Ukraine Institute of Plant Varieties Expertise, 524 pp.

Xie, Q., Mayes, S. & Sparkes, D.L2015. Spelt as a genetic resource for yield component improvement in bread wheat. *Crop Sci*. **55**, 2753–2765.

*Agronomy Research* **20**(1), 103–123, 2022
https://doi.org/10.15159/AR.22.005

# Research into properties of blue melilot and fenugreek cultivated using different sowing times

I. Fedosiy[1], I. Bobos[1], O. Zavadska[1], O. Komar[1], O. Tonkha[1], M. Furdyha[2], S. Polishchuk[3], M. Arak[4] and J. Olt[4,*]

[1]National University of Life and Environmental Sciences of Ukraine, 15, Heroyiv Oborony Str., UA03041 Kyiv, Ukraine
[2]Institute of Potato Growing of NAAS of Ukraine, 22 Chkalov Str., Nemishaeve Vlg, Borodyanka Dist., UA07853 Kyiv Region, Ukraine
[3]National Scientific Centre, Institute of Agriculture of NAAS of Ukraine, 2b, Mashinobudivnikiv Str., Chabany vil., Kyiv-Svyatoshin Dist., UA08162, Kyiv Region, Ukraine
[4]Estonian University of Life Sciences, Institute of Forestry and Engineering, 56 Kreutzwaldi Str., EE51006 Tartu, Estonia
[*]Correspondence: jyri.olt@emu.ee

Received: September 6th, 2021; Accepted: January 30th, 2022; Published: February 17th, 2022

**Abstract.** The paper presents the results of the research into the properties of blue melilot (*Melilotus caeruleus* (L.) Desr.) and fenugreek (*Trigonella foenum graecum* L.) with regard to the set of their economy-and-biology and biochemical indices in relation to the dates of their sowing. It has been established that the two species under consideration feature wide ranges of index variability depending on the sowing term and the weather conditions. The earliest ripening terms have been recorded for species in case of summer sowing dates (decade I of June), when short growing season lengths of 36–37 days were observed. At the same time, in terms of heavy plant herbage yield obtained from species in the green conveyor system, the early spring (decades II–III of April) and late spring (decade I of May) sowing terms are more suitable providing a herbage yield of 5.7–6.9 t ha$^{-1}$ in case of blue melilot and 7.3–9.3 t ha$^{-1}$ for fenugreek, with a solids content of 12.4–28.4%, total sugars of 2.5–5.0% and vitamin C - 38.0–51.8 mg (100 g)$^{-1}$. For the purpose of obtaining the spice named 'Greek hay' (foenum Graecum), a better choice is to cultivate fenugreek with early spring (decades II–III of April) and late spring (decade I of May) sowing times, as in this case a greater vegetation mass develops, resulting in a plant dry weight yield of 1.3–1.4 t ha$^{-1}$. An increase in the total precipitation by 1 mm has contributed to the variation of the herbage yield within the range of 15.0 to 77.3 kg ha$^{-1}$, dry matter yield - 0.693 to 25.9 kg ha$^{-1}$. High seed yield has been noted in case of sowing the species in early spring (decades II–III of April), where the seed yield of blue melilot was equal to 0.4 t ha$^{-1}$, fenugreek - 2.0 t ha$^{-1}$, their 1,000 seeds having a weight of 0.71 and 9.7 g, respectively.

**Key words:** blue melilot, fenugreek, sowing time, herbage and dry weight, pod, yield.

## INTRODUCTION

The current stage of development in the vegetable farming industry features multiple unresolved problems, the most marked ones being the insufficient vegetable crop species diversity, the low yield capacity and the low quality of the output vegetable products. At the same time, supplying the population with the food products that are rich with protein, a nutrient that is deficient in everyone's daily diet, remains a high priority topic (Pandian et al., 2002; Fernandez-Aparicio et al., 2008; Bobos, 2013; Bobos & Kokoyko, 2013; Bobos et al., 2019; Tonkha et al., 2020).

Legumes (*Fabaceae* Lindl.) are of high nutritional value. They are recognized, first of all, as a source of easily digestible proteins and vitamins. The global diversity of arable vegetable legumes is huge and includes over 40 species (Yakovlev, 1991; Pandian et al., 2002; Fernandez-Aparicio et al., 2008; Bobos, 2013; Bobos & Kokoyko, 2013; Bobos et al., 2019).

In cultivation, fenugreek (*Trigonella foenum graecum* L.) is the most commonly encountered species, but blue melilot (*Melilotus caeruleus* (L.) Desr.) is the most commonly not encountered species (Pandian et al., 2002; Bobos, 2013; Bobos & Kokoyko, 2013; Bobos, 2015; Shelyuto, 2013).

It is generally assumed that *Trigonella* species come from the eastern part of the Mediterranean. They are widely present and have the greatest diversity of species in Asia Minor and Central Asia. The value of the plant is recognized all over the globe and it is actively cultivated in many countries (Thirunavukkarasu & Anuradha, 2007; Acharya et al., 2008; Fernandez-Aparicio et al., 2008; Bobos, 2013; Abramchuk & Karpuhin, 2018).

*Trigonella* and blue melilot species are cultivated for obtaining spice and flavour mixtures and as fodder and green manure crops (Ates, 2016). Fresh herbage does not produce any pronounced intense flavour, it appears only after its drying in the process of storage. Young shoot apices harvested in the blooming period, dried and beaten to powder are used as a spice for meat dishes and in cheese-making. Moreover, ground seeds fenugreek and blue melilot powder plant smell like dried mushrooms and are used in gastronomy and the bread baking industry. Trigonella seeds are an irreplaceable component in the cooking of many dishes. Apart from that, trigonella seeds are used to obtain sprouts. Young plants are used for making salads, which are very good for health due to the biologically active substances contained in them (Thirunavukkarasu & Anuradha, 2007; Fernandez-Aparicio et al., 2008; Premanath et al., 2011; Bobos, 2013; Shelyuto, 2013; Bobos, 2015; Zemzmi et al., 2017).

In the USA, *Trigonella* is used for flavouring rum and maple drinks, sometimes it is added to dough. In India, coffee substitutes are made from its roasted seeds (Thirunavakkarasu & Anuradha, 2006; Acharya et al., 2008).

These crops ~~is~~ are also recognized as having medicinal properties. Fenugreek seeds gathered at the stage of biological ripeness are used in the capacity of drug raw materials. They contain alkaloids (trigonelline), essential oils, steroidal saponins, flavonoids, coumarins, polysaccharides, proteins (amino acids: alanine, arginine, glycine, methionine and other), carbohydrates (45–60%), vitamins (A, C, B, P), mineral salts (Ca, Mg, P, Fe, K, S and other) (Pandian et al., 2002; Devasena & Menon, 2003; Acharya et al., 2008 Premanath et al., 2011; Shelyuto, 2013; Arslan et al., 2016; Abramchuk& Karpuhin, 2018). The polyphenols of the plant possess pronounced antioxidative, hepatoprotective and antibacterial properties (Srinivasan, 2006; Kaviarasan et al., 2007; Al-Timimi, 2019).

The highest pharmacological activity is typical for the plant's steroidal saponins, which are used both for the preventive care and the treatment of cardiovascular diseases and atherosclerosis (Premanath et al., 2011; Shelyuto, 2013; Al-Timimi, 2019). Steroidal saponins are effective in the treatment of rheumatic diseases, hemolitic anemia, bronchial asthma, gastric ulcer (Devasena & Menon, 2003; Srinivasan, 2006; Plechishchik et al., 2010; Abramchuk & Karpuhin, 2018). In many countries, fenugreek seeds are included in the contents of the combined pharmaceuticals that have antidiabetic, antisclerotic, diuretic, laxative, anti-inflammatory effects (Srinivasan, 2006; Kaviarasan et al., 2007; Bafadam et al., 2019).

Despite the high importance of the above-mentioned species for a number of Asian and North African countries and the fact that they are cultivated in many countries, the data on their genetic diversity, the intraspecies and interspecies variation and the agronomic practices of their cultivation are limited (Dangi et al., 2004; Shelyuto, 2013; Bobos, 2015; Beyzi & Gürbüz, 2020; Xalxo & Keshavkant, 2020).

The crops under consideration are also of importance for feeding purposes and is a promising one in that sector. However, until recently it has been inadequately researched into and of limited occurrence for the purposes of increasing the production of fodder and plant proteins in the territories of the EU and other countries, including Ukraine. It is well-known that *Trigonella* species and blue melilot have agronomic importance in the improvement of soil fertility due to the ability of the plant to form nitrogen-assimilating tubercles (Randhawa et al., 1996; Plechishchik et al., 2010; Shelyuto, 2013; Bobos, 2015; Pavlista & Santra, 2016; Xalxo & Keshavkant, 2020).

In view of the above, research into the economically valuable properties of fenugreek and blue melilot as crops only recently introduced and little researched in the conditions of Ukraine is of great scientific and practical interest. No technology has been developed for cultivating *Trigonella* species in the conditions of Ukraine for the purpose of spice production. The primary method of technology implementation is the adaptation of species to the cultivation conditions. No domestic varieties has been bred for these species and vegetable growers just cultivate local forms. The varietal diversity of local specimen in Ukraine is rather large. At the same time, the local varieties have not until know been set in collections and systematised (Plechishchik et al., 2010; Bobos, 2013; Bobos & Kokoyko, 2013; Shelyuto, 2013; Bobos et al., 2019).

The authors have been carrying out work on research into the production methods and the development of the green conveyor for the cultivation of *Trigonella* and blue melilot as a valuable medical and spice-and-flavour crop. Therefore, the problem of the effect that the sowing terms have on the growth and development of *Trigonella* species and blue melilot in the context of widening the green crop species diversity remains a topical one (Bobos & Kokoyko, 2013; Sych & Bobos, 2013; Pavlista & Santra, 2016; Bobos et al., 2019; Xalxo & Keshavkant, 2020).

The aim of the completed study was to determine the properties of fenugreek and blue melilot in terms of exploring the sowing times for the purpose of delivering products in conveyor in the conditions of the Forest Steppe Region. The research into the economically valuable properties of the crop species would enable the development of technologies for the cultivation of a spice named 'mushroom grass', which would result in expanding the legume species diversity and improving the supply of cheap digestible protein to the population. The research target was in summary to determine the following: the timing of phenological stages, the growing season duration, the yield of

fresh and dried leaves, their biochemical composition and the seed productivity of the plants.

## MATERIALS AND METHODS

The research had been carried out for 3 years (2018–2020) in the National University of Life and Environmental Sciences of Ukraine (NUBiP) in the collection field of the Horticultural Garden situated in the Kiev Province, without watering. Two local specimen were under investigation: blue melilot and fenugreek (*Trigonella foenum graecum* L.). The investigations were carried out with three replicates using the two-factor experiment technique (Bondarenka & Yakovenka, 2001). Factor A - trigonella species, factor B - sowing date. The total recorded area was 120 $m^2$, one plot - 5 $m^2$.

The experimental design included four sowing time options for blue melilot and fenugreek. Both the species were sown simultaneously at the following four sowing terms: early spring - decades II–III of April (10.04. - the 1st year, 24.04. - the 2nd year, 10.04. - the 3rd year); late spring, term 1 - decade III of April - decade I of May (25.04. - the 1st year, 08.05. - the 2nd year, 29.04. - the 3rd year); late spring, term 2 - decade II of May (15.05. - the 1st year, 17.05. - the 2nd year, 14.05. - the 3rd year); summer - decade I of June (10.06. - the 1st year, 04.06. - the 2nd year, 05.06. - the 3rd year). The early spring sowing term (decades II–III of April) was assumed to be the reference case in the study.

The study employed the generally accepted approach, according to which *Trigonella* species should be cultivated in the production conditions suitable for legumes (Sych et al., 2010). The seeds were drilled manually following the 45×15 cm pattern. The sowing depth was 1.0–1.5 cm for blue melilot; 2.0–3.0 cm for fenugreek. After the appearance of seedlings, thinning was carried out with a target of setting the distance between the plants in a row at 15 cm, irrespective of the sowing time. At all sowing dates, the density of stand was arranged at 15 plants per $m^2$ (Maletić & Jevdjović, 2007).

During the growth of the plant, the following phenological stages were marked: start of (10%) and massive (75%) seedlings; start of and massive flowering; ripening of pods. Seedlings were recorded, when the seed lobes appeared on the surface of the soil. The beginning of pod ripening was recorded, when 60–70% of the seedpods had been yellowed. The duration of the vegetation period was counted from the appearance of seedlings to the beginning of pod ripening.

The territory of the research field is situated in the Forest Steppe Region. The climate of the area is moderately continental, with warm summer and not cold winter. According to the long-term data, the annual mean temperature is equal to 7.0 °C. The long-term mean temperature of the coldest month of January is equal to minus 6.5 °C, the warmest one, July + 19.8 °C. In accordance with the long-term monitoring data, the minimum temperature is equal to -36 °C, the maximum one - to +39 °C. The sum of effective temperatures above 10 °C is within the range of 2,440–2,700 °C, which is the evidence of high calorific resources available for growing various species of leguminous vegetable crops.

The soil in the field is medium-podzolic, roughly dusty, easy loamy soil, the reaction of the soil medium is slightly acid. The humus horizon thickness is equal to 24–28 cm. The experimental field features low humus content 4 - 1.5–2.2%, moderate contents of hydrolysable nitrogen - 26–38 mg $kg^{-1}$, labile phosphorus - 43–61 and potassium - 28–34 mg $kg^{-1}$ (Bobos et al., 2019; Zavadska et al., 2020).

The depth of top soil is 20–22 cm. The preceding backgrounds were as follows: black fallow in the 1st year, in the 2nd and 3rd years - cucumber plantings. The primary tillage of the soil for the crop involved autumnal eradication of the plant residues from the preceding crop and weeds, deep autumn ploughing. 7 days prior to seed sowing, the N60P40K90 fertiliser mixture (German saltpetre, superphosphate and potassium chloride) was applied. In the first decade of April and prior to sowing, the experimental field was tilled to depths of 12–15 cm and 6–8 cm, respectively, with the use of a KPSP-4 tiller unitised with a DT-75 tractor, then levelled off with a harrow and the seeds were sown. In the massive plant flowering period, the plants' vegetative mass was cut for hay in an area of 60 $m^2$. The herbage output in the massive flowering period was analysed.

The harvested vegetative mass had for 7 days been dried in the Shellab HF10-2 dry-air drying cabinet at a temperature of +35 °C. The moisture content in the specimen was equal to 80.2–80.5%. After drying the plants, the leaves and flower heads were separated from the stems and were weighed separately in order to determine the per cent content of different plant components in the plant as a whole.

In order to determine the seed productivity, the plants were harvested at a seed moisture content of 18–20%. After harvesting, the seeds had been finally dried for 7–10 days in the Shellab HF10-2 dry-air drying cabinet at a temperature of +35 °C, then they were sieved through a set of sieves with gauges of 1.0–2.5 mm. The variability was analysed for the following main economically valuable properties of the reproductive organs: the number of seedpods on a plant, the seedpod length, the seed productivity and yield, also the mass of 1,000 seeds. The seed productivity indices were determined at the seedpod biological ripening stage.

The analysis of the herbage obtained from species was carried out in the conditions of the research-and-study laboratory under the Department of Storage, Processing and Standardization of Crop Products named after Prof. B.V. Lesik, NUBiP, in accordance with the standard practices (Zavadska et al., 2020). The content of solid matter was determined in accordance with DSTU ISO 751 with the use of thermal gravimetric analysis by drying the sample in the drying cabinet at a temperature of 100–105 °C until the mass became constant. The content of sugars (total) was determined with the use of Bertrand's method; vitamin C - with the use of 2,6-dichlorophenolindophenol solution. For the purposes of research, 100 g of fresh herbage were sampled for each species with 3 replicates and immediately analysed with regard to the contents of the main biochemical components.

The obtained research results were statistically analysed with the use of the methods of the analysis of variance and the correlation and regression analysis (Rao, 2007).

The analysis of variance was applied in the form of the statistical research into the probable effect that the involved factors (species and sowing time) and their interaction had on the resulting property. The significance of the difference between means was estimated by the least significant difference (*LSD*). This statistical value was compared with the difference between arithmetic means (d). If $d \geq LSD$, the difference between the alternatives was significant, but if $d < LSD$ - it was not significant, inessential. The difference between the means that exceeded *LSD*, was calculated with a 5% significance level. The analysis was carried out for each year.

For the purpose of measuring the closeness and form of the relationship, the special statistical methods called correlation analysis and regression analysis were used.

## RESULTS AND DISCUSSION

It has been established that the growth and development of species depend on the sowing terms. In case of early spring sowing times, the vegetative season increases by 14–15 days as compared to summer sowing dates, on the average for three years. At the same time, in case of summer sowing terms, the earlier massive emergence of seedlings has been recorded for the researched species - on the 5$^{th}$ day after drilling. In case of early spring sowing terms, the massive emergence of seedlings becomes a lengthier process. That is due to the lower temperatures in the respective period. In case of the next sowing terms, fenugreek and blue melilot seedlings emerge 7–9 days earlier as compared to the reference case.

The duration of interstage periods differs for species under consideration and depends on the sowing date (Table 1). When the species are sown in summer, the duration of the period from seeding to massive seedlings is 6–8 days, according to the records, which is 4–6 days shorter, than in the reference case. This is due to the increased temperature of the air and soil in this period, which promotes the accelerated completion of all stages of plant growth and development.

**Table 1.** Impact of sowing terms on duration of phenological stages of growth and development for fenugreek and blue melilot species

| Sowing term (factor B) | Duration of periods [days] | | | |
|---|---|---|---|---|
| | Seeding - massive seedlings | Massive seedlings - start of flowering | Start of flowering - start of seedpod ripening | Massive seedlings - start of seedpod ripening |
| Blue melilot (factor A) | | | | |
| Early spring (decades II–III of April) (reference case) | 12 | 40 | 10 | 50 |
| Late spring, term 1 (decade III of April-decade I of May) | 9 | 37 | 9 | 46 |
| Late spring, term 2 (decade II of May) | 8 | 32 | 8 | 40 |
| Summer (decade I of June) | 6 | 29 | 7 | 36 |
| Fenugreek | | | | |
| Early spring (decades II–III of April) (reference case) | 13 | 38 | 14 | 52 |
| Late spring, term 1 (decade III of April-decade I of May) | 11 | 35 | 14 | 49 |
| Late spring, term 2 (decade II of May) | 9 | 32 | 13 | 45 |
| Summer (decade I of June) | 8 | 28 | 9 | 37 |

According to Güzel & Özyazıcı (2021), the time until the emergence of seedlings, the time until the 50% flowering of the plants and the growing period of various *Trigonella* genotypes vary within the ranges of 16.0 to 19.9 days, 160.9 to 170.4 days,

202.0 to 209.3 days, respectively. However, the highest values of these indices have been observed for the genotypes grown in Iraq and Afghanistan.

According to the results of investigations, it has been established that the sowing terms have effect on the duration of the stage from massive seedlings to the start of flowering, which has varied for the species within the range of 28 to 40 days. The earliest completion of it is typical for the species sown on summer sowing terms. Their stage duration is 28–29 days, which is 10–11 days shorter, than in the reference case. That results from hot weather and the rapid warming of the soil surface in the summer season, which accelerates the initiation of all species growth and development stages.

The economically valuable indices of the species that had been researched for 3 years are shown in Table 2.

**Table 2.** Impact of sowing terms on economically valuable indices of fenugreek and blue melilot herbage

| Species (factor A) | Sowing terms (factor B) | Mean productivity, g | Herbage yield in years, t ha$^{-1}$ | | | Mean yield, t ha$^{-1}$ | Yield increase | | Stability factor (S.F.) |
|---|---|---|---|---|---|---|---|---|---|
| | | | 1st year | 2nd year | 3rd year | | t ha$^{-1}$ | % | |
| Blue melilot | Early spring (decades II–III of April) (reference case) | 46.7 | | | | 6.9 | 0 | 100 | 1.9 |
| | Late spring 1st term (decade III of April-decade I of May) | 38.5 | 8.2 | 4.6 | 4.4 | 5.7 | -1.2 | -17 | 1.9 |
| | Late spring 2nd term (decade II of May) | 26.9 | 4.9 | 3.6 | 3.4 | 4.0 | -2.9 | -42 | 1.4 |
| | Summer (decade I of June) | 7.1 | 1.4 | 0.9 | 0.9 | 1.1 | -5.8 | -84 | 1.6 |
| Fenugreek | Early spring (decades II–III of April) (reference case) | 62.7 | 10.2 | 9.0 | 8.7 | 9.3 | 0 | 100 | 1.2 |
| | Late spring 1st term (decade III of April-decade I of May) | 47.9 | 8.8 | 7.0 | 6.1 | 7.3 | -2.0 | -21 | 1.4 |
| | Late spring 2nd term (decade II of May) | 29.0 | 5.4 | 3.8 | 3.7 | 4.3 | -5.0 | -54 | 1.4 |
| | Summer (decade I of June) | 8.0 | 1.7 | 1.0 | 0.9 | 1.2 | -8.1 | -87 | 1.9 |
| $HCP_{05}$ | | | 1.5 | 1.2 | 1.1 | | | | |
| *factor A* | | | 0.8 | 0.7 | 0.5 | | | | |
| *factor B* | | | 1.1 | 1.1 | 0.9 | | | | |

The species plant productivity and mean herbage yield capacity depend on the sowing term (factor B). That said, a significant difference has been detected between the reference, late spring (2 terms) and summer sowing term cases. As regards the economically valuable indices of blue melilot and those of fenugreek, no significant difference has been found.

The plant productivity defines the herbage yield and overall harvest. Fenugreek features a more developed vegetative mass, forming large size leaves and greater numbers of shoots, which has effect on its productivity. That said, the plant productivity amounts to 62.7 g in case of early spring sowing terms and decreases by 87.3% in case of summer seeding.

On the average for three years, the plant productivity has been higher in case of early spring sowing terms both for fenugreek and blue melilot, being equal to 46.7–62.7 g. The summer sowing terms result in reducing the plant productivity down to 7.1–8.0 g. This is related to the cold tolerance of the species, which have optimum conditions for their plant growth and development at moderate temperatures.

The yield of plant herbage to a significant extent depends on both the species and the sowing terms. The highest herbage yield capacity has been detected for early spring sowing terms, in which case it is equal to 6.9 t $ha^{-1}$ on the three years average for blue melilot, 9.3 t $ha^{-1}$ - for fenugreek. That said, blue melilot has been found to be less adaptable to the growing conditions, with a stability factor of 1.9. Blue melilot plants feature less developed vegetative mass, forming smaller size leaves and smaller numbers of shoots as compared to fenugreek, which results in their lower productivity. That said, species had low yield in dry spring of 2014, the dry conditions inflicting the formation of an underdeveloped vegetative apparatus and the more intensive progress of all the plant growth and development stages.

The low herbage yield of species plants in case of the late spring (decade II of May) and summer (decade I of June) sowing terms is due to the less developed vegetative apparatus of the plants. The high air and soil temperatures have contributed to the rapid completion of all plant growth and development stages. However, the intensity of the species' tops build-up has been recorded at lower levels. Therefore, such dates are not suitable for the cultivation of species in the Forest Steppe Region of Ukraine. The sowing on summer dates has resulted in the species herbage productivity decreasing by 84–87% in comparison with the reference case. At the same time, blue melilot has been found to be more adaptive to summer growing conditions with a stability factor of 1.6.

Meanwhile, no appreciable difference from the reference case has been revealed for the species in case of the first late spring sowing term. When sowing on this term, the three-year average herbage productivity of the species becomes equal to 5.7–7.3 t $ha^{-1}$, i.e. 17–21% less than in the reference case. Significantly lower herbage productivity is obtained with the summer sowing terms: fenugreek 0.9 to 1.7 t $ha^{-1}$, blue melilot - 0.9–1.4 t $ha^{-1}$ (Fig. 1). Muhammad et al. (2020) have found that IAA and $GA_3$ can be applied for increasing the foliage biomass output and the yield.

Saxena et al. (2019) have revealed that the fatty oil content in the seeds of various trigonella genotypes varies within the range of 2.62 to 5.33%. Beyzi et al. (2021) have reported about the fatty oil content in trigonella within the range of 4.75% to 5.54%. Ciftci et al. (2011) have stated that the oil content in trigonella varies within the range of 5.8 to 15.2% and the main fatty acids are: linolic acid (45.1–47.5%), α-linolenic (18.3–22.8%), oleic (12.4–17.0%), palmitic (9.8–11.2%) and stearic (3.8–4.2%) acids. The ratios between the n-6 and n-3 fatty acids vary within the range of 2.1 to 2.7. Seeds of the plant contain also 35% of alkaloids, 10% of flavonoids (100 mg per gram of *Trigonella* seeds), 4.8% of saponins and 0.2–0.9% of diosgenin (Jani et al., 2009; Meghwal & Goswami, 2012; Vaidya et al., 2013). Alkaloids, together with some other

volatile compounds, are the primary cause of the bitter taste and the typical flavour of *Trigonella* (Kumar et al., 2012, Faeste et al., 2009).

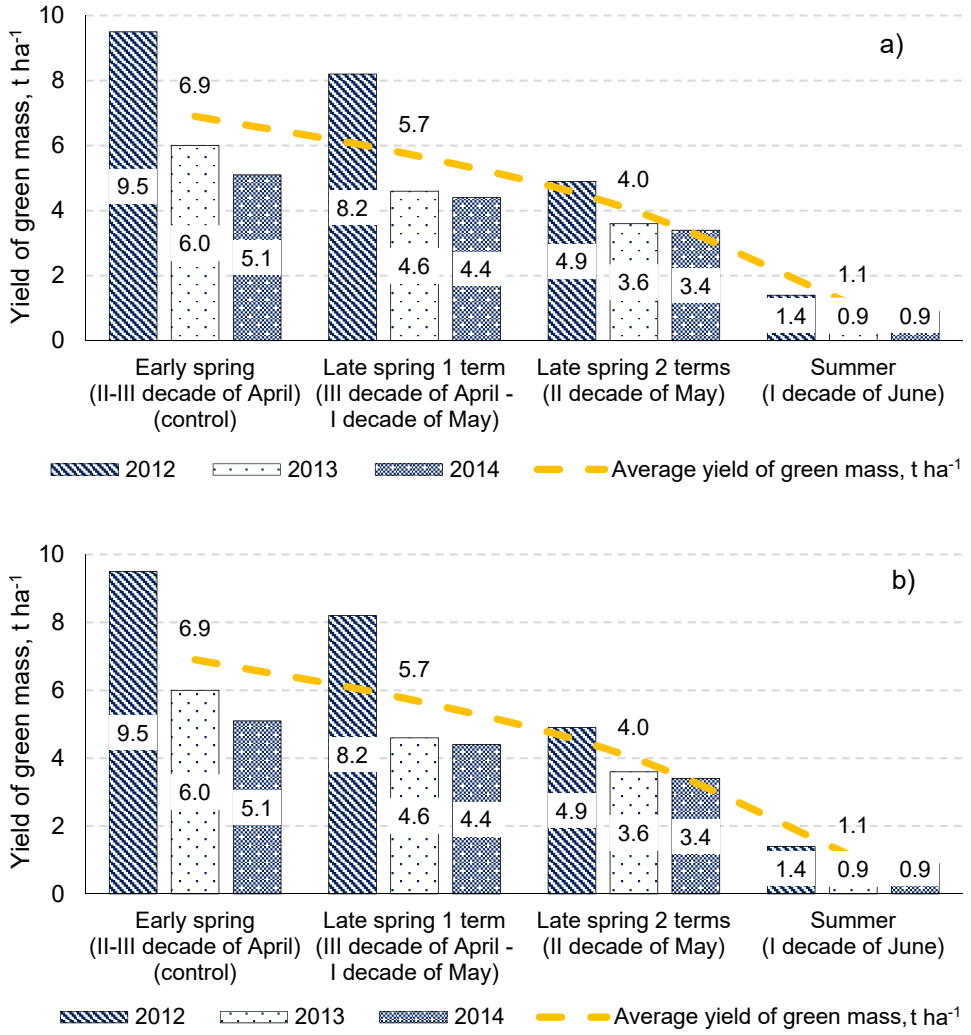


**Figure 1.** Herbage yield development dynamics: a) blue melilot; b) fenugreek.

It has been established in the research that the biochemical composition of the species herbage to a significant extent depends on both the species properties and the sowing terms (Table 3).

**Table 3.** Relation between sowing terms and biochemical indices of fenugreek and blue melilot herbage

| Species (factor A) | Sowing terms (factor B) | Solid matter, % | Sum of sugars, % | Vitamin C, mg (100 g)$^{-1}$ |
|---|---|---|---|---|
| Blue melilot | Early spring (decades II–III of April) (reference case) | 12.4 | 2.5 | 45.4 |
| | Late spring, term 1 (decade III of April- decade I of May) | 18.8 | 4.0 | 38.0 |
| | Late spring, term 2 (decade II of May) | 16.0 | 2.8 | 26.0 |
| | Summer(decade I of June) | 15.5 | 2.2 | 19.7 |
| Fenugreek | Early spring (decades II–III of April) (reference case) | 18.0 | 2.6 | 51.8 |
| | Late spring, term 1 (decade III of Aprisl-decade I of May) | 28.4 | 5.0 | 49.7 |
| | Late spring, term 2 (decade II of May) | 20.4 | 3.4 | 26.7 |
| | Summer (decade I of June) | 18.5 | 2.7 | 20.1 |
| $HIP_{05}$ | | | 4.9 | 0.7 |
| *factor A* | | | 2.4 | 0.4 |
| *factor B* | | | 3.4 | 0.5 |

According to the results of the biochemical analysis, the fresh herbage quality indices of species improve in case of late spring sowing terms (decade III of April-decade I of May). The solid matter content in this case is equal to 18.8–28.4%. The higher index values have been obtained for the herbage of fenugreek. The same trend is observed also in other indices. That can be explained by the great height of blue melilot plants, which results in the shading of the plants, the slowing down of the photosynthesis process and the reduced accumulation of solid matter and sugars.

With early spring sowing terms, the quality indices go down - in these cases, the solid matter and sugar contents in fenugreek species have been equal to 18.0 and 2.6%, respectively, in blue melilot species - 12.4 and 2.5%. That can be explained by the slowing down of photosynthesis in plants at lower temperatures. However, in case of early spring sowing terms, the vitamin C content in species increases. This index has been found to reach the highest level in the reference case, where it is equal to 51.8 mg (100 g)$^{-1}$ of raw matter for fenugreek, for blue melilot - 45.4 mg (100 g)$^{-1}$. With later sowing terms, the vitamin C content decreases, reaching the lowest level in case of summer seeding, where it has been equal to 19.7–20.1 mg (100 g)$^{-1}$ of raw matter.

The loss of vitamin C, when boiling in water or cooking in steam and frying, amounts to 10.8 and 7.4%, respectively, while the action of β- and γ-radiation on germinating seeds reduces the vitamin content as well (Khorshidian et al., 2016).

For the food purposes, the dried upper part of leaves and flower heads is the most frequently used part of these species. Accordingly, it is necessary to determine the economically valuable indices of dried output. It has been found on the average for three years that the dry matter yield capacity of blue melilot and fenugreek depends to a considerable extent on the sowing term (factor B) (Table 4).

**Table 4.** Relation between sowing terms and economically valuable indices of blue melilot and fenugreek dry matter

| Species (factor A) | Sowing terms (factor B) | Average water loss factor | Dry matter yield in years, t ha$^{-1}$ | | | Average dry matter yield, t ha$^{-1}$ | Increase of yield | | Stability factor (S.F.) |
|---|---|---|---|---|---|---|---|---|---|
| | | | 1st year | 2nd year | 3rd year | | t ha$^{-1}$ | % | |
| Blue melilot | Early spring (decades ii–iii of april) (reference case) | 6.5 | 1.3 | 1.2 | 1.0 | 1.2 | 0 | 100 | 1.3 |
| | Late spring 1st term (decade iii of april - decade i of may) | 5.7 | 1.3 | 1.1 | 0.9 | 1.1 | -0.1 | -8 | 1.4 |
| | Late spring 2nd term (decade ii of may) | 4.0 | 1.2 | 0.9 | 0.8 | 1.0 | -0.2 | -17 | 1.4 |
| | Summer (decade i of june) | 1.8 | 0.7 | 0.6 | 0.5 | 0.6 | -0.6 | -50 | 1.5 |
| Fenugreek | Early spring (decades ii–iii of april) (reference case) | 6.7 | 1.5 | 1.4 | 1.3 | 1.4 | 0 | 100 | 1.1 |
| | Late spring 1st term (decade iii of april- Decade i of may) | 5.9 | 1.4 | 1.3 | 1.1 | 1.3 | -0.1 | -7 | 1.3 |
| | Late spring 2nd term (decade ii of may) | 4.0 | 1.4 | 0.9 | 0.9 | 1.1 | -0.3 | -21 | 1.6 |
| | Summer (decade i of june) | 1.5 | 1.0 | 0.7 | 0.6 | 0.8 | -0.6 | -43 | 1.7 |
| $HCP_{05}$ | | | 0.5 | 0.5 | 0.4 | | | | |
| *factor A* | | | 0.2 | 0.1 | 0.1 | | | | |
| *factor B* | | | 0.3 | 0.3 | 0.2 | | | | |

It has been established that the dry matter yield of two species depends on the water loss factor, which has been found to be lower, at a value of 1.5–1.8, in case of summer sowing terms. That is due to the high temperatures of the summer season and the loss of turgor because of the intensive plant breathing. Higher water loss factors among the two species are observed in case of early spring sowing terms (6.5–6.7). That said, this index is lower for blue melilot. At the same time, blue melilot has been found to be less adaptive in case of early spring sowing terms, comparing to fenugreek, with a stability factor of 1.3.

Higher dry matter yield has been observed in case of early spring sowing terms and late spring term 1, which is due to the high plant herbage yield: it is equal to 1.1–1.2 t ha$^{-1}$ for blue melilot, for fenugreek - 1.3–1.4 t ha$^{-1}$. Lower dry matter yield is obtained from species in case of summer sowing terms (0.6–0.8 t ha$^{-1}$) (Fig. 2). That is due to the low herbage yield, despite the lower water loss factor in this period (1.5–1.8). On the average for three years, the dry matter yield in case of summer sowing terms has been reduced by 43–50% in comparison with the reference case.

The dry matter yield has been higher in case of fenugreek at all the sowing terms (0.8–1.4 t ha$^{-1}$), as compared to blue melilot (0.6–1.2 t ha$^{-1}$). At the same time, no significant difference with regard to the dry matter yield has been observed between the

cases of the early spring and 1st late spring sowing terms - in both cases it has been equal to 1.3–1.4 t ha$^{-1}$ for fenugreek. It has been established that late spring sowing term 2 (decade II of May) and the summer sowing terms (decade I of June) are impractical for the cultivation of species, since with these terms the lowest plant herbage and dry matter yields have been reached.

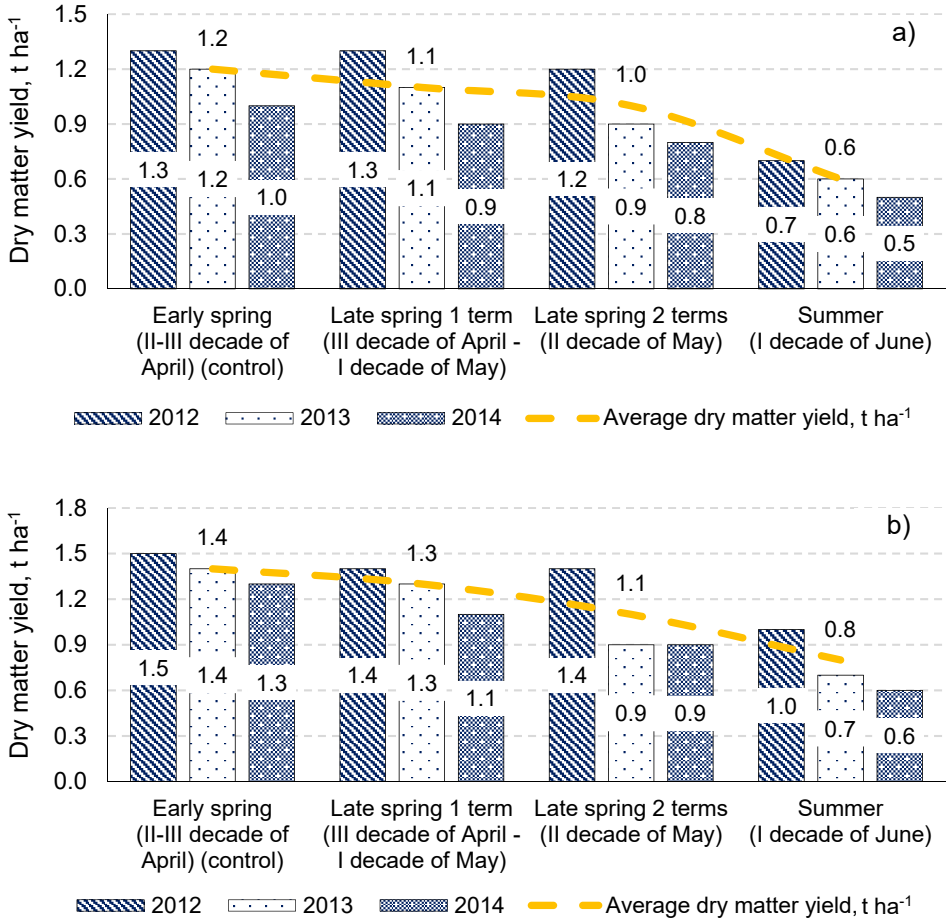


**Figure 2.** Dry matter yield development dynamics: a) blue melilot; b) fenugreek.

The above-mentioned results align with the data obtained in the state of Alberta for the production of hay from blue melilot and fenugreek. In this area, the recommended sowing term is from the middle of April to the middle of May (Acharya et al., 2008). In Kansas, Obour et al. (2015) have reported that the timing of sowing within the period from the 1st of April through the 22nd of May has no effect on the fodder yield. In Poland, Bieńkowski et al. (2016) have reported that the highest seed yield per plant was reached in case of the earliest sowing terms in spring, while the maximum recorded seed yield was equal to 840 kg ha$^{-1}$.

Although the cultivation of blue melilot and fenugreek are concentrated mostly in some countries of Africa and Asia, it is grown throughout the world in different

environmental conditions, where the annual rainfall varies within the range of 300–1,500 mm and the average yearly temperature - within the range of 7.8–27.5 °C (Solorio-Sánchez et al., 2014; Ahmad et al., 2016). *Trigonella* is considered a drought-resistant plant and its relatively low requirement to precipitation makes it suitable for the semi-arid conditions of the Great Plains, for example, in Alberta, Canada (Acharya et al., 2008), Kansas (Obour et al., 2015) and western Nebraska. *Trigonella* is sensitive to moisture deficiency, especially immediately after sowing (Żuk-Gołaszewska et al., 2015). That is supported by the results of the research into blue melilot by Akhalkatsi & Losch (2005). They have proved that shortage of water in the period of seed germination limits the germinating capacity and development of the plants. Seasonal irrigation is needed to achieve the maximum yield. In Iran, Dadrasan et al. (2015) have reported that insufficient irrigation (75%) not meeting the plants' demand reduces the seed yield by 27% and the fodder yield by 40%. In India, where *Trigonella* sp. were grown in winter with small amounts of rainfall, the irrigation resulted in an increase in the seed yield to a maximum of 1,300 kg $ha^{-1}$ (Kumar et al., 2000).

Plants need certain quantities of heat for their development (Reshma & Samir 2021). It is difficult to forecast the growth of plants by the calendar, because the temperature can greatly vary from year to year (Abou-Shleel, 2014). Instead of that, the 'Growing Degree Days' (GDD) method can be applied. The method is based on the actual temperatures, it is a simple, but accurate way of predicting when a certain plant development stage will be reached. Moreover, according to the paper (Ionescu & Roman, 2013), the maturity was reached in the third ten-day period of July, that is, after 95 days of growth, when the accumulation of the above-mentioned heating units totalled 922.2 GDD (St > 10 °C).

Within the recorded three years of cultivation, the sum of effective air temperatures (> 10 °C) in the species growth season varied, depending on the sowing terms, within the range of 316 to 508 °C, the precipitation total - within the range of 36 to 195 mm. At the same time, the herbage yield varied from 0.9 t $ha^{-1}$ to 10.2 t $ha^{-1}$, the dry matter yield - from 0.5 t $ha^{-1}$ to 1.5 t $ha^{-1}$. The above-mentioned data make it possible to determine the yield variability criterion per degree °C of the sum of effective air temperatures and per mm of the precipitation total. A strong direct relation between the species herbage yield and its dry matter yield has been established ($r$ = 0.88 to 0.99). A strong direct relation exists between the species dry matter yield at different sowing terms and the sum of effective air temperatures ($r$ = 0.66 to 0.99). Intermediate and strong inverse relations have been found between the species dry matter yield at different sowing terms and the precipitation total ($r$ = -0.48 to -0.99) (Table 5).

In order to establish the direction and type of the effect that the parameters of the sum of effective air temperatures (> 10 °C) and the precipitation total have on two species yield value at different sowing terms, the authors have generated and analysed the regression equations.

Basing on the results of the regression equation analysis, it has been established that an increase in the sum of effective air temperatures by 1 °C results in the variation of the blue melilot yield at different sowing terms: herbage yield - within the range of 4.82 to 128 kg $ha^{-1}$, dry matter yield - within the range of 0.401 to 6.06 kg $ha^{-1}$. Increasing the precipitation total by 1 mm results in the variation of the herbage yield within the range of 16.1 to 146 kg $ha^{-1}$, the dry matter yield - within the range of 0.145 to 22.7 kg $ha^{-1}$.

**Table 5.** Modelling of blue melilot and fenugreek yield development

| Sowing term | Regression equations | |
|---|---|---|
| | Herbage yield (y) | Dry matter yield (y) |
| Blue melilot | | |
| Early spring (decades II–III of April) (reference case) | $y = -71.408+0.1277 \cdot x_1+0.1465 \cdot x_2$ | $y = -2.3375+0.0061 \cdot x_1+0.0054 \cdot x_2$ |
| Late spring. term 1 (decade III of April-decade I of May) | $y = -21.5585+0.0533 \cdot x_1+0.0283 \cdot x_2$ | $y = -0.6787+0.0039 \cdot x_1+0.000145 \cdot x_2$ |
| Late spring. term 2 (decade II of May) | $y = 18.8633-0.0111 \cdot x_1-0.0967 \cdot x_2$ | $y = 4.1151-0.0018 \cdot x_1-0.0225 \cdot x_2$ |
| Summer (decade I of June) | $y = 4.2259-0.0048 \cdot x_1-0.0161 \cdot x_2$ | $y = 1.0105-0.0004 \cdot x_1-0034 \cdot x_2$ |
| Fenugreek | | |
| Early spring (decades II–III of April) (reference case) | $y = 0.2199+0.0141 \cdot x_1+0.015 \cdot x_2$ | $y = 0.4699+0.0016 \cdot x_1+0.0011 \cdot x_2$ |
| Late spring. term 1 (decade III of April-decade I of May) | $y = -11.5108+0.0339 \cdot x_1+0.0227 \cdot x_2$ | $y = 0.3536+0.0022 \cdot x_1-0.0007 \cdot x_2$ |
| Late spring. term 2 (decade II of May) | $y = -13.8269+0.0212 \cdot x_1+0.0773 \cdot x_2$ | $y = -4.7949+0.0066 \cdot x_1+0.0259 \cdot x_2$ |
| Summer (decade I of June) | $y = -4.0142+0.0102 \cdot x_1+0.0184 \cdot x_2$ | $y = -1.3691+0.0043 \cdot x_1+0.0068 \cdot x_2$ |

Note: $x_1$ – sum of effective air temperatures (> 10 °C); $x_2$ – precipitation total in mm.

An increase in the sum of effective air temperatures by 1 °C results in the variation of the fenugreek yield at different sowing terms: herbage yield - within the range of 10.25 to 33.9 kg $ha^{-1}$, dry matter yield - 1.58 to 6.63 kg $ha^{-1}$. Increasing the precipitation total by 1 mm results in the variation of the herbage yield within the range of 15.0 to 77.3 kg $ha^{-1}$, dry matter yield - within the range of 0.693 to 25.9 kg $ha^{-1}$.

The research into the cultivation of blue melilot and fenugreek has revealed a difference between their seed productivities (Table 6).

It has been established that the early spring (decades II–III of April) and late spring (decade III of April-decade I of May) sowing terms are the most favourable ones for the growth and development of species, that is, the optimal amount of precipitation in April and the increased temperatures during the second part of summer have positive effect on the seed productivity of species. In case of these terms, the plants develop the greatest amounts of pods and seeds in them. That results in the improved seed productivity of species, as compared to the summer sowing terms.

In the conditions of semi-arid high-altitude plains in the USA, the variation of the sowing terms within the range of the first ten-day period in May to the first ten-day period in June had no effect on the plant height (Pavlista & Santra, 2016). The heights of *Trigonellas* varied within the range of 33 to 41 cm for two varieties within the range indicated for *Trigonella* in Turkey, 36 to 44 cm (Tuncturk et al., 2011) and for *Trigonella* in India, 25 to 54 cm, depending on the genotype, 38 cm on the average (Chandra et al., 2000). In Canada, the height of the *Trigonella* in the time of flowering was equal to about 40 cm (Acharya et al., 2008).

**Table 6.** Relation between sowing terms and seed productivity of blue melilot and fenugreek

| Sowing terms (factor B) | Number of pods per plant, pcs | Length of pod, cm | Number of seeds per pod, pcs | Mean productivity, g | Seed yield, t $ha^{-1}$ | Mass of 1,000 seeds, g |
|---|---|---|---|---|---|---|
| Blue melilot (factor A) | | | | | | |
| Early spring (decades II–III of April) (reference case) | 133.5 ± 25.3 | 2.4 ± 0.4 | 27.3 ± 5.7 | 2.6 ± 0.4 | 0.40 ± 0.2 | 0.71 ± 0.24 |
| Late spring, term 1 (decade III of April-decade I of May) | 81.8 ± 12.7 | 1.8 ± 0.1 | 16.2 ± 4.3 | 0.9 ± 0.2 | 0.10 ± 0.05 | 0.65 ± 0.13 |
| Late spring, term 2 (decade II of May) | 56.3 ± 12.5 | 1.5 ± 0.3 | 13.5 ± 5.6 | 0.5 ± 0.3 | 0.07 ± 0.03 | 0.60 ± 0.09 |
| Summer (decade I of June) | 31.0 ± 8.6 | 1.3 ± 0.4 | 11.7 ± 4.8 | 0.2 ± 0.1 | 0.03 ± 0.01 | 0.52 ± 0.05 |
| Fenugreek | | | | | | |
| Early spring (decades II–III of April) (reference case) | 65.7 ± 14.7 | 15.0 ± 2.8 | 21.0 ± 4.5 | 13.3 ± 4.8 | 2.0 ± 0.7 | 9.7 ± 1.5 |
| Late spring, term 1 (decade III of April-decade I of May) | 46.5 ± 13.8 | 10.7 ± 1.5 | 15.3 ± 2.3 | 6.4 ± 2.4 | 0.9 ± 0.3 | 9.0 ± 1.1 |
| Late spring, term 2 (decade II of May) | 35.1 ± 10.2 | 9.5 ± 1.2 | 12.8 ± 3.1 | 3.9 ± 1.3 | 0.6 ± 0.2 | 8.7 ± 0.9 |
| Summer (decade I of June) | 21.0 ± 9.8 | 8.0 ± 0.9 | 10.8 ± 2.7 | 1.7 ± 0.8 | 0.2 ± 0.09 | 7.5 ± 0.6 |

Fenugreek produces low plants - up to 40 cm, with lower numbers of pods per plant (21.0–65.7 pcs). Moreover, in the years with the increased sums of effective air temperatures the productivity of fenugreek decreases. Another distinctive feature of fenugreek is that it produces long pods with a length of 8.0 to 15.0 cm, which contain small numbers of seeds (10.8–21.0 pcs per pod).

Özyazıcı (2020) has established that the seed yield positively and significantly correlated with the number of pods per plant ($r = 0.70$), the pod length ($r = 0.33$), the number of seeds per pod ($r = 0.51$), the mass of one thousand seeds ($r = 0.57$). Increases in these indices result in significant increases in the plant seed yield. The highest coefficients of correlation for the seed yield have been found in its relationships with the number of pods per plant, the number of seeds per pod and the mass of one thousand seeds. Parchin et al. (2019) have stated that there is a positive correlation between the number of pods per plant and the seed yield.

A positive and significant correlation has been determined between the plant height and the height of the first pod. Positive and significant correlations have been revealed between the number of pods per plant and the pod length as well as between the number of seeds per pod and the mass of one thousand seeds. Positive and significant interrelations have been found between the mass of one thousand seeds and the number of pods per plant as well as between the pod length and the number of seeds per pod. Many papers state that the number of seeds per pod, the number of pods per plant and the mass of one thousand seeds are the primary factors that have a direct effect on the seed yield (Patahk et al., 2014; Singh et al., 2019a; Singh et al., 2019b).

In the conditions of West Bengal, India, the number of seeds per pod varies within the range of 14.67 to 16.38 pcs for different times of sowing (Bhutia et al., 2017). Nandre et al. (2011) have established that the *Trigonella* plants sown on the 1st of November yield considerably greater numbers of seeds per pod. Bhutia & Sharangi (2016), Sultana et al. (2016) obtained the highest numbers of seeds per pod in case of sowing on the 23rd of November.

Blue melilot grows higher reaching plant heights of up to 100 cm. It blossoms with small blue flowers on the stem apices. The seeds are smaller comparing to fenugreek (approximately by a factor of 3–5). The scent is less pronounced. At the same time, blue melilot produces greater numbers of pods per plant at all sowing terms (31.0–133.5 pcs). However, blue melilot features short pods, in which small seeds develop, 1,000 seeds weighing 0.52–0.71 g. That results in the low seed productivity of the species, which is equal to 0.2–2.6 g per plant, despite the greater number of seeds per pod. Overall, the seed yield of blue melilot varies within the range of 0.03–0.40 t $ha^{-1}$.

Tuncturk et al. (2011) have reported that 1,000 seeds weigh 18 g in Turkey, which is heavier than in western Nebraska (12 g) for fenugreek. In Poland, the variation of the 1,000 seed weight within the range of 14 to 15 g has been recorded (Bieńkowski et al., 2016). The difference between seed masses is probably caused by the germinal plasma, because different germinal plasmas differ as regards the seed mass even for the plants grown close to each other in the same year (Pavlista & Santra, 2015).

Fenugreek produces seeds with greater sizes, 1,000 seeds weighing 7.5–9.7 g, which results in the higher seed productivity of its plants. The average seed productivity was recorded at higher levels in case of early spring sowing terms, where it was equal to 13.3 g per plant, resulting in the improvement of the seed yield, which reached 2.0 t $ha^{-1}$ for fenugreek. Moreover, its seeds after their grinding emitted intense pleasant mushroom aroma.

In the tropics, species for seed production is usually sown in the winter season. The maximum seed yield was obtained in case of sowing on the 30th of October (1.45 t $ha^{-1}$), the lowest one - when sowing on the 30th of December (0.93 t $ha^{-1}$) (Bhutia et al., 2017). According to the data by Nandre et al. (2011), the highest species seed yield per hectare was obtained in case of sowing on the 1st of November. Lal et al. (2003) have also revealed similar results for *Trigonella*. Bhutia & Sharangi (2016) and Sultana et al. (2016) obtained the highest seed yield after sowing on the 2nd of November. The possible cause of the low productivity in case of late sowing can be related to the insufficient time for vegetative growth due to the plant entering the reproductive phase more rapidly. Delays in harvesting increase the risk of pod dehiscence and seed loss. Petropoulos (2002) has also reported that the late sowing in spring has resulted in a reduced seed yield.

Lower seed yield was recorded in case of summer sowing terms, where it was equal to 0.2 t $ha^{-1}$, which was lower by 1.8 t $ha^{-1}$, as compared to the reference case. Moreover, with each succeeding sowing term fenugreek produced lower numbers of pods per plant, shorter pods, smaller numbers of seeds per pod and lower weights of 1,000 seeds, which resulted in lower seed yields as compared to the early spring sowing terms.

The time of sowing is of critical importance for the vegetative growth of plants and the procurement of the highest possible yield. Early or late seeding can impair the growth, the yield capacity and also the quality of the harvest (Al-Dalain et al., 2012). In case of *Trigonella*, early sowing results in early flowering, but then the plants are

vulnerable to damage in the event of severe cold and frost. Overall, the crop needs a cool climate during its vegetative growth and a warm dry climate at the ripening stage (Aggarwal et al., 2013). Plants sown on an optimal day have better chances of achieving the correct phenological development (Bieńkowski et al., 2016).

## CONCLUSIONS

Blue melilot and fenugreek species have a wide range of variability as regards their morphologic and economically valuable properties, depending on the time of their sowing. The earliest ripening of two species has been recorded in case of summer sowing terms - the vegetative season duration was equal to 36–37 days. In case of early spring sowing dates, the species growth period became longer and was equal to 50–52 days.

It has been established that the early spring sowing terms (decades II–III of April) and the late spring sowing terms (decade I of May) are more suitable for obtaining high herbage yields from the plants of blue melilot and fenugreek in the green conveyor system - with these sowing terms, the herbage yield is equal to 5.7–6.9 t $ha^{-1}$ for blue melilot and 7.3–9.3 t $ha^{-1}$ - for fenugreek, the herbage containing dry matter at levels of 12.4–28.4%, total sugars - 2.5–5.0% and vitamin C - 38.0–51.8 mg $(100\ g)^{-1}$.

For the purpose of obtaining the spice named 'mushroom grass', the promising development trend is to use fenugreek sown at the early spring terms (decades II–III of April) and the late spring terms (decade I of May), as it produces better developed vegetative mass and delivers a plant dry matter yield of 1.3–1.4 t $ha^{-1}$ and a seed yield of 0.9–2.0 t $ha^{-1}$, 1,000 seeds weighing 9.0–9.7 g.

It has been revealed that an increase in the sum of effective air temperatures by 1 °C results in the variation of the fenugreek yield at different sowing terms as follows: the herbage yield - within the range of 10.25 to 33.9 kg $ha^{-1}$, the dry matter yield - within the range of 1.58 to 6.63 kg $ha^{-1}$. An increase in the precipitation total by 1 mm results in the variation of the herbage yield within the range of 15.0 to 77.3 kg $ha^{-1}$, the dry matter yield – within the range of 0.693 to 25.9 kg $ha^{-1}$.

## REFERENCES


Abou-Shleel. S.M. 2014. Effect of Air Temperature on Growth, Yield and Active Ingredients of Fenugreek (*Trigonella foenum-graecum*). *Nature and Science* **12**(9), 50–54.

Abramchuk, A.V. & Karpuhin, M.Yu. 2018. Chemical composition and pharmacologic properties of fenugreek *(Trigonella foenum graecum* L.). *Bulletin of Biotechnologies* **3**, 6 p. http://bio.beonrails.ru/ru/issues/2018/3/170. Accessed: 3.09.2021. (in Russian)

Acharya, S.N., Thomas, J.E. & Basu, S.K. 2008. Fenugreek, an Alternative Crop for Semiarid Regions of North America. *Crop Science* **48**(3), 841–853. doi: 10.2135/cropsci2007.09.0519

Aggarwal, K.B., Ranjan, J.K., Rathore, S.S., Saxena, S.N. & Mishra, B.K. 2013. Changes in physical and biochemical properties of fenugreek (*Trigonella sp.* L.) leaf during different growth stages. *Int J Seed Spices* **3**(1), 31–5.

Ahmad, A., Alghamdi, S.S., Mahmood, K. & Afzal, M. 2016. Fenugreek a multipurpose crop: potentialities and improvements. *Saudi. J. Biol. Sci*. **23**(2), 300–310. doi: 10.1016/j.sjbs.2015.09.01

Akhalkatsi, M. & Losch, R. 2005. Water limitation effect on seed development and germination in Trigonella coerula (Fabaceae). *Flora* **200**(6), 493–501. doi: 10.1016/j.flora.2005.06.001

Al-Dalain, S.A., Abdel-Ghani, A.H., Al-Dala'een, J.A. & Thalaen, H.A. 2012. Effect of planting date and spacing on growth and yield of fennel (*Foeniculum vulgare* Mill.) under irrigated conditions. *Pak. J. Bio.l Sci*. **15**(23).1126–32. doi: 10.3923/pjbs.2012.1126.1132

Al-Timimi, L.A.N. 2019. Antibacterial and Anticancer Activities of Fenugreek Seed Extract. *Asian Pacific Journal of Cancer Prevention* **20**(12), 3771–3776. doi: 10.31557/APJCP.2019.20.12.3771

Ates, E. 2016. The Effect of Different Growth Stages on Some Forage Quality Characters of the Leaf and Stem in Four Newly Developed Genotypes of Blue Melilot (*Melilotus caeruleus* (L.) Desr.). *Greener Journal of Plant Breeding and Crop Science* **4**(5), 087–093. doi: 10.15580/GJPBCS.2016.5.082516139

Arslan, B., Culpan, E. & Ates, E. 2016. A New Alternative Species as a Medicinal, Aromatic and Forage Crop: Blue Melilot (Melilotus caeruleus (L.) Desr.). *Journal of Agricultural Faculty of Uludag University* **30**, Special Issue, 392–394.

Bafadam, S., Beheshti, F., Khodabakhshi, T., Asghari, A., Ebrahimi, B., Sadeghnia, H.R., Mahmoudabady, M.; Niazmand, S. & Hosseini, M. 2019. Trigonella foenum-graceum seed (Fenugreek) hydroalcoholic extract improved the oxidative stress status in a rat model of diabetes-induced memory impairment. *Horm. Mol. Biol. Clin. Investig*. **39**(2). doi: 10.1515/hmbci-2018-0074

Beyzi, E. & Gürbüz, B. 2020. Influence of sowing date and humic acid on fenugreek (*Trigonella foenum-graecum* L.) *Journal of Applied Research on Medicinal and Aromatic Plants* **16**, No. 100234. doi: 10.1016/j.jarmap.2019.100234

Beyzi, E., Safak, E.K., Gürbüz, P., Kosar, M. & Gürbüz, B. 2021. Fatty acid composition, diosgenin and trigonelline contents of fenugreek (*Trigonella foenum-graecum*): Effects of phosphorus fertilizer. Plant Biosyst. *Int. J. Deal. All Asp. Plant Biol*. **155**(4), 663–667. doi: 10.1080/11263504.2020.1769216

Bhutia, K.C., Bhutia, S.O., Chatterjee, R. & Chattopadhyay, N. 2017. Growth, Phenology and Yield of Fenugreek (*Trigonella foenum-graecum* L.) as Influenced by Date of Sowing. *International Journal of Current Microbiology and Applied Sciences* **6**(10), 1810–1817. doi: 10.20546/ijcmas.2017.610.218

Bhutia, P.H. & Sharangi, A.B. 2016. Effect of Dates of Sowing and Soil Moisture Level in Different Growth Stages and Yield Dynamics of Fenugreek (*Trigonella foenum-graecum* L.). *Natl. Acad. Sci. Lett*. **39**(2), 77–80. doi: 10.1007/s40009-016-0428-2

Bieńkowski, T., Żuk-Gołaszewska, K., Kurowski, T. & Gołaszewski, J. 2016. Agrotechnical indicators for *Trigonella foenum-gracum* L. Production in the environmental conditions of Northeastern Europe. Turkish Journal of Field Crops 21(1), 16–28. doi: 10.17557/tjfc.37573

Bobos, I.M. 2013. Seed productivity of mushroom grass. Variety research and protection of rights to plant varieties. Kiev: *Ukrainian Institute for Plant Variety Examination* **2**, 66–68 (in Ukrainian).

Bobos, I.M. & Kokoyko, V.V. 2013. Mushroom grass – a promising spice and flavour plant in Ukraine. *Scientific bulletin of NUBiP of Ukraine*: *Agronomy series. Publishing Centre of NUBiP of Ukraine* **183**(1), 114–119 (in Ukrainian).

Bobos, I.M. 2015. Growth and development of gunba at different sowing terms. In: *Proceedings of Sworld*, 23, **1**(38), 98–1001, http://elibrary.ru/item.asp?id=23301283 (in Ukrainian).

Bobos, I., Fedosy, I., Zavadska, O., Tonha, O. & Olt, J. 2019. Optimization of plant densities of dolichos *(Dolichos lablab l. var. lignosus)* bean in the right-bank of forest-steppe of Ukraine. *Agronomy Research* **17**(6), 2195–2202. https://doi.org/10.15159/AR.19.223

Bondarenka, G.L. & Yakovenka, K.I. 2001. *Methodology of experimenting in vegetable farming and melon growing*. Kharkiv: Osnova, 369 pp. (in Ukrainian).

Chandra, K., Sastry, E.V.D. & Singh, D. 2000. Genetic variation and character association of seed yield and its component characters in fenugreek. *Agricultural Science Digest* **20**, 93–95.

Ciftci, O.N., Przybylski, R., Rudzinska, M. & Acharya, S. 2011. Characterization of fenugreek (*Trigonella foenum-graecum*) seed lipids. *Journal of the American Oil Chemists' Society* **88**(10), 1603–1610. doi: 10.1007/s11746-011-1823-y

Dadrasan, M., Chaichi, M.R., Pourbabaee, A.A., Yazdani, D. & Keshavarz-Afshar, R. 2015. Deficit irrigation and biological fertilizer influence on yield and trigonelline production of fenugreek. *Industrial Crops and Products* **77**, 156–162. doi: 10.1016/j.indcrop.2015.08.040

Dangi, R.S, Lagu, M.D., Choudhary, L.B., Ranjekar, P.K. & Gupta, V.S. 2004. Assessment of Genetic Diversity in Trigonella Foenum-Graecum and Trigonella Caerulea Using ISSR and RAPD Markers. *BMC Plant Biology* **4**(13), 4–28. doi: 10.1186/1471-2229-4-13

Devasena, T. & Menon, V.P. 2003. Fenugreek affects the activity of β-glucuronidase and mucinase in the colon. *Phytotherapy Research* **17**(9), 1088–1091. doi: 10.1002/ptr.1331

Faeste, C.K., Namork, E. & Lindvik, H. 2009. Allergenicity and antigenicity of fenugreek (*Trigonella foenum-graecum*) proteins in foods. *Journal of Allergy and Clinical Immunology* **123**(1), 187–194. doi: 10.1016/j.jaci.2008.09.012

Fernandez-Aparicio, M., Emeran, A.A. & Rubiales, A. 2008. Control of Orobanche crenata in legumes intercropped with fenugreek (Trigonella foenum graecum L.). *Crop protection* **27**(3–5), 653–659. doi: 10.1016/j.cropro.2007.09.009

Güzel, Y. & Özyazıcı, G. 2021. Adoption of Promising Fenugreek (*Trigonella foenum-graceum* L.) Genotypes for Yield and Quality Characteristics in the Semiarid Climate of Turkey. *Atmosphere* **12**, 1199. doi: 10.3390/atmos12091199

Ionescu, A.M. & Roman, Gh.V. 2013. Research on biology, productivity and yield quality of *Trigonella foenum-graecum* L. species (Fenugreek) in the Central Part of the South Romanian Plain. *Scientific Papers Series A. Agronomy* **56**, 395–397.

Jani, R, Udipi, S.A. & Ghugre, P.S. 2009. Mineral content of complementary foods. *The Indian Journal of Pediatrics* **76**(1), 37–44. doi: 10.1007/s12098-009-0027-z

Kaviarasan, S., Viswanathan, P., Anuradha, C.V. 2007. Fenugreek seed (Trigonella foenum graecum L.) polyphenols inhibit ethanol-induced collagen and lipid accumulation in rat liver. *Cell Biol. Toxicol.* **23**(6), 373–380. doi: 10.1007/s10565-007-9000-7

Khorshidian, N., Asli, M.Y., Arab, M., Mortazavian, A.M. & Mirzaie, A.A. 2016. Fenugreek: potential applications as a functional food and nutraceutical. *Nutrition and Food Science* **3**(1), 5–16. doi: 10.18869/acadpub.nfsr.3.1.5

Kumar, P., Kale, R.K., McLean, P. & Baquer, N.Z. 2012. Antidiabetic and neuroprotective effects of Trigonella foenum-graecum seed powder in diabetic rat brain. *Prague Medical Report* **113**(1), 33–43. doi: 10.14712/23362936.2015.35

Kumar, V., Yadav, J.S., Singh, J. & Yadav, B.D. 2000. Irrigation and phosphorus requirement of fenugreek (*Trigonella foenum-graecum*) on light soil. *Indian Journal of Agricultural Sciences* **70**(8), 515–517.

Lal, S., Rana, M.K. & Pratap, P.S. 2003. Effect of date of sowing and green cuttings on quality of different fenugreek genotypes. *Haryana J. Hort. Sci.* **32**(3/4), 262–265.

Maletić, R. & Jevdjović, R. 2007. Sowing date – the factor of yield and quality of fenugreek seed (*Trigonella foenum graecum* L). *Journal of Agricultural Sciences* **52**(1), 1–8. doi: 10.2298/JAS0701001M

Meghwal, M. & Goswami, T.K. 2012. A review on the functional properties, nutritional content, medicinal utilization and potential application of fenugreek. *Journal of Food Processing and Technology* **3**(9), 181. doi: 10.4172/2157-7110.1000181

Muhammad, T., Khalid, H., Iqra, I., Khalid, N., Noshia, A., Sana, J. & Usman, A. 2020. Efficacy of IAA, GA3 and Riboflavin for Morpho-biochemical and Yield Attributes of Fenugreek (*Trigonella foenum-graecum* L.) in Pakistan. *Legume Research* **43**(6), 780–787. doi: 10.18805/A-575

Nandre, D.R., Ghadge, R.G. & Rajput, B.S. 2011. Effect of sowing dates and nutrient management on growth and seed yield fenugreek. *Adv. Res. J. Crop Improv* **2**(2), 215–220. doi: 10.1007/s40009-016-0428-2

Obour, A., Obeng, E. & Holman, J.D. 2015. Influence of different seeding dates on fenugreek (*Trigonella foenum-graecum* L.) forage yield and nutritive value. *Kansas Agricultural Experiment Station Research Reports* **1**(2). doi: 10.4148/2378-5977.1032

Özyazıcı, G. 2020. Responses of sulfur and phosphorus doses on the yield and quality of fenugreek (*Trigonella foenum-graecum* L.). *Appl. Ecol. Environ. Res*. **18**(5), 7041–7055. doi: 10.15666/aeer/1805_70417055

Pandian, R.S., Anuradha, C.V. & Viswanathan, P. 2002. Gastroprotective effect of fenugreek seeds (Trigonella foenum graecum) on expermental gastric ullcer in rats. *J. Ethnopharmacol*. **81**(3), 393–397. doi: 10.1016/s0378-8741(02)00117-4

Parchin, R.A., Ghomi, A.A.N., Hasanali, N.B., Eskandari, A., Navabpour, S. & Mehrafarin, A. 2019. Growth characteristics and phytochemical responses of Iranian fenugreek (*Trigonella foenum-graecum* L.) exposed to gamma irradiation. *Industrial Crops & Products* **139**, 111593.

Patahk, A.R., Patel, A.I., Joshi, H.K. & Patel, D.A. 2014. Genetic variability, correlation and path coefficient analysis in fenugreek (*Trigonella foenum-graecum* L.). *Trends in Bios* **7**(4), 234–237.

Pavlista, A. & Santra, D.K. 2015. Seed Yield of Fenugreek in Response to Planting Date, Irrigation, and Harvest Time. *Hortscience* **50**(9), 134.

Pavlista, A.D. & Santra, D.K. 2016. Planting and harvest dates, and irrigation on fenugreek in the semi-arid high plains of the USA. *Industrial Crops and Products* **94**, 65–71. doi: 10.1016/j.indcrop.2016.07.052

Petropoulos, G.A. 2002. Cultivation. In: Petropoulos, G.A. (Ed.), Fenugreek The genus Trigonella. CRC Press, Boca Raton, FL, USA, 26–72.

Plechishchik, Ye.D., Goncharova, L.V., Sprodovich, E.V. & Peshotnikov, V.N. 2010. Fenugreek as a source of wide spectrum of bioactive compounds. *Proceedings of BSU* **4**(2), 1–19.

Premanath, R., Sudisha, J., Lakshmi Devi, N. & Aradhya, S.M. 2011. Antibacterial and Anti-oxidant Activities of Fenugreek *(Trigonella foenum graecum* L*.)* leaves. *Research Journal of Medical Plants* **5**(6), 695–705. doi: 10.3923/rjmp.2011.695.705

Randhawa, G.S., Gill, B.S., Saini, S.S. & Singh, J. 1996. Agronomic technology for production of fenugreek (Trigonella foenum graecum L.) Seeds. *Journal of Herbs, Spices and Medicinal Plants* **4**(3), 43–49. doi: 10.1300/J044v44v04n03_06

Rao, G.N., 2007. *Statistics for Agricultural Sciences*, 2nd ed., BS Publications, p. 466.

Reshma, M.I.S. & Samir, E.T. 2021. Evaluation of Fenugreek (*Trigonella foenum-graecum*) Cultivars in Relation to Herbage and Seed Yield in Prayagraj Agro-climatic Condition. *International Journal of Current Microbiology and Applied Sciences* **10**(01), 2575–2580. doi: 10.20546/ijcmas.2021.1001.299

Saxena, S.N., Kakani, R.K., Sharma, L.K., Agarwal, D., John, S. & Sharma, Y. 2019. Effect of water stress on morpho-physiological parameters of fenugreek (*Trigonella foenum-graecum* L.) genotypes. *Legume Res*. **42**, 60–65. doi: 10.18805/LR-3830

Shelyuto, B. 2013. Productivity and economic efficiency of cultivating fenugreek, (*Trigonella foenum graecum* L.) Chiadonha variety, in conditions of north-eastern Belarus, in relation to sowing terms. *Agrarian Economics* **5**, 50–55.

Singh, A., Pandey, V.P., Kumar, P., Kumar, M., Kumar, S. & Vaishya, D.V. 2019a. To study of correlation coefficient and path coefficient analysis for different characters in germplasm of fenugreek (*Trigonella foenum graecum* L.). *Journal of Pharmacognosy and Phytochemistry* **8**(1). 857–861.

Singh, A.K., Singh, D.R., Singh, A., Maurya, J.K., Pandey, V.P. & Sriom, D.R. 2019b. Studies on character association and path analysis of yield with important yield contributing traits in fenugreek (*Trigonella foenum-graecum* L.). *Journal of Pharmacognosy and Phytochemistry* **8**(3), 4616–4619.

Solorio-Sánchez, F., Solorio-Sánchez, B., Basu, S.K., Casanova-Lugo, F., Sarabia-Salgado, L., Ku-Vera, J. & Cetzal-Ix, W. 2014. Opportunities to grow annual forage legume fenugreek (*Trigonella foenum-graecum* L.) under mexican sylvopastoral system. *Am. J. Social Issues Humanities*, 86–95.

Srinivasan, K. 2006. Fenugreek (*Trigonella foenum graecum* L.)*:* A review of health beneficial physiological effect. *Food Reviews International* **22**(2), 203–224. doi: 10.1080/87559120600586315

Sultana, S., Das, G., Das, B. & Sarkar, S. 2016. Influence of dates of sowing on growth and yield dynamics of fenugreek (*Trigonella foenum-graecum* L.). *International Journal of Green Pharmacy* **10**(4), 236. doi: 10.22377/ijgp.v10i04.788

Sych, Z.D. & Bobos, I.M. 2013. The new vegetable plants are in modern vegetable business. Earth Bioresources and Quality of Life. *International Scientific Electronic Journal Earth* http://gchera-ejournal.nubip.edu.ua.

Sych, Z.D., Bobos, I.M., Kotyuk, N.B., Kutovenko, V.B., Fedosiy, I.A., Strigin, V.M., Kovalchuk, D.P. & Popovich, I.G. 2010. *Guidelines on cultivation of less common leguminous vegetable crops in the Forest Steppe Region of Ukraine*. NUBiP of Ukraine, 41 pp. (in Ukrainian).

Thirunavukkarasu, V. & Anuradha, C.V. 2007. Gastroprotective effect of fenugreek seeds (Trigonella foenum graecum) on experimental gastric ulcer in rats. *Journal of Herbs, Spices and Medicinal Plants* **12**(3), 13–25. doi: 10.1300/j044v12n03_02

Tonkha, O., Menshov, O., Bykova, O., Pikovska, O. & Fedosiy, I. 2020. Magnetic methods application for the physical and chemical properties assessment of Ukraine soil. Conference Proceedings, XIV International Scientific Conference «Monitoring of Geological Processes and Ecological Condition of the Environment». *European Association of Geoscientists & Engineers,* **2020**, pp. 1–5. doi: 10.3997/2214-4609.202056027

Tuncturk, R., Celen, A.E. & Tuncturk, M. 2011. The effects of nitrogen and sulphur fertilizers on the yield and quality of fenugreek (*Trigonella foenum-graecum* L.). *Turkish Journal of Field Crops* **16**(1), 69–75.

Vaidya, K., Ghosh, A., Kumar, V., Chaudhary, S., Srivastava, N., Katudia, K., Tiwari, T. & Chikara, S.K. 2013. De Novo transcriptome sequencing in L. to identify genes involved in the biosynthesis of diosgenin. *The Plant Genome* **6**(2), 1–11. doi: 10.3835/plantgenome2012.08.0021

Xalxo, R. & Keshavkant, S. 2020. Growth and antioxidant responses of *Trigonella foenum-graecum* L. seedlings to lead and simulated acid rain exposure. *Biologia* **75**(8), 1115–1126. doi: 10.2478/s11756-020-00478-y

Zavadska, O., Bobos, I., Fedosiy, I., Podpryatov, G. & Olt, J. 2020. Studying the storage and processing quality of the carrot taproots (Daucus carota) of various hybrids. *Agronomy Research* **18**(3), 2271–2284. https://doi.org/10.15159/ar.20.199

Zemzmi, J., Mabrouki, S., Abdouli, H. & Najar, T. 2017. Preliminary characterization of fenugreek seed gum for use as prebiotic in rabbits' nutrition. In *Proceedings of the 20th International Symposium on Housing and Diseases of Rabbits, Fur Providing Animals and Pet Animals*, Celle, Germany, 17–18 May, pp. 179–186.

Żuk-Gołaszewska, K., Wierzbowska, J. & Bieńkowski, T. 2015. The effect of potassium fertilization, Rhizobium inoculation and water deficit on the yield and quality of fenugreek seeds. *Journal of Elementology* **20**(2), 513–524. doi: 10.5601/jelem.2014.19.4.775

*Agronomy Research* **20**(1), 124–133, 2022
https://doi.org/10.15159/AR.22.006

# Effects of some agronomic practices on the quality of starch content of maize grains

P. Fejér*, A. Széles, É. Horváth, T. Rátonyi and P. Ragán

University of Debrecen, Faculty of Agricultural and Food Sciences and Environmental Management, Institute of Land Use, Engineering and Precision Farming Technology, 138 Böszörmenyi str., HU4032 Debrecen, Hungary
*Correspondence: fejerp@agr.unideb.hu

Received: February 1st, 2021; Accepted: January 15th, 2022; Published: February 28th, 2022

**Abstract.** The use of maize, both as main and by-product, is extremely versatile and diverse. The highest amount of carbohydrate within maize is found in the form of starch (C6H10O5)x. In terms of industrial starch, maize is the most important raw material. Fodder maize is primarily an energy source due to its high starch content, and its protein and oil content are less important. It was found that starch and protein content, which are negatively correlated with each other, are significantly affected by fertilizer doses. The experiment is located in the Hajdúság Loess Plateau, its soil is loess-based deep humus layered calcareous chernozem. The following treatments were applied in the scope of the polyfactorial experiment: Tillage: T1 = winter ploughing, T2 = strip tillage, T3 = ripping. Crop years: 2017, 2018 and 2019. Fertilization treatments: N 0 kg ha$^{-1}$ $P_2O_5$ 0 kg ha$^{-1}$ $K_2O$ 0 kg ha$^{-1}$ (control); N 80kg ha$^{-1}$ $P_2O_5$ 60 kg ha$^{-1}$ $K_2O$ 90 kg ha$^{-1}$ and N 160 kg ha$^{-1}$ $P_2O_5$ 60 kg ha$^{-1}$ $K_2O$ 90 kg ha$^{-1}$. Analysis of the nutritional component was carried out by means of a Foss Infratec TM 1241 Grain Analyser.
In terms of fertilization treatments, the highest (64.42%) maize starch content was measured for the control treatment, while the lowest starch content was recorded in the case of the 160 kg N ha$^{-1}$ treatment (62.62%). The analysis of the crop year effect showed that 2018 was the most favourable year for the maize starch content of the examined samples (65.76%). Of the studied years, the lowest starch content was measured in 2017 (61.78%).

**Key words:** starch content, starch yield, fertilization, crop year, tillage.

## INTRODUCTION

In the last few decades food insecurity was considered as one of the vital issues that facing humanity, which should be solved by increasing the quantity and the quality of agricultural products. On the other hand, world population is projected to reach 9 billion by 2050 (Roberts, 2011; Mohammed et al., 2021a); which create another pressure on the agricultural sector. Thus, the development of the agricultural sector is one of the main solutions to face this dilemma (Ramasamy & Moorthy, 2006). Yet, agricultural production still facing many obstacles, such as, climate change (Juhász et al., 2020), green houses gases emission (Harsányi et al., 2021a; Mohammed et al., 2021b), drought (Harsányi et al., 2021b), land degradation (Hateffard et al., 2021; Khallouf et al., 2021; Takács et al.,

2021), soil salinisation and contamination (Mohammed et al., 2021c), and many others. Thus, the united nation lunched the UN-2030 Agenda to solve the earths problems, which include zero hunger under Goal 2 (i.e., SDG-2) (Elbeltagi et al., 2021).

Maize is one of the important crops that plays an important role in human diet, worldwide (Prasanna et al., 2001). Globally, maize equipped around 192.50 million hectares of agricultural land, with yearly production of 1,112.40 million metric tons (Hulmani, 2021).

The use of maize, both as main and by-product, is extremely versatile and diverse (Nagy, 2007). In the world and in Hungary, maize is mainly considered as an energy-rich animal feed, but in developing and food-stricken countries, about 80–90% of the crop is used for human consumption (Pepó & Sárvári, 2011). The highest amount of carbohydrate within maize is found in the form of starch $(C_6H_{10}O_5)_x$. In terms of industrial starch, maize is the most important raw material. Fodder maize is primarily an energy source due to its high starch content, and its protein and oil content are less important. It was found that starch and protein content, which are negatively correlated with each other, are significantly affected by fertilizer doses. Appropriate hybrid selection plays a crucial role, which greatly influences yield and quality (Pepó, 2017). Nutrient replenishment is required to achieve adequate yields. Fertilizer has been shown to play a key role in the uptake of macro- and microelements (Nagy, 2017; Sadeghi et al., 2018). Giving above introduction, the main goals of this research were to: 1) analyse the effect of different level of fertilization doses (N 0 kg ha$^{-1}$ $P_2O_5$ 0 kg ha$^{-1}$ $K_2O$ 0 kg ha$^{-1}$ (control); N 80 kg ha$^{-1}$ $P_2O_5$ 60 kg ha$^{-1}$ $K_2O$ 90 kg ha$^{-1}$ and N 160 kg ha$^{-1}$ $P_2O_5$ 60 kg ha$^{-1}$ $K_2O$ 90 kg ha$^{-1}$) on starch content of maize grains, 2) analyse the effect of three tillage systems (winter ploughing (27 cm), strip tillage (23 cm), ripping) on starch content of maize grains, 3) analyse the year effect (climate effect) on starch content of maize grains, and 4) analyse the accumulative impact of these factors on the quality of starch content of maize grains.

## MATERIALS AND METHODS

**Experimental design:**

The Experimental Station of the University of Debrecen is located in the Hajdúság Loess Plateau, its soil is loess-based deep humus layered calcareous chernozem. The following treatments were applied in the scope of the polyfactorial experiment: Tillage: T1 = winter ploughing (27 cm), T2 = strip tillage (23 cm), T3 = ripping (45 cm). Fertilization treatments: N 0 kg ha$^{-1}$ $P_2O_5$ 0 kg ha$^{-1}$ $K_2O$ 0 kg ha$^{-1}$ (control); N 80 kg ha$^{-1}$ $P_2O_5$ 60 kg ha$^{-1}$ $K_2O$ 90 kg ha$^{-1}$ and N 160 kg ha$^{-1}$ $P_2O_5$ 60 kg ha$^{-1}$ $K_2O$ 90 kg ha$^{-1}$.

Fig. 1 shows the experimental design within the research station.

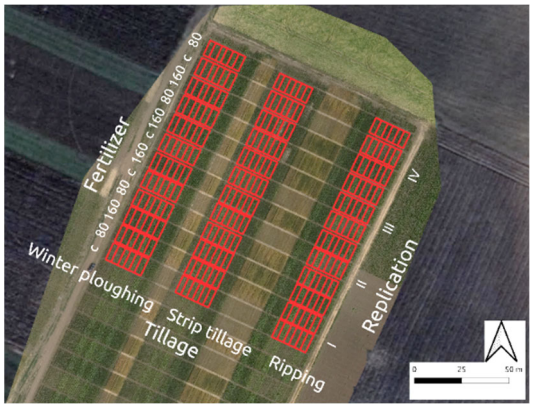


**Figure 1.** the experimental design in the Hajdúság Loess Plateau (Hungary).

Three maize hybrids have been utilized in the scope of the field trial, they are shown in Table 1.

**Table 1.** Hybrid composition of the field trials 2017–2019

| 2017 | | 2018 | | 2019 | |
|---|---|---|---|---|---|
| Hybrid name | FAO no. | Hybrid name | FAO no. | Hybrid name | FAO no. |
| *Armagnac* | FAO 490 | *Armagnac* | FAO 490 | *Armagnac* | FAO 490 |
| *Loupiac* | FAO 380 | *Loupiac* | FAO 380 | *Loupiac* | FAO 380 |
| *Fornad* | FAO 420 | *Fornad* | FAO 420 | *Fornad* | FAO 420 |

*Source: own editing.*

**Maize sampling and statistical analysis:**

Maize samples were collected for three years, between 2017 and 2019. Analysis of the nutritional component of the collected samples was carried out by means of a Foss Infratec TM 1241 Grain Analyser (FITM) at the Institute of Land Use, Engineering and Precision Farming Technology.

The FITM is a grain analyser that uses near-infrared to analyze several parameters (moisture, protein, oil, starch, etc.) in a variety of grains and oilseeds. The FITM has a number of advantages, including being quick, reliable, and simple to operate.

Weather data was evaluated based on the findings of Gombos & Nagy (2019) The 2017 crop year was 0.9 °C warmer and 91.1 mm moister than the 30-year average. The growing season in 2018 was 1.4 °C warmer and it was an average year in terms of precipitation (+ 1.5 mm). The year 2019 was 2.7 °C warmer and 191 mm drier than average (Fig. 2).

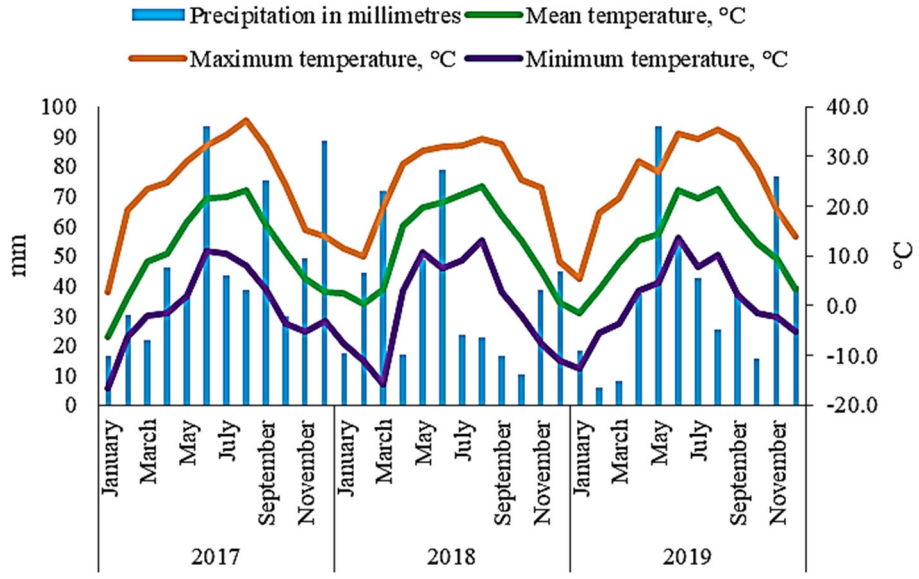


**Figure 2.** Temperature and precipitation data in Debrecen between 2017 and 2019. (https://www.ksh.hu/stadat_files/kor/en/kor0071.html)

For statistical analysis the Analysis of variance (ANOVA) was used to compare the differences among means (Huzsvai & Balogh, 2015). Then, the Least Significant Difference (LSD) was carried out to compare between means. All analysis was conducted by using RStudio.

## RESULTS AND DISCUSSION

### Impact of different fertilization does on starch content

In terms of fertilization treatments, the highest (64.42%) maize starch content was measured for the control treatment, while the lowest starch content was recorded in the case of the 160 kg Nha treatment (62.62%). The least significant difference among fertilizer treatments was 0.428%.

### Impact of different crop year effect on starch content

The analysis of the crop year effect (climatic effects of the crop year) showed that 2018 was the most favourable year for the maize starch content of the examined samples (65.76%). Of the studied years, the lowest starch content was measured in 2017 (61.78%). The least significant difference between the crop years was 0.309%.

### Impact of different tillage system and crop year on starch content

The effect of tillage and crop year also had a statistically significant effect on the starch content of maize. The lowest starch content was measured in 2017 in addition to in the case of strip tillage. This year, there was no statistically significant difference between winter ploughed and ripped primary tillage. In the following year, i.e. in 2018, the starch content of maize was outstanding, in this crop year there was no significant difference among different tillage treatments. In 2019, significantly lower starch contents were measured for all tillage methods than in 2018, however, compared to 2017, the starch content was higher. There was no statistical difference among tillage treatments in the 2019 crop year either (Fig. 3).

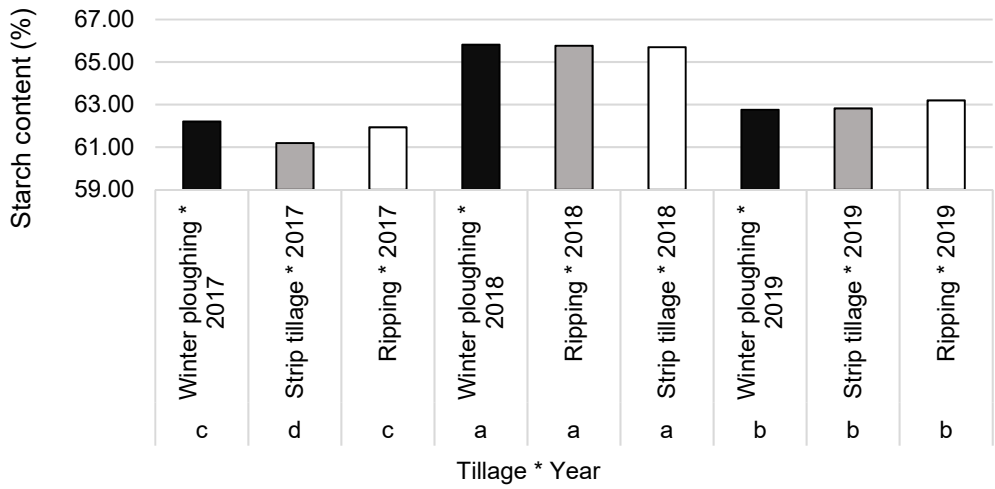


**Figure 3.** Effect of primary tillage and crop year on the starch content of maize (Debrecen-Látókép 2017–2019).

**Impact of fertilization and crop year on starch content**

The analysis showed that fertilization and crop year had a significant effect on the starch content of the examined maize samples. In 2018, there was no significant difference among the three tillage methods. In 2019, there was no statistical difference among the tillage methods in terms of protein content. Compared to the previous year, starch content was verifiably lower for all tillage types. The least significant difference between tillage and crop year was 0.536.

Fertilization and crop year also had a joint influence on the starch content of maize. In 2017, the lowest starch content of the examined period was measured in the 160 kg N $ha^{-1}$ treatment (60.67%). In all the studied years, fertilization reduced the starch content of maize compared to the control. In 2018, starch content of maize increased significantly with all fertilizer treatments compared to the previous year. The statistically highest starch content (66.43%) of the examined period was measured in the control plot in 2018. In 2019, compared to the previous year, starch content decreased significantly at all fertilizer levels (Fig. 4).

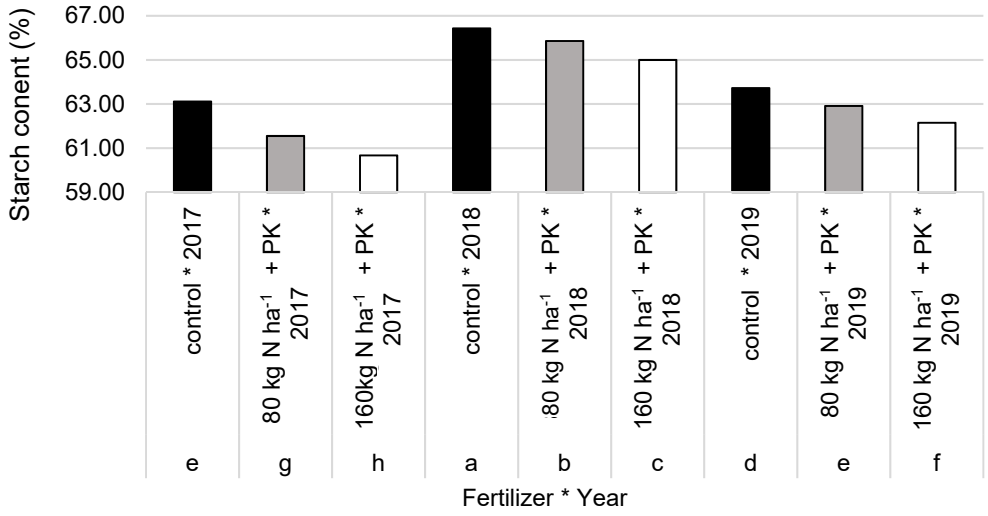


**Figure 4.** Effect of fertilization and crop year on the starch content of maize (Debrecen-Látókép 2017–2019).

**Impact of tillage and fertilization on starch content**

The effect of fertilization, tillage, and crop year on maize starch yield was also examined. Among the applied tillage methods, the highest starch yield was measured in the average of the examined years with the ripped (6.17 t $ha^{-1}$) primary tillage, while the winter ploughed (5.69 t $ha^{-1}$) and strip tillage (5.63 t $ha^{-1}$) did not differ from each other. The three analysed fertilizer doses differed significantly in terms of starch yield, the yield of the control was 4 t $ha^{-1}$, the 80 kg N $ha^{-1}$ + PK dose provided 6.3 t $ha^{-1}$, and the 160 kg N $ha^{-1}$ + PK fertilizer treatment resulted in 7.1 t $ha^{-1}$. Tillage and fertilization

together also affected the starch yield of maize. The lower starch yields were measured on the control plots, of which the significantly lowest was recorded in the case of the autumn ploughed primary tillage (3.7 t ha$^{-1}$). There was no significant difference between the control plots with strip tillage band cultivation (4.16 t ha$^{-1}$) and ripping (4.22 t ha$^{-1}$). At the 80 kg N ha$^{-1}$ + PK fertilizer dose, the lowest starch yield was recorded in the case of strip tillage. The highest starch yield (7.69 t ha$^{-1}$) was measured in the average of the studied years with the ripping primary tillage at the dose of 160 kg N ha$^{-1}$ + PK. There was no significant difference in this fertilizer dose between autumn ploughed (6.98 t ha$^{-1}$) and strip tillage (6.7 t ha$^{-1}$) (Fig. 5).

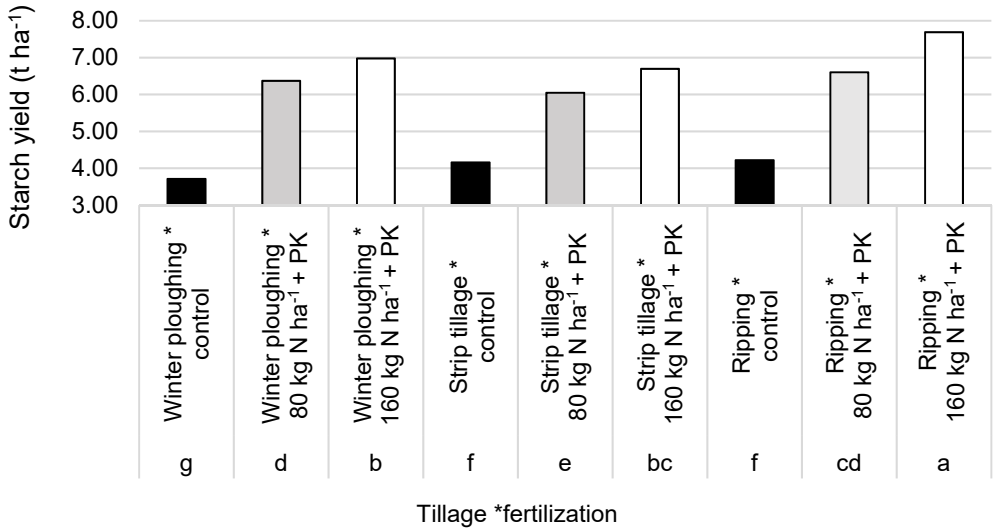


**Figure 5.** Effect of tillage and fertilization on the starch yield of maize (Debrecen-Látókép 2017–2019).

**Impact of tillage and crop year on starch content**

The crop year greatly influenced the starch yield of maize; 2017 was an unfavourable year for starch yield (5.37 t ha$^{-1}$) and there was no significant difference between 2018 (6.08 t ha$^{-1}$) and 2019 (6.02 t ha$^{-1}$). In the more rainy and warmer crop year of 2017, starch yield was higher in the case of to the ripped primary tillage, this year there was no significant difference between winter ploughing and strip tillage. In the 2018 crop year, which was average in terms of rainfall and temperature, the ripped primary tillage treatment provided the highest starch yield of the examined period (6.54 t ha$^{-1}$). There was no difference between strip tillage and winter ploughed treatment this year either. In the drier and warmer crop year of 2019, there was also a difference between autumn ploughed and strip tillage, and in this case higher starch yield (6.33 t ha$^{-1}$) was also measured with ripping as primary tillage (Fig. 6).

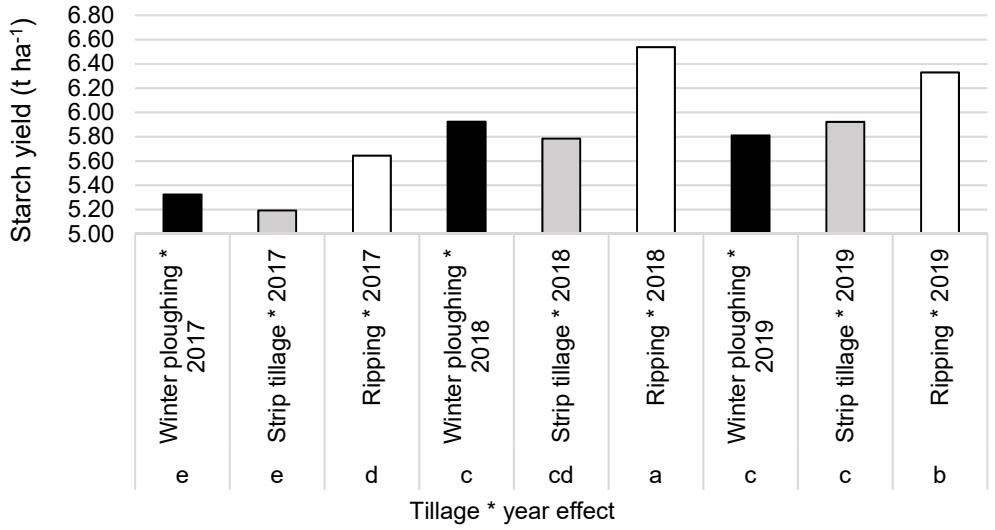


**Figure 6.** Effect of tillage and crop year on the starch yield of maize (Debrecen-Látókép 2017–2019).

**Impact of fertilization and crop year on starch content**

Fertilization and crop year together also influenced the starch yield of maize. Among the examined years, the lowest starch yield was measured in the average of tillage in 2017 on the control plots (3.4 t $ha^{-1}$). In each of the examined years, fertilization increased the starch yield of maize. The highest starch yield data of the studied period were measured in the 160 kg N $ha^{-1}$ + PK treatment (Fig. 7).

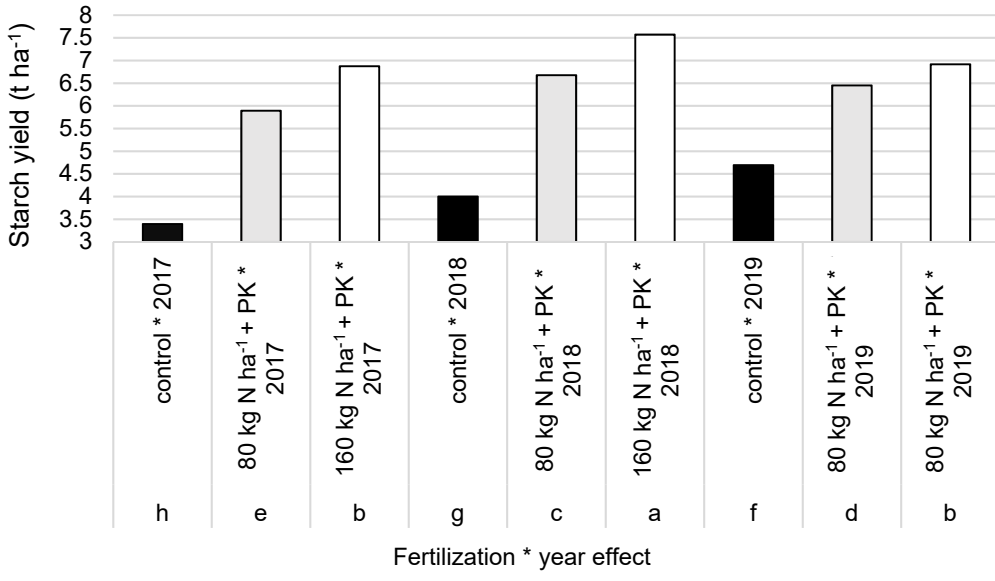


**Figure 7.** Effect of fertilization and crop year on the starch yield of maize (Debrecen-Látókép 2017–2019).

In the scope of the present research, the quality of starch content of maize grains was analyzed as a function to weather conditions (crop year), three tillage systems and different fertilization does. These agronomic practices were asses to use them as factors to verify their influence in relation to the variable content of starch in cultivated maize. The output of this research exhibited the importance of different agronomic practices on the quality of starch content of maize grains. For instance, good weather conditions will positively affect the starch content. In our research result showed that 2018 was the most favourable year for the maize starch content, where the weather namely rainfall and temperature was the best compared with other years (Fig. 1). In this sense, Butts-Wilmsmeyer et al. (2019) stresses the importance of temperature, rainfall and soil water content on the quality and compositional of maize grains. On the other hand, increased temperature (Heat stress) during different grain filling stages decreased starch content and grain weight (Lu et al., 2013).

Tillage system also influence the maize grain yield which mainly corelated with soil characteristics, drainage and many other factors (Boomsma et al., 2010). In this context, Cociu et al. (2017) reported that conservation tillage practices could produce the same quality of wheat, maize and soybean yields as traditional practices, which is similar to our results in Fig. 3. However, in 2018, there was no significant difference among the three tillage methods. In 2019, there was no statistical difference among the tillage methods in terms of protein content. Compared to the previous year, starch content was verifiably lower for all tillage types. The least significant difference between tillage and crop year was 0.536.

Fertilization also plays an important role in starch content and plant growth, where availability of N is crucial for optimal growth, photosynthesis, profitable yield (Butts-Wilmsmeyer et al., 2019, Széles et al., 2019a, 2019b). Our results showed that fertilization and crop year had a significant effect on the starch content of the examined maize samples. Fertilization and crop year also had a joint influence on the starch content of maize. However, the complex interaction between different agronomic practices were previously highlighted by many researchers, for example, Viswakumar et al. (2008) reported that drought had a negative impact on maize yield which minimize the influence to tillage or N application.

All in all, it is good to mention here that the quality of maize grain including starch content is the final output of the ultimate interaction between genetic (hybrid), environmental conditions (crop year), and agronomic management factors (Cook et al., 2012; Butts-Wilmsmeyer et al., 2019, Horváth et al., 2021). The key funding of this research is an output of three monitoring years (2017–2019), the output will be fostered by continuing with the research goals. Thus, we could present results in a period covering from 5 to 10 years of research and presenting the combination variants of cultivation and fertilizer dosage, analyzing the crop yields of starch from the point of view of field operations, crop year and tillage management.

## CONCLUSIONS

Based on the results of the field trial, it was confirmed that the tillage method, the intensity of nutrient supply and the crop year determine the amount of starch content of maize grains and the starch yield of grains that can be harvested from a unit of production area. In the studied crop years, starch content was not influenced by the applied tillage

method, but it had a significant influence on the starch yield. The highest starch content and starch yield were measured in the crop year with average rainfall supply, and the lowest in the rainy crop year. Starch yield was significantly highest in the case of the ripping primary tillage treatment in all three studied years.

As the amount of applied fertilizer increased, the starch content decreased significantly, while the starch yield increased significantly. The agro-technical treatment combination to be applied in the examined production area in order to increase starch yield of maize: ripped primary tillage with 160 kg N $ha^{-1}$ + PK nutrient supply.

ACKNOWLEDGEMENTS. 'The above research was supported by project no. TKP2021-NKTA-32 which has been implemented with the support provided from the National Research, Development and Innovation Fund of Hungary, financed under the TKP2021-NKTA funding scheme and the EFOP-3.6.3-VEKOP-16-2017-00008 project'.

## REFERENCES

Boomsma, C.R., Santini, J.B., West, T.D., Brewer, J.C., McIntyre, L.M. & Vyn, T.J. 2010. Maize grain yield responses to plant height variability resulting from crop rotation and tillage system in a long-term experiment. *Soil and Tillage Research* **106**(2), 227–240.

Butts-Wilmsmeyer, C.J., Seebauer, J.R., Singleton, L. & Below, F.E. 2019. Weather during key growth stages explains grain quality and yield of maize. *Agronomy* **9**(1), 16.

Cociu, A.I. & Alionte, E. 2017. Effect of different tillage systems on grain yield and its quality of winter wheat, maize and soybean under different weather conditions. *Agric. Res*. **1**, 59–67.

Cook, J.P., McMullen, M.D., Holland, J.B., Tian, F., Bradbury, P., Ross-Ibarra, J., ... & Flint-Garcia, S.A. 2012. Genetic architecture of maize kernel composition in the nested association mapping and inbred association panels. *Plant physiology* **158**(2), 824–834.

Elbeltagi, A., Azad, N., Arshad, A., Mohammed, S., Mokhtar, A., Pande, C., ... & Deng, J. 2021. Applications of Gaussian process regression for predicting blue water footprint: Case study in Ad Daqahliyah, Egypt. *Agricultural Water Management* **255**, 107052.

Gombos, B. & Nagy, J. 2019. Weather assessment based on the results of maize (Zea mays L.) yield trials. *Növénytermelés* **68**(2), 5–23 (in Hungarian).

Harsányi, E., Bashir, B., Almhamad, G., Hijazi, O., Maze, M., Elbeltagi, A., ... & Szabó, S. 2021a. GHGs Emission from the Agricultural Sector within EU-28: A Multivariate Analysis Approach. *Energies* **14**(20), 6495.

Harsányi, E., Bashir, B., Alsilibe, F., Alsafadi, K., Alsalman, A., Széles, A., ... & Mohammed, S. (2021b). Impact of Agricultural Drought on Sunflower Production across Hungary. *Atmosphere* **12**(10), 1339.

Hateffard, F., Mohammed, S., Alsafadi, K., Enaruvbe, G.O., Heidari, A., Abdo, H.G. & Rodrigo-Comino, J. 2021. CMIP5 climate projections and RUSLE-based soil erosion assessment in the central part of Iran. *Scientific reports* **11**(1), 1–17.

Horváth, É., Gombos, B. & Széles, A. 2021. Evaluation phenology, yield and quality of maize genotypes in drought stress and non-stress environments. *Agronomy Research* **19**(2), 408–422. https://doi.org/10.15159/AR.21.073

Hulmani, S. 2021. Accumulation of growing degree days, photothermal units and heliothermal units in winter maize as influenced by sowing windows and fertility levels. In Virtual National Conference On Strategic Reorientation For Climate Smart Agriculture V-Agmet 2021 (Vol. **2021**, pp. 26).

Huzsvai, L. & Balogh, P. 2015. *Linear models in R. Seneca Books*. Debrecen, pp. 109–124. (in Hungarian).

Juhász, C., Gálya, B., Kovács, E., Nagy, A., Tamás, J. & Huzsvai, L. 2020. Seasonal predictability of weather and crop yield in regions of Central European continental climate. *Computers and Electronics in Agriculture* **173**, 105400.

Khallouf, A., Talukdar, S., Harsányi, E., Abdo, H.G. & Mohammed, S. 2021. Risk assessment of soil erosion by using CORINE model in the western part of Syrian Arab Republic. *Agriculture & Food Security* **10**(1), 1–15.

Lu, D., Sun, X., Yan, F., Wang, X., Xu, R. & Lu, W. 2013. Effects of high temperature during grain filling under control conditions on the physicochemical properties of waxy maize flour. *Carbohydrate polymers* **98**(1), 302–310.

Mohammed, S., Alsafadi, K., Hennawi, S., Mousavi, S.M.N., Kamal-Eddin, F. & Harsanyie, E. 2021c. Effects of long-term agricultural activities on the availability of heavy metals in Syrian soil: A case study in southern Syria. *Journal of the Saudi Society of Agricultural Sciences* **20**.

Mohammed, S., Gill, A.R., Alsafadi, K., Hijazi, O., Yadav, K.K., Hasan, M.A., ... & Harsanyi, E. 2021a. An overview of greenhouse gases emissions in Hungary. *Journal of Cleaner Production* **314**, 127865.

Mohammed, S., Mirzaei, M., Pappné Törő, Á., Anari, M.G., Moghiseh, E., Asadi, H., ... & Harsányi, E. 2021b. Soil carbon dioxide emissions from maize (Zea mays L.) fields as influenced by tillage management and climate. *Irrigation and Drainage* **71**.

NAGY, J. 2017. Climate change and the impact of fertilizer application on maize on the yield of maize in a tank experiment in Debrecen. *Növénytermelés* **66**(3), 11–32 (in Hungarian).

Nagy, J. 2007. *Maize production*. Akadémiai Kiadó. Budapest, **276** (in Hungarian).

Pepó, P. 2017. Temperature experiments as indicators of climate change. *Növénytermelés* **66**(3), 33–46.

Pepó, P. & Sárvári, M. 2011. *Cultivation of cereal crops*. Debreceni Egyetem, Debrecen, (in Hungarian).

Prasanna, B.M., Vasal, S.K., Kassahun, B. & Singh, N.N. 2001. Quality protein maize. *Current science* **81**, 1308–1319.

Ramasamy, J. & Moorthy, P. 2006. Managing food insecurity and poverty in India in the era of globalization. *International Journal of Multidisciplinary Research* **2**.

Roberts, L. 2011. 9 Billion?. *Science* **333**(6042). doi: 10.1126/science.333.6042.540

Sadeghi, S.M., Noorhosseini, S.A., & Damalas, C.A. 2018. Environmental sustainability of corn (Zea mays L.) production on the basis of nitrogen fertilizer application: the case of Lahijan, Iran. *Renewable and Sustainable Energy Reviews* **95**, 48–55.

Széles, A., Nagy, J., Rátonyi, T. & Harsányi, E. 2019b. Effect of differential fertilisation treatments on maize hybrid quality and performance under environmental stress condition in Hungary. *Maydica* **64**(2), 14.

Széles, A. & Nagy, J., Ratonyi, T. & Harsányi, E. 2019. Effect of differential fertilisation treatments on maize hybrid quality and performance under environmental stress condition in Hungary. *Maydica* **62**, 11–14.

Takács, I., Amiri, M., Károly, K. & Mohammed, S. 2021. Assessing soil quality changes after 10 years of agricultural activities in eastern Hungary. *Irrigation and Drainage* **70**.

Viswakumar, A., Mullen, R.W., Sundermeier, A. & Dygert, C.E. 2008. Tillage and nitrogen application methodology impacts on corn grain yield. *Journal of Plant Nutrition* **31**(11), 1963–1974.

*Agronomy Research* **20**(1), 134–147, 2022
https://doi.org/10.15159/AR.21.158

# The impact of ventilation type on the heat load of dairy cows

A. Hauliková*, J. Lendelová, Š. Mihina and P. Kuchar

Slovak University of Agriculture in Nitra, Faculty of Engineering, Department of Building Equipment and Technology Safety, Trieda Andreja Hlinku 2, CZ949 76 Nitra, Slovak Republic
*Correspondence: xhaulikova@uniag.sk

Received: January 31th, 2021; Accepted: March 27th, 2021; Published: November 26th, 2021

**Abstract.** Heat load in cattle causes deterioration of health and reduced production of milk. Therefore, it is necessary to protect cows by appropriate passive and active means and monitor the air quality in barns. Based on several indicators of environmental quality, is possible to make a more comprehensive assessment of the microclimate and more precise conclusions. This study, was monitoring the values of air temperature, relative humidity, and air velocity in two barns with the same volume and layout with floor dimensions of 26.6 m × 62.1 m. In barn 1, roof ridge of which had underwent only partial reconstruction, there were installed fourteen basket fans with a total fan performance $Q(1)_{fans}$ = 218,400 $m^3$ $h^{-1}$. In barn 2, there were twelve panel fans with a total fan performance $Q(2)_{fans}$ = 289,320 $m^3$ $h^{-1}$. The resulting THI, HLI and ETIC values were compared in relation to each other and in relation to the recommended values.
Despite the operating ventilation technology and enlargement of wall openings, the above-limit values of climatic characteristics were observed in both barns during tropical days. There were no differences between the barns ($p > 0.05$), in barn 1: THI(1) = 83.10 ± 0.51; HLI(1) = 85.62 ± 1.42; ETIC(1) = 27.24 ± 0.31, and in barn 2: THI(2) = 83.12 ± 0.34; HLI(2) = 85.77 ± 1.50; ETIC(2) = 27.29 ± 0.28, however, there were found significant differences in values of temperature indices obtained in the detailed measurements at points arranged perpendicularly, as well as parallelly, to the direction of air velocity in the animal zone ($p < 0.05$).

**Key words:** air flow speed, cattle, heat load index, temperature - humidity index.

## INTRODUCTION

Currently, climate change is becoming topical issue, because high temperatures adversely affect health and productivity of livestock (Sheikh et al., 2017). Reduced production and decrease of health cause significant economic losses in animal husbandry (Fournel et al., 2017). Several climate models calculate that, at the end of the 21st century, surface air warming can rise from 1.1 °C to 6.4 °C. Global warming is concerning not only for tropical and southern regions, but also countries with a temperate climate (Bernabucci, 2019). Cattle is housed in buildings with natural ventilation, and therefore, these objects are so dependent on the weather (Hempel et al., 2019). In last decades, many studies have observed the heat load of dairy cows and confirmed that it

affects the cow's health (Kovács et al., 2018), production (Broucek et al., 2019), behaviour (Nordlund et al., 2019).

Animals react to their environment through physiological indicators (respiratory rate, rectal temperature) and behavioural indicators (activity, rest, feed intake); these indicators are mostly used for detecting of heat stress (Galan et al., 2018). The other indicators used to identify heat load in cows are heart rate, body weight, water intake and rumination (Hoffmann et al., 2019). Milk production can fall by up to 50% due to reduced feed intake. Heat load affects not only the quantity, but also the quality of milk (Sheikh et al., 2017).

According Fournel et al. (2017), Brown-Brandl (2018), the environment affects the thermal comfort of animals and is characterized by basic physical elements (microclimatic parameters), such as air temperature, relative humidity, air flow speed and sunlight. The heat load can be evaluated by calculating and measuring of microclimatic parameters.

The temperature humidity index (THI) is the most used index for assessing thermal comfort in cattle. This index combines air temperature and relative humidity into one value to estimate the heat load (Hoffmann et al., 2019). Heat stress have several levels: mild heat stress $72 < THI < 79$, moderate stress $80 < THI < 89$ and severe heat stress $THI > 89$ (Armstrong, 1994; Akyuz et al., 2010).

High temperatures negatively affect high-yielding cows, which are more sensitive than cows with average milk production (Pragna et al., 2017). According to recent studies by Heinicke et al. (2018), the threshold value for dairy cows begins at a THI value of 67. According to Pinto et al. (2020), the threshold value for the heat load of dairy cows is THI 65.

Fournel et al. (2017) claim, that THI does not consider other factors that may affect the thermal comfort of dairy cows, such as air velocity and solar radiation. The environmental index that considers not only temperature and humidity, but also the air flow speed and solar radiation is the Heat load index (HLI). According to Gaughan et al. (2008), HLI have four categories: thermoneutral zone $HLI \leq 70$, warm environment area $70 < HLI < 77$, hot environment area $77 < HLI < 86$, very hot environment area $HLI > 86$.

Another index for air flow evaluation is Equivalent temperature index for cattle (ETIC). According to Hempel et al. (2019), equivalent temperature index has 4 categories: mild category $18 \leq ETIC < 20$, moderate category $20 \leq ETIC < 25$, severe category $25 \leq ETIC < 31$, emergency category $31 \leq ETIC$. Monitoring of climate and indoor microclimatic parameters could help to mitigate the effects of heat stress in cattle (Herbut et al., 2019). Buildings for livestock do not always have the technical capabilities to protect against weather conditions and animals are forced to deal with heat on their own (Lendelova et al., 2019).

One of the solutions to alleviate heat stress in cattle are cooling systems such as shades, ventilation, evaporative cooling, or their combination (Becker & Stone, 2020). To make dairy production more efficient, it is necessary to adjust the indoor environment in the form of ventilation (Fournel et al., 2017). Measuring the air velocity in housing facilities is quite demanding (Bustos-Vanegas et al., 2019). The performance of a ventilation system is affected by several factors that disturb the efficiency of ventilation equipment such as animal concentration or structural elements (Mondaca et al., 2019). The air flow speed should be directed to the zone where the animals are located and thus improve the cooling effect of the fans (Zhou et al., 2019).

## MATERIALS AND METHODS

The research took place at an experimental dairy farm located in southern Slovakia at an altitude of 220 m above sea level. Records were collected in the summer of 2018 from two identical barns with floor plan dimensions of 26.6 m × 62.1 m and a volume of 7,943 $m^3$.

Both barns were reconstructed from a tie- to free-housing, while the openings in the side walls were enlarged to improve natural ventilation and a ridge slots (55 m × 1.2 m) with deflectors were built. Due to the frequent occurrence of tropical days, motor ventilation was additionally installed to both buildings. In both barns, there are 4 groups of animals of 32 with an average annual milk yield of 9,520 kg per animal in the given year and the feed corridors, straw bedding, and system and frequency of cleaning are the same.

In barn 1, fourteen basket fans (each with fan performance of 15,600 $m^3\ h^{-1}$) with a total fan performance of 218,400 $m^3\ h^{-1}$ were installed. The fans were arranged in two rows 3.5 m away from the longitudinal axis of the building. They were mounted to the ceiling structure at a height of 2.8 m above the floor and inclined to the animal zone at an angle of 10° (Fig. 1).

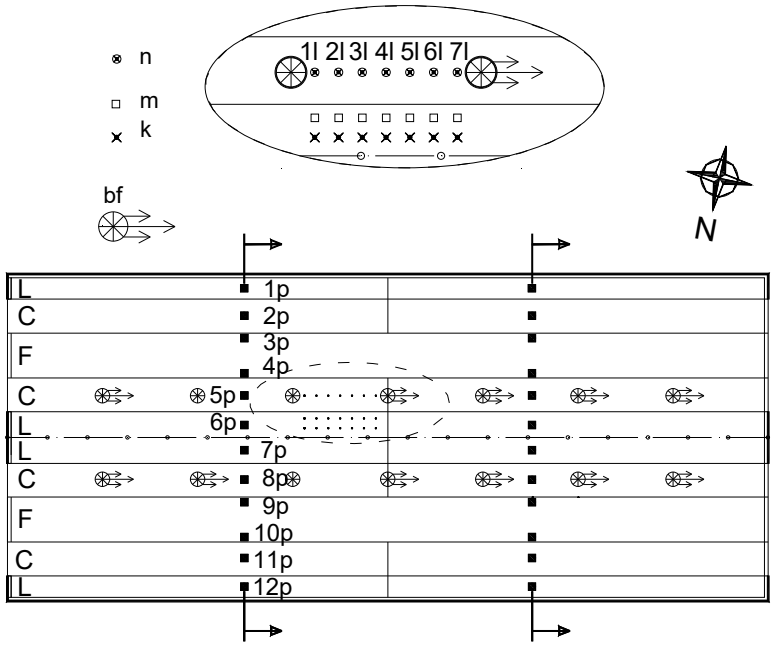


**Figure 1.** Layout of barn 1 with locations of basket fans and measuring points.

(bf Brangule basket fan; 1l–7l are measuring points in the longitudinal direction of the object spaced 1,200 mm apart; k – places of lying area with measurements at a height of 500 mm; m – measuring places of lying area with measurements at a height of 1,200 mm; n – moving alley with measurements at a height of 1,200 mm; 1p – 12p are measuring points in the direction perpendicular to the longitudinal axis of the object; L – lying zone; C – movement corridor; F – feeding corridor).

In barn 2, twelve panel fans were installed (4 devices with fan performance of 36,530 $m^3 h^{-1}$ and 8 devices with fun performance of 17,900 $m^3 h^{-1}$) with a total fan performance of 289,320 $m^3 h^{-1}$. All fans were mounted to the existing steel columns located at the longitudinal building axis (Fig. 2).

COM S3121 data loggers were installed in both buildings and outdoors for continuous climate measurements, and ambulant measurements were performed-using ALMEMO 2490-1L instruments with temperature range of -20 °C ÷ + 60 °C, relative humidity range of 0% ÷ 100% and measurement accuracy 0.03% with hot-wire thermoanemometric probe with air flow velocity measuring range of 0.08 ÷ 2 m $s^{-1}$ measurement accuracy ± 0.04 m $s^{-1}$ ± 1% and omnidirectional probe of the appropriate range with air flow velocity measuring range of 0.05 ÷ 5 m $s^{-1}$ and measurement accuracy ± 0.02 m $s^{-1}$ ± 1.5%.

Ambulant measurements were performed on days when the outside air temperature exceeded 30 °C and the air speed did not exceed 2.0 m $s^{-1}$. The measurements usually took place between 1:00 pm and 5:00 pm. During the measurements, the same procedure was always followed in both objects (at the measuring points according to (Fig. 1; Fig. 2), and, following the same order, the measurements were alternated in the lines of observation points arranged perpendicularly to the object axis and longitudinally to the object axis).

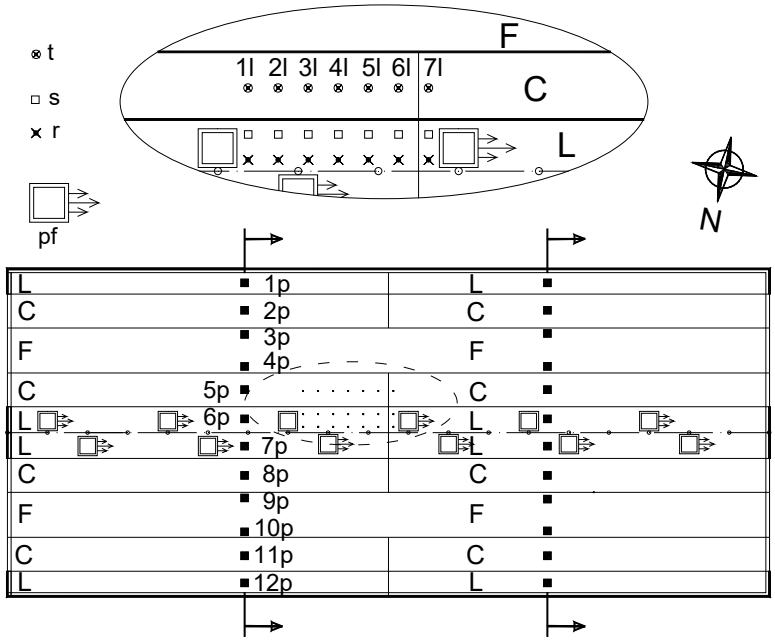


**Figure 2.** Layout of barn 2 with locations of panel fans and measuring points.

(pf – panel fan; 1l–7l are measuring points in the longitudinal direction of the object spaced 1,200 mm apart; r – places of lying area with measurements at a height of 500 mm; s – measuring places of lying area with measurements at a height of 1,200 mm; t – moving alley with measurements at a height of 1,200 mm; 1p – 12p are measuring points in the direction perpendicular to the longitudinal axis of the object; L – lying zone; C – movement corridor; F – feeding corridor).

The average values of climatic parameters were used for the calculation part to determine selected thermal indices THI, HLI and ETIC (Eq. 1; Eq. 2; Eq. 3). Index calculations were performed according to the recommendations of Fournel et al. (2017) and Wang et al. (2018a). The following equations for the Temperature humidity index (THI), Heat load index (HLI) and Equivalent temperature index for cattle (ETIC) were used:

$$\mathrm{THI} = (1.8 \cdot \mathrm{Tdb} + 32) - \left((0.55 - 0.0055 \cdot \mathrm{RH}) \cdot (1.8 \cdot \mathrm{Tdb} - 26.8)\right) \quad (1)$$

where Tdb – The dry bulb temperature, °C; RH – Relative humidity, % (Kelly & Bond, 1971)

$$\mathrm{HLI}(\text{if } \mathrm{Tbg} \geq 25) = 8.62 + (0.38.\,\mathrm{RH}) + (1.55.\,\mathrm{Tbg}) - (0.55.\,\mathrm{WS}) + e^{2.4-\mathrm{WS}} \quad (2)$$

where Tbg – Black globe temperature, °C; RH – Relative humidity, %, WS – Wind speed, m $s^{-1}$ (Gaughan et al., 2008)

$$\mathrm{ETIC} = \mathrm{Tdb} - 0.0038 \cdot \mathrm{Tdb} \cdot (100 - \mathrm{RH}) - 0.1173 \cdot |\mathrm{WS}|^{0.707} \cdot (39.2 - \mathrm{Tdb}) + 1.86 \cdot 10^{-4} \cdot \mathrm{Tdb} \cdot \mathrm{SR} \quad (3)$$

where Tdb – Black globe temperature, °C; RH – Relative humidity, %; WS – Wind speed, m $s^{-1}$ (Wang et al., 2018a).

Statistical analyses were under taken using STATISTICA 10. These involved descriptive statistics followed by an analysis of variance (ANOVA).

## RESULTS AND DISCUSSION

The level of heat load in both buildings was first evaluated using the THI Temperature-humidity index. The measurement results obtained from measuring points 1 to 12, which were arranged in a line perpendicular to the direction of air flow, are shown in Figs 3 and 4.

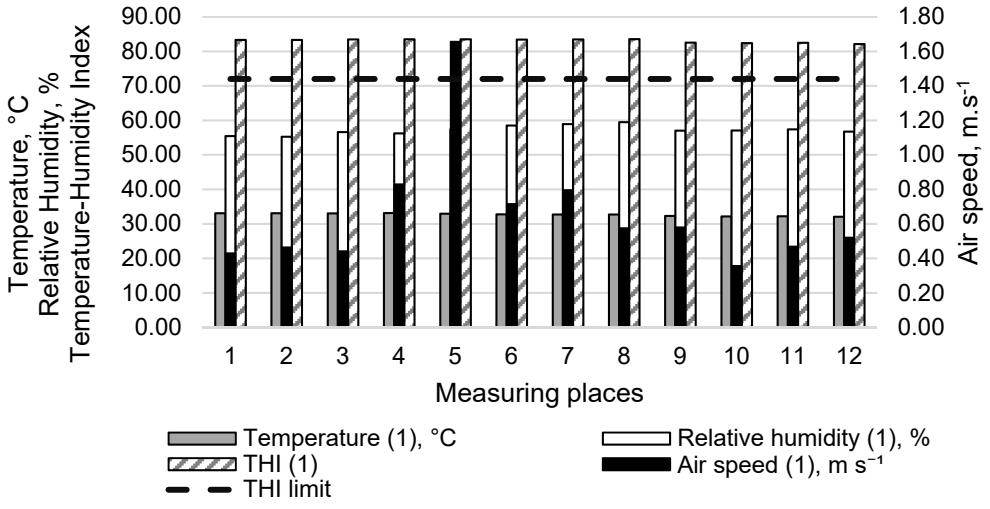


**Figure 3.** Results of the measured microclimatic variables in barn 1 with the corresponding temperature-humidity index THI (1).

It was found that the average air temperature measured (in 1p – 12p according to Figs 1 and 2 in the animal zone in two cross sections) was $T(1)_{ai,avg} = 32.69 \pm 0.40$ °C in barn 1 and $T(2)_{ai,avg} = 32.85 \pm 0.31$ °C in barn 2. The temperature detected in 1p and 2p located at the left longitudinal barn wall was higher than the temperature at 11p and 12p at the right wall due to its exposure to sun and partial penetration of solar radiation through the left wall openings.

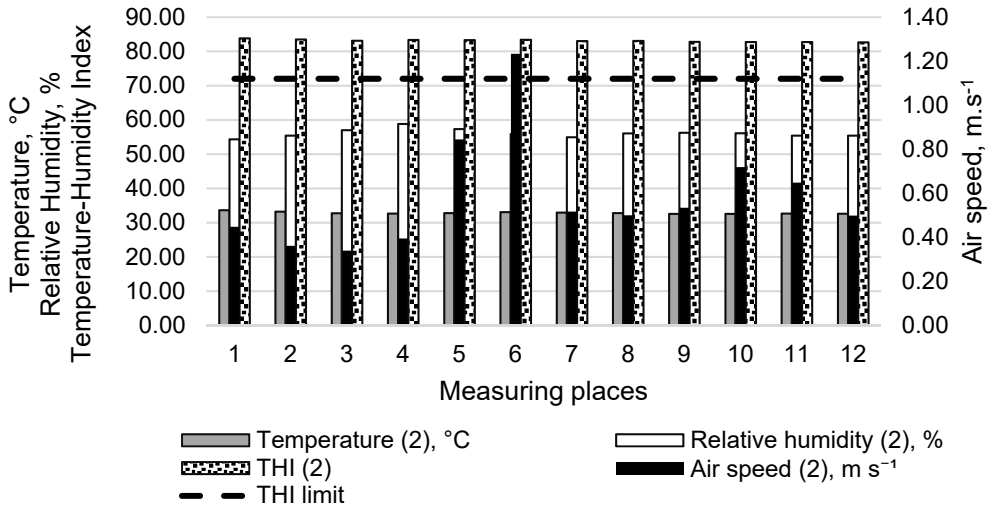


**Figure 4.** Results of the measured microclimatic quantities in barn 2 with the corresponding temperature-humidity index THI (2).

The air temperature near the longitudinal perimeter walls in barn 1 was even lower (but not significantly, $p > 0.05$) than the temperature in barn 2 (in all places 1p, 2p, 11p and 12p), however, the ventilation of fan performance in barn 2 was higher by 32% (289,320 $m^3\ h^{-1}$ vs. 218,400 $m^3\ h^{-1}$). The air temperature measured at locations of groups housed in the middle of barn at 5p, 6p, 7p and 8p showed more balanced-values: from $T_{ai} = 32.18$ °C to $T_{ai} = 33.07$ °C.

The average relative humidity in the barn 1 was $RH(1)_{avg} = 57.18\%$, and $RH(2)_{avg} = 56.08\%$ in the barn 2, while the highest values were found in the middle barn areas (from places of 4p to 8p). With the exception of the left feed corridor area (3p, 4p and 5p), the relative humidity in the animal zone was always higher ($p < 0.05$) in barn 1 compared to barn 2, which corresponds to the size difference of openings in the side walls $A(1)_{op} = 77.82\ m^2$ in barn 1 in contrast to, $A(2)_{op} = 212.5\ m^2$ in barn 2.

The average air flow speed from cross sections was $v(1)_{avg} = 0.65\ m\ s^{-1}$ and $v(2)_{avg} = 0.59\ m\ s^{-1}$. The air velocity in the middle barn area, were significantly higher ($p < 0.05$) in both buildings, especially in measuring points 5p, 6p, 7p and 8p (the average air speed was $v(1)_{(5,6,7,8)} = 0.93\ m\ s^{-1}$ and $v(2)_{(5,6,7,\ 8)} = 0.77\ m\ s^{-1}$) in barn 2 in contrast to points at the perimeter walls ($v(1)_{(1,2,11,12)} = 0.47\ m\ s^{-1}$ in barn 1 and $v(2)_{(1,2,11,12)} = 0.49\ m\ s^{-1}$ in barn 2).

Based on the determined performance of operating fans, the theoretical air exchange in objects with the same air volume was $ACH(1)_{theor} = 27.49\ h^{-1}$ for barn 1, and $ACH(2)_{theor} = 36.43\ h^{-1}$ for barn 2, however, based on results acquired, there was worse air exchange in main animal zone in barn 2 in comparison to barn 1 even though it is equipped with ventilation technology with higher performance.

For the calculations from experimental measurements in the animal zone, two simplified logical assumptions were introduced: 1) the velocity vector direction is the same in all places of the animal life zone (identical to the air pressure direction driven by fans); 2) if there is the same number of animals housed in-in barn 1 and barn 2, then the extent of the cumulative resistance that the animals present by their bodies as the partial barriers affecting the air flow rates in both barns will be the same.

However, the barn 2 showed worse ventilation ($ACH(1)_{exp} = 37.74\ h^{-1}$, $ACH(2)_{exp} = 34.25\ h^{-1}$) using the average air velocity ($v(1)_{avg} = 0.65\ m\ s^{-1}$ in barn 1; $v(2)_{avg} = 0.59\ m\ s^{-1}$ in barn 2).

By subsequent determination of selected temperature indices (THI, HLI and ETIC according to the methodology, using formula 1, 2 and 3, it was found that the heat load levels in the interior of both barns, which were calculated using the measured data from all measuring points, are in the equally dangerous category.

In barn 1, $THI(1) = 83.1 \pm 0.51$ and in barn 2, $THI(2) = 83.12 \pm 0.34$ (it means that, in both barns, there is a category of severe stress with conditions of $80 < THI < 89$). However, observed level of THI indicates that the environment in both barns is equally risky in terms of animal heat load, despite the better ventilation capacity in barn 2.

Based on the calculations of HLI, it was found that $HLI(1) = 85.62 \pm 1.42$ for barn 1 is almost identical to $HLI(2) = 85.77 \pm 1.51$ for barn 2 (Fig. 5). This index also confirmed the high level of heat load in both barns when the animals - despite the establishment of technical measures in the summer - were exposed to the so-called category of hot environment ($77.1 \leq HLI \leq 86$) in both barns.

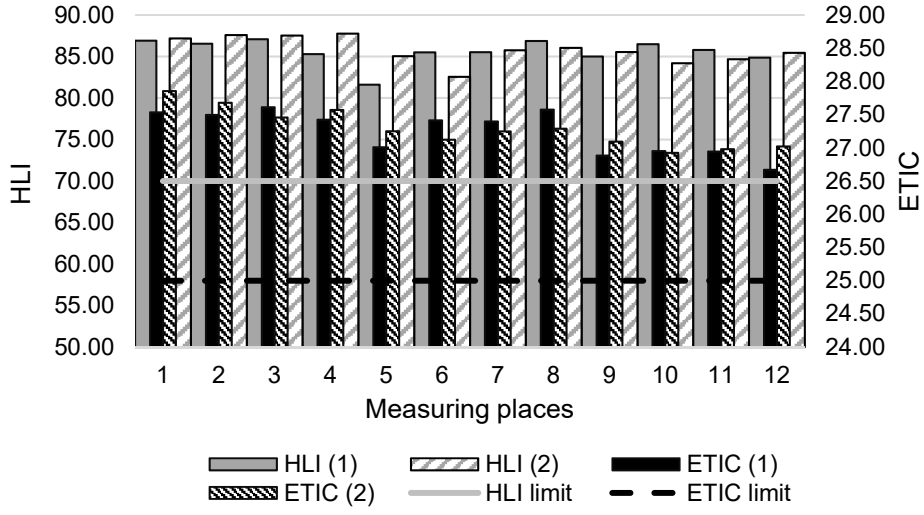


**Figure 5.** Results of environment evaluation state using HLI and ETIC in both barns.

A comparison of differences between the values of THI, HLI and ETIC indices found in the peripheral areas (1p, 2p, 11p and 12p) and the inner areas (5p, 6p, 7p and 8p) of the animal zone showed better results for barn 1 with basket fans in terms of heat load in the vicinity of the longitudinal masonry walls. The deviation in HLI index ($\Delta HLI_{avg} = 1.32\%$) were larger than the deviations in THI and ETIC ($\Delta THI_{avg} = 0.50\%$ and $\Delta ETIC_{avg} = 0.56\%$, respectively), however, a significant difference in the objects was not confirmed ($p > 0.05$).

It was found that the heat load calculated by means of ETIC, which, takes into account the multifactor influence of the environment in addition to temperature, showed almost the same heat load in both buildings. In barn 1, $ETIC(1) = 27.24 \pm 0.31$; $ETIC(2) = 27.29 \pm 0.81$ in barn 2.

The differences were also demonstrated in the control calculation of the partial air exchanges in the building determined according to the evaluated speed levels at individual measuring points and in the recalculation of the ETIC coefficient in the network of points arranged parallelly to the axis of the fan arrangement (in 3 rows of places 1l–7l). According to these results, the level of heat load was lower in barn 1, however, the above-limit values were observed in both buildings (severe stress, ETIC > 25).

For adding more motor ventilation devices, different fan mounting points were selected in the buildings, which used the existing steel structural elements. In barn 1, basket fans were installed at a height of 2.8 m and inclined at an angle of 10° towards the animals. In the barn 2, panel fans were used to move the air horizontally from the entrance to the in-farm dungstead.

In barn 2, the panel fans were concentrated directly along the longitudinal axis at a height of 3.8 m above the opposite heads of the lying animals. Although their higher performance ensured a more intensive air exchange in its entire, it did not affect the environment of the animal life zone to any significant extent.

The course of ETIC coefficient values is shown in Fig. 6. The average value in the longitudinal measuring field $ETIC(1)_{long}$ at the height of 1,200 mm was $ETIC(1)_{avg, long} = 27.01$ in barn 1, and $ETIC(2)_{avg, long} = 27.70$ in barn 2. For measurements at 500 mm, $ETIC(1)_{avg, long} = 27.71$ in barn 1, and $ETIC(2)_{avg, long} = 27.69$ in barn 2. The values obtained by measurements in the direction of air flow between adjacent fans carried out successively at seven places located 1.2 m apart from each other (in compliance with the bed size) ranged from $ETIC(1)_{min} = 26.14$ to $ETIC(1)_{max} = 27.9$ in barn 1, and from $ETIC(2)_{min} = 26.87$ to $ETIC(2)_{max} = 28.61$ in barn 2 (Fig. 6).

Based on the ETIC results obtained from measurements along the air flow between adjacent fans, it was found that the reduction of the heat load occurs especially in areas located 2 to 5 m from the fan.

An average decrease of this index was in barn 1, $\Delta ETIC(1)_{avg} = 1.67$ and $\Delta ETIC(2)_{avg} = 1.38$ in barn 2. Furthermore, the lowest values of $ETIC(1)_{min} = 26.17$ were achieved in barn 1, the maximum values were obtained in barn 2, $ETIC(2)_{max} = 28.16$.

The ETIC values inversely corresponded to a gradual decrease in the air flow rate in the direction along the air flow between the fans. This development did not correspond to the development of ETIC in the peripheral barn areas near the perimeter walls, in which no changes in the air flow in the longitudinal direction initiated by the fans were observed. Insufficient air exchange in the peripheral barn areas creates unequal living

conditions for housed animals, which should be further addressed by a multi-level process of heat load modification, including the utilization of computer climate modeling.

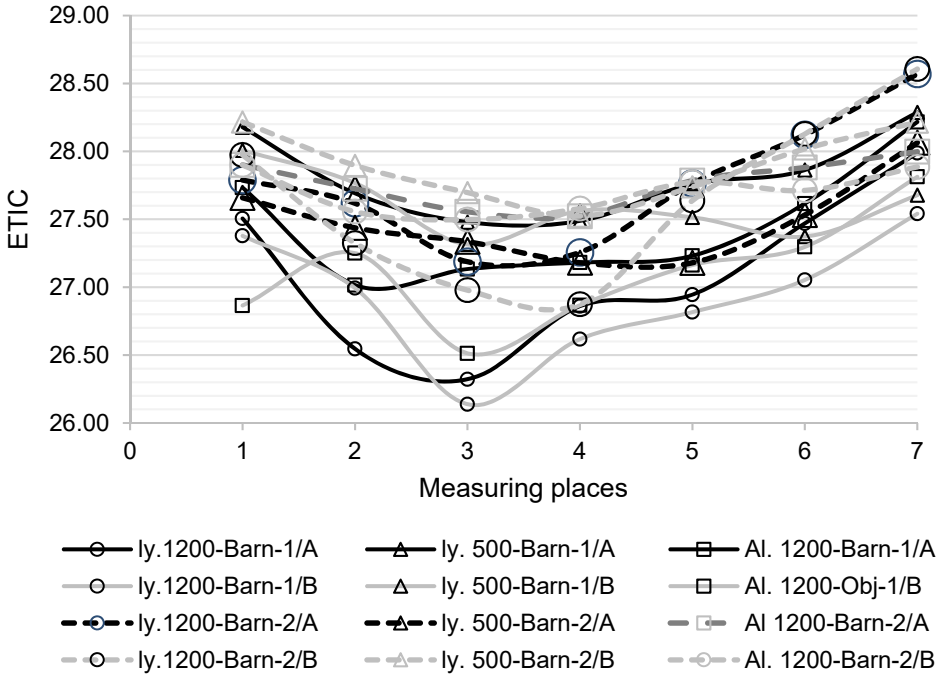


**Figure 6.** Results of the ETIC evaluation in the longitudinal direction of the barns in the area of adjacent fans (in the lying area at a height of 1,200 mm and 500 mm and in the movement alleys at a height of 1,200 mm – see Fig. 1 and Fig. 2).

Every year, in the Slovak lowlands, more than half of the days with air temperatures above 25 °C occur during the summer months, and the number of tropical days also increases. The limit value of the thermoneutral zone for dairy cows may vary, the older literature Berman et al. (1985) recommends a value up to 25 °C, newer articles report a threshold value up to 15 °C (Garner et al., 2017).

At higher air temperatures, heat production also increases, with high-producing cows being at greater risk of heat stress than low-producing cows (Pragna et al., 2017; Liu et al., 2019). The temperature in stables culminates especially in the afternoon when its maximum level can remain even for several hours.

In the study presented, it was found that the average afternoon indoor temperature was higher than 32 °C in both buildings ($T(1)_{ai,avg}$ = 32.69 °C ± 0.40 °C in barn 1; $T(2)_{ai,avg}$ = 32.85 ± 0.31 °C in barn 2), reaching the highest level in the inner barn sections. For this reason, the location of ventilation technology is especially important in this area.

Heat load affects the reduction of feed intake, which in turn leads to lower milk production, and therefore, it is necessary to create some procedures to reduce heat stress in dairy cows (Könyves et al., 2017).

Several authors, i.e. Wang et al. (2018b) and Tyson, (2010), recommend using airflows ranging from 2.0 m $s^{-1}$ to 3.0 m $s^{-1}$ for cooling the cattle housing during summer. It is important to achieve a suitable speed and direction of flow in the zone occupied by animals (Wang et al., 2018b; Zou et al., 2020).

The air flow rate found in study presented did not reach the level of 2.0 m $s^{-1}$ ($v_{max}$ < 2.0 m $s^{-1}$). In the individual profiles of cross section, the average afternoon air velocity did not reach nor the level of 1.0 m $s^{-1}$ ($v(1)_{avg}$ = 0.65 m $s^{-1}$ in barn 1; $v(2)_{avg}$ = 0.59 m $s^{-1}$ in barn 2), which raises the need to properly supplement the ventilation system in a manner that there would be better opportunities for cooling the animals even in the peripheral barn areas.

For the purposes of such solutions, it is advantageous to use computer modelling and effective utilization of geometric potential of the building, as well as possibility to adjust the motor ventilation capacity (Yi et al., 2019; Saha et al., 2020). The heat load in dairy cows can be assessed using several methods, but they provide different threshold values (Hammami et al., 2013; Ji et al., 2020).

THI results can be evaluated according to various recommended criteria, however, according to several studies, negative reactions to heat load already occur at values above THI = 68, Zimbelman & Collier (2011) or THI = 72, Bernabucci et al. (2014), respectively Liu et al. (2019) state that dairy cows feel a mild stress when the THI value rises above 72.

Heat stress can be alleviated by various cooling devices, such as fans and sprayers. These measures have been found to improve air quality in barns (Chen et al., 2015; Tresoldi et al., 2018; Chen et al., 2020). There are some different possibilities to solve other concept in building science, too (Kic et al., 2017; Leso et al., 2017; Salama, 2017).

In the study presented, the above-limit level of THI was recorded in both barns (THI(1) = 83.1 ± 0.51 in barn 1; THI(2) = 83.12 ± 0.34 in barn 2) even though both objects were intensively ventilated stables with an insulated roof, causing severe stress level according to most authors (Bohmanova et al., 2007; Akyuz et al., 2010; Bernabucci et al., 2014).

Several authors, i.e., Ammer et al. (2018), Liu et al. (2019), argue that it is required to consider other factors that affect environmental indices in terms of assessing the THI.

As THI does not include the influence of air velocity and other environmental factors, both objects were further evaluated using HLI and ETIC indices.

When evaluating the heat load using the HLI index, it was also confirmed that the animals are in a stressful environment in both buildings after taking into account the flow rate (HLI(1) = 85.62 ± 1.42, and HLI(2) = 85.77 ± 1.51). Even the addition of motor ventilation did not improve the conditions in barn 2. It is believed that the air flow in this building was driven mainly over the animals, because the axial height of the panel fans was 3.3 m. In the windy climate situation at this level, there is better interference of the transport of air masses Yi et al. (2019), but these phenomena are rare at the farm location and do not usually take place during the hottest days.

If the external wind situation does not improve the condition inside the buildings, HLI regularly rises above HLI = 70 in the afternoon in the summer. Study by Van lear et al. (2015), examined the relationship of HLI to the production parameters of dairy cows and found that increasing HLI reduced milk yield, where, a decrease in milk was 1.0 kg per animal at a daily average HLI of 85. Vitali et al. (2019) stated that, during the summer study from June to September, the HLI values ranged from 72 to 80. They found

that the incidence of clinical mastitis had also been shown to increase in connection to above-limit HLI values.

However, the ventilation technology used cannot guarantee the elimination of these risks. Furthermore, according to the evaluation of the Equivalent temperature index for cattle, the animals in both buildings were exposed to the conditions of severe heat load ($25 < ETIC < 31$), as in both buildings the $ETIC = 25$ limit was exceeded ($ETIC(1) = 27.24 \pm 0.31$ in barn 1, and $ETIC(2) = 27.29 \pm 0.28$ in barn 2).

At the measuring points arranged perpendicularly to the flow direction, there were observed $ETIC_{min} = 26.79$ and $ETIC_{max} = 27.73$. In the measurements close to the center and parallel to the driven air flow, there were observed $ETIC_{min} = 26.14$ and $ETIC_{max} = 28.67$. The differences were higher along axis of the flow, although the values at the perimeter walls were worse due to lower local air exchange. By getting closer to the fan, the differences became more pronounced, which also demonstrated by the animal behaviour - the cattle grouped at better ventilated place. However, at the place with the highest ventilation effect, it was found that the ETIC was reduced only by 1.6, which is not sufficient at this level of heat load.

## CONCLUSIONS

The work aim was to investigate the relationship of ventilation technology to the heat load of dairy cows in two structurally and dispositional identical barns with different total fan performance: $Q(1)_{fans} = 218{,}400\ m^3\ h^{-1}$ and $Q(2)_{fans} = 289{,}320\ m^3\ h^{-1}$, with longitudinal air flow and fans situated around the object longitudinal axis. It was found that the values of temperature indices showed a high temperature load, but the differences between the objects were not significant ($p > 0.05$), when the Temperature humidity index was $THI(1) = 83.10 \pm 0.51$ in barn 1, and $THI(2) = 83.12 \pm 0.34$ in bar 2, as well as for Heat load index: $HLI(1) = 85.62 \pm 1.42$ and $HLI(2) = 85.77 \pm 1.50$ also for the Equivalent temperature index for cattle, which was $ETIC(1) = 27.24 \pm 0.31$ and $ETIC(2) = 27.29 \pm 0.28$.

Based on detailed climatic measurements, it was found that, according to measurements at 12 points arranged always in a direction perpendicular to the building axis, the central barn area was more cooled than the side areas near the longitudinal barn walls. However, based on the measurements in the longitudinal direction, it was found that, in the central part of the object within a direct reach of fans in almost half of the measuring points, there was sufficient reduction in heat load ($ETIC < 0.5$), but better results were obtained in barn 1 with a two–row fan arrangement.

For both barns, the calculations pointed the need to further intensify the cooling of animals in order to adequately improve the possibility of heat excess dissipation. Using computer modelling, it is possible to improve the conditions so that they are evenly available to as many animals as possible.

ACKNOWLEDGEMENTS. This publication was supported by the Operational Programme Integrated Infrastructure within the project: Sustainable smart farming systems taking into account the future challenges 313011W112, cofinanced by the European Regional Development Fund.

## REFERENCES


Ammer, S., Lambertz, C., von Soosten, D., Zimmer, K., Meyer, U., Danicke, S. & Gauly, M. 2018. Impact of diet composition and temperature-humidity index on water and dry matter intake of high-yielding dairy cows. *Journal of Animal Physiology and Animal Nutrition* **102**(1), 103113. doi: 10.1111/jpn.12664

Akyuz, A., Boyaci, S. & Cayli, A. 2010. Determination of critical period for dairy cows using temperature humidity index. *J. Anim. Vet. Adv.* **9**(3), 1824–1827.

Armstrong, D.V. 1994. Heat stress interaction with shade and cooling. *Journal of Dairy Science* **77**(7), 2044–050. https://doi.org/10.3168/jds.S0022- 0302(94)77149-6

Becker, C.A. & Stone, A.E. 2020. Graduate Student Literature Review. Heat abatement strategies used to reduce negative effects of heat stress in dairy cows. *Journal of Dairy Science* **103**, 2020–18536. https://doi.org/10.3168/jds.2020-18536

Berman, A., Folman, Y., Kaim, M., Mamen, m., Herz, Z., Wolfenson, D., Aireli, A. & Garber, Y. 1985. Upper critical temperatures and forced ventilation effects for high-yielding dairy cows in a subtropical climate. *J. Dairy Sci.* **68**, 1488–1495. https://doi.org/10.3168/jds.S0022-0302(84) 81501-5

Bernabucci, U. 2019.Climate change: Impact on livestock and how can we adopt. *Animal Frontiers* **9**(1), 3–5. doi: 10.1093/af/vfy039

Bernabucci, U., Biffani, S., Buggiotti, L., Vitali, A., Lacetera, N. & Nardone, A. 2014. The effects of heat stress in Italian Holstein dairy cattle. *Journal of Dairy Science* **97**(1), 471–486. doi: 10.3168/jds.2013-6611

Bohmanova, J., Misztal, I. & Cole, J.B. 2007. Temperature-humidity indices as indicators of milk production losses due to heat stress. *J. Dairy Sci*. **90**, 1947–1956.

Broucek, J., Ryba, S., Dianova, M., Uhrincat, M., Soch, m., Sistkova, M., Mala, G. & Novak, P. 2019. Effect of evaporative cooling and altitude on dairy cows milk efficiency in lowlands. *International Journal of Biometeorology* **64**, 433–444. https://doi.org/10.1007/s00484-019-01828-5

Brown-Brandl, T.M. 2018. Understanding heat stress in beef cattle. *Revista Brasileira de Zootecnia Brazilian. Journal of Animal Science* **47**, 1–9. e20160414.

Bustos-Vanegas, J.D., Hempel, S., Janke, D., Doumbia, m., Judith Streng, J. & Amon, T. 2019. Numerical simulation of airflow in animal occupied zones in a dairy cattle building. *Biosystems Engineering* **186**, 100–105. //doi.org/10.1016/j.biosystemseng.2019.07.002

Fournel, S., Rousseau, Alain N. & Laberge, B. 2017. Rethinking environment control strategy of confined animal housing systems through precision livestock farming. *Biosystems Engineering* 1**55**, 96–123. https://doi.org/10.1016/j.biosystemseng.2016.12.005

Galan, E., Llonch, P., Villagra, A., Levit, H., Pinto, S. & del Prado, A. 2018. A systematic review of non-productivityrelated animal-based indicators of heat stress resilience in dairy cattle. *Plos One* **13**(11) e0206520. https://doi.org/10.1371/journal. pone.0206520

Garner, J., Douglas, M., Williams, S.R.O., Wales, W.J., Marett, L.C., Digiacomo, K., Leury, B.J. & Hayes, B.J. 2017. Responses of dairy cows to short – term heat stress in controlled – climate chambers. *Animal Production Science* **57**(7) 1233–1241. doi: 10.1071/AN16472

Gaughan, J.B., Mader, T.L., Holt, S. & Lisle, A. 2008. A new heat load index for feedlot cattle. *J. Anim. Sci*. **86**, 226–234.

Heinicke, J., Hoffmann, G., Ammon, C., Amon, B., Amon, T. 2018. Effects of the daily heat load duration exceeding determined heat load thresholds on activity traits of lactating dairy cows. *J. Therm. Biol.* **77**, 67–74.

Hammami, H., Bormann, J., M´hamdi, N., Montaldo, H.H. & Gengler, N. 2013. Evaluation of Heat stress effects on produstion traits and somatic cell score of Holsteins in a temperature environment. *J. Dairy. Sci*. **96**, 1844–1855.

Hempel, S., Menz, CH., Pinto, S., Galán, E., Janke, D., Estellés, F., Müschner-Siemens, T., Wang, X., Heinicke, J., Zhang, G., Amon, B., del Prado, A. & Thomas, A. 2019. Heat stress risk in European dairy cattle husbandry under different climate change scenarios - uncertainties and potential impacts. *Earth System Dynamics* **10**, 859–884. https://doi.org/10.5194/esd-10-859-2019

Herbut, P., Angrecka, S., Godyń, D. & Hoffmann, G. 2019. The physiological and productivity effects of heat stress in cattle – a review. *Ann. Anim. Sci.* **19**, 579–593. https://doi.org/10.2478/aoas-2019-0011

Hoffmann, G., Herbut, P., Pinto, S., Heinicke, J., Kuhla, B. & Thomas, A. 2019. Animal-related, non-invasive indicators for determining heat stress in dairy cows. *Biosystems Engineering* **199**, 83–96.

Chen, E., Narayanan, V., Pistochini, T. & Rasouli, E. 2020. Transient simultaneous heat and mass transfer model to estimate drying time in a wetted fur of a cow. *Biosystems Engineering* **195**, 116–135.

Chen, J., Schutz, K.E. & Tucker, C.B. 2015. Cooling cows efficiently with sprinklers: Physiological responses to water spray. *Journal of Dairy Science* **98**(10), 6925–6938.

Ji, B., Banhazi, B, Ghahramani, A., Bowtell, L., Wang, Ch. & Li, B. 2020. Modelling of heat stress in a robotic dairy farm. Part 4: Time constant and cumulative effects ofheat stress. *Biosystems Engineering* **199**, 58–72.

Kelly, C.F. & Bond, T.E. 1971. Bioclimatic factors and their measrurments. National Research Council (Ed.), A guide to enviromenmental research on animals, pp. 7–92.

Kic, P. 2017. Effect of construction shape and materials on indoor microclimatic conditions inside the cowsheds in dairy farms. *Agronomy Research* **15**(2), 426–434.

Kovács, L., Kézér, F.L., Ruff, F., Jurkovich, V. & Szenci, O. 2018. Heart rate, cardiac vagal tone, respiratory rate, and rectal temperature in dairy calves exposed to heat stress in a continental region. *International Journal of Biometeorology* **62**(10), 1791–1797. doi: 10.1007/s00484-018-1581-8

Könyves, T., Zlatković, N., Memiši, N., Lukač, D., Puvača, N., Stojšin, M., Halasz, A. & Miscevic, B. 2017. Relationship of temperature-humidity index with milk production and feed intake of holstein-frisian cows in different year seasons. *Thai Journal of Veterinary Medicine* **47**(1), 15–23.

Lendelová, J., Mihina, Š., Žitňak, M., Nemethova, M. & Botto, L. 2019. Thermo-technical parameters of the different bedding surgaces in cubicles for dairy cows as a factor of their well-being in winter and summer. *American Society of Agricultural and Biological Engineers – ASABE* Meeting Presentation, Paper No. 1900268, https://doi.org/10.13031/aim.201900268

Leso, L., Morshed, W., Conti, L. & Barbari, M. 2017. Evaluating thermal performance of experimental building solutions designed for livestock housing: the effect of greenery systems. *Agronomy Research* **15**(1), 239–248.

Liu, J.J., Li, L.Q., Chen, X.L., Lu, Y.Q. & Wang, D. 2019. Effects of heat stress on body temperature, milk production, and reproduction in dairy cows: a novel idea for monitoring and evaluation of heat stress - A review. *Asian – Australasian Journal of Animal Sciences* **32**(9) 1332–1339. doi.org/10.5713/ajas.18.074

Mondaca, M.R., Choi, C.Y. & Cook, N.B. 2019 Understanding microenvironments within tunnel-ventilated dairy cow freestall facilities: examination using computational fluid dynamics and experimental validation. *Biosyst Eng* **183**, 70–84. https://doi.org/10.1016/j.biosystemseng.2019.04.014

Nordlund, K.V., Strassburg, P., Bennett, T.B., Oetzel, G.R. & Cook, N.B. 2019. Thermodynamics of standing and lying behavior in lactating dairy cows in freestall and parlor holding pens during conditions of heat stress. *Journal of Dairy Science* **102**, 6495–6507. https://doi.org/10.3168/jds.2018-15891

Pinto, S., Hoffmann, G., Ammon, C. & Amon, T. 2020 Critical THI thresholds based on the physiological parameters of lactating dairy cows. *Journal of Thermal Biology* **88**, 102523. https://doi.org/10.1016/j.jtherbio.2020. 102523

Pragna, P., Archana, P.R., Aleena, J., Sejian, V., Krishnan, G., Bagath, m., Manimaran, A., Beena, V., Kurien, E.K., Varma, G. & Bhatta, R. 2017. Heat Stress and Dairy Cow: Impact on Both Milk Yield and Composition. *International Journal of Dairy Science* **12**(1) 1–11. doi: 10.3923/ijds.2017.1.11

Saha, K. Ch., Yi, Q., Janke, D., Hempel, S., Amon, B. & Amon, T. 2020. Opening Size Effects on Airflow Pattern and Airflow Rate of Naturally Ventilated Dairy Building – CFD. *Applied Sciences* **10**, 6054, 1–17. doi:10.3390/app10176054

Salama, W. 2017. Design of concrete buildings for disassembly: An explorative review. *International Journal of Sustainable Built Environment.* Volume **6**, Issue 2, December, pp. 617–635. https://doi.org/10.1016/j.ijsbe.2017.03.005

Sheikh, A.A., Bhagat, R., Islam, S.T., Dar, R.R., Sheikh, S.A., Wani, J.M. & Dogra, P. 2017. Effect of climate change on reproduction and milk production performance of livestock. *Journal of Pharmacognosy and Phytochemistry* **6**(6), 2062–2064.

Tresoldi, G., Schutz, K.E. & Tucker, C. 2018. Cooling cows with sprinklers: Spray duration affects physiological responses to heat load. *Journal of Dairy Science,* **101**(5), 4412–4423.

Tyson, J.T. 2010. Dairy heat abatement system selection tool. Paper presented at the 2010 ASABE Annual International Meeting, Pittsburgh, Pennsylvania.

Vitali, A., Felici, A., Lees, A.M., Giacinti, G., Maresca, C., Bernabucci, U., Gaughan, J.B., Nardone, A. & Lacetera, N. 2020. Heat load increases the risk of clinical mastitis in dairy cattle. *Journal of Dairy Science* **103**(9), 8378–8397. doi: 10.3168/jds.2019-17748

Wang, X., Gao, H., Gebremedhin, K.G., Bjerg, B.S., Van Os, J., Tucker, C.B. & Zhang, G. 2018a. A predictive model of equivalent temperature index for dairy cattle (ETIC). *Journal of Thermal Biol*ogy. **76**, 165–170. doi.org/10.1016/j.jtherbio.2018.07.013

Wang, X., Zhang, G. & Choi, CH. Y. 2018b. Effect of airflow speed and direction on convective heat transfer of standing and reclining cows. *Biosystems Engineering* **167**, 87–98. https://doi.org/10.1016/j.biosystemseng.2017.12.011

Yi, Q., Wang, X., Thang, G., Li, H., Janke, D. & Amon, T. 2019. Assessing effects of wind speed and wind direction on discharge coefficient of sidewall opening in a dairy building model – A numerical study. *Computers and Electronics in Agriculture* **162**, 235–245. https://doi.org/10.1016/j.compag.2019.04.016

Zimbelman, R.B. & Collier, R.J. 2011. Feeding strategies for high-producing dairy cows during periods of elevated heat and humidity. In: *Tristate dairy nutrition conference*, Fort Wayne, Indiana, USA, pp. 111–125.

Zou, B., Heber, A.J., Shi, Z., Du, S., Jin, Y. & Lim, T.T. 2020. Comparison of direct and indirect determinations of dynamic ventilation rate in a modern dairy free stall barn. *Int. J. Agric. & Biol. En.* **13**(6) 41–46.

Zou, B., Wang, X., Mondaca, m.R., Rong, L. & Choi, CH.Y. 2019. Assessment of optimal airflow baffle locations and angles in mechanically-ventilated dairy houses using computational fluid dynamics. *Computers and Electronics in Agriculture* **165**, 104930.

*Agronomy Research* **20**(1), 148–160, 2022
https://doi.org/10.15159/AR.22.007

# Morphophysiological peculiarities of productivity formation in columnar apple varieties

O. Havryliuk[1,*], T. Kondratenko[1], B. Mazur[1], V. Kutovenko[1], B. Mazurenko[1], O. Voitsekhivska[2] and Y. Dmytrenko[1]

[1]National University of Life and Environmental Sciences of Ukraine, 12 A Heroiv Oborony Str., UA03041 Kyiv, Ukraine
[2]Taras Shevchenko National University of Kyiv, Plant biology department, 60 Volodymyrska Str., UA03127 Kyiv, Ukraine
[*]Correspondence: o.havryliuk@nubip.edu.ua

Received: December 30th, 2021; Accepted: February 22nd, 2022; Published: March 4th, 2022

**Abstract.** Differentiation of generative buds is one of the most important biological processes of plant transition from vegetative to generative state. This process is key to the problem of creating regular fruit-bearing and early-fruiting plantations. The article provides information on the organogenesis of buds in plants of columnar apple varieties in the Forest-Steppe of Ukraine, which allows establishing the features of this process in complex fruit formations of different ages, and the levels of their productivity and longevity. Research to study the organogenesis of different-age fruit formations of columnar apple varieties was conducted in the northern part of the Forest-Steppe of Ukraine during 2016–2020. The efficiency of realization the plants biological potential of all studied columnar apple varieties at III–IV and V–IX stages of organogenesis was high: the largest number of buds from their total number differentiated into generative on trees varieties 'Sparta', 'President', 'Bilosnizhka', 'Valuta' and 'Tantsivnytsia' (37–51%), the smallest in 'Favoryt' and 'Bolero'. The biggest number of flowers per one potentially generative bud was formed by plants of 'Tantsivnytsia' and 'Bilosnizhka' varieties. The lowest level of ovarian loss during the X stage of organogenesis was observed on plants of 'Valuta', 'President', and 'Tantsivnytsia' varieties (41–49%), and the highest - in 'Favoryt' variety (up to 83%). More effective realization of potential productivity at the XI stage of organogenesis occurred in plants of 'President', 'Valuta' and 'Tantsivnytsia' varieties; their trees on one potentially generative bud formed - 0.27–0.38 fruits. The coefficient of determination indicates that the influence of meteorological conditions of the year on the passage of III–IV stages of organogenesis is 46%; V–IX stages - 42%; Stage X - 17%; Stage XI - 24%.

**Key words:** columnar apple, productivity, organogenesis, differentiation of generative buds, fruit formations.

## INTRODUCTION

According to Isaeva (1989), the productivity of the apple tree is the totality of all organic matter formed during the process of photosynthesis, and in the economic sense, it is an integral part of biological productivity, which is realized in the form of fruit yield

(Zamorskyi, 2007). Isaeva (1974) recommends studying the productivity of apple trees in the process of their formation by analyzing the formation of rudimentary organs and their consistent development into vegetative and generative organs, which are elements of productivity (Rather et al., 2018; Vasylenko et al., 2021). It follows that productivity should be understood as the total number of elements formed on the fruit tree, and not just the fruit yield (El-Sabagh et al., 2012; Zuo et al., 2018; Mezhenskyj et al., 2020).

To periodize the process of shoot formation Isaeva (1989) proposed to modify the scheme Cooperman (1984). The modified scheme reveals the sequence of vegetative and generative organs formation, ie the process of productivity. The author considers the latter as the effectiveness of the realization of productivity potential at each stage of organogenesis. The effectiveness of realization is determined by the genotype of the variety and the conditions of its cultivation in a particular year (Isaeva, 1989; Palubicki et al., 2009; Kovalyshyna et al., 2020a; Kovalyshyna et al., 2020b).

Differentiation of generative buds is one of the most important biological processes of plant transition from vegetative to generative state (Duric et al., 1997; Mazurenko et al., 2020). It is the key in the problem of creating regularly fruitful and early fruiting plantations (Benko, 1967; Konarska, 2012). It is known that the laying and beginning of inflorescences and flowers formation in apple trees takes place in the previous year of the growing season. In the yield formation, III–V stages of organogenesis Isaeva (1989) considers critical, because the fate of the yield depends on the availability of conditions for the transition of potential fruiting points to the laying of flower buds. At the IV–V stages due to the formation of embryonic flowers is the laying of the elements of the yield, thus determining the total yield of the tree in the form of rudimentary flowers (Shevchuk et al., 2021).

The share of potential productivity, formed in the form of embryonic flowers (which successfully overwintered), is largely decided during pollination and fertilization (stage IX); it is at these stages that the possibility of realizing the potential in the fruit yield is largely determined (Havryliuk et al., 2019a). At the X–XII stages of organogenesis, the efficiency of flower realization in fruits is determined, the latter acquires a certain mass, which together determines the yield. But at the same time, there is a loss of productivity potential due to the reduction of flowers, ovaries, and fruits. The main reason for the reduction in productivity at the IX–XI stages of organogenesis in the apple tree is the excessive number of rudimentary flowers. The tree is not able to form fruit from all their number. At this time, potential productivity is lost, which is not provided with assimilates and therefore can not be realized (Havryliuk et al., 2019b). According to the nature of the reduction of productivity elements at the X–XII stages of organogenesis, apple cultivars Isaeva (1989) divided into several groups.

In studies conducted by Kondratenko (2013) in the conditions of Polissya and Forest-Steppe of Ukraine, the potential of productivity and efficiency of its realization in common apple varieties was determined. The scientist concluded that modern apple varieties of the domestic and foreign selection form a high potential for productivity; the most significant differences between varieties are found in III–IV and X–XII stages of organogenesis; the degree of reproductive elements reduction at the X stage of organogenesis depends on the variety and does not depend on the growing area; the potential of productivity is realized more effectively by the newest grades at cultivation on intensive technologies.

Scientific research hypothesis. The study of the productivity of columnar appletrees in the process of its formation, by analyzing the formation of rudimentary organs and their consistent development into vegetative and generative organs, which are elements of productivity, will establish the features of this process in complex fruit formations of different ages and levels of productivity and longevity. Knowing the level of influence of meteorological factors on the passage of II–XII stages of organogenesis, we can recommend more specific soil and climatic conditions for growing columnar varieties.

## MATERIALS AND METHODS

The research was performed during 2016–2020 at the Department of Horticulture named after Professor Volodymyr Levkovych Symyrenko of the National University of Life and Environmental Sciences of Ukraine. The experimental basis for the research was the planting of apple trees of the primary variety test at the Institute of Horticulture of the National Academy of Agrarian Sciences of Ukraine.

The subject of research - 7 apple varieties of columnar type ('Tantsivnytsia', 'Sparta', 'Favoryt', 'Bilosnizhka' (Ukraine); 'President', 'Valuta' (Russia); 'Bolero' (England)) of three ecological and geographical groups of Ukrainian and foreign selection.

The object of research - the processes of potential and real (economic) productivity formation of apple trees varieties in the fruiting orchard.

The garden was laid in 2002 and 2010 according to the method of primary variety testing. Planting is not irrigated. Trees on rootstock 54–118 were planted according to the scheme of 4×1 m.

Meteorological data for the trial evaluation years were obtained at the Vantage Pro2 Plus weather station. The hydrothermal coefficient (SCC Selyanova) was calculated by dividing the amount of precipitation in mm by the sum of active temperatures of 10 °C and above for the period of growth and development of fruits. The obtained data were decreased 10 times.

**Instruments.** The buds were selected in five repetitions from complex flushes located in the middle part of the trunk of a certain age. Anatomical sections of buds 30–60 μm thick were made using a freezing microtome OmE. The obtained material was viewed using a microscope MBI-6 at a magnification of 90–180 times.

**Methods.** Quantitative evaluation of apple varieties productivity formation at III–IV stages of organogenesis and the effectiveness of their elements into the real yield (V–XI stages of organogenesis) was performed according to the method of Isaeva (1974). SEC (statistical evaluation coefficient) was calculated as the ratio of the number of reproductive elements at a certain stage of organogenesis to the number of buds that reached stage II of organogenesis.

**Description of the Experiment.** The number of elements of reproduction at certain stages of organogenesis was analyzed during the research. We also conducted a correlation analysis of the weather factors influence over 5 years on the actual number of potential fruiting points depending on the stage of organogenesis.

**Sample preparation:** The number of buds on the plant was calculated in early August. When the air temperature was less than 5 °C, the number of buds that differentiated into generative ones was counted. From the onset of subzero temperatures, anatomical and morphological analysis of the buds was performed under a microscope to determine their condition in the pre-winter period. During the IX stage of

organogenesis (flowering), the total number of flowers on plants was counted. After the fall of the ovary in June (stage X of organogenesis), the number of ovaries that did not fall was counted. At the XI stage of organogenesis, the number of fruits was counted.

**Number of samples analyzed:** seven varieties of columnar type apple trees took part in the research. Each variety is represented by five plants (35 trees in total). The number of reproductive elements at certain stages of organogenesis was counted on each of the trees.

### Statistical analysis

Using correlation analysis, the strength of the connection between meteorological elements for the years of the field experiment and the number of elements of reproduction at a certain stage of organogenesis. The influence of the factor by the correlation coefficient is weak ≤ 0.29, moderate: 0.30–0.49, noticeable: 0.50–0.69, high: 0.70–0.89, very high: 0.90–0.99 (*LSD*: Least significantly difference at $P < 0.05$). Statistical processing was performed in Microsoft Excel 2016 in combination with XLSTAT.

## RESULTS AND DISCUSSION

The experimental site is located in the zone of the Western Forest-Steppe of Ukraine. The climate of the area is temperate continental and is characterized by mild winters and warm summers. The average annual temperature is 7.4 °C. The coldest month is January, with an average monthly temperature of minus 5.8 °C, and the warmest is July (19.6 °C). The first autumn frosts are observed from the second decade of October. Winter begins in the second decade of November. Permanent snow cover is established in December and disappears in the second decade of March. Thawing during the winter period (December-February) lasts an average of 40 days (repeated 8 to 10 times with a duration of 5 days). Spring frosts are likely by mid-May.

The growing season in fruit crops, according to long-term data, begins in the first decade of April. Active growth and development of fruit plants are observed in the third decade of April. The sum of active temperatures of 10 °C and above ($\Sigma_{akt}t \geq 10$ °C) is 2,850 °C, the number of days with a temperature of 10 °C and above - about 160. The average annual rainfall reaches 597 mm, most of which falls from April to October (400 mm). The wettest are the summer months - from June to August, an average of 68–81 mm of precipitation per month. In the period from November to March, about 230 mm of precipitation falls. The average number of days with precipitation is 160.

The soil of the experimental plot is dark gray podzolic medium loamy on carbonate loess, typical for the right-bank part of the Western Forest-Steppe. The humus content in the arable soil layer (0–40 cm) is 1.00–1.90%, the pH of the aqueous extract is 6.22–8.33.

During the III–IV stages of organogenesis due to the rudimentary flowers formation in the generative buds is the laying of potential yield elements of the tree (Buntsevich, 2014; Kohek et al., 2015). During this period, there is a loss of potential productivity in conventional varieties due to vegetative shoots, and in columnar (in most varieties) - vegetative buds on simple and complex shoots, which do not differentiate generative buds (buds with incomplete cycle of organogenesis). Kolomiets (1976) and Kobel (1984) investigated the dependence of generative buds differentiation on meteorological conditions (El Yaacoubi et al., 2020). According to the results of five-year experiments Isaeva (1989) found that this process begins earlier in warm and fairly dry summers than

cold and rainy, but, in the opinion of the scientist, the difference in the timing of generative buds differentiation in different weather is insignificant and reaches 7–14 days. Kondratenko (2003) found a varietal difference in the timing of the beginning of generative buds' differentiation, in the degree of development of the latter in the pre-winter period, as well as in the timing and duration of IX–X stages of organogenesis for traditional apple genotypes. Information on the organogenesis of buds in plants of columnar apple cultivars, which would make it possible to establish the features of this process in complex shoot of different ages, is currently missing, as well as the levels of their productivity and longevity (Koutina et al., 2007; Yareshchenko et al., 2012).

Plants of the columnar varieties studied by us at the II stage of organogenesis formed, depending on the variety, 144–871 pcs. buds/tree. At the III–IV stages of organogenesis varieties differed in the efficiency of generative buds differentiation both among themselves and by years (Table 1).

**Table 1.** Efficiency of potential productivity realization by plants of columnar apple varieties at III–IV stages of organogenesis (SEC). IH NAAS, 2016–2019

| Stages of organo-genesis | Year | Variety | | | | | | |
|---|---|---|---|---|---|---|---|---|
| | | Tantsivnytsia | Sparta | President | Valuta | Favoryt | Bilosnizhka | Bolero (c) |
| II | | 1.000 | 1.000 | 1.000 | 1.000 | 1.000 | 1.000 | 1.000 |
| III–IV | 2016 | 0.248 bc | 0.163 bc | 0.527 a | 0.548 a | 0.071 c | 0.425 a | 0.308 b |
| | 2017 | 0.922 a | 0.636 b | 0.496 b | 0.560 b | 0.337 c | 0.481 b | 0.288 c |
| | 2018 | 0.022 d | 0.205 b | 0.022 d | 0.021 d | 0.214 b | 0.341 a | 0.084 c |
| | 2019 | 0.852 a | 0.506 b | 0.422 bc | 0.482 b | 0.296 c | 0.346 bc | 0.243 c |
| Average for 4 years | | 0.511 a | 0.377 b | 0.367 b | 0.403 b | 0.230 c | 0.398 b | 0.231 c |

Means in lines with the different letter are highly significantly different according to the Fisher's test ($P \leq 0.05$).

On average, over the four years of the study, the biggest number of generative buds out of their total number was formed on 'Tantsivnytsia' trees (51%), the smallest - in 'Favoryt' and 'Bolero' (23%).

According to the coefficient of determination, the influence of the conditions of the year on the differentiation of generative buds on average for all varieties is 46%; of variety - 10%; interaction of conditions of the year and variety - 36%. Weather conditions had a strong influence on the differentiation of buds in the variety 'Tantsivnytsia', as evidenced by the correlation coefficient (Table 2).

**Table 2. C**orrelation coefficient between SEC and weather factors during III–IV organogenesis

| Variety | HTC | $\Sigma_{akt}t \geq 10$ °C | Σ precipi-tation | Average daily air temperature |
|---|---|---|---|---|
| Tantsivnytsia | 0.95 | -0.80 | -0.95 | -0.91 |
| Sparta | 0.87 | -0.60 | -0.96 | -0.79 |
| President | 0.71 | -0.91 | -0.52 | -0.80 |
| Valuta | 0.78 | -0.96 | -0.60 | -0.87 |
| Favoryt | 0.52 | -0.16 | -0.69 | -0.40 |
| Bilosnizhka | 0.60 | -0.60 | -0.53 | -0.61 |
| Bolero (c) | 0.67 | -0.87 | -0.48 | -0.76 |

The influence of precipitation, $\Sigma_{akt}t \geq 10$ °C and average daily air temperature on the flower buds formation for varieties 'Favoryt' and 'Bilosnizhka' was weak and

moderate. For the introduced varieties ‘Bolero’, ‘President’ and ‘Valuta’, as well as for domestic variety ‘Sparta’, a high negative correlation coefficient was established between the number of generative buds relative to their total number and $\Sigma_{akt}t \geq 10$ °C The influence of precipitation, $\Sigma_{akt}t \geq 10$ °C and average daily air temperature on the flower buds formation for varieties ‘Favoryt’ and ‘Bilosnizhka’ was weak and moderate. For the introduced varieties ‘Bolero’, ‘President’ and ‘Valuta’, as well as for domestic variety ‘Sparta’, a high negative correlation coefficient was established between the number of generative buds relative to their total number and $\Sigma_{akt}t \geq 10$ °C and the average daily air temperature and positive - with elevated HTC.

Thus, the differentiation of flower buds on plants of columnar varieties, one way or another, is influenced by certain meteorological factors (Lenz et al., 2016; Unterberger et al., 2018). Plants of introduced apple cultivars in the period of generative potential formation at III–IV stages of organogenesis are negatively affected by increase of level $\Sigma_{akt}t \geq 10$ °C and average daily air temperature, as well as decrease of HTC (hydrothermal coefficient). For most domestic varieties, the influence of these factors on the laying of flower buds is weak and moderate, which indicates a better adaptability of these varieties to the conditions of the Western Forest-Steppe of Ukraine.

Different numbers of flowers are formed in the generative buds of different types of fruit formations. On fruit twigs, terminal buds of shoots and shuts of ordinary varieties there are more of them (5–7 pcs.), And on fruiting shoots and in axillary buds of shoots - less (3–5). As a result, the participation of each type of fruit formations in the formation of productivity at stages IV–VIII of organogenesis changes. In the studied columnar varieties, the vast majority of fruit formations are represented by simple and complex shoots, in the generative buds of which, depending on the characteristics of the variety, 5 to 7 flowers were formed.

At the V stage of organogenesis of buds reduction of a considerable quantity of reproduction elements as a result of action on rudimentary flowers of low minus temperatures is possible (Amasino, 2010; Zuo et al., 2018; Xing et al., 2019). Kondratenko (2002) reports that in stages V–VIII during the winter-spring pruning of the crown in conventional varieties, more than 35% of generative buds are removed, ie the number of potential fruiting points is artificially reduced (Xing et al., 2016; Zhu et al., 2018). The realization of the productivity potential available in the form of flowers (IX stage of organogenesis) (Fig. 1) depends on the success of pollination and fertilization, which is influenced by meteorological conditions during flowering, as well as the presence of pollinating varieties and insects (Ryadnova & Eremin, 1964; Mir et al., 2016). In rainy and cool weather, pollination is complicated. Simultaneous and gradual flowering on the tree allows you to pollinate most of them (Srivastava et al., 2017). Thus, the asynchrony of flower bloom is one of the devices for the effective realization of the potential of productivity in the real yield.

On average, in 2017–2020, the largest number of formed flowers per potentially generative bud was observed in plants of varieties ‘Tantsivnytsia’ and ‘Bilosnizhka’, the smallest - in ‘Favoryt’ (Table 3).


**Figure 1.** Plants crown of studied apple varieties during mass flowering. IH NAAS, 2018: a – 'President'; b – 'Valuta'; c – 'Favoryt'; d – 'Bilosnizhka'; e – 'Sparta', f – 'Tantsivnytsia'.

**Table 3.** The efficiency of the elements of reproduction implementation at the V–IX stages of organogenesis in plants of columnar varieties (SEC). IH NAAS, 2017–2020

| Stages of organo-genesis | Year | Variety | | | | | | |
|---|---|---|---|---|---|---|---|---|
| | | Tantsivnytsia | Sparta | President | Valuta | Favoryt | Bilosnizhka | Bolero (c) |
| II | | 1.000 | 1.000 | 1.000 | 1.000 | 1.000 | 1.000 | 1.000 |
| V–IX | 2017 | 1.737 a | 0.475 a | 1.743 a | 2.033 a | 0.296 a | 2.034 a | 1.711a |
| | 2018 | 6.326 a | 3.178 bc | 2.480 cd | 2.799 bc | 1.684 cd | 3.368 b | 1.969 cd |
| | 2019 | 0.157 d | 1.025 b | 0.108 d | 0.105 d | 1.068 b | 2.387 a | 0.580 c |
| | 2020 | 5.865 a | 1.928 bc | 2.033 bc | 2.432 b | 1.479 c | 2.090 bc | 1.704 c |
| Average for 4 years | | 3.521 a | 1.651 b | 1.591 b | 1.842 b | 1.132 bc | 2.470 a | 1.491 b |

Means in lines with the different letter are highly significantly different according to the Fisher's test ($P \leq 0.05$).

According to the coefficient of determination, the influence of meteorological factors of the year on the efficiency of the implementation of the reproduction elements at the V–IX stages of organogenesis was 42%; varietal characteristics - 16%; interaction of year conditions and varietal characteristics - 29%. In all studied varieties, with more rainfall during the V–IX stages, a smaller number of flowers was observed (Table 4); under conditions of higher average daily temperature and $\Sigma_{akt}t \geq 10$ °C their number per one potentially generative bud was higher.

**Table 4.** Correlation coefficient between SEC and weather factors during V–IX organogenesis

| Variety | HTC | $\Sigma_{akt}t \geq 10$ °C | Σ precipi-tation | Average daily air temperature |
|---|---|---|---|---|
| Tantsivnytsia | -0.96 | 0.84 | -0.89 | 0.75 |
| Sparta | -0.90 | 0.99 | -0.68 | 0.97 |
| President | -0.78 | 0.48 | -0.88 | 0.35 |
| Valuta | -0.75 | 0.45 | -0.85 | 0.32 |
| Favoryt | -0.60 | 0.84 | -0.31 | 0.88 |
| Bilosnizhka | -0.73 | 0.83 | -0.53 | 0.82 |
| Bolero (c) | -0.55 | 0.29 | -0.66 | 0.19 |

Therefore, under conditions of warm ($\Sigma_{akt}t \geq 10$ °C not less than 500) and not rainy spring (HTC not more than 0.50) during the IX stage of organogenesis in columnar apple varieties fully retains the number of flowers laid in the IV stage, which provides a high the level of realization of potential productivity.

At the X stage of organogenesis, the ovary increases in size, in the seed there is growth of endosperm and nucellus (Isaeva, 1989). There is also growth of unfertilized ovaries, which are reducing over the time. The duration of this process depends on the variety and is two to three weeks (Kuzin et al., 2018). At the XI stage the formation of the endosperm and embryo, as well as the hereditary size of the fetus determined for each variety is completed; depending on the conditions of a particular year, the size of the fruit may vary slightly. Thus, during the X–XI stages of organogenesis, along with yield formation due to a certain number of fruits and their average weight, there is a loss of its potential due to the reduction of ovaries and fruits. This process Gareev (1970), Kobel (1984) and others are divided into two periods.


**Figure 2.** Plants of the 'Valuta' variety at a certain stage of organogenesis, IH NAAS, 2018: a – Stage X; b – Stage XI.

In general, on average in 2017–2020 studies, significantly lower levels of ovarian loss relative to control during stage X of organogenesis were observed in plants of Tantsivnytsia, 'Valuta' and 'President'varieties (41–49%) (Fig. 2), the highest - in 'Favoryt', up to 83% (Table 5).

The coefficient of determination indicates that the influence of the year conditions on the passage of the X stage of organogenesis is 17%; varietal features - 13%; interaction between the conditions of the year and variety - 39%.

**Table 5.** The efficiency of the elements of reproduction implementation at the X stage of organogenesis in columnar varieties of apples (SEC). IH NAAS, 2017–2020

| Stages of organo-genesis | Year | Variety | | | | | | |
|---|---|---|---|---|---|---|---|---|
| | | Tantsivnytsia | Sparta | President | Valuta | Favoryt | Bilosnizhka | Bolero (c) |
| II | | 1.000 | 1.000 | 1.000 | 1.000 | 1.000 | 1.000 | 1.000 |
| X | 2017 | 0.346 ab | 0.173 ab | 0.407 ab | 0.531 a | 0.090 b | 0.099 b | 0.274 ab |
| | 2018 | 0.694 ab | 0.148 bc | 0.892 a | 0.699 a | 0.176 bc | 0.152 bc | 0.377 bc |
| | 2019 | 0.035 c | 0.337 ab | 0.031 c | 0.046 a | 0.245 b | 0.349 a | 0.107 c |
| | 2020 | 0.572 a | 0.158 bc | 0.640 a | 0.567 a | 0.169 c | 0.124 c | 0.246 b |
| Average for 4 years | | 0.412 ab | 0.204 b | 0.492 a | 0.461 a | 0.170 b | 0.181 b | 0.251 b |

Means in lines with the different letter are highly significantly different according to the Fisher's test ($P \leq 0.05$).

For the introduced varieties 'Bolero', 'President', 'Valuta' and domestic variety 'Tantsivnytsia', a negative correlation was found between the number of ovaries at the end of stage X of organogenesis and meteorological factors such as $\Sigma_{akt}t \geq 10$ °C and the amount of precipitation, and a significant positive correlation coefficient - with an average daily temperature (Table 6).

**Table 6.** Correlation coefficient between SEC and weather factors during the X stage of organogenesis

| Variety | HTC | $\Sigma_{akt}t \geq 10$ °C | Σ precipi-tation | Average daily air temperature |
|---|---|---|---|---|
| Tantsivnytsia | -0.59 | -0.43 | -0.51 | 0.65 |
| Sparta | 0.80 | 0.71 | 0.76 | -0.49 |
| President | -0.69 | -0.54 | -0.61 | 0.64 |
| Valuta | -0.81 | -0.69 | -0.75 | 0.60 |
| Favoryt | 0.81 | 0.90 | 0.87 | 0.06 |
| Bilosnizhka | 0.85 | 0.84 | 0.86 | -0.27 |
| Bolero (c) | -0.79 | -0.63 | -0.71 | 0.71 |

For the varieties 'Sparta', 'Favoryt' and 'Bilosnizhka' at the X stage of organogenesis, a high positive correlation coefficient was found between the amount of preserved ovary and $\Sigma_{akt}t \geq 10$ °C and the amount of precipitation. Therefore, by increasing the average daily air temperature in varieties 'Tantsivnytsia', 'Bolero', 'President' and 'Valuta' minimizes the reduction of reproductive elements at this stage of organogenesis. In the varirties 'Sparta', 'Favoryt' and 'Bilosnizhka', the reduction decreased with the decrease of $\Sigma_{akt}t \geq 10$ °C and the amount of precipitation. This means that under optimal meteorological conditions for a certain variety at the X stage of organogenesis, the coefficient of the reproduction elements realization will be much higher.

The highest level of potential productivity realization on average for 2017–2020 was observed in the varieties ‘President’, ‘Valuta’ and ‘Tantsivnytsia’; their trees per one potentially generative bud formed 0.27–0.38 fruit. The lowest level of potential productivity realization was found in plants of the control variety ‘Bolero’ (Table 7).

**Table 7.** Implementation of reproductive elements in trees of columnar apple varieties at the XI stage of organogenesis (SEC). IH NAAS, 2017–2020

| Stages of organo-genesis | Year | Variety | | | | | | |
|---|---|---|---|---|---|---|---|---|
| | | Tantsivnytsia | Sparta | President | Valuta | Favoryt | Bilosnizhka | Bolero (c) |
| II | | 1.000 | 1.000 | 1.000 | 1.000 | 1.000 | 1.000 | 1.000 |
| XI | 2017 | 0.174 b | 0.063 b | 0.354 a | 0.325 a | 0.071 b | 0.119 b | 0.078 b |
| | 2018 | 0.611 a | 0.148 b | 0.770 a | 0.541 a | 0.158 b | 0.122 b | 0.155 b |
| | 2019 | 0.019 b | 0.169 a | 0.017 b | 0.024 b | 0.151 a | 0.172 a | 0.046 b |
| | 2020 | 0.290 c | 0.131 d | 0.376 b | 0.409 a | 0.140 d | 0.054 e | 0.103 d |
| Average for 4 years | | 0.273 a | 0.128 b | 0.379 a | 0.328 a | 0.130 b | 0.117 b | 0.095 b |

Means in lines with the different letter are highly significantly different according to the Fisher’s test ($P \leq 0.05$).

According to the coefficient of determination, the influence of the year conditions on the fruits reduction during the XI stage of organogenesis is 24%; varietal characteristics - 21%; interaction of conditions of the year and variety - 42%. In general, for almost all studied varieties it was found that the increase in useful ovaries, ie a decrease in fruit reduction during stage XI, is positively affected by an increase in the level of $\Sigma_{akt}t \geq 10$ °C, rainfall and average daily air temperature. A strong influence on the preservation of the reproductive potential of plants varieties ‘Tantsivnytsia’, ‘President’, ‘Valuta’ and ‘Bolero’ had an increase in the level of precipitation during the XI stage of organogenesis ($r$ = 0.85-0.98) (Table 8).

**Table 8.** Correlation coefficient between SEC and weather factors during the XI stage of organogenesis

| Variety | HTC | $\Sigma_{akt}t \geq 10$ °C | Σ precipi-tation | Average daily air temperature |
|---|---|---|---|---|
| Tantsivnytsia | 0.87 | 0.74 | 0.87 | 0.47 |
| Sparta | 0.19 | 0.53 | 0.20 | 0.77 |
| President | 0.89 | 0.08 | 0.88 | 0.09 |
| Valuta | 0.86 | 0.58 | 0.85 | 0.20 |
| Favoryt | 0.38 | 0.65 | 0.39 | 0.80 |
| Bilosnizhka | -0.31 | -0.09 | -0.31 | 0.15 |
| Bolero (c) | 0.98 | 0.81 | 0.98 | 0.50 |

The fruit reduction decrease in all varieties, except for ‘Bilosnizhka’, was significantly and positively caused by an increase in $\Sigma_{akt}t \geq 10$ °C. The increase in the average daily air temperature contributed to the increase in the number of useful ovaries in the varieties ‘Sparta’ and ‘Favoryt’.

According to Kondratenko (2002), the realization rate of potential productivity less than 0.100 indicates serious violations in the technology of care for the variety, the inconsistency of the climatic zone of cultivation or the impact of adverse weather conditions in a particular year. The low realization rate was characteristic of the ‘Bolero’ variety, probably due to low rainfall ($r$ = 0.98) during the XI stage of organogenesis.

## CONCLUSIONS

In the conditions of the western Forest-Steppe of Ukraine, columnar apple cultivars react differently to environmental conditions at certain stages of organogenesis. The efficiency of differentiation of generative buds and the reduction of reproductive elements of columnar varieties are influenced in one way or another by meteorological factors. The efficiency of plants biological potential realization of all studied columnar apple varieties at III–IV and V–IX stages of organogenesis was high: the higgest number of buds from their total number differentiated into generative on trees varieties 'Sparta', 'President', 'Bilosnizhka', 'Valuta' and 'Tantsivnytsia' (37–51%), the smallest in 'Favoryt' and 'Bolero'. The largest number of flowers per one potentially generative bud is formed by plants of varieties 'Tantsivnytsia' and 'Bilosnizhka'. The lowest level of ovarian loss during stage X of organogenesis was observed in plants varieties 'Valuta', 'President' and 'Tantsivnytsia' (41–49%), and the highest - in 'Favoryt' variety (up to 83%). More effective realization of potential productivity at the XI stage of organogenesis occurred in plants of varieties 'President', 'Valuta' and 'Tantsivnytsia'; their trees on one potentially generative bud formed - 0.27–0.38 fruits.

## REFERENCES


Amasino, R. 2010. Seasonal and developmental timing of flowering. *The Plant Journal* **61**, 1001–1013. https://doi.org/10.1111/j.1365-313X.2010.04148.x

Benko, B. 1967. Morphological differentiation of flower buds in Apple-Trees. *Biologia Plantarum*. **9**(4), 263. https://doi.org/10.1007/BF02929766

Buntsevich, L. & Sergeeva, N. 2014. Morphophysiological effects of various foliar nutrition regimes in apple in the south of Russia. *Universal Journal of Plant Science* **2**(3), 63–68. https://doi.org/10.13189/ujps.2014.020301

Cooperman, F.M. 1984. *Morphophysiology of plants*. Moscow, Russia: Higher school, 240 pp. (in Russian).

Duric, G., Micic, N., Cerovic, R. & Plazinic, R. 1997. Degree of differentiation of generative buds as a factor of bearing in apricot. *In XI International Symposium on Apricot Culture.* Veria-Makedonia, Greece. 488, pp. 351–356. https://doi.org/10.17660/ActaHortic.1999.488.55

El Yaacoubi, A., El Jaouhari, N., Bourioug, M. El Youssfi, L., Cherroud, S., Bouabid, R., Chaoui, M. & Abouabdillah, A. 2020. Potential vulnerability of Moroccan apple orchard to climate change–induced phenological perturbations: effects on yields and fruit quality. *Int. J. Biometeorol* **64**, 377–387. https://doi.org/10.1007/s00484-019-01821-y

El-Sabagh, A.S., Othman, S.A. & AlAbdaly, A.N. 2012. Performance of Anna apple cultivar grown on two different rootstocks in response to hydrogen cyanamide winter spraying. *World J. Agric. Sci.* **8**(1), 01–12. ISSN 1817-3047

Gareev, E.Z. 1970. *Features of the formation of flower buds in an apple tree*. Frunze, Kyrgyzstan: Ilim, 192 pp. (in Russian).

Havryliuk, O., Kondratenko, T. & Goncharuk, Y. 2019a. Features of formation of productivity of columnar apple-tree. *Bulletin of Agricultural Science* **97**(6), 27–34. https://doi.org/10.31073/agrovisnyk201906-04

Havryliuk, O. & Kondratenko, T. 2019b. Specific of the Assimilation Surface of Columnar Apple-Tree. *Agrobiodiversity for Improving Nutrition, Health and Life Quality* **3**, 57–65. https://doi.org/10.15414/agrobiodiversity.2019.2585-8246.057-065

Isaeva, I.S. 1974. *Morphophysiology of fruit plants*. Moscow, Russia: Moscow State University. M.V. Lomonosov, 135 pp. (in Russian).

Isaeva, I.S. 1989. *Apple tree productivity*. Moscow, Russia: Moscow State University. M.V. Lomonosov, 149 pp. (in Russian).

Kobel, F. 1984. *Fruit growing on a physiological basis*. Moscow, Russia: GISL, 375 pp. (in Russian).

Kohek, Š., Guid, N., Tojnko, S., Unuk, T. & Kolmanič, S. 2015. EduAPPLE: Interactive Teaching Tool for Apple Tree Crown Formation, *HortTechnology* **25**(2), 238–246. https://doi.org/10.21273/HORTTECH.25.2.238

Kolomiets, I.A. 1976. *Overcoming the frequency of fruiting apple trees.* Kiev, Ukraine: Harvest, 240 pp. (in Ukraine).

Konarska, A. 2012. Differences in the fruit peel structures between two apple cultivars during storage. *Acta Scientiarum Polonorum-Hortorum Cultus* **11**(2), 105–116.

Kondratenko, T. E. 2002. *Fundamentals of the formation of an industrial assortment of apple trees in Ukraine*: PhD Thesis, Kiev, Ukraine, 326 pp. (in Ukraine).

Kondratenko, T.E. 2003. Potential productivity of apple varieties and the level of its implementation depending on the technology and growing area. *Collection of scientific works of Uman State Agrarian University "Biological sciences and problems of crop production".* Uman, Ukraine: UDAU. pp. 470–474 (in Ukraine).

Kondratenko, T.E. 2013. Columnar apple orchard. *Modern agricultural technologies* **4**, 58–63 (in Ukraine).

Koutina, G., Koutinas, N. & Pepelyankov, G. 2007. Rootstock influence on the time of cessation of the shoot growth and the time of differentiation of flower buds in two apple cultivars. *In I. Balkan Symposium on Fruit Growing.* Plovdiv, Bulgaria, **825**, pp. 231–236. https://doi.org/10.17660/ActaHortic.2009.825.36

Kovalyshyna, H., Dmytrenko, Y., Makarchuk, O., Slobodyanyuk, N. & Mushtruk, M. 2020a. The donor properties of resources resistance against the exciter of wheat rust wheat. *Potravinarstvo Slovak Journal of Food Sciences* **14**, 821–827. https://doi.org/10.5219/1427

Kovalyshyna, H., Dmytrenko, Y., Tonkha, O., Makarchuk, O., Demydov, O., Humenyuk, O., Kozub, N., Karelov, A., Sozinov, I. & Mushtruk, M. 2020b. Diversity of winter common wheat varieties for resistance to leaf rust created in the V. M. Remeslo Myronivka Institute of Wheat. *Potravinarstvo Slovak Journal of Food Sciences* **14**, 1001–1007. https://doi.org/10.5219/1447

Kuzin, A.I., Trunov, Yu.V. & Solovyev, A.V. 2018. Effect of fertigation on yield and fruit quality of apple (*Malus domestica* Borkh.) in high-density orchards on chernozems in Central Russia*. Acta Hortic* **1217**, 343–350. https://doi.org/10.17660/ActaHortic.2018.1217.43

Lenz, A., Hoch, G., Körner, C. & Vitasse, Y. 2016. Convergence of leaf-out towards minimum risk of freezing damage in temperate trees. *Funct Ecol*. **30**, 1480–1490. https://doi.org/10.1111/1365-2435.12623

Mazurenko, B., Honchar, L., Novytska, N. & Kalenska, S. 2020. Grain yield response of facultative and winter triticale for late autumn sowing in different weather conditions. *Agronomy research* **18**(1), 183–193. https://doi.org/10.15159/AR.20.008

Mezhenskyj, V., Kondratenko, T., Mazur, B., Shevchuk, N., Andrusyk, Y. & Kuzminets, O. 2020. Results of ribes breeding at the national university of life and environmental sciences of ukraine. *Research for Rural Development* **35**, 22–26. https://doi.org/10.22616/rrd.26.2020.003

Mir, J.I., Ahmed, N., Singh, D.B., Sharma, O.C., Sharma, A., Shafi, W., Zaffer, S. & Hamid, A. 2016. Effect of planting densities on productivity of different cultivars in apple (Malus× domestica). *Indian Journal of Agricultural Sciences* **86**(8), 1059–62. http://epubs.icar.org.in/ejournal/index.php/IJAgS/article/view/60538

Palubicki, W., Horel, K., Longay, S., Runions, A., Lane, B., Měch, R. & Prusinkiewicz, P. 2009. Self-organizing tree models for image synthesis. *ACM Transactions on Graphics* (TOG), **28**(3), 1–10. https://doi.org/10.1145/1531326.1531364

Rather, J.A., Misgar, F.A., Dar, G.A. & Qurashi, S.N. 2018. Effects of Rootstocks on Horticultural Characteristics of Various Exotic Apple Cultivars in Kashmir Climatic Conditions. *Int. J.Curr. Microbiol. App. Sci.* **7**(04), 2341–2348. https://doi.org/10.20546/ijcmas.2018.704.268

Ryadnova, I.M. & Eremin, G.V. 1964. *Winter hardiness of fruit trees in the south of the USSR*. Moscow, Russia: Kolos, 208 pp. (in Russian).

Shevchuk, L., Grynyk, I., Levchuk, L., Babenko, S., Podpriatov, H. & Kondratenko, P. 2021. Fruit Quality Indicators of Apple (Malus domestica Borkh.) Cultivars Bred in Ukraine. *Journal of Horticultural Research* **29**(2), 95–106. https://doi.org/10.2478/johr-2021-0019

Srivastava, K., Singh, D., Kumar, D., Singh, S., Sharma, O. & Lal, S. 2017. Effect of planting densities and varieties on yield and yield associated characters of apple (Malus × dometica) on semi-dwarfing rootstock. *The Indian Journal of Agricultural Sciences* **87**(5). http://epubs.icar.org.in/ejournal/index.php/IJAgS/article/view/70107

Unterberger, C., Brunner, L., Nabernegg, S., Steininger, K.W., Steiner, A.K., Stabentheiner, E., Monschein, S. & Truhetz, H. 2018. Spring frost risk for regional apple production under a warmer climate. *PLoS ONE*, **13**(7). https://doi.org/10.1371/journal.pone.0200201

Vasylenko, O., Kondratenko, T., Havryliuk, O., Andrusyk, Y., Kutovenko, V., Dmytrenko, Y., Grevtseva, N. & Marchyshyna, Y. 2021. The study of the productivity potential of grape varieties according to the indicators of functional activity of leaves. *Potravinarstvo Slovak Journal of Food Sciences* **15**, 639–647. https://doi.org/10.5219/1638

Xing, L., Zhang, D., Qi, S., Chen, X., An, N., Li, Y., Zhao, C., Han, M. & Zhao, J. 2019. Transcription profiles reveal the regulatory mechanisms of spur bud changes and flower induction in response to shoot bending in apple (*Malus domestica* Borkh.). *Plant Mol. Biol.* **99**(1–2), 45–66. https://doi.org/10.1007/s11103-018-0801-2

Xing, L., Zhang, D., Zhao, C., Li, Y., Ma, J., An, N. & Han, M. 2016. Shoot bending promotes flower bud formation by miRNA-mediated regulation in apple (*Malus domestica* Borkh.). *Plant Biotechnol. J*. **14**(2), 749–770. https://doi.org/10.1111/pbi.12425

Yareshchenko, A., Tereshchenko, Y., Pryimachuk, L., Todosyuk, E. & Mazur, B. 2012. Ribes breeding programmes in Ukraine-recent achievements. *Acta Horticulturae* **946**, 177–182. https://doi.org/10.17660/ActaHortic.2012.946.27

Zamorskyi, V. 2007. The role of the anatomical structure of apple fruits as fresh cut produce. *In International Conference on Quality Management of Fresh Cut Produce*. Bangkok, Thailand. *Acta Hortic.* **746**, 509–512. https://doi.org/10.17660/ActaHortic.2007.746.64

Zhu,, Z., Jia, Z., Peng, L., Chen, Q., He, L., Jiang, Y. & Ge, S. 2018. Life cycle assessment of conventional and organic apple production systems in China. *Journal of Cleaner Production* **201**, 156–168. https://doi.org/10.1016/j.jclepro.2018.08.032

Zuo, X., Zhang, D., Wang, S., Xing, L., Li, Y., Fan, S., Zhang, L., Ma, J., Zhao, C., Shah, K., An, N. & Han, M. 2018. Expression of genes in the potential regulatory pathways controlling alternate bearing in 'Fuji' (*Malus domestica* Borkh.) apple trees during flower induction. *Plant Physiology and Biochemistry* **132**, 579–589. https://doi.org/10.1016/j.plaphy.2018.10.003

*Agronomy Research* **20**(1), 161–173, 2022
https://doi.org/10.15159/AR.22.008

# The potential and limitations for applications of oat proteins in the food industry

M. Ibrahim[1,2,*], A. Aav[1,2] and I. Jõudu[1,2]

[1]Estonian University of Life sciences, Institute of Veterinary Medicine and Animal Sciences, Chair of Food Science and Technology, Kreutzwaldi 56/5, EE51006 Tartu, Estonia
[2]Estonian University of Life sciences, Institute of Veterinary Medicine and Animal Sciences, ERA-Chair for Food (By-) Products Valorisation Technologies (VALORTECH), Kreutzwaldi 56/5, EE51006 Tartu, Estonia
[*]Correspondence: monica.nabil@student.emu.ee

Received: February 1st, 2022; Accepted: March 4th, 2022; Published: March 14th, 2022

**Abstract.** Oat proteins have gained high attractive popularity in the market as future protein alternatives in various food products. The extracted oat protein fractions are characterised by a relatively high protein content and a unique amino acid profile compared to other cereal grains. From another aspect, the oat protein is separated unintentionally during the production of oat flours, oat drinks, and oat flakes which encourages the incorporation of oat proteins in the food industry to valorise the food wastes. Therefore, commercial oat proteins possess poor techno-functionality and water solubility in the usual environmental conditions for most food products; therefore, modification of oat proteins functionalities is highly recommended. Several modification methods, including chemical, physical and enzymatic, have been proposed to improve the techno-functionality of native oat proteins and their biological activities. This review highlights the nutritional value of the oat protein fractions, their techno-functional properties and their food industrial challenging limitations. Additionally, it summarises several prospective methods effective for boosting the functionality of oat protein fractions and broadening their application in a range of food industries (bakery, dairy, meat, and their alternative products) with an overview of their impact on humans, animals, and environmental health.

**Key words:** oat proteins, nutritional benefits, biological activity, techno-functionality, modification methods, food industrial application.

## INTRODUCTION

In the last decade, consumer awareness regarding a healthy lifestyle and dietary protein sources has increased (Boukid, 2021a). As a result, the market demand for innovative healthy food products rich in alternative non-animal proteins has increased remarkably (Sterna et al., 2020; Boukid, 2021a). Meanwhile, the proteins derived from plant sources are attracting enormous food industrial interest owing to health, religious, ethical, cost, and dietary habits for some consumers (vegetarian, vegan, flexitarian), in

addition to sustainable and environmental concerns (Nieto-Nieto et al., 2014; Boukid, 2021b).

The comparison of Boukid (2021a) between the nutritional composition of grains and seeds (cereals, legumes, oil seeds) highlighted the particularly high protein content in oat grains among the whole major cereal categories. The protein content of oat groats ranges from 15 to 20% by weight, depending on genotype and growing environment (David, 2011; Kruma et al., 2018), in contrast to the protein contents of wheat (10.69–13.68%), brown rice (7.50%), barley (9.91%), sorghum (10.62%), millet (11.02%) and rye (10.34%) (Kumar et al., 2021). The main storage protein of most cereals (wheat, barley, and rye) is prolamin except for oat grains, where the predominant storage protein is globulin (which represents 70–80% of the total oat protein fraction) (Nieto-Nieto et al., 2014; Sargautis et al., 2021). Oat globulin is characterised by having a better amino acids composition, which is significantly higher in essential ones such as lysine and threonine, for human and animal nutrition than the prolamin of the other cereals (David, 2011; Nieto-Nieto et al., 2014). From the biological activity aspect, the oat globulin is characterized by particular bioactive peptides sequences such as angiotensin-converting enzyme inhibitor, antiamnestic (PEP-inhibitor), DPP-IV-inhibitor, antioxidant, and hypotensive peptides (Cavazos & Gonzalez de Mejia, 2013). Moreover, oat protein is a gluten-free source that suits the requirements of people suffering from coeliac disease (Kumar et al., 2021).

The annual marketing observations have indicated a prominent increment for oat protein acceptance by consumers compared to the other plant protein alternatives such as soy, pea, and lupine proteins since no off-flavours concerns are raised (Boukid, 2021a). Therefore, the research and markets (2019) predict growth in the global oat protein market at a CAGR of 1.22% during the forecast period (2019–2024). Furthermore, from the sustainability and the environmental perspectives, Mogensen et al. (2020) confirmed the potential reduction in greenhouse gas emissions by 8% and the land use by 14% if 24% of animal-based food is replaced by oat protein concentrate-based food. In this regard, the oat grains became valuable and attractive for research and commercial interests as a superior cereal source of low-cost dietary proteins with a prominent demand for its oat protein fractions in all the food industries (Boukid, 2021a).

Recently, oat protein preparations have been produced industrially (Fig. 1) in the following forms: oat protein isolates (OPI), oat protein concentrates (OPC), and fraction rich-in-proteins. The oat protein isolates (containing ≈ 90% protein) are extracted by wet methods (alkaline iso-electrically extraction, saline extraction, and acidic extraction) or an enzymatically isolation method (Boukid, 2021a; Immonen et al., 2021; Kumar et al., 2021). Oat protein concentrates (containing ≈ 70% protein) are produced with a production yield of up to 5% as the by-product of oat flour dry fractionation (including fine milling and air classification) into oat bran, oat starch, and $\beta$-glucan (Jiang et al., 2015; Immonen et al., 2021; Kumar et al., 2021). Additionally, the oat protein concentrates can be recovered as a by-product from the industrial production of $\beta$-glucan isolates (Brückner-Gühmann et al., 2019a).

The dry fractionation process is incorporated in the production of a fraction rich in proteins containing 42% protein (Boukid, 2021a). The study of Kumar et al. (2021) illustrated the unintentional removal of oat proteins during the physical separation step

of fibres in the production processes of oat flours, oat flakes and oat drinks that have a potential in oat protein fraction preparation. Theoretically, the oat protein possesses potential functional properties that contribute to the production of plant protein-enriched food products characterised by their improved quality (Jiang et al., 2015; Mäkinen et al., 2017; Kumar et al., 2021).

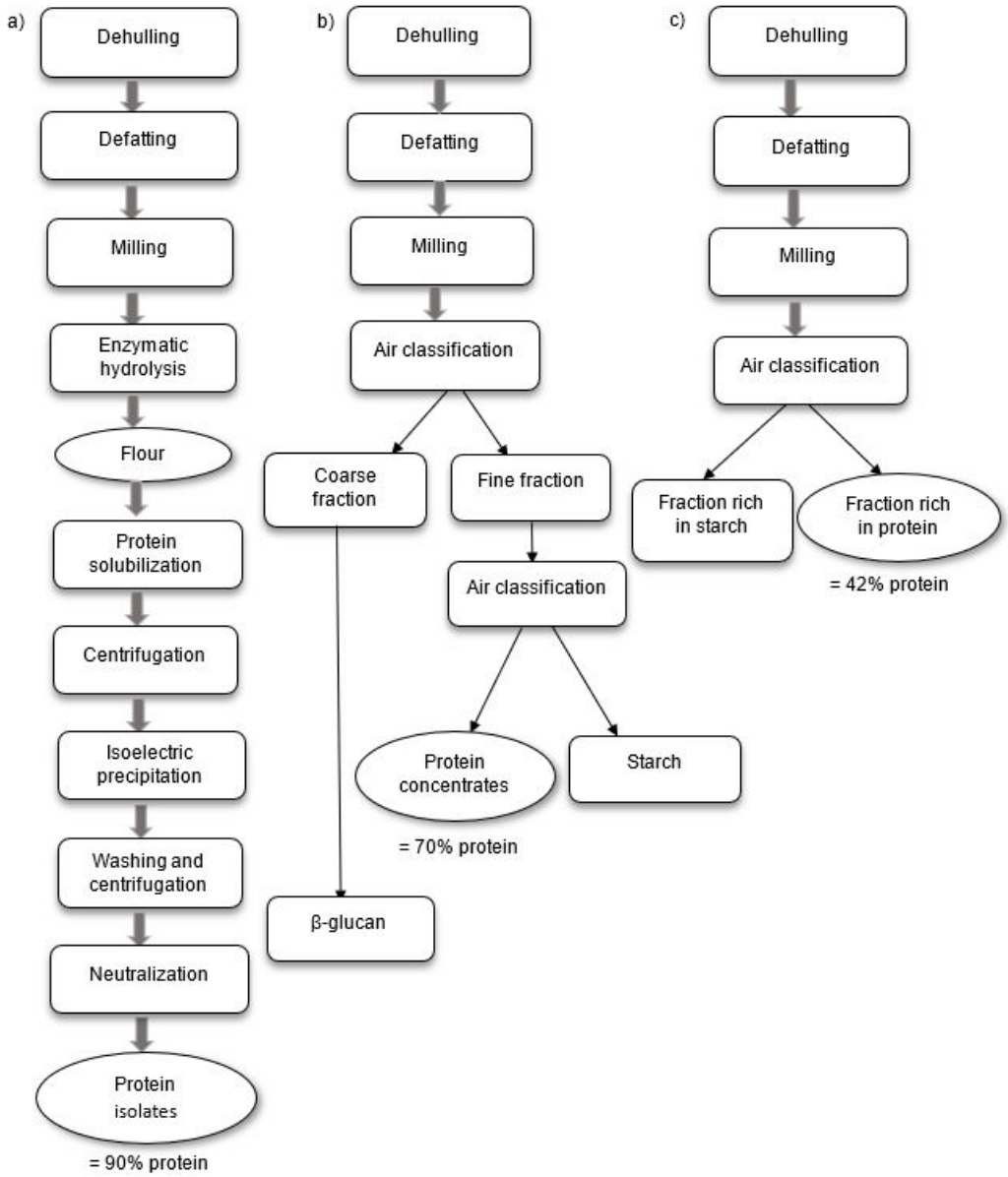


**Figure 1.** Schematic demonstration of the three potential industrial processing methods for producing oat protein preparations: a) alkaline extraction method, b) eecovery of oat concentrate from *β*-glucan production chain, and c) dry fractionation (Boukid, 2021a).

Although the market availability for the oat protein preparations and its unique proteinaceous profile and good amino acid compositions, the oat protein utilisation in the food industry remains limited and challenging due to the limited techno-functionality of the native oat protein under the typical aqueous food conditions (Mäkinen et al., 2017; Li & Xiong, 2020; Kumar et al., 2021). Thus, the demand has increased for the development of new modification strategies to enhance the techno-functionality of oat proteins and boost their application in various food industries (Brückner-Gühmann et al., 2018; Boukid, 2021a). Therefore, the purpose of this review is to demonstrate the nutritional value of the oat protein fractions, their biological activities, their techno-functional properties, and their food industrial challenging limitations. Additionally, this study summarises several prospective methods effective for boosting the functionality of oat proteins and broadening their application in various food industries with an overview of their impact on humans, animals, and environmental health.

**The unique nutritional value of oat proteins and their biological activities**

Typically, oat proteins have the following distribution in the layers of oat groats: 12% protein in the starchy endosperm, 18–30% in the bran, and 29–38% in the germ (Immonen et al., 2021). Four different varieties of proteins have been discovered in the oat grains based on the Osborne classification: globulins (70–80%), prolamins (4–14%); in oats called avenins, albumins (1–12%) and glutelins (< 10%), each as a percentage of the total oat proteins (Immonen et al., 2021; Spaen & Silva, 2021). Moreover, the essential amino acid composition in oat proteins is basically the same as the standard required for the daily intake of the human body, which can effectively promote the growth and development of the human body, in parallel to its regular consumption helps in treating the lysine deficiency (Tang et al., 2022).

The globulins represent the major fraction in oat proteins. Their amino acid profile is typically more valuable when compared to glutelin rich crops such as wheat or maize (Kruma et al., 2016). The amino acid composition for oat globulin is similar to soya glycinin, with the exception of tyrosine and phenylalanine, which were higher in oat globulin, and aspartic acid, proline, and lysine which were lower (Sargautis et al., 2021).

The distribution of oat amino acids varies between the structural parts of the grain (the germ, the endosperm, and the husk). The lysine content was found higher in oat germs than in either endosperm or the husk (Kumar et al., 2021). Mäkinen et al. (2017) identified higher glutamic acid and proline content in oat endosperm, particularly in comparison with the husk. In contrast, the same research found that the phenylalanine husk content is higher than in both the embryo and endosperm. Sterna et al. (2016) reported that the dehulled oat grains (45.60 g $kg^{-1}$) usually have a more significant amount of essential amino acids than the hulled grains (38.65 g $kg^{-1}$).

Both albumin and globulin in the oat grains play essential roles as contributors of lysine, and these have been found to have greater lysine contents, about 8.18 and 5.53 g amino acid 16 $g^{-1}$ of N, respectively (Kumar et al., 2021). Furthermore, Spaen & Silva (2021) determined that the prolamins of oats are rich in sulphur and contain high amounts of glutamic acid.

Apart from the nutritional value of oat proteins, the isolated oat protein fractions characterized by high digestibility (90.3–94.2%), biological value (74.5–79.6%) as well as net protein utilisation rate (69.1–72.4) (Kumar et al., 2021). The high utilisation rate

of the oat protein in the human body was reported by Tang et al. (2022), in addition to the superior oat protein efficiency ratio (PEP) that exceeds 2.0, compared to wheat and maize's PEP (< 1.5). Recent studies showed the presence of a bioactive peptides sequence in oat globulins that have the following biological activities: ACE-inhibitor, antiamnestic (PEP-inhibitor), DPP-IV-inhibitor, antioxidant, hypotensive peptides, antidiabetic peptides and antithrombotic peptides (Cavazos & Gonzalez de Mejia, 2013; Ramírez-Fuentes et al., 2021). An *in-vivo* study by Zhang et al. (2015a) showed that oat peptides, at a high dosage, had a hypoglycaemic effect on STZ-induced diabetic mice stimulating insulin secretion, increasing insulin sensitivity and elevating glycogenesis. Sánchez-Velázquez et al. (2021) explained the dependence of the biological activity and the functionality of oat protein on its solubility and digestibility, which can be enhanced by the digestive enzymes in the GIT (gastrointestinal tract). Consequently, oat protein modifications, especially limited proteolytic hydrolysis, are highly recommended for unfolding the complex structure of native oat protein and promoting its solubility and bioactivity (Sánchez-Velázquez et al., 2021). The previous nutritional profile and bioactivity of oat proteins justify its potential future application in the food industry and its particular techno-functional properties.

**The techno-functional properties of oat proteins and their challenging limitations in the food industries**

The functionality of the various oat protein fractions has a promising value in the novel healthy food industry. Kumar et al. (2021) and Spaen & Silva (2021) reported the oat proteins' functional properties, including gelling ability, emulsification properties, water-holding capacity (WHC), fat-binding capacity (FBC) and foaming properties, which enable the oat proteins to function as thickeners, emulsifiers, texture modifiers, and stabilisers in food products. Furthermore, the similar structure between the oat 12S globulin and the soya glycinin 11S globulin, which is known for its good gelling and emulsifying properties, suggesting the potential of oat protein to act as a gelling agent (Nieto-Nieto et al., 2015; Li & Xiong, 2020).

However, the functionality of native proteins is poor and limited in neutral and slightly acidic pH conditions (4−7), which is the typical pH range for food products, and consequently restricts its utilisation in many food industries (Mäkinen et al., 2017; Kumar et al., 2021). The reason for functionality limitation is that the oat globulins are insoluble under slightly acidic and neutral conditions due to their unfolding structure, resulting in transition from $\beta$-sheet to a random coil conformation and the formation of insoluble aggregates (Brückner-Gühmann et al., 2019a; Ma et al., 2000). Further explanation was illustrated by Mäkinen et al. (2017), who attributes the solubility difference between the oat globulins and the soya glycinins to some changes in the oat globulin surface properties. These changes arise from the existing glutamine-rich repeats of eight amino acids near the C-terminus of the acidic polypeptide exposed to solvents. Thus, these surface changes render the oat globulins less hydrophilic compared to other globulins, and explain the higher salt concentrations needed for solubilizing the oat globulin.

The oat protein preparations (OPC and OPI) could be used as an additional source of proteins to enrich dairy alternative products (Spaen & Silva, 2021) and producing meat analogue products (Mäkinen et al., 2017; Boukid, 2021a), or as a replacement for

skimmed milk powder in hybrid (dairy/plant based) yoghurt production (Brückner-Gühmann et al., 2019b). However, the main commercially available oat protein preparations (OPC and OPI) have poor techno-functionality and solubility in most relevant liquid and semi-solid food products (Spaen & Silva, 2021). Brückner-Gühmann et al. (2019b) investigated the potential of substituting skimmed milk powder with an oat protein preparation OPC (containing 43% protein and 33% starch) or OPI (containing 90% protein and less than 1% starch) in a cow's milk-based yoghurt. The results showed a decrease in syneresis with an increment in the viscosity and the sensorial characteristics of yoghurt containing OPC (43% proteins and 33% starch). Brückner-Gühmann and co-workers attributed this observation to the high amount of starch in the OPC rather than to the aggregated gelatinous oat protein particles due to their poor functionality and solubility (Brückner-Gühmann et al., 2019b; Spaen & Silva, 2021). Mäkinen et al. (2017) reported results of producing wheat bread containing OPC (3% and 6%) or OPI (5%) based on total flour weight. The trial outcomes showed increments in the loaf volume containing OPC, in contrast to a significant reduction in the loaf volume containing OPI which also had an increment in bread hardness and chewiness. Thus, modifying the oat protein preparations, especially the OPI, functionality, is critical for broadening their food application.

The good solubility of oat protein is a critical precondition property to achieve good emulsifying, foaming, and gelling properties (Jiang et al., 2015; Zhang et al., 2021). The US patent, US2016/0309762A1 (Chen, 2016) described the very weak gel formation and the poor water-holding capacity for oat proteins in acidic and neutral pH conditions. However, the oat proteins' gelling properties improve from a pH value of 8, and strong gels can be formed at pH 9–10 (Nieto-Nieto et al., 2015; Chen, 2016). The oat proteins' compact structure and heat stability explain the high-temperature (90–100 °C) needed to initiate a limited oat globulin dissociation into subunits to ameliorate its solubility and gelation properties (David, 2011). Nevertheless, this heating temperature doesn't suit a wide range of food systems, except those requiring high thermal stability, and consequently limits the utilisation of oat proteins in food products (David, 2011; Nieto-Nieto et al., 2015). Furthermore, the solubility and functionality of protein fractions vary by the extraction method used, where the alkaline method is the most efficient compared to both the saline and acidic methods (Kumar et al., 2021). In short, the alteration in the functionality of oat protein depends on its molecular size, structure, and charge distribution, as well as the presence of other components (lipids, starch, $\beta$-glucans) in association (Mäkinen et al., 2017). Therefore, various investigations have evaluated several modification procedures of the native oat protein to enhance its physicochemical and functional properties in typical food industrial conditions (Nieto-Nieto et al., 2014; Kumar et al., 2021).

**The industrial modification procedures of oat protein to broaden its food application**

Several chemical, physical and enzymatic modification methods (Table 1) have been studied to change the net charge and the hydrophilicity of proteins, leading to improvements in the solubility, surface properties and overall techno-functionality of oat protein fractions (Mäkinen et al., 2017; Brückner-Gühmann et al., 2018).

**Table 1.** Highest potential modification methods to enhance oat protein techno-functionality

| Modification categories | Modification methods | Impact on oat protein structure | References |
|---|---|---|---|
| Chemical modifications | Acetylation | Formation of acyl linkage | Kumar et al., 2021 |
| | Succinylation | Transfer the succinyl group and add negative charge | Mäkinen et al., 2017 |
| | Acidity regulator or Ionic salts | Altering the surface distribution of protein charges | Li & Xiong, 2020 |
| | Acidic deamidation | Degradation of protein and change its charge | Jiang et al., 2015 |
| Physical modifications | Glycation by controlled Maillard reaction | Enable the conjugation of protein with polysaccharides (dextrin, *β*-glucan, inulin) | Zhang et al., 2015b; Nieto-Nieto et al., 2015 |
| | Cold-set gelation | Proteins' denaturation followed by adding $Ca^{2+}$ or glucono-*δ*-lactone | Chen, 2016; Boukid, 2021a |
| Enzymatic modifications | Partial protein hydrolysis with trypsin or alcalase | Changing the molecular size and the conformation of tertiary protein structure | Spaen & Silva, 2021; Nieto-Nieto et al., 2014 |
| | Protein-glutaminase | Catalyse the deamidation of the side chain amino group of protein-bound glutaminyl residues | Jiang et al., 2015 |
| | Transglutaminase | Catalyse the formation of an isopeptide linkage between a glutamine and the amino group of protein-bound lysine | Mohamed et al., 2009 |

The chemical modifications by acetylation and succinylation were reported by Jiang et al. (2015) and Immonen et al. (2021) as efficient methods of altering the isoelectric point and the functionality profiles of oat protein. Protein acetylation includes adding an acetyl group to a specific amino acid of a protein in an esterification reaction with acetic acid or acetic anhydride to change the basic groups into neutral groups (Kumar et al., 2021). The succinylation process comprises attaching a succinyl group to proteins in a reaction with succinic anhydride to change the positive groups into negative groups (Mirmoghtadaie et al., 2009). Both modifications render the net charge towards the negative, leading to an increment in the negative charge repulsion and subunits dissociation (Mäkinen et al., 2017; Kumar et al., 2021). Of both treatments, succinylation was more effective in improving the techno-functionalities of modified oat protein, including its solubility, emulsification, gelation hardness, fat-binding capacity, and foaming properties (Mirmoghtadaie et al., 2009; Mohamed et al., 2009). The acetylation treatment showed improvement in the emulsification activity index of the native protein isolate (NPI) from 60.8 $m^2 g^{-1}$ protein to 76.2 $m^2 g^{-1}$ protein; however, it decreased the emulsion stability index of NPI from 29.0 min to 12.1 min (Mohamed et al., 2009; Spaen & Silva, 2021). Otherwise, these modifications still have legal issues related to the utilisation of succinic anhydride and acetic anhydride in food protein processing and other food safety concerns (Jiang et al., 2015; Zhang et al., 2015b). David (2011) mentioned the linoleate/potassium linoleate treatment's ability to modify the oat protein solubility at pH 4–7, in addition to its emulsifying capacity and stability. The potential factors of the aqueous environment affecting the oat protein functionality are the pH and

the ionic strength. In industrial operations, the addition of ionic salts (sodium chloride (NaCl) or sodium phosphate ($Na_2HPO_4$ / $NaH_2PO_4$)) or acidity regulators (dipotassium phosphate or trisodium citrate) in food formulations promote the protein solubility and the formation of firm gel with a smooth texture and good water-holding capacity (Li & Xiong, 2020; Vikenborg & Stensson, 2020). Chemical deamidation can be done by mild acid or alkaline treatment to increase the negative charge of the protein and lead to changes in its functionality (Mäkinen et al., 2017). The acidic deamidation is recognised to perform severe degradation to the protein which negatively affects some protein functionality and results in a bitter taste (Jiang et al., 2015).

Some physical modification methods were noticed to be effective in strengthening and altering oat protein techno-functionality. Glycation is a promising way for oat protein modification which is achieved by the Maillard reaction under controlled dry-heating conditions to enable the oat protein conjugation with several polysaccharides such as *Pleurotus ostreatus* $\beta$-glucan, inulin, and dextran (Zhang et al., 2015b; Boukid, 2021a). The conjugated form of isolated oat protein-$\beta$-glucan exhibits improved solubility, emulsifying capacity and thermo-stability compared to unconjugated oat protein (Boukid, 2021a). A promising industrial future for the conjugated protein-$\beta$-glucan form is in the $\beta$-carotene encapsulation process to increase its stability, bioavailability, and antioxidant activity (Zhong et al., 2019). The dextran-linked oat protein isolate had more effective emulsification properties than its native protein (Zhang et al., 2015b). The inulin associated oat protein-containing low concentration inulin (0.1–0.5%) resulted in strong oat protein gels formation at neutral pH (Nieto-Nieto et al., 2015). A novel physical method was described by Chen (2016) as an alternative gelling method for oat protein named cold-set gelation. This method consists of two steps; initially a heating step to enable proteins denaturation and then polymerization followed by a cooling and the addition of $Ca^{2+}$ or glucono- $\varepsilon$ -lactone (GDL), resulting in the formation of three-dimensional soluble protein aggregates (a gel network) at ambient temperature (Chen, 2016; Boukid, 2021a). The oat protein cold-set gel is characterised by its resistance to acidic juice and pepsin digestion, thereby protecting against both $\alpha$-amylase enzyme activity and the viability of probiotics in harsh gastric conditions, that is why it has the potential to be used as a delivery vehicle for sensitive compounds in food production (Boukid, 2021a). A stronge effect of the homogenisation process on oat protein functionality was observed by Vikenborg & Stensson (2020) and indicated improvement in the protein solubility from approximately 4% for the non-homogenised proteins to approximately 6% for the homogenised proteins. The investigation of the same study explained the solubility changes resulting from the effect of homogenization on decreasing the protein particle size to < 10 μm and disrupting the aggregates with their enabling to refold (Vikenborg & Stensson, 2020). Effect of homogenisation promoted the stability and solubility of oat protein concentrate, in parallel with the addition of the $\beta$-glucan extract, in the smoothie and the pudding products rich in protein and fibres (Vikenborg & Stensson, 2020). The physical deamidation of oat protein carried out by dry heating at 70 °C, for 2 h in an aqueous phase boosted some functional properties such as solubility, foaming capacity, and emulsifying activity and decreased the foaming stability and the emulsion stability (Mirmoghtadaie et al., 2009).

Currently, the modification category which is under investigation for oat protein modification includes enzymatic treatments. Studies have pointed out that enzymatic hydrolysis is a powerful tool to improve the techno-functionalities of oat protein fractions (Nieto-Nieto et al., 2014; Mäkinen et al., 2017). Studies were performed to evaluate the solubility and the gelling properties of oat protein treated with trypsin (Guan et al., 2007; Sargautis et al., 2021). The evaluations' results showed the formation of a weak gel structure and no change in functionality after the trypsin treatment due to the development of protein molecules with a small size that can no longer associate to form a strong gel matrix (Nieto-Nieto et al., 2014). Guan et al. (2007) mentioned that the harsh excessive enzymatic hydrolysis modification could impair the oat protein functionality. Nevertheless, limited enzymatic proteolysis can improve the functional properties of proteins by changing the molecular size, conformation, and strength of the inter-and intramolecular bonds of the protein molecules (Nieto-Nieto et al., 2014). Therefore, the proteolysis reaction must be carefully monitored and controlled in order to manufacture oat protein isolated products with desired functionality (Guan et al., 2007). For example, the effect of limited trypsin hydrolysis was cited by Spaen & Silva (2021), where the oat protein solubility at pH 5 increased from 7.3% in its native form into 68.2% in its trypsin-treated form with a degree of hydrolysis (DH) of 8.3%. In addition, the improved solubility of limited trypsin modified oat protein promoted improvement of the emulsifying activity index and the foaming ability (Guan et al., 2007). The same solubility observation at pH 4 was reported by Brückner-Gühmann et al. (2018). However, that the solubility of trypsin-treated oat protein was not improved at pH 7 was explained by the exposure of hydrophobic patches and subsequent protein-protein interactions and aggregation. Further inspection for the partial hydrolysis of oat protein isolate was carried out by alcalase which changed the native protein solubility at pH 4 from 17.6% without treatment to 50.3% with trypsin treatment (DH = 3%) (Spaen & Silva, 2021). Nieto-Nieto et al. (2014) reported that the partial enzymatic hydrolysis by trypsin or alcalase could improve the gelling properties of oat protein fractions by encouraging the gel formation from plant origin with similar properties to those from animal proteins such as egg white. Therefore, oat protein value increases in the industry as new plant gelling ingredients in food formulations such as meat binding and fat replacer or in meat analogues (Nieto-Nieto et al., 2014; Kumar et al., 2021). In the baking industry, partially hydrolysed OPI resulted in similar mechanical properties and water-holding capacity in wheat bread to that of egg white (Mäkinen et al., 2017). This could enable the use of OPI as a texturizing and structure-forming ingredient to replace animal protein in bakery products (Mäkinen et al., 2017).

A second enzymatic category to improve the oat protein functionality without causing severe hydrolysis is the oat protein deamidation with a food-grade commercial enzyme ‘protein-glutaminase’ (PG) that specifically catalyses the deamidation of the side chain amino group of protein-bound glutaminyl residues (Jiang et al., 2015; Immonen et al., 2021). The PG deamidation was able to double the protein water solubility compared to its native form (Jiang et al., 2015; Sargautis et al., 2021). Moreover, PG deamidated oat protein (59% deamidation degree) assisted the stability of the emulsion for longer than 30 days (Jiang et al., 2015). The transglutaminase, a protein cross-linking enzyme, can also induce deamidation with high enzyme to substrate ratios (Mohamed et al., 2009). The Transglutaminase mechanism catalyses the formation of an isopeptide

linkage between a glutamine and the amino group of protein-bound lysine (Mäkinen et al., 2017). The transglutaminase effectively increased protein solubility, foaming properties and emulsification (Boukid, 2021a). All the previous modifications aimed to change the oat protein fraction's surface properties to boost their techno-functionality and broaden their food industrial applications (dairy, meat, bakery, and their alternative products).

**Impact of oat protein modification methods on humans, animals and the environment**

The effect of oat protein modification methods may have important effects on human and animal health, in parallel to those on the environment. Due to the modification methods of oat proteins being understudied recently, their impact on humans, animals and the environment is only partially understood. It has been established that the chemical deamidation, acetylation and succinylation methods have drawbacks for human and animal health and may pollute the environment (Kutzli et al., 2021). The drawbacks of these modification methods are concerning problems with food-safety regulations arising from the requirement for various chemicals, which in some cases are toxic (Jiang et al., 2015; Kutzli et al., 2021). Mohamed et al. (2009) cited non-alteration in the nutritional value of the acylated oat proteins while its digestibility was significantly increased.

Oat and pea protein glycation significantly affect protein digestibility, which can be increased or reduced depending on the carbohydrate types and the conditions of protein glycation (Kutzli et al., 2021). The causative agents of coeliac disease(prolamins and glutelins) are very low in oat compared to other cereals (Rasane et al., 2015). However, enzymatic deamidation was reported to decrease the allergenicity of plant-based proteins, including the prolamins and glutelins (Nikbakht Nasrabadi et al., 2021). The most popular method for the oat protein modification is enzymatic treatment, particularly for incorporating the modified proteins in food production, since this process is environmentally friendly and less energy-consuming without the production of toxic by-products (Nikbakht Nasrabadi et al., 2021). In addition to the modulation of oat protein functionality, enzymatic treatment has the ability to improve the protein's nutritional quality including digestibility, bioavailability, and its biological activity such as antioxidant and antimicrobial properties (Nikbakht Nasrabadi et al., 2021; Sargautis et al., 2021). Tang et al. (2022) identified the formation of a new type of angiotensin-converting enzyme (ACE), an inhibitory peptide with strong antioxidant activity when the oat protein is hydrolysed by trypsin. The influence of the oat protein modification methods on different aspects are still not well known, which is why further detailed research needs to be carried out in the near future.

## CONCLUSIONS

In the framework of mapping new sources of alternative proteins of plant origin, the oat protein concentrates, and isolates have been shown to have a potential future in various food industries. Oat protein could be considered a good plant-derived protein source from its relatively superior amino acid and nutritional profiles compared with other cereal grains (wheat, barley, and rye). Moreover, the oat protein preparations possess good functional properties such as solubility, emulsification, foaming and

gelling properties, additionally to valued bioactivities. Noteworthily, native oat proteins present poor techno-functionality in most food products' typical production conditions, which restricts in its use in industrial food production. Therefore, several research studies have investigated the potential of diverse modification methods to improve the oat protein functionality and expand its industrial food incorporation. The common proposed modification categories include chemical, physical, and enzymatic treatments, where the enzymatic methods have been shown to be a powerful safe and environmentally friendly strategy to change the functionality and promote the oat protein as a novel nutritious plant protein source without the production of toxic by-products. More investigations are required to optimise the extraction methods of oat protein fractions from food by-products for their valorisation and promote their modification methods for boosting their quality to meet the food industry requirements.

ACKNOWLEDGEMENTS. This work was supported by the Estonian Ministry of Education and Research programme 'Support for research and development on resource valorisation' ResTA focus theme 'Food: Innovative valorisation of food and food ingredients' research project RESTA28 'Valorisation of cereal and oilseed crops' and by the project VALORTECH funded from the European Union's Horizon 2020 research and innovation programme under grant agreement No 810630.

## REFERENCES

Boukid, F. 2021a. Oat proteins as emerging ingredients for food formulation: where we stand? *European Food Research and Technology* **247**, 535–544. doi: 10.1007/s00217-020-03661-2

Boukid, F. 2021b. Plant-based meat analogues: from niche to mainstream. *European Food Research and Technology* **247**, 297–308. doi: 10.1007/s00217-020-03630-9

Brückner-Gühmann, M., Heiden-Hecht, T., Sözer, N. & Drusch, S. 2018. Foaming characteristics of oat protein and modification by partial hydrolysis. *European Food Research and Technology* **244**(12), 2095–2106. doi:10.1007/s00217-018-3118-0

Brückner-Gühmann, M., Vasil'eva, E., Culetu, A., Duta, D., Sözer, N. & Drusch, S. 2019a. Oat protein concentrate as alternative ingredient for non-dairy yoghurt-type product. *Journal of the Science of Food and Agriculture* **99**(13), 5852–5857. doi:10.1002/jsfa.9858

Brückner-Gühmann, M., Benthin, A. & Drusch, S. 2019b. Enrichment of yoghurt with oat protein fractions: Structure formation, textural properties and sensory evaluation. *Food Hydrocolloids* **86**, 146–153. doi.org/10.1016/j.foodhyd.2018.03.019

Cavazos, A., Gonzalez de Mejia, E. 2013. Identification of Bioactive Peptides from Cereal Storage Proteins and Their Potential Role in Prevention of Chronic Diseases. *Comprehensive Reviews in Food Science and Food Safety* **12**(4), 364–380. doi:10.1111/1541-4337.12017

Chen, L. 2016. Oat protein gels. US patent 2016/0309762A1.

David, M.P. 2011. Chapter 8 - Storage Proteins. In Francis, H.W. & Peter, J.W. (eds), *Oats: Chemistry and Technology, 2nd ed.* American Associate of Cereal Chemists International, St. Paul, Minnesota, 123–142.

Guan, X., Yao, H., Chen, Z., Shan, L. & Zhang, M. 2007. Some functional properties of oat bran protein concentrate modified by trypsin. *Food Chemistry* **101**(1), 163–170. doi:10.1016/j.foodchem.2006.01.011

Immonen, M., Myllyviita, J., Sontag-Strohm, T. & Myllärinen, P. 2021. Oat Protein Concentrates with Improved Solubility Produced by an Enzyme-Aided Ultrafiltration Extraction Method. *Foods* **10**(12), 1–15. doi: 10.3390/foods10123050

Jiang, Z.-q., Sontag-Strohm, T., Salovaara, H., Sibakov, J., Kanerva, P. & Loponen, J. 2015. Oat protein solubility and emulsion properties improved by enzymatic deamidation. *Journal of Cereal Science* **64**, 126–132. doi:10.1016/j.jcs.2015.04.010

Kruma, Z., Tomsone, L., Galoburda, R., Straumite, E., Kronberga, A. & Åssveen, M. 2016. Total phenols and antioxidant capacity of hull-less barley and hull-less oats. *Agronomy research* **14**(S2), 1361–1371.

Kruma, Z., Galoburda, R., Tomsone, L., Gramatina, I., Senhofa, S., Straumite, E., Klava, D., Kince, T., Cinkmanis, I., Zagorska, J. & Kunkulberga, D. 2018. Changes in the nutritional value of breakfast cereals containing germinated spring grain flakes during storage. *Agronomy Research* **16**(S2), 1405–1416. doi.org/10.15159/AR.18.130

Kumar, L., Sehrawat, R. & Kong, Y. 2021. Oat proteins: A perspective on functional properties. *LWT - Food Science and Technology* **152**(3), 1–9. doi:10.1016/j.lwt.2021.112307

Kutzli, I., Weiss, J. & Gibis, M. 2021. Glycation of Plant Proteins Via Maillard Reaction: Reaction Chemistry, Technofunctional Properties, and Potential Food Application. *Foods* **10**(2), 376–416. doi:10.3390/foods10020376

Li, R. & Xiong, Y.L. 2020. Sensitivity of oat protein solubility to changing ionic strength and pH. *Journal of Food Science* **86**(1), 78–85. doi:10.1111/1750-3841.15544

Ma, C.-Y., Rout, M.K., Chan, W.-M. & Phillips, D.L. 2000. Raman Spectroscopic Study of Oat Globulin Conformation. *J. Agric. Food Chem* **48**(5), 1542–1547. doi:10.1021/jf991222n

Mäkinen, O.E., Sozer, N., Ercili-Cura, D. & Poutanen, K. 2017. Chapter 6 - Protein From Oat: Structure, Processes, Functionality, and Nutrition. In Sudarshan, R.N., Wanasundara, J.P.D. & Scanlin, L. (eds), *Sustainable Protein Sources, 1st ed.* Academic press, Elsevier, London-San Diego-Cambridge-Kidlington, United Kingdom-United States, 105–119.

Mirmoghtadaie, L., Kadivar, M. & Shahedi, M. 2009. Effects of succinylation and deamidation on functional properties of oat protein isolate. *Food Chemistry* **114**(1), 127–131. doi:10.1016/j.foodchem.2008.09.025

Mogensen, L., Heusale, H., Sinkko, T., Poutanen, K., Sözer, N., Hermansen, J.E. & Knudsen, M.T. 2020. Potential to reduce GHG emissions and land use by substituting animal-based proteins by foods containing oat protein concentrate. *Journal of Cleaner Production* **274**, 1–9. doi:10.1016/j.jclepro.2020.122914

Mohamed, A., Biresaw, G., Xu, J., Hojilla-Evangelista, M.P. & Rayas-Duarte, P. 2009. Oats protein isolate: Thermal, rheological, surface and functional properties. *Food Research International* **42**(1), 107–114. doi: 10.1016/j.foodres.2008.10.011

Nieto-Nieto, T.V., Wang, Y.X., Ozimek, L. & Chen, L. 2014. Effects of partial hydrolysis on structure and gelling properties of oat globular proteins. *Food Research International* **55**, 418–425. doi:10.1016/j.foodres.2013.11.038

Nieto-Nieto, T.V., Wang, Y.X., Ozimek, L. & Chen, L. 2015. Inulin at low concentrations significantly improves the gelling properties of oat protein – A molecular mechanism study. *Food Hydrocolloids* **50**, 116–127. doi:10.1016/j.foodhyd.2015.03.031

Nikbakht Nasrabadi, M., Sedaghat Doost, A. & Mezzenga, R. 2021. Modification approaches of plant-based proteins to improve their techno-functionality and use in food products. *Food Hydrocolloids* **118**, 1–23. doi:10.1016/j.foodhyd.2021.106789

Ramírez Fuentes, L., Richard, C. & Chen, L. 2021. Sequential alcalase and flavourzyme treatment for preparation of α-amylase, α-glucosidase, and dipeptidyl peptidase (DPP)-IV inhibitory peptides from oat protein. *Journal of Functional Foods* **87**, 1–10. doi.org/10.1016/j.jff.2021.104829

Rasane, P., Jha, A., Sabikhi, L., Kumar, A. & Unnikrishnan, V.S. 2015. Nutritional advantages of oats and opportunities for its processing as value added foods - a review. *Journal of Food Science and Technology* **52**(2), 662–675. doi:10.1007/s13197-013-1072-1

Research and markets. 2019. Oat Protein Market—Growth, Trends and Forecasts (2019–2024). https://www.researchandmarkets.com/reports/4622348/oat-protein-market-growth-trends-and-forecasts.

Sánchez-Velázquez, O.A., Cuevas-Rodríguez, E.O., Mondor, M., Ribéreau, S., Arcand, Y., Mackie, A. & Hernández-Álvarez, A.J. 2021. Impact of in vitro gastrointestinal digestion on peptide profile and bioactivity of cooked and non-cooked oat protein concentrates. *Current Research in Food Science* **4**, 93–104. doi:10.1016/j.crfs.2021.02.003

Sargautis, D., Kince, T. & Sargautiene, V. 2021. Review: current trends in oat protein recovery and utilization in aqueous food systems. In Treija, S. & Skujeniece, S. (eds): *proceedings of the annual 27th International scientific conference on Research for Rural Development 2021*. Latvia University of Life Sciences and Technologies, Jelgava, Latvia, pp. 77–83. doi: 10.22616/rrd.27.2021.011

Spaen, J. & Silva, J.V.C. 2021. Oat proteins: Review of extraction methods and techno-functionality for liquid and semi-solid applications. *LWT - Food Science and Technology* **147**, 1–8. doi:10.1016/j.lwt.2021.111478

Sterna, V., Zute, S. & Brunava, L. 2016. Oat Grain Composition and its Nutrition Benefice. *Agriculture and Agricultural Science Procedia* **8**, 252–256. doi:10.1016/j.aaspro.2016.02.100

Sterna, V., Zute, S., Jansone, I., Ence, E. & Strausa, E. 2020. Evaluation of various legume species and varieties grown in Latvia as a raw material of plant-based protein products. *Agronomy Research* **18**(4), 2602–2612. doi.org/10.15159/AR.20.215

Tang, Y., Li, S., Yan, J., Peng, Y., Weng, W., Yao, X., Gao, A., Cheng, J., Ruan, J. & Xu, B. 2022. Bioactive Components and Health Functions of Oat. *Food Reviews International* **38**, 1–20. doi.org/10.1080/87559129.2022.2029477

Vikenborg, C. & Stensson, F. 2020. *Functionality of oat based food ingredients*. Master's thesis degree of Food Technology, department of Food Technology, Engineering and Nutrition, Lund University in cooperation with Lantmännen, Lund, Sweden, 90 pp.

Zhang, H. & Wang, J. 2015a. Peptides Derived from Oats Improve Insulin Sensitivity and Lower Blood Glucose in Streptozotocin-Induced Diabetic Mice. *Journal of Biomedical Sciences* **4**(1), 1–7. doi:10.4172/2254-609x.100007

Zhang, B., Guo, X., Zhu, K., Peng, W. & Zhou, H. 2015b. Improvement of emulsifying properties of oat protein isolate–dextran conjugates by glycation. *Carbohydrate Polymers* **127**, 168–175. doi: 10.1016/j.carbpol.2015.03.072

Zhang, Y., Sharan, S., Rinnan, Å. & Orlien, V. 2021. Survey on Methods for Investigating Protein Functionality and Related Molecular Characteristics. *Foods* **10**(11), 1–18. doi: 10.3390/foods10112848

Zhong, L., Ma, N., Wu, Y., Zhao, L., Ma, G., Pei, F. & Hu, Q. 2019. Gastrointestinal fate and antioxidation of *β*-carotene emulsion prepared by oat protein isolate-Pleurotus ostreatus *β*-glucan conjugate. *Carbohydrate Polymers* **221**, 10–20. doi: 10.1016/j.carbpol.2019.05.085

*Agronomy Research* **20**(1), 174–187, 2022
https://doi.org/10.15159/AR.22.002

# Bonding performance of wood of fast-growing tree species eucalyptus (*Eucalyptus grandis*) and radiata pine (*Pinus radiata* D. Don) with polyvinyl acetate and emulsion polymer isocyanate adhesives

J. Iejavs[1,*], K. Šķēle[1], E. Grants[1] and A. Uzuls[2]

[1]Forest and Wood Products Research and Development Institute, Dobeles iela 41, LV–3001 Jelgava, Latvia
[2]'Kokpārstrāde 98' Ltd., 'Dižkoki', Allažu pagasts, Siguldas novads, LV–2154, Latvia
[*]Correspondence: janis.iejavs@e–koks.lv

Received: July 11th, 2021; Accepted: December 5th, 2021; Published: January 25th, 2022

**Abstract.** Fast-growing imported plantation tree species have become an available wood resource for Europe's wood industry in the last decades. This sustainable alternative may reduce the gap between the increasing demand for and decreasing supply of the local tree species. The aim of the study was to evaluate the performance of eucalyptus (*Eucalyptus grandis*) and radiata pine (*Pinus radiata* D. Don) wood in face-bonding with polyvinyl acetate (PVAc) and emulsion polymer isocyanate (EPI) adhesive for the production of non-structural semi-finished glued laminated timber members for window manufacturing. Test specimen preparation and testing were performed according to European standards. Tensile shear strength and wood failure percentages were determined as bonding performance indicators for 3 adhesives and 3 selected bonding parameters (pressure, pressing time and adhesive spread) in 27 variations after boiling the specimens in water. According to the results, the bonding variables influence the glue-line tensile shear strength and wood failure percentages. Bonding pressure and pressing time were evaluated as the most significant factors influencing shear strength of bonded joints. For all bonding variations the average level of shear strength from 3.45 to 5.23 MPa were reached for PVAc adhesive and from 3.78 to 9.65 MPa for EPI adhesives. Both EPI adhesives provide higher performance compared to PVAc adhesive. In the case of bonding fast-growing tree species, the highest shear strength values were achieved using the lowest pressure of 0.8 MPa, adhesive spread from 150 to 180 g $m^{-2}$ and longest pressing time of 40 min. Based on the general evaluation of the results, it can be stated that the wood of eucalyptus and radiata pine bonded with both EPI adhesives presents great potential for non-structural semi-finished glued laminated timber member production, especially for the use in humid conditions.

**Key words:** bonding, EPI, *Eucalyptus grandis*, fast-growing wood, *Pinus radiata* D. Don, PVAc.

## INTRODUCTION

Fast-growing imported plantation tree species have become an available wood resource for the European wood industry. Two tree species - eucalyptus (*Eucalyptus grandis*) and radiata pine (*Pinus radiata* D. Don) are at the top of the list in this respect.

These sustainable alternatives may replace some of the local tree species for the production of wooden windows and structural elements (Liao et al., 2017).

Radiata pine (*Pinus radiata* D. Don*)* is the most widely spread commercial forestry fast-growing tree species covering an estimated 1.8 million ha in New Zealand (Palmer et al., 2010) where its rotation period is 28 years for sawlog production and the annual growth rate is evaluated at 17 $m^3$ $ha^{-1}$ $year^{-1}$ (Cubbage et al., 2010). In total, 13.7 million $m^{-3}$ of radiata pine pulpwood and sawn timber were exported from New Zealand in 2011 (Ministry of Primary Industries, 2020).

Eucalyptus is one of the fastest growing tree species in the world and the most commonly planted forest species in Uruguay (over 0.25 million ha) (Rachid–Casnati et al., 2019). Its rotation period is 16 years for sawlog production and the annual growth rate is evaluated at 30 $m^3$ $ha^{-1}$ $year^{-1}$ in Uruguay (Cubbage et al., 2010) and up till 50 $m^3$ $ha^{-1}$ $year^{-1}$ in Turkey (Gürses et al., 1995). The availability of eucalyptus sawn timber is evaluated at 0.7 million $m^{-3}$ according to Dieste et al. (2019).

Physical and mechanical properties of eucalyptus and radiata pine wood differ significantly depending on the growth region and growth conditions. The majority of radiata pine wood properties do not differ significantly from Scots pine (*Pinus sylvestris* L.) properties but some of mechanical properties of eucalyptus even exceed the properties of the common European oak (*Quercus robur*) which is a conventional species for manufacturing wood windows in Europe (Iejavs et al., 2021). Good shape, acceptable price, mechanical properties and high growth rate of fast-growing plantation wood species Eucalyptus and Radiata pine make them an ideal choice for local wood species substitution in Europe (Iejavs et al., 2018).

The declining availability and decrease in the quality of wood resources significantly increase the importance of wood bonding in the woodworking industry in Europe. The strength of the glued joint is of crucial importance in the production of glued wood products; therefore, special attention should be paid to the process of manufacturing the glued joint and the selection of appropriate bonding technological parameters. Glued joints should be compatible with environmental conditions to which the wooden structure will be subjected during its service life (Pereira et al., 2016).

Polyvinyl acetate (PVAc) is one of the most common adhesives used in non-structural applications. PVAc is capable of producing strong and durable bonds on both hardwoods and softwoods. However, PVAc adhesives are not generally recommended for joints under continuous load or those subjected to high temperature and/or high humidity (Jokerst, 1981; Vassiliou et al., 2006).

Emulsion Polymer isocyanate adhesive (EPI) is a two-component adhesive that combines an emulsion component and an isocyanate functional cross-linking componet. The glue line is cold curing, it has high flexibility, low creep, contains no formaldehyde and provides excellent water resistance in both cold and boiling water. EPI systems have very good adhesion to wood and metal and glues difficult wood species. EPI adhesive systems have been used since the early 1970s in Japan but the first EPI adhesive was approved for structural glued laminated timber production in Europe only in 2005 (Grøstad & Bredesen, 2014), therefore there is a lack of information about the EPI adhesive performance for non-structural glued laminated timber production, especially for fast-growing plantation wood species.

The choice of optimal bonding parameters is crucial to obtain an appropriate bonding strength of the joint. Too low of bonding pressure does not ensure the mechanical

penetration of the glue into the wood, which forms mechanical adhesion, but too high of a pressure leads to a thin bond line, which reduces the cohesion strength of the bond line (Vick, 1999; Tienne et al., 2008). Pressing time plays an important role in the process of bonding to provide the necessary mechanical strength of the glued joint (Vick, 1999; Mölleken et al., 2016). The pressing time should be as short as possible to reduce the production time of glued products. The increase of adhesive spread can significantly increase the strength of the glued joint (Vick, 1999; Follrich et al., 2010; Fonte & Trianoski, 2015), but the economical aspect of the adhesive losses during at the bonding process should be taken into consideration. Surface preperation before bonding (sawing, planing and sanding) has a significant effect on the final bond strength. Both closed and open assembling time during the bonding process affects the bonding quality, especially when 2 component EPI adhesives are used with very short open assembling time (Pitzner & Lind, 2005). In general, the increase in wood surface roughness significantly reduces the strength of bonded joints (Vick, 1999; Iždinský et al., 2021), but under certain specific conditions the surface roughness increases the bondig area, resulting in the increased shear strength of the bonded joint (Follrich et al., 2010).

Wood moisture content during the bonding process and the end use conditions affect the bond strength. According to Bomba et al. (2014), for PVAc adhesive and beech wood (*Fagus sylvatica* L.) shear strength of the joint decreases by 37% if wood with moisture content of 20% is bonded instead of 8%. Test specimen immersion in water for 24 hours decreases shear strength of joint by 87% for PVAc adhesive.

The temperature of the environoment and the wood during the bonding process affect the strength of solid wood and wood joints. Wood joints with PVAc and EPI adhesives are more sensitive to temperature decrease from 20 °C to -20 °C compared to PUR and PRF (phenol-resorcinol-formaldehyde adhesive) (Pitzner & Lind, 2005; Wang et al., 2015). A significant decrease in timber bending strength of fingerjointed aspen (*Populus tremula* L.) was observed for PVAc adhesive when wood temperature increased from 20 °C to 100 °C (Iejavs et al., 2018).

The strength of thermoplastic PVAc and EPI adhesive joints is most significanly influenced by the combined effect of incresed temperatures and humidity, reducing the shear strength by 88% (Bomba et al., 2014). Such specimen pretreatment is provided by standard LVS EN 204 (2016) conditioning sequence 5. According to Iwakiri et al. (2019) shear strength results of bonded eycalyptus wood species, after humid pretreatment, were not found in the literature.

Limited or inconsistent information is available on bonding fast growing imported plantation wood species, especially with EPI adhesives (Calil Neto, 2010; Calil Neto et al., 2016) in contrast to conventional wood species such as Beech (*Fagus sylvatica* L.), Scots pine (*Pinus sylvestris* L.) and Spruce (*Picea abies* L.), which have been frequently investigated and used industrially in Europe (Pitzner & Lind, 2005; Vassiliou et al., 2006; Bomba et al., 2014; Wang et al., 2015; Konnerth et al., 2016). The determination of the optimal bonding parameters of fast growing wood species allows us to choose appropriate adhesives and bonding regimes for industrial manufacturing of wooden window blanks and other non-structural wood products with PVAc and EPI adhesives.

Therefore, the main goal of the study was to find the correlation between changing bonding parameters of polyvinyl acetate (PVAc) and emulsion polymer isocyanate (EPI) adhesives and the degree of shear strength of the glued fast-growing imported plantation

timber species eucalyptus (*Eucalyptus grandis*) and radiata pine (*Pinus radiata* D. Don) wood after boiling pre-treatment.

## MATERIALS AND METHODS

### Wood

For this study the wood of two fast-growing plantation tree species eucalyptus (*Eucalyptus grandis*) from Uruguay ('Rivera' Department) and radiata pine (*Pinus radiata* D. Don) from New Zealand ('Taupo' region) was used. The raw material was kiln dried sawn timber (moisture content = 12 ± 3%) with nominal cross section dimensions of 35x150 mm and a length of 4 m. A total of 30 straight grained, defect free boards were randomly selected from both wood species with an angle between the growth rings and the surface between 30° to 90° to prepare test specimens according to standard LVS EN 205 (2016). After the timber delivery, all boards were conditioned to a constant mass in a standard atmosphere (air temperature 20 ± 2 °C; air humidity 65 ± 2%). The average moisture content after the conditioning of timber was 12.0% for eucalyptus and 12.7% for radiata pine. The corresponding average density was 588 kg $m^{-3}$ for eucalyptus and 504 kg $m^{-3}$ for radiata pine. Other physical and mechanical properties of timber used in the study are presented in the literature (Iejavs et al., 2021).

### Adhesives and bonding parameters

Three different adhesives were used in this study to assess their ability to bond fast-growing wood species in face bonding: a one-component cross-linking polyvinyl acetate emulsion (PVAc) Dynea Prefere 6415 and 2 two-component emulsion polymer isocyanate adhesives (EPI–1) Dynea Prefere 6151 with hardener 6651 and (EPI-2) Dynea Prefere 6170 with hardener 6670. All materials and adhesives for this study were kindly provided by 'Kokpārstrāde 98' Ltd. The technical data of the adhesives are presented in Table 1.

**Table 1.** Technical data of the adhesives

| Characteristics | Adhesive codes | | | | |
|---|---|---|---|---|---|
| | PVAc | EPI–1 | | EPI–2 | |
| | | adhesive | hardener | adhesive | hardener |
| Commercial name | Prefere 6415 | Prefere 6151 | Prefere 6651 | Prefere 6170 | Prefere 6670 |
| Adhesive type | PVAc | EPI | | EPI | |
| Durability class LVS EN 204 (2016) | D4 | D4 | | D4 | |
| Appearance | white, viscous liquid | white, viscous liquid | brown liquid | milky-white liquid | brown liquid |
| No. of components | 1 | 2 | | 2 | |
| Viscosity at 23 °C, mPa $s^{-1}$ | 6,500–8,500 | 6,000–10,000 | 250–400 | 5,000–6,000 | 200 |
| Density, kg $m^{-3}$ | 1,100 | 1,260 | 1,240 | – | – |
| pH | 2.5–3.5 | 6.5–8.5 | – | 6.4–8.4 | – |
| Solid content, % | 49–52 | 59–61 | – | 56–60 | – |
| Glue spread, g $m^{-2}$ | 100–250 | 175–400 | | 120–250 | |
| Pressure, MPa | 0.5–1.2 | 0.6–1.2 | | 0.7–1.6 | |
| Minimal pressing time, min | 15–35 | 10–30 | | 15 | |
| Wood moisture content, % | – | 6–15 | | 6–15 | |
| Mixing ratio | – | 100 | 15 | 100 | 15 |

From each of the boards several pairs of panels were prepared with nominal dimensions of 7×130×350 mm to bond 2 fast-growing wood species with 3 different adhesives. Shortly before bonding, all the surfaces to be bonded were lightly planed to obtain panels with a nominal thickness of 5 mm.

In total, a full factorial design (3×3×3) with 27 bonding parameter combinations (pressure 0.8, 1.0 and 1.2 MPa, pressing time 20, 30 and 40 min and adhesive spread 150, 180 and 210 g $m^{-2}$) were used in the study for each species and adhesive combination. For both EPI adhesives, the adhesive and hardener were mixed in a ratio of 100:15 (based on the weight percentage). The adhesive was applied on one side of the panel using a hand roller and the glue spread was controlled by a weighing method (Fig. 1, a). Pressing was done with the 1,500 kN press 'Joos' LAP 150 (Fig. 1, b). Maximum open assembling time was 1 min, and maximum close assembling time was 5 min in all cases.

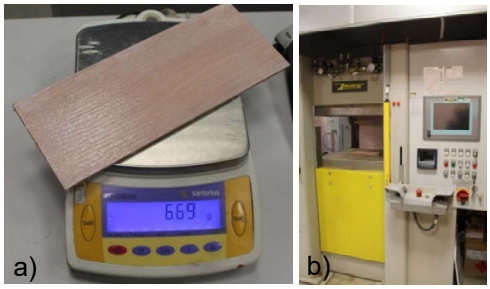


**Figure 1.** Adhesive spread control (a) and panel pressing (b).

**Test specimens and pre-treatment**

The cutting of test pieces was done 7 days after specimen pressing and keeping in standard atmosphere. Each bonded panel with definite bonding parameters was cut into 10 test specimens with nominal dimensions of 20×150 mm. The final thickness was 10 mm. Flat bottomed cuts 2.5 mm wide in the bonded section across the grain were made completely through the bond line, so that the overlap of length was 10 mm. The final shear area of the test pieces was 10×20 mm. In total, for 2 wood species, 3 adhesives and 27 bonding parameter combinations 1,620 specimens were produced and tested. As a reference, 20 solid wood specimens of eucalyptus and radiata pine were produced and tested in the same manner as for glued specimens, with the exception of panel bonding, to compare the results with the solid timber shear strength. Test specimen dimension, test arrangement according to LVS EN 205 (2016) and a graphic of shear strength results for one set of 10 test specimens are presented in Fig. 2.

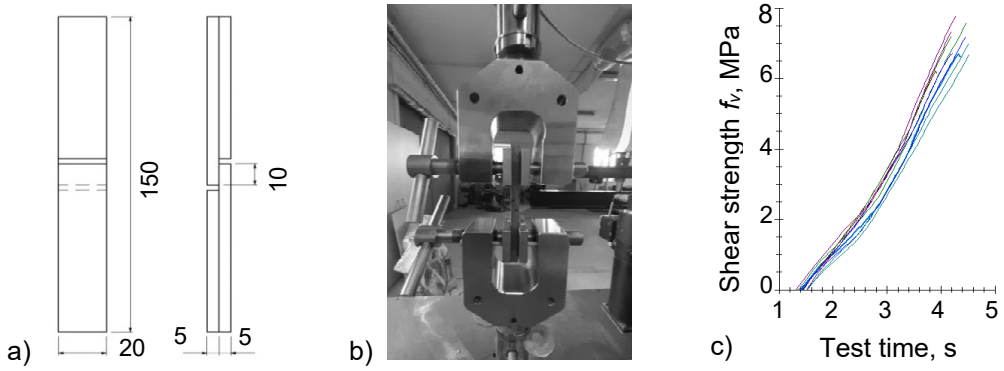


**Figure 2.** Test specimen dimensions in mm (a), tensile shear test arrangement (b) and the graphic example of 10 test specimens set shears strength results (c).

Each bonded specimen was marked with: wood species symbol G – for eucalyptus and R – for radiata pine; followed by adhesive symbol 64 (for PVAc adhesive 6415), 61 (for EPI–1 adhesive Prefere 6151/6651) and 617 (for EPI–2 adhesive Prefere 6170/6670), pressure symbol 0.8, 1.0 or 1.2 MPa; adhesive spread symbol 150, 180 or 210 g $m^{-2}$ pressing time symbol 20, 30 or 40 min; and specimen No. from 1 to 10 within each bonded panel.

The following pre-treatment was applied to all specimens keeping them for 7 days in a standard atmosphere; 6 h in boiling water and 2 h in water at 20 °C before testing according to LVS EN 204 (2016) sequence 5. This pre-treatment is part of a procedure to determine the shear strength of adhesives for durability class D4 (for exposure to running or condensed water in the interior or for exterior use exposed to weather with an adequate surface coating).

**Test procedure and evaluation**

The test was carried out according to standard LVS EN 205 (2016) p. 6.5. procedure with Zwick Z100 test machine to determine tensile shear strength and an extra parameter - wood failure percentage *Wf*. Test speed 50 mm $min^{-1}$ was used for all mechanical tests. The target average shear strength $f_v$ of bond line should be equal or greater than 4 MPa according to the standard LVS EN 204 (2016). *Wf* was evaluated as suggested in standard LVS EN 314–1 (2005) with a 25% step and was as follows: 0%; 25%; 50%, 75% or 100% for individual specimens. Individual and average shear strength and *Wf* values were determined in 10 test specimens for each bonded panel. An example of *Wf* failure mode is presented in Fig. 3.

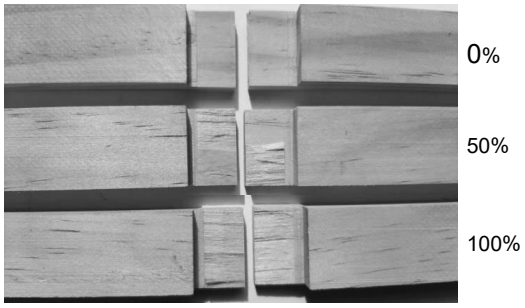


**Figure 3.** Wood failure percentage examples with wood failure 0%, 50% and 100%.

The results were analysed using programme 'R' version 4.1.0. Tukey *HSD* test at 5% significance level was performed to determine the difference between the grand average of shear strength (average between all bonding regimes within the wood species and adhesive combination) between adhesives. The average shear strength between bonding regimes (adhesive spread, pressing pressure and pressing time) was compared with pairwise *t*–test with 'Bonferroni' adjusted *p*–values with 95% confidence level. Analysis of variance (ANOVA) with interaction effects was used to identify the most significant factors and interaction effects influencing bonded joint shear strength. Due to the properties of wood failure percentage data (lack of normal distribution) no statistical analysis of these data was carried out.

## RESULTS AND DISCUSSION

Both wood species with full factorial analysis of 3 adhesives and 3 selected bonding parameter combinations (pressure, pressing time and adhesive spread) in 27 variations provide a certain level of *fv*. Bonded joint failure during the specimen boiling procedure

was not observed. The results of the study are presented in Fig. 4 for eucalyptus and in Fig. 5 for radiata pine. The average values of *fv* and standard deviation *SD* as the average wood failure percentage *Wf* are given for each adhesive and bonding regime. All tests were carried out in wet condition of the specimens. The target *fv* value for each species, adhesive and bonding parameter combination was ≥ 4 MPa according to standard LVS EN 204 (2016).

**Shear strength of solid timber**

The shear strength of 20 solid wood samples was also determined in the same manner as for glued samples for comparison. The results were as follows: the mean $f_v$ was 8.40 MPa (standard deviation *SD* 1.25 MPa) for eucalyptus wood and 5.83 MPa (*SD* 1.08 MPa) for radiata pine.

**Shear strength and wood failure percentage of bonded eucalyptus wood**

The average values of *fv* for bonded eucalyptus wood varied from 3.45 MPa with PVAc adhesive (bonding pressure *P* – 1.2 MPa; adhesive spread *S* – 150 g $m^{-2}$ and pressing time *T* – 20 min) to 9.65 MPa with EPI–1 (*P* – 0.8 MPa; *S* – 150 g $m^{-2}$ and *T* – 40 min) according to Figure 4. The highest value 9.65 MPa for EPI–1 adhesive was significantly higher ($p < 0.05$) compared to other adhesives and bonding parameter combinations. The shear strength of the bonded joint even exceeds *fv* of solid timber by 15%. This can be explained by the difference between the average solid timber and individual bonded panel density. The average density of eucalyptus was 588 kg $m^{-3}$ but maximum reached 738 kg $m^{-3}$ with a 25% difference (Iejavs et al., 2021). The next highest result for EPI–1 adhesive was 8.68 MPa obtained with the same pressure and bonding time, but with an increased adhesive spread to 210 g $m^{-2}$. Similar shear strength results from 4.94 MPa to 8.07 MPa were obtained by Iwakiri et al. (2019) after the immersion of specimens for 24 h in water for 2 eucalyptus wood species (*Eucalyptus camaldulensis*, *Eucalyptus urophylla*) bonded with PVAc and EPI adhesives. According to Iwakiri et al. (2014) the adhesive spread used industrially for face bonding varies from 180 to 220 g $m^{-2}$.

From 27 bonding regimes in bonding eucalyptus wood with PVAc adhesive, 11 bonding regimes did not reach the average target shear strength value of 4 MPa according to LVS EN 204 (2016). Both EPI adhesives within all bonding regimes exceeded that of 4 MPa threshold value.

Statistically significant differences ($p < 0.05$) were found between the grand average *fv* between all adhesives used (Fig. 4). EPI–1 adhesive *fv* was significantly higher than for EPI–2 and PVAc. Accordingly, EPI–2 adhesive provides significantly higher *fv* compared to PVAc adhesive. The same tendencies can be observed for *Wf* data. *Wf* values vary within great amplitude between each wood species and adhesive combination. The highest values for eucalyptus were observed for EPI–1 and the lowest for PVAc adhesive. For 13 gluing parameter combination of 27, the lowest average *Wf* 0% was observed for PVAc adhesive and the highest for EPI–1 in 4 cases reaching *Wf* from 95 to 98%. A significant decrease in both *fv* and *Wf* values was observed for wet specimens (24 h immersion in water) compared to the dry (after air conditioning) specimens when several eucalyptus species were bonded with PVAc and EPI adhesives as described by Iwakiri et al. (2019) and when 13 hardwood species were bonded with PVAc adhesive by Iždinský et al. (2021).

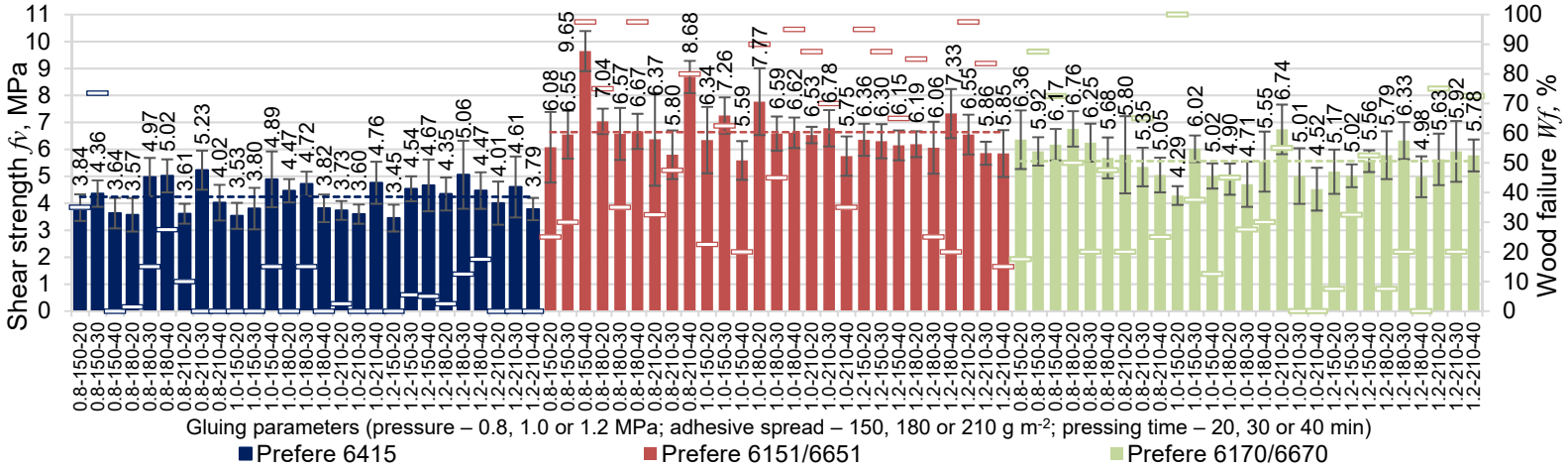


**Figure 4.** Average shear strength and wood failure percentage of bonded eucalyptus wood joints with three adhesives.

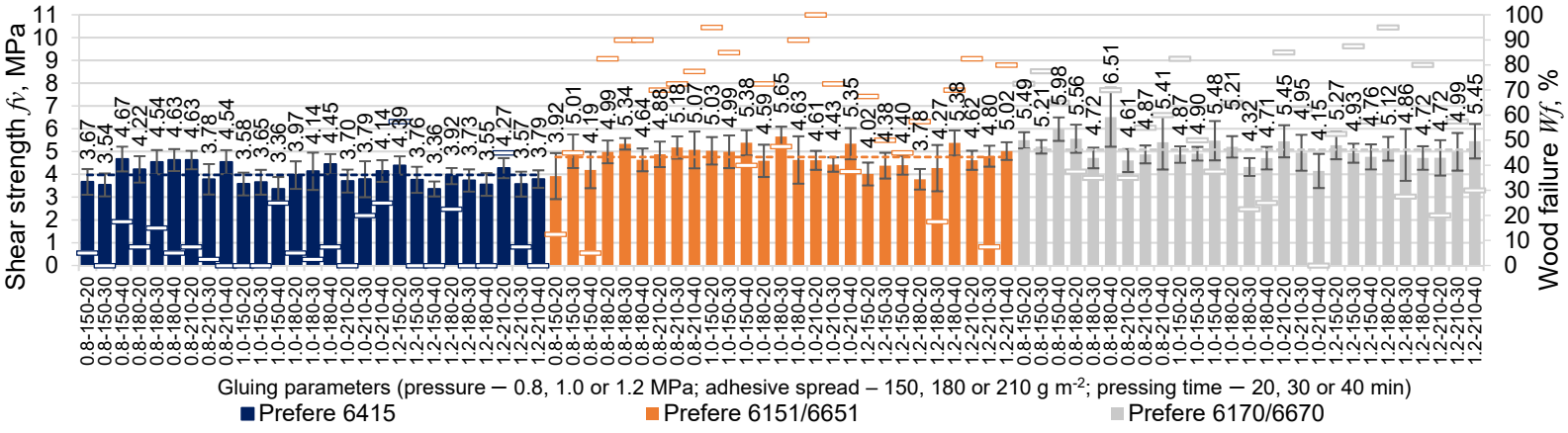


**Figure 5.** Average shear strength and wood failure percentage of bonded radiata pine wood joints with three adhesive.

This study confirmed the superiority of both EPI adhesives over PVAc adhesives, when testing eucalyptus wood in wet conditions. Previously the same conclusion was reported by Iwakiri et al. (2019). The differences in shear strength found for EPI and PVAc adhesives were attributed to their different penetration ability resulting from their chemical structures as well as their physicochemical characteristics such as rheological properties. The bonding of the wood is complex manufacturing process where majority of bonding parameters and timber characteristics matters. Usually umber joints should be kept under certain pressure and time period until they have enough strength to withstand handling stresses that tend to separate the pieces of wood.

The EPI adhesives used in the study compared to lower curing reactivity PVAc adhesive are designed so that the added hardener minimizes the time required for pressing the samples, as a result of which sufficient mechanical strength of the joint is achieved already during short 20 min pressing, but with increased pressing time of 40 min adhesives continues currying reaction with lower speed, which significantly improves the mechanical strength of the joint, especially, it can be seen with 0.8 MPa pressing pressure.

According to Vick (1999) time for cold pressing of lumber can be little as 15 min or as long as 24 h, depending on the temperature of the room and the wood, the curing characteristics of the adhesive, and the thickness, density, and absorptive characteristics of the wood.

The bonding performance between eucalyptus and EPI adhesive 6151/6651 was affected by bonding pressure ($p < 0.05$) and pressing time ($p < 0.05$). The adhesive spread ($p = 0.17$) had insignificant effects for a single bonding parameter. The interaction between bonding pressure and pressing time most significantly influences the shear strength of bonded joint ($p < 0.05$) according to Fig. 6a. No significant effect between other bonding parameters was observed.

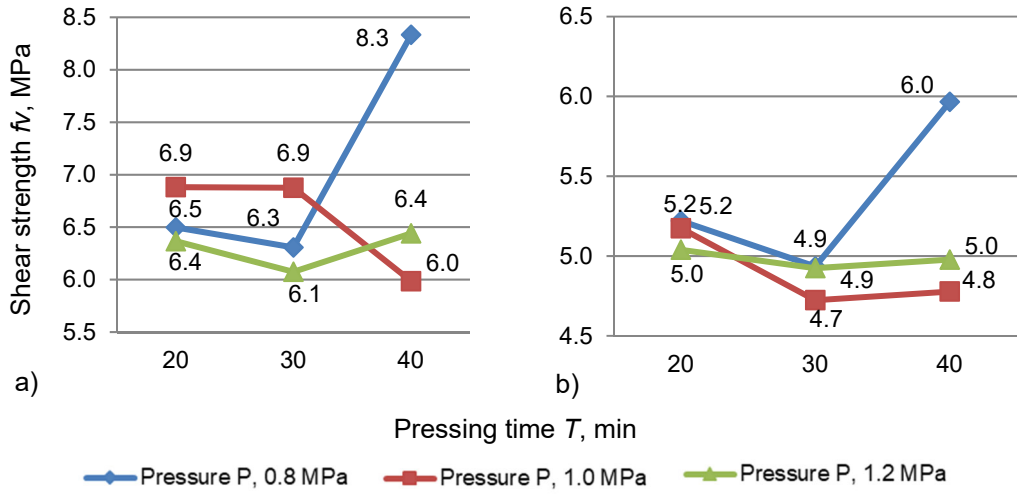


**Figure 6.** The influence of pressing time $T$ and bonding pressure $P$ interaction on the shear strength of: a – eucalyptus wood bonded with EPI–1 adhesive and b – radiata pine wood bonded with EPI–2 adhesive.

Boding pressure *P* 0.8 MPa and 1.2 MPa interacted with pressing time *T* 20 and 30 min showed an insignificant ($p = 0.52–0.09$) decrease in bond line *fv* of eucalyptus wood according to Fig. 6a. The most significant increase ($p < 0.05$) in *fv* was observed for *P* 0.8 MPa and *T* 40 min when *fv* 8.3 MPa was observed. For *P* 1.2 MPa the increase in *T* from 30 to 40 min did not influence *fv* significantly ($p = 0.11$). For *P* 1.0 MPa the same average *fv* values were observed for T 20 and 30 min, but a significant decrease ($p < 0.05$) was observed when *T* 40 min was used for bonding of specimens. No significant effects between other bonding parameters were observed.

The relationship between adhesive consistency and bonding pressure strongly affects adhesive wetting, flow, and penetration, particularly the transfer of adhesive to an unspread wood surface, when pressure is applied to the assembly. Since in the study the highest shear strength values of the joint with EPI adhesives was reached with relatively low bonding pressure of 0.8 MPa, it means, that pressure is optimal: to entrap the air from the joint, to brings adhesive into molecular contact with the wood surface; to form the optimal thickness adhesive film and holds the assembly in position while the adhesive cures. When pressure is too high, the adhesive can overpenetrate porous wood and cause starved joints that are inferior in bond strength (Vick, 1999).

**Shear strength and wood failure percentage of bonded radiata pine wood**

The average values of *fv* for bonded radiata pine wood varied from 3.36 MPa with PVAc adhesive (*P* – 1.0 MPa; *S* – 150 g $m^{-2}$ and *T* – 40 min) to 6.51 MPa with EPI–2 (*P* – 0.8 MPa; *S* – 150 g $m^{-2}$ and *T* – 40 min) according to Fig. 5. The obtained shear strength values of radiata pine wood are comparable with values of *Pinus Teada* wood (3.36 to 5.36 MPa) bonded with PVA adhesive according to Endo et al. (2017).

The value 6.51.MPa and corresponding bonding regime for EPI–2 adhesive provide a significantly ($p < 0.05$) higher *fv* value compared to the 20 bonding regimes, but *fv* of 6 regimes did not differ significantly ($p = 0.2–1.0$). For example, the bonding regime: *P* – 0.8 MPa, *S* – 150 g $m^{-2}$, *T* – 40 min provided 5.98 MPa average *fv* value and *P* – 0.8 MPa, *S* – 180 g $m^{-2}$, *T* – 40 min provided 5.98 MPa. EPI–1 adhesive with bonding regime *P* – 1.0 MPa, *S* – 180 g $m^{-2}$, *T* – 30 min provided comparable ($p = 0.06$) *fv* result 5.65 MPa to the highest value of EPI–2 adhesive. In all other cases the results are significantly lower ($p < 0.05$). All PVAc adhesive bonding regimes for radiata pine provide significantly lower results compared to EPI–1 and EPI–2 adhesives. The highest *fv* of a bonded joint exceeds *fv* of solid radiata pine wood by 12%. This can be explained in the same way as for eucalyptus wood. The average density of radiata pine was 504 kg $m^{-3}$ but the maximum can reach 568 kg $m^{-3}$ with a 13% difference (Iejavs et al., 2021).

From 27 bonding regimes in bonding radiata wood with PVAc adhesive, 16 bonding regimes did not reach the average target shear strength value of 4 MPa according to LVS EN 204 (2016). Two bonding regimes with the lowest *T* – 20 min (*P* – 0.8 MPa, *S* – 150 g $mm^{-2}$, *T* – 20 min and *P* – 1.2 MPa, *S* – 180 g $mm^{-2}$, *T* – 20 min) with EPI–1 adhesive did not reach 4 MPa threshold value.

Statistically significant differences ($p < 0.05$) were found between grand average *fv* of all adhesives used (Fig. 4). EPI–2 adhesive *fv* was significantly higher than for EPI–1 and PVAc. Accordingly, EPI–1 adhesive provided significantly higher *fv* compared to PVAc adhesive.

Despite the significantly higher grand average *fv* values of EPI–2 adhesive compared to EPI–1 adhesive, high *Wf* rates are more often observed for EPI–1 adhesive reaching 90–100% for 5 bonding regimes instead of 1 EPI–1 bonding regime. For 11 gluing parameter combinations of all the adhesives the lowest average wood failure percentage 0% was observed for 10 PVAc bonding regimes and 1 for EPI–2 adhesive.

Radiata pine and EPI–2 adhesive bonding performance is affected by adhesive spread *S* ($p < 0.05$) and bonding pressure *P* ($p < 0.05$), pressing time *T* had insignificant ($p = 0.42$) effects on bonding performance for the single bonding parameters.

The bonding pressure and pressing time interaction most significantly influence the shear strength of bonded radiata pine joints ($p < 0.05$) according to Fig. 6b. For bonding *P* 0.8 MPa interacted with *T* 20 and 30 min, a significant ($p < 0.05$) decrease in *fv* was observed. But the most significant increase ($p < 0.05$) in *fv* from 4.9 to 6.0 MPa for *P* 0.8 MPa was observed when pressing time increases from 30 to 40 min. The most significant decrease ($p < 0.05$) in *fv* from 5.2 to 4.7 MPa was observed for *P* 1.0 MPa when *T* was increased from 20 to 30 min. Insignificant *fv* changes ($p = 0.55$ and 0.78) were observed when *P* 1.2 MPa was used between pressing time variations. The results of the study show that for *Eucalyptus grandis* and *Pinus radiata* D. Don wood the best bonding performance with EPI adhesives was achieved with a low bonding pressure of 0.8 MPa compared to 1.0 MPa, in contrary to the study carried out by Martins et al. (2013) when *Eucalyptus benthamii* Maiden et Cambage wood was bonded with PVAc adhesive. According to River & Okkonen (1991), Corrêa (1997) and Muenchow (2002) bonding pressure from 0.9 to 1.3 MPa are optimal to bond medium density wood.

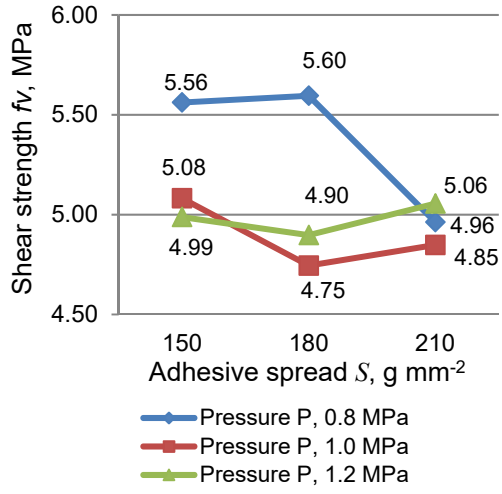


**Figure 7.** The influence of adhesive spread *S* and bonding pressure *P* interaction on shear strength of radiata pine wood bonded with EPI–2 adhesive.

The second significant interaction was observed for *P* and *S* according to Fig. 7 for radiata pine and EPI–2 adhesive. In this case only for the lowest *P* 0.8 MPa and highest *S* 210 g mm$^{-2}$ interaction, significant ($p < 0.05$) changes were observed when the average *fv* decreased from 5.6 MPa to 4.96 MPa with increased *S* from 180 to 210 g m$^{-2}$. A significant effect between other bonding parameters was not observed.

Regarding the adhesive spread, no significant increase in shear strength values was observed when adhesive spread was increased from 150 to 210 g m$^{-2}$ within the range recommended by the adhesives manufacturer (Table 1), as a result the adhesive joint of optimal thickness is formed, which does not significantly affect the shear strength of the glued joint. In cases when the adhesive spread is too small, there are not enough adhesives in the pores of the wood, as a result of which the optimal adhesion force between the adhesive and the wood is not achieved, which significantly reduces the mechanical strength of the glued joint. In turn, increased adhesive application results in

too thick bond line, which reduces the internal cohesion forces of the adhesive joint itself, which also leads to a reduced mechanical strength of the bonded joint (Follrich et al., 2010). These results indicate that it is possible to use the lowest glue spread for non-structural semi-finished glued laminated timber member production from eucalyptus and radiata pine wood. Similar statements were reported by Iwakiri et al. (2016), Campelo et al. (2017) and Iwakiri et al. (2019).

In other studies was concluded that bonding pressure and glue spread have a significant effect on the shear strength of the glue joint, while after sufficient hardening the pressing time does not have a significant effect on the bonding quality (Li et al., 2015; Mölleken et al., 2016). But the effect of glue spread on the shear strength was not observed (Fonte & Trianoski, 2015). The range of gluing parameters considered in various studies is crucial for assessing their effect on the shear strength of glued joints.

The anatomical structure, density and porosity of wood, as well as the chemical composition and absorption properties of adhesives in the wood can be mentioned as the most important factors causing the difference between PVAc and EPI adhesive bonds (Iwakiri, 2005).

## CONCLUSIONS

Eucalyptus (*Eucalyptus grandis*) and radiata pine (*Pinus radiata* D. Don) wood in face bonding with PVAc and EPI adhesives provides certain level of bond line shear strength. Failures of bonded joints after boiling pre–treatment were not observed within the range of bonding parameters used.

The bonding performances of both EPI adhesives were significantly higher compared to PVAc.

Bonding pressure and pressing time were evaluated as the most significant interacting factors influencing shear strength of eucalyptus and radiata pine wood bonded with EPI adhesive Prefere 6151/6651 or EPI adhesive Prefere 6170/6670.

Based on the general evaluation of the results, it can be stated that the wood of eucalyptus and radiata pine bonded with both EPI adhesives presents great potential for non-structural semi-finished glued laminated timber member production, especially for the use in humid conditions.

ACKNOWLEDGEMENTS. In accordance with the contract No. 1.2.1.1/18/A/004 between ‘Forest Sector Competence Centre’ Ltd. and the Central Finance and Contracting Agency, concluded on 17th of April, 2019, the study was conducted by ‘Kokpārstrāde 98’ Ltd. with the support from the European Regional Development Fund (ERDF) within the framework of the project ‘Forest Sector Competence Centre’.

## REFERENCES

Bomba, J., Sedivka, P., Cvach, J. & Sarvašová Kvietková, M. 2014. Strength of PVAc joints. *BioResources* **9**(1), 1027–1037.

Calil Neto, C. 2010. Species – treatment – adhesives combinations using Brazilian reforestations species for glulam purpose. WCTE 2010 Vol. 4. Available at http://support.sbcindustry.com/Archive/2010/june/Paper_215.pdf?PHPSESSID=ju29kfh90oviu5o371pv47cgf3

Calil Neto, C., Molina, J.C., Calil, J.C. & Lahr, F.R. 2016. Specie - treatment - adhesive combinations for glulam purpose. *CAPA* **3**(2). Available at https://doi.org/10.18256/2358-6508/rec-imed.v3n2p16-23

Campelo, S., Iwakiri, S., Trianoski, R. & Aguiar, O.R. 2017. Use of the Genipa Americana milling machine for the production of side gluing panels – EGP. *Floresta, Curituba* **47**(1), 129–135 (in Portuguese).

Corrêa, C.G. 1997. *Techniques for Gluing Wood with Vinyl Adhesive*. Chemical Border. Indústria e Comércio Ltda, Brasil, 68 pp. (in Portuguese).

Cubbage, F., Koesbandana, S., Donagh, P.M., Rubilar, R., Balmelli, G., Olmos, V.M., De La Torre, R., Murara, M., Hoeflich, V.A., Kotze, H., Gonzalez, R., Carrero, O., Frey, G., Adams, T., Turner, J., Lord, R., Huang, J., MacIntyre, C., McGinley, K., Abt, R. & Phillips, R. 2010. Global timber investments, wood costs, regulation, and risk. *Biomass and Bioenergy* **34**, 1667–1678.

Dieste, A., Cabrera, M.N., Clavijo, L. & Cassella, N. 2019. Analysis of wood products from an added value perspective: The Uruguayan forestry case. *Maderas. Ciencia y tecnología* **21**(3). Available at https://scielo.conicyt.cl/scielo.php?pid=S0718-221X2019000300305&script=sci_arttext&tlng=p

Endo, C., Trianoski, R. & Iwakiri, S. 2017. Production of edgewise glued panels with different PVAc adhesives and pressing systems. *Floresta e Ambiente* **24**, 1–8 (in Portuguese).

Follrich, J., Vay, O., Veigel, S. & Müller, U. 2010. Bond strength of end-grain joints and its dependence on surface roughness and adhesive spread. *Journal of Wood Science* **56**(5), 429–434.

Fonte, A.P.N. & Trianoski, R. 2015. Effect of grammage on the bonding quality of glue side of Tectona grandis wood. *Lages* **14**, 224–233.

Grøstad, K. & Bredesen, R. 2014. EPI for Glued Laminated Timber. In: Aicher, S., Reinhardt, H.W. & Garrecht, H. (eds) Materials and Joints in Timber Structures. *RILEM Bookseries*, vol. **9**. Springer, Dordrecht, 354–365. Available at https://doi.org/10.1007/978-94-007-7811-5_32

Gürses, M.K., Gülbaba, A.G. & Özkurt, A. 1995. Report about improves eucalyptus cultivation in Turkey. *Journal of DOA* **V**, 8.

Pitzner, B. & Lind, P. 2005. Gluing of Norway spruce and Scots pine with an EPI adhesive, Report No. 60, Norwegian Institute of Wood Technology, 1–33. Available at https://www.treteknisk.no/resources/filer/publikasjoner/rapporter/Rapport-60.pdf

Rachid–Casnati, C., Mason, E.G. & Woollons, R.C. 2019. Using soil–based and physiographic variables to improve stand growth equations in Uruguayan forest plantations. *iForest - Biogeosciences and Forestry* **12**(3), 237–245.

Iejavs, J., Podnieks, M. & Uzuls, A. 2021. Some physical and mechanical properties of wood of Fast-growing tree species eucalyptus (Eucalyptus grandis) and radiata pine (Pinus radiata D. Don). *Agronomy Research* **19**(2), 434–443. Availabe at https://doi.org/10.15159/AR.21.038

Iejavs, J., Spulle, U., Jakovlevs, V., Buksana, E. & Zelmenis, A. 2018. Effect of environmental temperature on bending strength of the finger jointed aspen lumber. *Agronomy Research* **16**(4), 1677–1685. Available at https://doi.org/10.15159/AR.18.193

Iwakiri, S. 2005. Reconstituted Wood Panels. Curitiba: FUPEF. 2005, 254 pp. (in Portuguese).

Iwakiri, S., Matos, J.M.L., Trianoski, R., Parcehn, C.F.A., Castro, V.G. & Iwakiri, V.T. 2014. Characteristics of glued laminated beams made with teak wood (*Tectona grandis*). *Floresta e Ambiente* **21**(2), 269–275 (in Portuguese).

Iwakiri, S., Trianoski, R., Fonte, A.P.N., Franca, M.C., Lau, P.C. & Molleken, R. 2016. Potential of using wood from *Dinizia excels* Ducke and *Protium puncticulatum* J.F. Mach for the production of EGP panels. *Scientia Forestalis* **44**(111), 709–717 (in Portuguese).

Iwakiri, S., Trianoski, R., Stupp, Ā.M. & Cabral, B. 2019. The use of Eucalyptus camaldulensis and Eucalyptus urophylla wood in the production of Edge Glued Panels. *Floresta* **49**(2), 317–324.

Iždinský, J., Reinprecht, L., Sedliačik, J., Kúdela, J. & Kučerová, V. 2021. Bonding of Selected Hardwoods with PVAc Adhesive. *Applied Scienses.* **11**(67). Available at https://dx.doi.org/10.3390/app11010067

Jokerst, R.W. 1981. Finger Jointed Wood Products. U.S. Department of Agriculture, Forest Service, Forest Products Laboratory. 24 p.

Li, R., Guo, X., Ekevad, M., Marklund, B. & Cao, P. 2015. Investigation of glueline shear strength of pine wood bonded with PVAc by response surface methodology. *BioRes*. **10**(3), 3831–3838.

Liao, Y.C., Tu, D.Y., Zhou, J.H., Zhou, H., Yun, H., Gu, J. & Hu C. 2017. Feasibility of manufacturing cross–laminated timber using fast-grown small diameter eucalyptus lumbers. *Construction and Building Materials* **132**, 508–515.

LVS EN 204. 2016. 'Classification of thermoplastic wood adhesives for non-structural applications'. European Committee for Standardization. Brussels.

LVS EN 205. 2016. 'Adhesives – Wood adhesives for non-structural applications - Determination of tensile shear strength of lap joints'. European Committee for Standardization. Brussels

LVS EN 314–1. 2005. 'Plywood – Bonding quality - Part 1: Test methods'. European Committee for Standardization. Brussels.

Konnerth, J., Kluge, M., Schweizer, G., Miljkovic, M. & Gindl–Altmutter, W. 2016. Survey of selected adhesive bonding properties of nine European softwood and hardwood species. *European Journal of Wood and Wood Products* **74**, 809–819.

Martins, S.A., Del Menezzi, Claudio, H.S., Ferraz, J.M. & de Sauza, M.R. 2013. Bending behaviour of Eucalyptus benthamii wood to manufacture edge glued panels. *Maderas, Ciencia y techologia* **15**(1), 79–92.

Ministry of Primary Industries of New Zealand, 2020. Wood product markets. Data on forestry imports and exports and indicative log prices. Annual exports. Available at https://www.mpi.govt.nz/forestry/new-zealand-forests-forest-industry/forestry/wood-product-markets/

Mölleken, R.E., Trianoski, R. & Neto, S.C. 2016. Evaluation of pressing time in the production of edge glued panel with adhesive polyurethane derived from castor oil. *Appl. Adhes Sci.* **4**(9). Available at https://doi.org/10.1186/s40563-016-0066-4

Muenchow, J. 2002. The steps of the high frequency side gluing and face gluing process. Material téchnico – Franklin International, 10 p. (in Portuguese).

Palmer, D.J., Watt, M.S., Kimberley, M.O., Höck, B.K., Payn, T.W. & Lowe, D.J. 2010. Mapping and explaining the productivity of *Pinus radiata* in New Zealand. *New Zealand Journal of Forestry* **55**(1), 15–21.

Pereira, M.C. de M., Calil Neto, C., Icimoto, F.H. & Calil Junior, C. 2016. Evaluation of tensile strength of a Eucalyptus grandis and Eucalyptus urophylahybrid in wood beams bonded together by means of finger Joints and polyurethane–based glue. *Materials Research* **19**, 1270–1275. Available at http://dx.doi.org/10.1590/1980-5373-MR-2016-0072

River, B.H. & Okkonen, E.A. 1991. Delamination of edge glued wood panels: Moisture effects. U.S. Department of Agriculture, Forest Service, Forest Products Laboratory, 11 p.

Tienne, D.L.C., Nascimento, A.M., Garcia, R.A. & Silva, D.B. 2008. Adhesion quality of quaruba ceder wood glued joints under internal and external service conditions. *Floresta e Ambiente* **15**(1), 20–33.

Vassiliou, V., Barboutis, I. & Karastergiou, S. 2006. Effect of PVAc bonding on finger–joint strength of steamed and unsteamed beech wood (*Fagus sylvatica*). *Journal of Applied Polymer Science* **103**(3), 1664–1669.

Vick, C.B. 1999. Adhesive bonding of wood materials. Wood handbook: wood as an engineering material. Madison, WI: USDA Forest Service, Forest Products Laboratory, General technical report FPL, GTR–113. 9.1–9.24.

Wang, X., Hagman, O., Sundqvist, B., Ormarsson, S., Wan, H. & Niemz, P. 2015. Impact of cold temperatures on the shear strength of Norway spruce joints glued with different adhesives, *Eur. J. Wood Prod.* **73**, 225–233. Available at https://doi.org/10.1007/s00107-015-0882-4

*Agronomy Research* **20**(1), 188–199, 2022
https://doi.org/10.15159/AR.22.026

# Utilization of *Pachysolen tannophilus* and *Pichia kudriavzevii* for the production of xylitol on undetoxified corn cob hydrolysates

O. Jolayemi[1], M.A. Oke[2], L. Rocha-Meneses[3,4] and P.F. Omojasola[1,*]

[1]University of Ilorin, Faculty of Life Sciences, Department of Microbiology, Nigeria
[2]Smallfood Inc., Dartmouth, Nova Scotia, Canada
[3]University of Sharjah, Research Institute of Sciences and Engineering, 27272 Sharjah, Biomass & Bioenergy Research Group, Center for Sustainable Energy and Power Systems Research, United Arab Emirates
[4]Estonian University of Life Sciences, Institute of Forestry and Engineering, Chair of Biosystems Engineering, Kreutzwaldi 56, EE51006 Tartu, Estonia
[*]Correspondence: jasola@unilorin.edu.ng

Received: February 19th, 2022; Accepted: April 24th, 2022; Published: April 29th, 2022

**Abstract.** Xylitol is a natural polyol with broad applications in the food and pharmaceutical industries. However, its large-scale production through chemical means is still an expensive and not environmentally friendly process. Therefore, great attention has been paid to low-cost and renewable substrates like corn cobs (CC), which can be utilized to improve the economic outlook of xylitol production. In this study, CC were used as a feedstock for xylitol production, with the help of yeasts and filamentous fungi. The results obtained in this study showed that the amount of xylitol produced from CC hydrolysate was similar to the amount of xylitol obtained on xylose substrate. Overall, yeast produced higher amounts of xylitol than filamentous fungi. *Pachysolen tannophilus* had the highest xylitol production at pH 5.0, 72 h fermentation time, substrate concentration 15%, and inoculum size $1.5\times10^8$ cfu $mL^{-1}$, while *Pichia kudriavzevii* performed better at pH 5.0, with a 72 h fermentation time, substrate concentration of 20%, and inoculum size of $2.5\times10^8$ cfu $mL^{-1}$. When comparing the combined optimal parameters with and without supplementation, supplementation with 1.5% methanol, has increased the xylitol production of *P. tannophilus* and *P. kudriavzevii* by 31% and 18.6%, respectively. These findings demonstrate the robustness of these yeast strains for sustainable and cost-effective xylitol production from CC waste.

**Key words:** corn cob hydrolysate, *P. tannophilus*, *P. kudriavzevii*, xylose, xylitol production.

## INTRODUCTION

Xylitol is a polyol composed of five carbon atoms (Cristobal-Sarramian & Atzmüller, 2018). It can be used for various applications, such as a building block for organic synthesis, as a sugar substitute in the management of diabetes, and as a sweetener in food industries (Mathew et al., 2018; Baptista et al., 2021).

Xylitol can be produced from various lignocellulosic residues, such as wheat straw/bran, rice straw, sugarcane, corncobs, corn stalks, and corn stover (Ribeiro et al. 2016; Venkateswar Rao et al., 2016; Bedő et al., 2021). These feedstocks are commonly composed of three main polymers: hemicellulose (20–40%), cellulose (40–60%), and lignin (10–25%) (Rocha-Meneses, 2019). The conversion of cellulose and hemicellulose into xylitol is commonly done by hydrolysis and hydrogenation processes (Hilpmann et al., 2018).

The hydrogenation process uses hydrogen gas and heterogeneous catalysts to convert xylose into xylitol (Ayubi et al., 2021; Lu et al., 2021). Some of the heterogeneous catalysts commonly employed in this process include nickel, ruthenium, rhodium, platinum, palladium, and copper (Carvalho, 2021). The hydrogenation process occurs at temperatures between 80–130 °C and pressures between 40–70 bar (Hilpmann et al., 2018).

Delgado-Arcaño et al. (2021) investigated the conversion of hemicellulose from corncob into xylitol using hydrolysis-hydrogenation processes. The results obtained in their study show that it is possible to simultaneously hydrolyze and hydrogenate CC with the help of Ru catalysts. The authors concluded that it is possible to make the process cost-effective by decreasing the reaction times and the energy input requirements. Another study by Ribeiro et al. (2017) utilized corncob for the simultaneous conversion of cellulose and xylan. The authors were able to achieve 75% yields of sorbitol and 77% of xylitol in a six hours reaction. The authors concluded that this strategy can efficiently maximize conversion yields. Ahuja et al. (2022) studied the detoxification process of corncob hydrolysates for further xylitol production. For this, activated carbon was used in the detoxification process. The results obtained in this study show that removing 93% of furfurals and 94% of phenolic compounds is possible. The detoxified material can be further converted into xylitol by means of fermentation. The authors obtained 122.47 g $L^{-1}$ of xylitol fermentation, with a selectivity of 95%, and concluded that it is possible to reduce the operational costs of xylitol production by approximately 38%. Although the chemical synthesis of xylitol is a very attractive process, it still has energetic, environmental, and economic limitations mainly due to the complex separation and purification steps that require the utilization of expensive catalysts, high pressures, and temperatures (Queiroz et al., 2022). Therefore, there is a search for alternative biotechnological processes that will make the chemical synthesis of xylitol cheaper and environmentally friendly (Queiroz et al., 2022). As a result, great attention has been paid to the utilization of corn cobs (CC) as a feedstock for xylitol production due to their low-cost, vast abundance, renewability, and high cellulose and hemicellulose content (Mohlala et al., 2016). However, the majority of the studies currently available focus mainly on the conversion of cellulose derivates for xylitol production, and there are limited studies on the conversion of the hemicellulose fraction CC into xylitol (Baptista, 2018).

In this study, robust and efficient microbial strains (yeasts and filamentous fungi) were isolated and analyzed for the conversion of undetoxified CC hydrolysates into xylitol. The optimum operational parameters that produced the highest xylitol concentrations were identified, seeking an improvement of the economic outlook of xylitol production.

## MATERIALS AND METHODS

### Isolation and identification of microorganisms

Three filamentous fungi (*Rhizopus stolonifer, Aspergillus niger, Penicillium digitatum*) and three yeasts (*Pachysolen tannophilus, Pichia kudriavzevii,* and *Saccharomyces cerevisiae*) were isolated from soil samples and wood shavings and used in the experiments.

The soil samples and wood shavings were obtained from sawdust dump sites located at sawmills in Tanke, Ilorin, Nigeria. The soil samples were diluted with physiological saline, and the suspension was homogenized in a shaker at 150 rpm for 3 h. Aliquots (1 mL) of $10^{-1}$ to $10^{-3}$ serial dilutions were inoculated in agar plates containing xylose medium using the spread plate method. The medium had the following composition: xylose 20 g $L^{-1}$, peptone 15 g $L^{-1}$, ammonium sulphate 1 g $L^{-1}$, $KH_2PO_4$ 1 g $L^{-1}$, $MgSO_4$ 0.5 g $L^{-1}$, yeast extract 10 g $L^{-1}$, and agar 20 g $L^{-1}$ (Zhang et al., 2013). The plates were incubated at room temperature for 2 days, and distinct colonies were sub-cultured on fresh plates of the xylose medium until pure cultures of the isolates were obtained and transferred to agar slants of the xylose medium. Identification of the isolates was carried out using molecular techniques as described by Altschul et al. (1997).

### Substrate preparation and hydrolysis

Corn cobs collected from a food waste dump site were dried in the sun until the moisture content was reduced to about 10%. The dried CC were crushed to a particle size of about 15 mm. The CC were hydrolyzed with 1% $H_2SO_4$ at 15% (w/v) solid loading for 60 min at 121 °C. The hydrolysates were then neutralized using 1N NaOH.

### Fermentation

The inoculum was prepared by washing off spores of a fully-sporulated (5-day old) culture of each isolated fungus from potato dextrose agar slant using sterile distilled water. Colonies from a 48-hour old culture were suspended in sterile distilled water for the yeast isolates. The spore and cell suspensions were adjusted to a concentration of about $1.0\times10^5$ spores $mL^{-1}$ or cfu $mL^{-1}$ for fungi and yeast, respectively. Inoculum size was set using the improved Neubauer haemocytometer (Narasimha et al., 2006). The fermentation medium was adjusted according to Srivani & Pydi Setty (2012) method with 15% (w/v) of D-xylose or CC as separate carbon sources in the media. The hydrolyzed corncob was supplemented with nutrients and mineral salts with the following composition: yeast extract (2 g), $MgSO_4.7H_2O$ (0.4 g), $KH_2PO_4$ (5 g), and $(NH_4)_2SO_4$ (2 g). The initial medium pH was set at 5.0. In the batch fermentation, $2.0\times10^8$ spores $cfu^{-1}$ per mL of isolated yeasts or fungi were used on 100 mL of each fermentation medium (D-xylose vs. CC hydrolysate) at pH 5. The fermentation was performed in 250 mL Erlenmeyer flasks on a rotary shaker (LH Fermentation, Model Mk V orbital shaker) at 150 rpm for 120 hours. The amount of xylitol produced was measured every 24 h.

### Optimization of xylitol production

The following parameters were varied to know the effects on xylitol production: CC hydrolysate concentration (5–25% w/v), pH (3–7), inoculum size

($1.0\times10^8$–$3.0\times10^8$ cfu $mL^{-1}$) and fermentation time (24–120 h), using the 2 highest xylitol producers on CC hydrolysates (the constant conditions used are 15% (w/v) CC hydrolysate, pH 5, inoculum size $2.0\times10^8$ cfu $mL^{-1}$, temperature 25 °C and fermentation time of 120 h.

**Methanol supplementation**

The effect of 1.5% (v/v) methanol supplementation on each isolate was monitored using combined optimized parameters. (El-Batal & Khalaf, 2004). The initial pH was maintained at pH 5, and the flasks were incubated with the spore suspensions of the isolated organisms. Batch fermentation was performed at 25 °C with an agitation speed of 150 rpm for 168 h. Samples were assayed for xylitol content at 24 h intervals.

**Xylitol assay**

Fermentation samples were centrifuged at 150 rpm for 30 min at 25 °C, and the supernatant was analyzed for xylitol content by spectrophotometric measurement at 412 nm (Searchtech 752N UV-VIS) as described by Sánchez (1998). A 0.5 mL volume of 0.5 M formic acid was added to 1 mL of the sample in a glass tube. Then, 1 mL of 5 mM sodium periodate was added to the solution and vortexed. After vortexing, the glass tube was exposed to room temperature for 15 seconds, after which a 1mL solution comprising 0.1 M acetylacetone, 2 M ammonium acetate, and 0.02 M sodium thiosulfate was added. The tube was sealed and boiled in water for 2 minutes. Next, it was cooled under running water, and the absorbance was measured at 412 nm. The amount of xylitol was calculated from a xylitol standard curve, which was obtained by conducting the assay under similar conditions using standard concentrations of xylitol (99% purity).

**Statistical analysis**

Statistical significance was measured using ordinary one-way analysis of variance (ANOVA), while Duncan's multiple comparisons test established multiple comparisons between means. The statistical analysis was performed in the software IBM SPSS and SigmaPlot for Windows version 10.0 (SysStatSoftwares Inc.). All the data are expressed as means of triplicates ± SEM, and values of $p < 0.05$ were considered significant.

## RESULTS AND DISCUSSION

**Screening of isolates for xylitol production on xylose and CC hydrolysate**

Fig. 1 shows the production of xylitol on xylose-containing media using isolated organisms. As it can be seen from the figure, the utilization of filamentous fungi gives lower xylitol concentrations than when yeasts are utilized. For instance, *A. niger P. digitatum* and *R. stolonifera* had a relatively low xylitol production, with their concentrations being 0.07–0.79 g $L^{-1}$, 0.23–0.80 g $L^{-1}$, and 0.17–1.57 g $L^{-1}$, respectively. These results are similar to the findings reported by Sampaio et al. (2003). In their experiments, *Aspergillus* and *Penicillium* sp. yielded small amounts of xylitol in xylose-containing media. In addition, Kang et al. (2016) showed that only trace quantities of xylitol were produced during fermentation with *Aspergillus* sp. A rationale for the low accumulation of xylitol by filamentous fungi could be a result of the discrepancy between the oxygen requirement that advances xylitol accumulation and the oxygen

required for fungal growth. Most fungi are obligate aerobes, while xylitol production and accumulation favour microaerobic or reduced conditions.

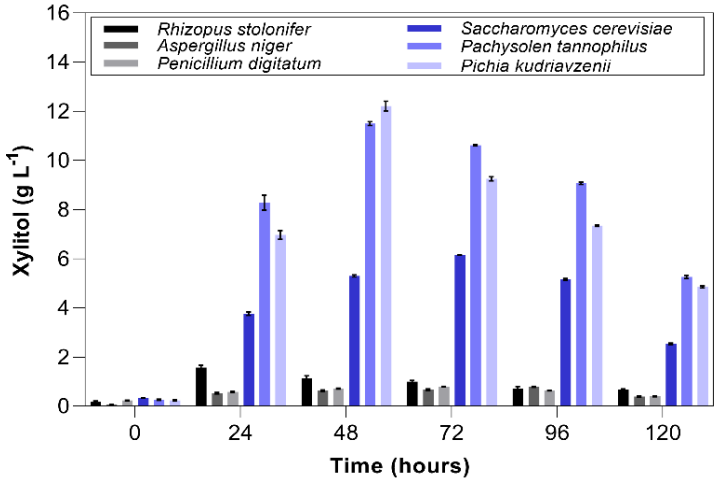


**Figure 1.** Production of xylitol using isolated organisms by submerged fermentation on xylose-containing media.

On the other hand, the three different types of yeasts utilized in this study had more appealing results, being 0.34–6.15 g $L^{-1}$ for *S. cerevisiae,* 0.26–11.50 g $L^{-1}$ for *P. tannophilus,* and 0.23–12.21 g $L^{-1}$ for *P. kudriavzenii*. *R. stolonifera* achieved its highest xylitol production at 24h, while *A. niger* reached its highest concentrations after the 96 h reaction. *P. digitatum* and *S. cerevisiae* reached their highest xylitol production at 72 h, and *P. tannophilus* and *P. kudriavzenii* at 48 h of reaction.

The yeasts *P. tannophilus* and *P. kudriavzevii* were selected as the best xylitol-producing strains. Despite growing on undetoxified hydrolysate, the yeasts utilized in this study produced xylitol concentrations higher than those reported in previous studies (Gong et al., 1981; Barbosa et al., 1988; Dahiya et al., 1991; Vandeska et al., 1995), which confirms their relatively high tolerance for inhibitors present in the hydrolysate. *P. tannophilus* has been shown to tolerate up to 2 g $L^{-1}$ of furfural in a xylose broth (Yang et al., 2012).

Fig. 2 shows xylitol production by submerged fermentation using isolated organisms on CC hydrolysate. Similar to Fig. 1, filamentous fungi had lower xylitol concentrations than when yeasts were utilized. For instance, *R. stolonifera*, *A. niger*, and *P. digita*tum had xylitol concentrations between 0.55–0.82 g $L^{-1}$, 0.58–1.23 g $L^{-1}$, and 0.35–1.71 g $L^{-1}$, respectively. When *S. cerevisiae* was used as yeast in the fermentation process, the xylitol concentrations varied between 0.71–5.82 g $L^{-1}$, while *P. tannophilus* produced 0.38–12.15 g $L^{-1}$L, and *P. kudriavzenii* 0.44–12.02 g $L^{-1}$. As shown in Fig. 2, *P. tannophilus* and *P. kudriavzenii* had similar amounts of xylitol on both xylose-containing media and CC hydrolysate. Their xylitol concentrations were significantly higher ($p < 0.05$) than that of the filamentous fungi *A. niger* and *P. digitatum.*

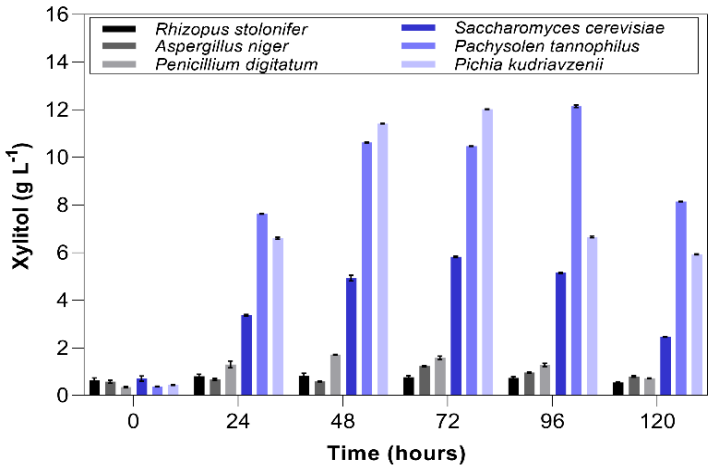


**Figure 2.** Production of xylitol by submerged fermentation using isolated organisms on CC hydrolysate.

**Optimization of xylitol production on CC hydrolysate**

The optimization experiments were performed under the following constant parameters: pH 5, inoculum size $2.0\times10^{8}$ cfu $mL^{-1}$, and 15% (w/v) CC hydrolysate.

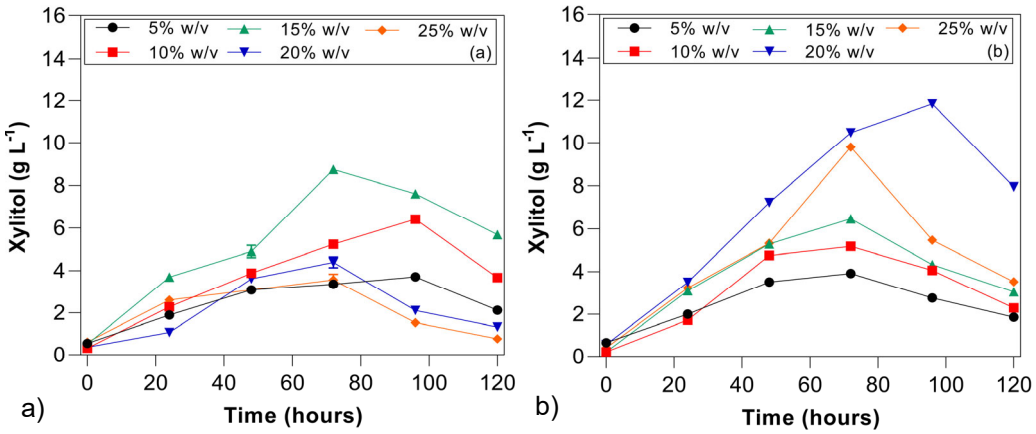


**Figure 3.** Effect of varying substrate concentration on xylitol production by (a) *P. tannophilus* and (b) *P. kudriavzevii* using CC hydrolysates.

Fig. 3 shows the effect of CC concentration on xylitol production using *P. tannophilus* and *P. kudriavzevii*. As can be seen from the figure, *P. tannophilus* had the highest xylitol production (8.75 g $L^{-1}$) at a substrate concentration of 15%, while *P. kudriavzevii* achieved its highest xylitol concentrations (11.83 g $L^{-1}$) at a substrate concentration of 20% w/v. Both organisms had a large drop in the xylitol production when substrate concentrations higher than 15% w/v and 20% w/v were used. These results can be caused by substrate inhibition since research has shown that substrate inhibition affects xylitol productivity by limiting the specific growth rate of the yeasts. This inhibition depends on the type of yeast and the complex nature of hemicellulose,

and the multiple compounds present upon sugar breakdown, including aliphatic or phenolic acids, furaldehydes, and other weak acids. It is known that many of these compounds inhibit the growth of the microorganisms during conversion to xylitol (Queiroz et al., 2022).

The influence of pH on the production of xylitol using *P. tannophilus* and *P. kudriavzevii* on CC hydrolysate is shown in Fig. 4. As can be seen from the figure, the maximum xylitol concentration was recorded at pH 5.0 for both *P. tannophilus* and *P. kudriavzevii* showing xylitol amounts of 8.84 g $L^{-1}$ and 11.74 g $L^{-1}$, respectively. The initial pH of the fermentation medium seemed to be an influential factor in the growth of the isolates, their physiological activities, and the compounding of xylitol in the fermentation medium. From 24 h of fermentation, *P. tannophilus* and *P. kudriavzevii* have shown a significant increase ($p < 0.05$) in the xylitol concentration produced at pH 5.0. These observations are supported by Kresnowati et al. (2016), which reported that the optimum initial pH of cultivation is highly yeast dependent.

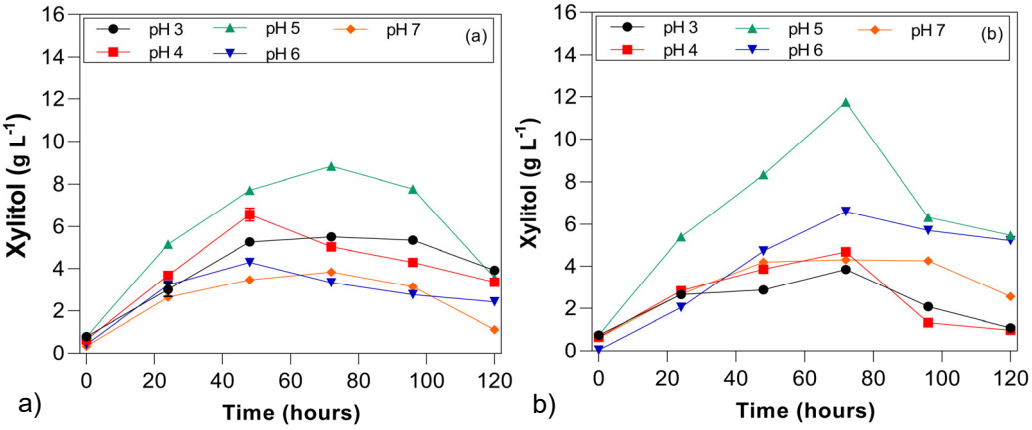


**Figure 4.** Effect of varying pH on xylitol production by (a) *P. tannophilus* and (b) *P. kudriavzevii* using CC hydrolysates.

The influence of the inoculum size on xylitol concentrations of *P. tannophilus* and *P. kudriavzevii* is shown in Fig. 5. As it can be seen from the figure, *P. tannophilus* had the highest xylitol concentration (12.82 g $L^{-1}$) when an inoculum size of $1.5\times10^8$ cfu $mL^{-1}$ was used. At the same time, *P. kudriavzevii* achieved its higher value with an inoculum size of $2.5\times10^8$ cfu $mL^{-1}$. Compared to $1.0\times10^8$ cfu $mL^{-1}$, *P. tannophilus* had a spike in xylitol concentration at $1.5\times10^8$ cfu $mL^{-1}$, which is dissimilar to the steady increase in xylitol production seen in *P. kudriavzevii* as the inoculum size increased. Although observations reported in *P. kudriavzevii* align with some works that report an increase in inoculum concentration to a linear rise in xylitol production, Manjarres-Pinzón et al. (2021) found that xylitol is a metabolite directly associated with cell density. Kresnowati et al. (2016) also reported that xylitol concentration increased, and biomass growth and concentration reduced markedly over an initial concentration range of $2\times10^7$ cells $mL^{-1}$ to $6\times10^7$ cells $mL^{-1}$. When yeast cell concentration was hiked to $6\times10^7$ cells $mL^{-1}$, 0.102 g $L^{-1}$ xylitol was derived from D-xylose. This characteristic was also replicated

with *Debaryomyces hansenii* (Kresnowati et al., 2016). Therefore, further studies are required in order to identify the optimum inoculum size for each microorganism.

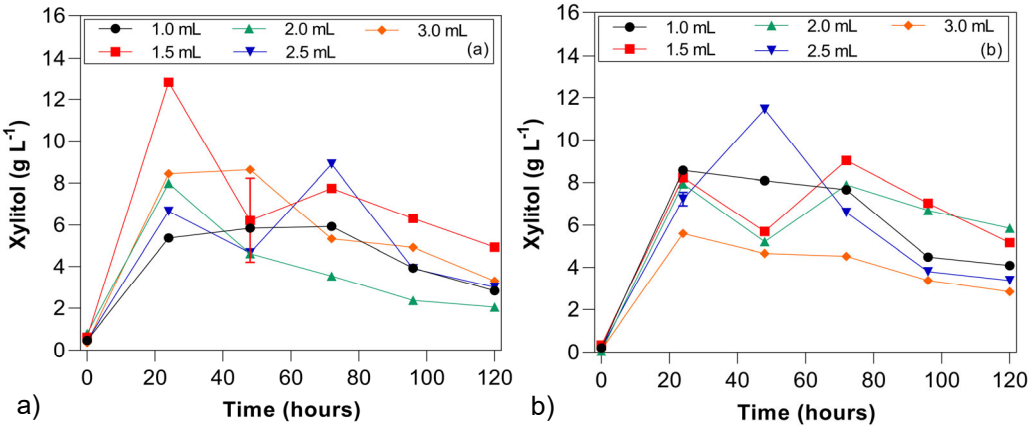


**Figure 5.** Effect of the inoculum size on xylitol production by (a) *P. tannophilus* and (b) *P. kudriavzevii* using CC hydrolysates.

The effect of fermentation time on xylitol concentrations is reported in Fig. 6. As it can be seen from the figure, there was a very high xylitol production at 96 h and 72 h by *P. tannophilus* and *P. kudriavzevii*, respectively. These results align with the findings of Jeevan et al. (2011). The authors reported that *Pichia* sp. had the highest xylitol accumulation at 72 h in synthetic and corncob hemicellulosic media. Interestingly, the media used by Jeevan et al. (2011) was detoxified using pH adjustment and charcoal adsorption before fermentation, unlike what was used in our study. Similar studies were reported by Narisetty et al., 2021., where *P. fermentans* was used in undetoxified sugarcane bagasse hydrolysate media for xylitol production. Under these conditions, the authors achieved a maximum xylitol production after 192 h of fermentation. They concluded that the rate of xylitol production by yeasts is influenced by inhibitors and the high glucose to xylose ratio in the hydrolysate.

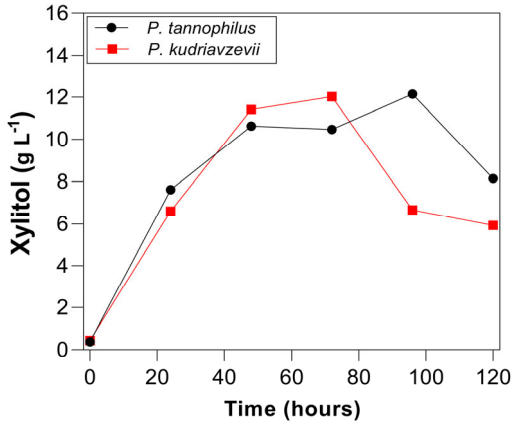


**Figure 6.** Effect of varying fermentation time on the production of xylitol on CC hydrolysates.

Fig. 7 shows the xylitol production by *P. tannophilus* and *P. kudriavzevii* on CC hydrolysates supplemented with 1.5%v/v methanol. As seen from the figure, without methanol supplementation, *P. tannophilus had a* xylitol production of 9.07 g $L^{-1}$. However, when supplemented with 1.5% methanol under combined optimal parameters, the xylitol concentrations increased to 11.9 g $L^{-1}$, a 31.0% increase. On the other hand,

*P. kudriavzevii* had a xylitol concentration of 11.6 g $L^{-1}$ in non-supplemented conditions and 13.7 g $L^{-1}$ with methanol supplementation, a 18.6% increase.

Overall, the xylitol production in pre-optimization experiments was higher than combined optimal conditions. However, the addition of methanol highly improved xylitol concentrations in both yeasts. El-Batal & Khalaf (2004) observed that all concentrations (0.5 to 10%) of methanol aaded to the fermentation medium resulted in increased xylitol production by *Candida tropicalis* compared to the control medium which had no methanol supplementation. This increase in concentration with supplementation can be due to the oxidation of methanol providing NADH, which is one of the co-factors that drive xylitol accumulation to the medium (Boontham et al., 2014). Xylitol concentrations increased due to the optimization experiments, and *P. kudriavzevii* was more influenced by optimized factors than *P. tannophilus*. These results suggest that the starting parameters utilized in the fermentation process were more conducive for the growth and xylitol production of *P. tannophilus* than *P. kudriavzevii.*

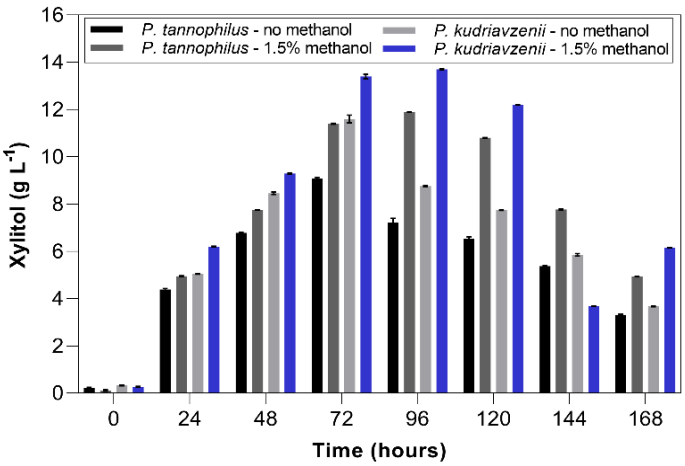


**Figure 7.** Xylitol production by *P. tannophilus* and *P. kudriavzevii* on CC hydrolysates supplemented with 1.5%v/v methanol.

## CONCLUSIONS

In this study, undetoxified CC hydrolysates were used for xylitol production with the help of isolated strains of yeasts and fungi. In screening experiments, the isolated wild-type yeasts and filamentous fungal strains produced similar amounts of xylitol in xylose-containing and CC hydrolysate media. The yeasts *P. tannophilus* and *P. kudriavzevii* produced significantly higher amounts of xylitol than the filamentous fungi, demonstrating the robustness of these yeasts.

The optimal fermentation conditions for *P. tannophilus* and *P. Kudriavzevii* were reported at pH 5.0, 72 h fermentation time, substrate concentration of 15% and 20%. The optimum inoculum size for *P. Tannophilus* was $1.5\times10^8$ cfu $mL^{-1}$, and for *P. kudriavzevii* $2.5\times10^8$ cfu $mL^{-1}$. Under these conditions, when supplemented with

1.5% methanol, *P. tannophilus* and *P. kudriavzevii* enhanced their xylitol concentration by 31.0% and 18.6%, respectively.

These results suggest that removing the substrate detoxification step can help achieve sustainable and cost-effective pathways for xylitol production. Another interesting implication of this study is that it demonstrates dual prospects of the overall process since using agricultural waste can significantly reduce the environmental impacts caused by the utilization of specifically grown feedstocks.

## REFERENCES


Ahuja, V., Kshirsagar, S., Ghosh, P., Sarkar, B., Sutar, A., More, S. & Dasgupta, D. 2022. Process development for detoxification of corncob hydrolysate using activated charcoal for xylitol production. *Journal of Environmental Chemical Engineering* **10**(1), p. 107097.

Altschul, S.F., Madden, T.L., Schaffer, A.A., Zhang, J., Zhang, Z., Miller, W. & Lipman, D.J. 1997. Gapped BLAST and PSI-BLAST: a new generation of protein database search programs. *Nucleic Acids Research* **25**, 3389–3402.

Ayubi, M.M., Werner, A., Steudler, S., Haase, S., Lange, R., Walther, T. & Hilpmann, G. 2021. Enhanced xylan conversion to xylitol in a bio- and chemocatalytic one-pot process. *Catalysis Today* 3**67**, 137–144. doi:https://doi.org/10.1016/j.cattod.2020.06.009

Baptista, S.L., Cunha, J.T., Romaní, A. & Domingues, L. 2018. Xylitol production from lignocellulosic whole slurry corn cob by engineered industrial Saccharomyces cerevisiae PE-2. *Bioresource Technology* **267**, 481–491.

Baptista, S., Romaní, A. & Domingues, L. 2021. Biotechnological Advancements, Innovations and Challenges for Sustainable Xylitol Production by Yeast. *Encyclopedia of Mycology*. Ó. Zaragoza and A. Casadevall. Oxford, 420–427.

Barbosa, M.F.S., Medeiros, M.B. & Mancilha, I.M., Schneider, H. and Lee, H. 1988. Screening of yeasts for production of xylitol from D-xylose and some factors which affect xylitol yield in Candida guilliermondii. *Journal of Industrial Microbiology* **3**, 241–251.

Bedő, S., Fehér, A., Khunnonkwao, P., Jantama, K. & Fehér, C. 2021. Optimized Bioconversion of Xylose Derived from Pre-Treated Crop Residues into Xylitol by Using Candida boidinii. *Agronom*y **11**(1). doi:10.3390/agronomy11010079

Boontham, W., Srisuk, N., Kokaew, K., Treeyoung, P., Limtong, S., Thamchaipenet, A. & Yurimoto, H. 2014. Xylitol Production by Thermotolerant Methylotrophic Yeast Ogataea siamensis and Its Xylose Reductase Gene (XYL1) Cloning. *Chiang Mai J. Sci*. **41**(3), 491–502.

Carvalho, S.L.B.V., de Moraes Medeiros, E.B., de Souza Wanderley, A., Ribeiro, L.d.M., da Silva, J.G., de Almeida Simões, I.T., de Lima Filho, N.M. 2021. Production of xylitol from acidic hydrolysates of lignocellulosic biomass by catalytic hydrogenation over a Ni–Ru/C catalyst. *Chemical Engineering Research and Design* **174**, 11–18. doi:https://doi.org/10.1016/j.cherd.2021.07.025

Cristobal-Sarramian, A. & Atzmüller, D. 2018. Yeast as a production platform in biorefineries: conversion of agricultural residues into value-added products. *Agronomy Research* **16**(2), 377–388.

Dahiya, J.S. 1991. Xylitol production by Petromyces albertensis grown on medium containing D-xylose. *Canadian Journal of Microbiology* **37**, 14–18.

Delgado-Arcaño, Y., Mandelli, D., Carvalho, W.A. & Pontes, L.A.M. 2021. Valorization of Corncob by Hydrolysis-Hydrogenation to Obtain Xylitol Under Mild Conditions. *Waste and Biomass Valorization* **12**(9), 5109–5120. doi:10.1007/s12649-021-01348-7

El-Batal, A.I. & Khalaf, S.A. 2004. Xylitol production from corn cobs hemicellulosic hydrolyzate by Candida tropicalis immobilized cells in hydrogel copolymer carrier. *International Journal of Agricultural Biology* **l6**, 1066–1073.

Gong, C.S., Chen, L.F. & Tsao, G.T. 1981. Quantitative production of xylitol from D-xylose by a high xylitol producing yeast mutant Candida tropicalis HXP2. *Biotechnology Letters* **3**, 125–130.

Hilpmann, G., Steudler, S., Ayubi, M.M., Pospiech, A., Walther, T., Bley, T. & Lange, R. 2019. Combining Chemical and Biological Catalysis for the Conversion of Hemicelluloses: Hydrolytic Hydrogenation of Xylan to Xylitol. *Catalysis Letters* **149**(1), 69–76. doi:10.1007/s10562-018-2598-7

Jeevan, P., Nelson, R. & Edith Rena, A. 2011. Optimization studies on acid hydrolysis of Corn cob hemicellulosic hydrolysate for Microbial production of xylitol. *Journal of Microbiology and Biotechnology Research* **1**(4),114–123.

Kang, T.Z., Mohammad, S.H., Murad, A.M.A., Illias, R.M. & Jahim, J.M. 2016. Fermentative production of xylitol: a first trial on xylose bifurcation. *Ind. J. Sci. Technol*., **9**, 1–5.

Kresnowati, P., Setiadi, T., Tantra, T. & Rusdi, D. 2016. Microbial Production of Xylitol from Oil Palm Empty Fruit Bunch Hydrolysate: Effects of Inoculum and pH. *Journal of Engineering and Technological Sciences* **48**, 523–533. 10.5614/j.eng.technol.sci.2016.48.5.2.

Lu, X., Junghans, P., Weckesser, S., Wärnå, J., Hilpmann, G., Lange, R. & Grénman, H. 2021. One flow through hydrolysis and hydrogenation of semi-industrial xylan from birch (betula pendula) in a continuous reactor – Kinetics and modelling. *Chemical Engineering and Processing - Process Intensification* **169**, 108614. doi:https://doi.org/10.1016/j.cep.2021.108614.

Manjarres-Pinzón, K., Barrios Ziolo, L., Arias Zabala, ME., Correa Londoño, G. & Rodriguez Sandoval, E. 2021. Kinetic study and modeling of xylitol production using Candida tropicalis in different culture media using unstructured models. *Journal of the National School of Agronomy Medellín* **74**(2), 9583–9592.

Mathew, A.K., Abraham, A., Mallapureddy, K.K. & Sukumaran, R.K. 2018. Chapter 9 - Lignocellulosic Biorefinery Wastes, or Resources? In T. Bhaskar, A. Pandey, S. V. Mohan, D.-J. Lee, & S. K. Khanal (Eds.), *Waste Biorefinery*, 267–297.

Mohlala, L.M., Bodunrin, M.O., Awosusi, A.A., Daramola, M.O., Cele, N.P. & Olubambi, P.A. 2016. Beneficiation of corncob and sugarcane bagasse for energy generation and materials development in Nigeria and South Africa: A short overview. *Alexandria Engineering Journal* **55**(3), 3025–3036.

Narasimha, G., Sridevi, A., Viswanath, B., Chandra, M.S. & Rajasekhar, R.B. 2006. Nutrient effects on production of cellulolytic enzymes by Aspergillus niger. *Afr. J. Biotechnol*. **5**, 472–476.

Narisetty, V., Castro, E., Durgapal, S., Coulon, F., Jacob, S., Kumar, D. & Kumar, V. 2021. High level xylitol production by Pichia fermentans using non-detoxified xylose-rich sugarcane bagasse and olive pits hydrolysates. *Bioresource Technology* **342**, 126005.

Queiroz, S.S., Jofre, F.M., Mussatto, S.I. & Felipe, M.D.G.A. 2022. Scaling up xylitol bioproduction: Challenges to achieve a profitable bioprocess. *Renewable and Sustainable Energy Reviews* **154**, 111789. doi:https://doi.org/10.1016/j.rser.2021.111789

Ribeiro, L.S., Delgado, J.J., de Melo Órfão, J.J. & Ribeiro Pereira, M.F. 2016. A one-pot method for the enhanced production of xylitol directly from hemicellulose (corncob xylan). RSC Advances **6**(97), 95320–95327. doi:10.1039/C6RA19666G..

Ribeiro, L.S., Órfão, J.J.d.M. & Pereira, M.F.R. 2017. Simultaneous catalytic conversion of cellulose and corncob xylan under temperature programming for enhanced sorbitol and xylitol production. *Bioresource Technology* **244**, 1173–1177. doi:https://doi.org/10.1016/j.biortech.2017.08.015

Rocha-Meneses, L., Raud, M., Orupõld, K. & Kikas, T. 2019. Potential of bioethanol production waste for methane recovery. *Energy* **173**, 133–139. doi:https://doi.org/10.1016/j.energy.2019.02.073

Sampaio, F.C., da Silviera, W.B., Chaves-Alves, V.M., Passos, F.M.L. & Coelho, J.L.C. 2003. Screening of filamentous fungi for production of xylitol from xylose. *Braz. J. Microbiol*. **34**, 325–328.

Sánchez, J. 1998. Colorimetric Assay of Alditols in Complex Biological Samples. *Journal of Agricultural and Food Chemistr*y **46**(1), 157–160. doi:10.1021/jf970619t.

Srivani, K. & Pydi Setty, Y. 2012. Parametric optimization of xylitol production from xylose by fermentation. *Asia-Pacific Journal of Chemical Engineering* **7**(S3), S280–S284.

Vandeska, E., Amartey, S., Kuzmanova, S. & Jeffries, T.W. 1995. Effects of environmental conditions on production of xylitol by Candida boidinii. *World Journal of Microbiology and Biotechnology* **11**, 213–218.

Venkateswar Rao, L., Goli, J. K., Gentela, J. & Koti, S. 2016. Bioconversion of lignocellulosic biomass to xylitol: An overview. *Bioresource Technology* **213**, 299–310. doi:https://doi.org/10.1016/j.biortech.2016.04.092

Yang, P., Zheng, Z., Luo, S., Jiang, S., Chen, M. & Gao, S. 2012. Tolerance of Saccharomyces cerevisiae and Pachysolen tannophilus to diluted acid hydrolysis inhibitor. Nongye Jixie Xuebao. *Transactions of the Chinese Society for Agricultural Machinery* **43**(4), 88–92.

Zhang, B., Li, L., Zhang, J., Gao, X., Wang, D. & Hong, J. 2013. Improving ethanol and xylitol fermentation at high temperature through substitution of xylose reductase in Kluyveromyces marxianus. *J. Ind. Microbiol. Biotechnol*. **40**, 305–316

*Agronomy Research* **20**(1), 200–214, 2022
https://doi.org/10.15159/AR.22.024

# Opposite tendency between yield and taste of organic tomato by increasing biochar doses in a slightly humous arenosol

T. Kocsis[1,*], Z. Kotroczó[2], K. Juhos[2], B. Ferschl[3], V. Rozmann[4], A. Brückner[1] and B. Biró[2]

[1]Hungarian University of Agriculture and Life Sciences, Department of Food Microbiology, Hygiene, and Safety, Somlói Str. 14–16, H-1118 Budapest, Hungary
[2]Hungarian University of Agriculture and Life Sciences, Department of Agro-Environmental Studies, Budapest, Villányi Str. 29–43, H-1118 Budapest, Hungary
[3]Hungarian University of Agriculture and Life Sciences, Department of Ecological and Sustainable Production Systems, Budapest, Villányi Str. 29–43, H-1118 Budapest, Hungary
[4]Hungarian University of Agriculture and Life Sciences, Department of Agricultural and Food Machinery, Villányi Str. 29–43, H-1118 Budapest, Hungary
[*]Correspondence: kocsis.tamas.jozsef@uni-mate.hu

Received: February 4th, 2022; Accepted: April 6th, 2022; Published: April 28th, 2022

**Abstract.** The tomato is the edible berry of the plant *Solanum lycopersicum*. Tomato plants are widely grown in temperate climates worldwide and are mostly cultivated as annuals. The objective of this study was to understand the interrelation between fruit quality of tomato, some soil biological parameters, and the addition of increasing biochar (BC) soil amendment doses. BC is an industrial product, made from organic waste by pyrolysis. Its use in the soil is known to improve fertility and several soil functions. Among organic, ecological conditions, a field experiment was performed in a type of slightly humous arenosol soil. Effect of increasing doses of biochar (BC) (0.5-, 1.0-, 2.5-, 5.0, 10 m/m% and control) was studied. Nutrient content and Total Soluble Solid (TSS) of the fruits, the ripeness, and the marketable/non-marketable ratio of yield were assessed. The presence of some cultivable microbial physiological groups (fungi, bacteria) and the soil-dehydrogenase activity (DHA) was estimated. Results represented that the changes of fruit TSS content was not linear with the increasing doses of BC. The increased yield (+53%) had an inverse correlation with the TSS content of the berry's pulps, and the content was lowest at the highest BC dose. Optimum doses of BC were considered, like 1–2.5 m/m%, supported by the nutritive element content (+55% N, +76% P, +83% K) and enhanced microbial activities (+45% DHA). Grouping the parameters by Pearson Correlation Coefficient, the biochar amendment was a driving factor for tomato growth, with certain dose limits in the studied organic agricultural practice.

**Key words:** biochar, ecological farming, nutrient uptake, soil biology, tomato.

## INTRODUCTION

Recently, increasing consumer concerns about several issues, such as food quality, environmental safety, and soil conservation, have led to sustainable agricultural practices (Belák et al., 2014). Due to urbanization and globalization, the development and supply of organic fertilizers are becoming scarce (Ali et al., 2019). Finding alternative solutions may be the most critical task, particularly for horticulture and viticulture. Organic soil amendments are essential for nutrient supplementation of crops and for improving soil chemical, physical and biological properties (Ringer et al., 2021).

A possible way to improve soil characteristics and functions is to apply biochar (BC) products (Gao & De Luca, 2018; Gaffar et al., 2021). BC may offer direct and indirect benefits when applied to soils. Available research information supports the application of BC products in soils, particularly in low-quality or degraded soils. Among them, soils with relatively low soil organic matter (SOM) are mainly studied (El-Naggar et al., 2019). Most of the available results approve that BC might improve the physical, chemical, and even biological characteristics of amended soils. The effect of biochar on sustainable plant growth along with nutrient management (preventing the loss of essential nutrients from the soil-plant environment) is considered beneficial, as well (Lehmann et al., 2011). Currently, the platform of circular economy applications of BC is growing dramatically. Faced with the burning issue of global warming, the development and application of BC appear to be a way of removing carbon from the carbon cycle and sequestering it in the soil (Xu et al., 2021). BC in the soil is a promising option for mitigating climate change and improving soil fertility/soil quality (Vaccari et al., 2015). BC might be considered an intact industrial material produced from organic waste by reductive pyrolysis (Mohan et al., 2006). Many organic materials can be used to produce biochar, but it might be critical that the used substances come from environmentally and climate-friendly sources. Usually, BC is a 2–5 mm long black granulated material, which can be used similarly as a synthetic or inorganic soil amendment agent (Dencső et al., 2017). Previous studies showed that BC is a highly porous material with a high soil-aeration and water-storage potential (Ahmad et al., 2014). During production, the literature distinguishes two major groups in terms of the initial raw materials. The first group is made on a relatively low (450–550 °C) pyrolyzing temperature, using mainly high-carbon-content substances. The products are capable of long-term binding the groundwater and dissolved ions; usually are originating from plant residues, by-products, and/or animal manures. The second group has been produced from animal bones at high temperatures (> 600–650 °C) with a relatively high calcium phosphate content and significantly lower carbon contents. The metal sorption of BC is possible through electrostatic attraction, ion exchange, surface complexation and some precipitation process. Metal ions can heavily adsorb on active sites of biochar that comprise phenolic and carboxylic functional groups present on the surface (Sobik-Szołtysek et al., 2021). Heavy metals can become stabilized on BC surfaces by metal ion exchange with $Ca^{2+}$, $Mg^{2+}$ or other cations; metal complexation by functional groups and inner complexation by hydroxyl groups; mechanisms based on electrostatic interactions or by physical adsorption and precipitation (Kocsis, 2018; Sobik-Szołtysek et al., 2021). Most of the microorganisms in soils are generally quite sensitive to drought-stressed conditions. BC application in soils might ensure the better survival of microbes (Głąb et al., 2016), control the degradation of soil (Abrol et al., 2016), maintain the

moisture content of the soil (Teixeira et al., 2021), and increase the bioavailable inorganic minerals in the soil (Lehmann et al., 2011). Literature suggests that biochar application increases the production of humic substances (Abd El-Rahim et al., 2021), which enhances microbial activity in the soil (Fekete et al., 2021). BC acts as an adsorption matrix and protects soil microorganisms due to its high porosity and large surface area (Ragályi et al., 2019). It has been reported on the other hand, that the application of a biochar and compost combination has a rather limited effect on the soil enzyme activities, in comparison to non-amended control plots (Gao & De Luca, 2018). In general, a change in enzymatic activity might respond to increased soil carbon content and the chemical composition after applying BC and/or compost (Dencső et al., 2017). Enzyme activity was shown to increase in sludge-biochar treated soils compared to untreated sewage sludge. This indicates that pyrolyzed organic matter may enhance biochemical properties. However, the effect on enzyme activities may be variable as a function on the soil and the type of enzymes (Joseph et al., 2021). It was also found that the hormone-like activity of solubilized humic substances might play a crucial role after the application of BC in drought-stressed conditions (Atik et al., 2013). In contrast, in temperate climates and alkaline soils, the application of BC often had a transient effect on crop yield and soil quality (Gaffar et al., 2021). Several studies have reported also, that the BC might somehow limit the crop production, even in very fertile soils (Xu et al., 2016; Liu et al., 2013). Based on the facts mentioned, the effect of BC highly depends on the certain site characteristics (soil and climate context) than on crop types or the type and preparation of BC.

Tomato (*Solanum lycopersicum* L.) is one of the most important vegetable crops, with global production estimated at 180 million tons of fresh fruit in 2020 (WPTC 2020). Tomatoes can optimally be grown in well-watered, loose-textured, nutrient-rich soil, where they require regular irrigation. Numerous studies and research have been carried out regarding the application of BC in soil on the quantity- and/or quality of tomato yields (Raave et al., 2020; Liao et al., 2021). It has been proven that biochar application significantly increases the carbon content in the soil, the capacity of soil cation exchange (CEC), and the availability of $NH_4^+$, P, and K in a tropical environment (Raave et al., 2020).

The present study aimed to measure tomato crop production, nutrient uptake, and soil microbiota in biochar treated soil (i.e. slightly humous, low-carbon content Arenosol). The study intends to examine crop production and some soil health parameters to identify critical issues at practical application of BC. Based on our hypothesis, the beneficial effects of increasing biochar doses might have some limitations on tomato nutrient uptake, amount of tomato yield and quality and some soil microbiological parameters.

## MATERIALS AND METHODS

### Study site and experimental setup

Field experiments were conducted at the Ecological Farm of the Hungarian University of Agriculture and Life Sciences, Soroksár, Hungary (47° 39’ N; 19° 15’E); certified by Biokontroll Hungária Inspection and Certification Nonprofit Ltd. The landscape has an altitude under 200 meters, flat, with moderately hot and dry temperatures. The average hours of sunshine are less than 2000 in a year. The average annual temperature is 10–11 °C. The average annual precipitation is around 500–550 mm.

The soil-forming rock is glacial and alluvial sediment, while the soil type is sandy soil with low humus-content (Arenosol) (MEPAR, 2013). Regarding the field experiment, tomato (*Solanum lycopersicum* L. var. Mobil) was grown as a test plant, and increasing doses of biochar were used. The locally grown tomato seeds were germinated and pre-grown in a greenhouse. They were planted in the experimental plots at the age of eight weeks, then grown from May 1 to September 8 in 2016 without irrigation. Thebiochar used in this study was produced from mixed wood chips (oak and beech) at a temperature of 600 °C initially with 30% water content. The prepared biochar product was dried at a temperature of 60 °C until its constant weight before applying to the soil.

The characteristic of the applied biochar is represented in Table 1.

**Table 1.** Nutrient content and chemical properties of applied biochar in field experiment, Soroksár, Hungary

| Characteristics (mg $kg^{-1}$) | Biochar values |
|---|---|
| $pH_{H2O}$ | 9.8 |
| sulfate | 445 |
| Mg | 33.7 |
| Na | 19.6 |
| $P_2O_5$ | 1,210 |
| $K_2O$ | 10,100 |
| N (%) | 0.48 |
| Cu | 1480 |
| Mn | 10.6 |
| Zn | 3.9 |
| salinity (m/m%) | < 0.02 |

The assessment were conducted by following the available standards for the studied soil characteristics, such as the pH: TS ISO 10390; water-soluble sulphate content: MSZ 14043-10; $P_2O_5$: MSZ EN 16170:2017; Mg-, $K_2O$-, Cu-, Mn: MSZ EN 16170:2017; salinity: MSZ-08-0206-2:1978.

Each experimental plot was 4 m ×2.5 m (10 $m^2$). The biochar was incorporated into the upper 20 cm layer of the soil. The dry weight was used to set the correct applied doses of biochar, as a percentage of 0.5%, 1%, 2.5%, 5%, 10%, and the control (without any treatment). The soil surface in the plots was covered with agro textile to prevent weeds and keep water in the soil. Soil samples were taken with a 20 mm diameter Pürckhauer 1175/1000 mm soil sampling auger (Bürkle GmbH, Switzerland). There were four plots per replicates in all treatments. From each plot, soil samples were taken randomly and finally a composite sample was used. Thus, we worked on four soil treatment replicates for showing of one average mean results. Considering the physical-chemical soil characteristics, main parameters are shown in Table 2.

**Table 2.** Nutrient content and some physical-chemical properties of the slightly humous sandy soil in the field experiment (Soroksár, Hungary)

| Characteristics (mg $kg^{-1}$) | Experimental soil |
|---|---|
| $pH_{H2O}$ | 6.8 |
| sulfate | 70.0 |
| Mg | 81.3 |
| Nitrate-N | 10.1 |
| Nitrite-N | 0.2 |
| Na | 77.7 |
| $P_2O_5$ | 357.0 |
| $K_2O$ | 215.0 |
| Cu ( | 2.4 |
| Mn | 98.3 |
| Zn | 2.9 |
| $CaCO_3$ (m/m%) | 0.7 |
| SOM (m/m%) | 1.6 |
| salinity (m/m%) | 30.0 |
| Arany-type texture (KA) | < 0.02 |

The measurements were conducted based on the following standards: pH: TS ISO 10390; water-soluble sulfate content: MSZ 14043-10; Nitrate-N-, Nitrite-N: MSZ 20135:1999; $P_2O_5$: MSZ EN 16170:2017; Ca $CO_3$: MSZ-08-1783-26:1985; Mg-, Na-, $K_2O$-, Cu-, Mn-, Zn: MSZ EN 16170:2017; SOM: MSZ-08-0012-6:1987; salanity: MSZ-08-0206-2:1978; Arany-type texture: MSZ-08-0205:1978.

The spatial position of the tomato plants was 50×40 cm per plot. That means five plants in six rows. One week before planting the seedlings, a Viano [VIANO MIXPROF BIO1 9-3-3+2Ca] type granulated organic fertilizer, approved for organic farming, was applied, in 1.32 kg plot$^{-1}$ (660 kg ha$^{-1}$) doses. From the inner rows, four plants were randomly selected for the study. Thus, we had sixteen plant samples (from four plots) per treatment. The fruit yield of the 16 plants in all treatments was measured, and the berries were classified into marketable/non-marketable groups, to get data on yield quality by the BC treatments. Non-marketable group was selected, as mechanically damaged or as contaminated by pathogens.

**Precipitation and temperature during the field experiment**

Regarding the environmental conditions there were 298 mm total precipitation with three peaks; temperature values were between 1.9 °C, as a minimum, and 39.1 °C, as a maximum during the investigated periods (Fig. 1).

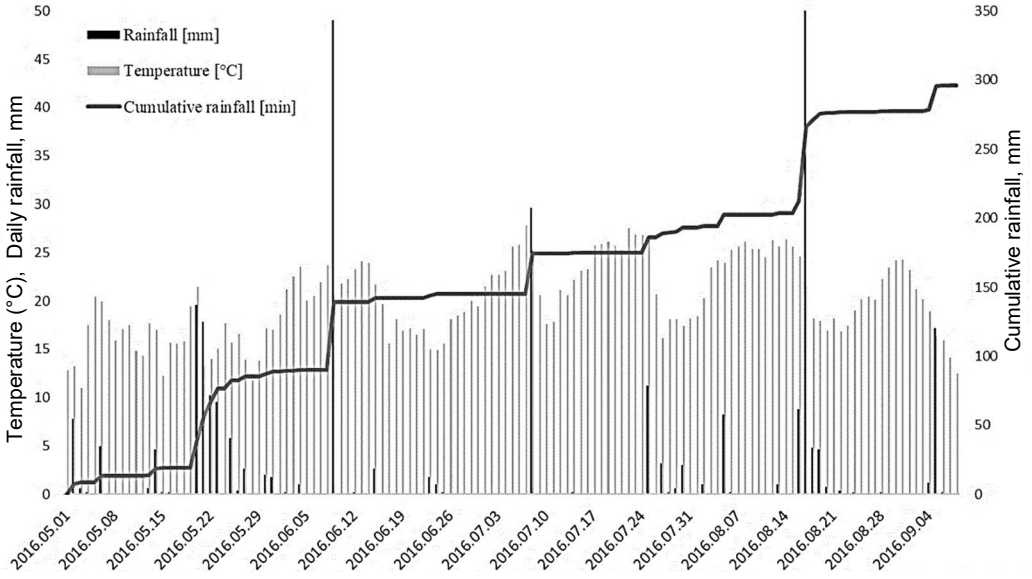


**Figure 1.** Measured average daily air temperature (°C) and precipitation data (mm) during the experiment at the research site (Soroksár, Hungary).

**Testing of soil-plant nutrient content and biochar contaminants**

The macro-nutrients (N, P, K), meso-nutrients (Ca, Mg), and micro-nutrients (Mn, Zn) were estimated in the shoot (i.e., the leaves and stem residues of tomato). The 16 plants per treatment collected during sampling were averaged by quadruplicates; thus, four samples per treatment were prepared in a drying oven for 24 hours at 60 °C. For that purpose, 1.0 g of dried finely ground plant shoot sample was weighed and transferred to the digestion tube. The volume of 10 mL concentrated sulfuric acid (≥ 99%) containing 0.5% of Se (as metal) powder was added into it (Sahrawat et al., 2002). After adding the digestion mixture, the tubes were **transferred to a block digester and preheated to 400 °C. About 4 hours** were needed for completing the digestion until a clear and colourless digest solution was left. The extract was diluted to

50 mL with distilled water. The K, Ca, Mg, Mn, and Zn concentrations were measured by atomic absorption spectrophotometer (AAS, Trace Aurora AI-1200 type). The colorimetric determination of phosphorus in plant extracts was carried out with an ammonium vanadate - ammonium molybdate reagent (≥ 99%). Determination of ammonium nitrogen content in the digest was carried out by steam distillation with 40% sodium hydroxide to liberate ammonia and then titrated (Mohammad et al., 2004).

**Fruit quality parameters**

The concentration of total soluble solids (TSS) can be determined from the smashed fruit juice using a hand-held refractometer (type Hanna HI 96801) (Cavalcanti et al., 2013). The fruits (skins and fruit-pulp) were crushed and homogenized with a blender and stored at a temperature of -25 °C until analysis. From each fruit pulp sample, 2 g was diluted with 2 mL of deionized water. One mL of the mixture was pipetted out and filtered through a 0.45 μm Syringe Driven Filter Unit. Colorimetric measurement of the fruit juice was also determined in the CIE (Commission International de l'Eclairage) chromaticity in tristimulus coordinate system L* (lightness/darkness), a* (red/green component), and b* (yellow/blue component) by the CR-400 Chroma Meter. Before the sample measurements, the instrument was calibrated with a white reference plate (CR-A43). 1 mL of juice sample was spread out to the target plate, and the L* value was measured at several points of each sample. The water content was calculated from the L* value (Kocsis, 2018). The pH of the tomato juice samples was measured using a digital pH meter (Model 420A, Orion Benchtop pH meter, Allometrics Inc., Seabrook, USA). The device was calibrated with commercial buffer solutions at pH 7.0 and 4.0. Ten milliliters of the sample were placed in a beaker with a magnetic stirrer and measured at 20 ± 0.5 °C. Measurements were taken at weekly intervals during the vegetation growth of the tomato.

**Soil microbiological parameters**

Besides general physicochemical soil parameters, soil-microbiological status (aerobic/anaerobic bacteria and microscopic fungi) was assessed by the Most Probable Number (MPN) method, described by Downes & Ito (2001). Since the technique is based on statistical estimation, we used an average sample per treatment inoculated in 5 replicates. The essence of the method is that the microorganisms were grown in a liquid medium on 96-well microplate plates, and based on the number of (positive) wells showing microbial growth, we can statistically infer the number of microorganisms. A basic suspension was prepared from the soil samples to be examined, and a dilution series was designed from this on a decimal basis. Determination of the most probable live colony-forming unit count on microplate plates was performed by 5–5 parallel inoculations. The first step in the assessment is to determine the key number after five days of incubation. A key number is a five-digit number determined from the number of positive wells showing microbial growth at three consecutive dilution levels. We then retrieved the set point for the key number obtained from the Hoskins table and multiplied it by the dilution ratio for the first member of the key number. The value thus obtained was converted to normal to give the test result (Cochran, 1950).

Soil functioning, i.e., the specific enzyme analysis of soil microorganisms, was assessed by the dehydrogenase enzyme assay (DHA), based on the reduction of the 2.3.5-triphenyl-tetrazolium chloride (≥ 98%) (TTC) method (Veres et al., 2013).

A standard curve was plotted using a range of triphenyl-formazan (≥ 90%) (TPF) concentrations between 0 and 40 µg TPF $mL^{-1}$. The DHA levels were expressed as µg TPF g dry $soil^{-1}$ $day^{-1}$. The soil microbiological measurements were made at the 14th week of tomato growth, the point of the highest microbial activity in the soil-plant system suggested by the literature (Dudás et al., 2017). Soil moisture content was given as a percentage by weight. The water content was calculated from the difference between the weight of the wet and dry soil samples (which was applied to the dried soil). Moisture content was calculated from the average of 5 subsamples per plot.

**Data analysis**

One-way ANOVA was applied to the test result. The Kolmogorov-Smirnov test ($p > 0.05$, $p = 0.200$) or the Shapiro-Wilk test ($p > 0.05$) were used to prove the assumption of normality, while the Levene's test ($p > 0.05$) was used to prove the homogeneity of variances. If the data showed homogeneity of variance, Tukey's honestly significant difference (HSD) post hoc test was used. If the data were heterogeneous, Games-Howell's post hoc analysis was used. The statistical method of Cochran was applied to calculate MPN values. One-way ANOVA Tukey test with logMPN values and standard logMPN errors was used to determine whether MPN values of field experiment soil samples were significantly different at the 95% confidence level (> 0.05). Pearson correlation analysis (2-tailed) was carried out to identify relationships between soil characteristics and plant components. Values of $r^2$ for significant correlations (*, $p < 0.05$ or **, $p < 0.01$) and correlation trends ($p < 0.1$) were reported.

## RESULTS AND DISCUSSION

**Yield and quality of tomato fruits under increasing doses of biochar**

In the case of the yield parameters, biochar application did not result in any differences between the tomato fruit's intact and non-intact (marketable/non-marketable) ratio. On the other hand, significantly higher fruit weight was recorded at the highest (2.5%, 5%, 10%) BC doses-, compared to the untreated control (Fig. 2).

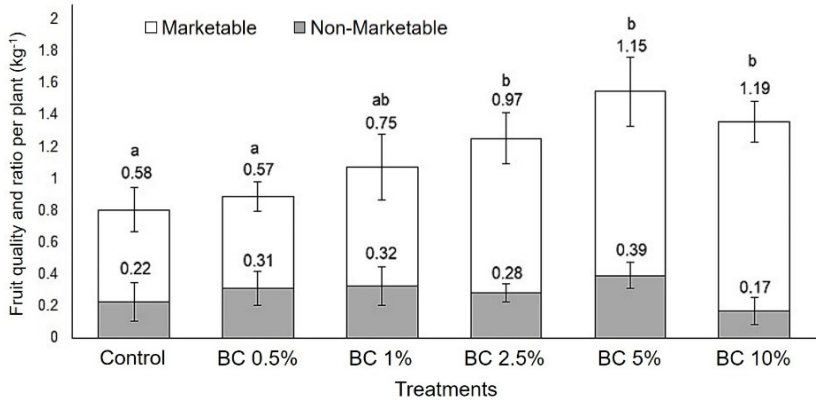


**Figure 2.** The average yield of tomato (*Solanum lycopersicum* var. Mobil) plants resulted from the increasing biochar doses (0-, 0.5-, 1-, 2.5-, 5-, 10%) of the upper soil layer (20 cm) in a slightly humous sandy soil ($n = 16$/ treatment, $P < 0.05$). Fruits were categorized as either marketable or non-marketable (small, misshapen, or diseased).

**As doses were increased, a significantly larger amount of marketable crop was harvested.** Referring to the annual precipitation (Fig. 1), biochar can retain the runoff rainwater that is determinative to the amount of yield. This result suggests that the water-absorbing capacity of biochar had a potentially greater effect on yield than its nutrient binding capacity. During the studied period, the average soil moisture content in the treatments was as follows: Control: 9.02%, BC 0.5%: 11.94%, BC 1%: 16.96%, BC 2.5%: 18.60%, BC 5%: 25.05%, BC 10%: 33.27%.

Hardie et al. (2014) had similar results when directly measuring the soil water content under different biochar treatments. Consequently, the application of biochar can increase the available water content of the soil through a direct contribution from the enlarged surfaces and its pores.

Besides the tomato yield, the nutritional properties were also examined. To determine the effect of various biochar doses on fruit quality, the TSS content and color intensity of the tomato fruits were also investigated. The increasing concentration of biochar resulted in a decrease in the TSS content of the fruit (Fig. 3, a). In contrast, the sample's L* (water content) value was increased parallel with the BC doses (Fig. 3, b).

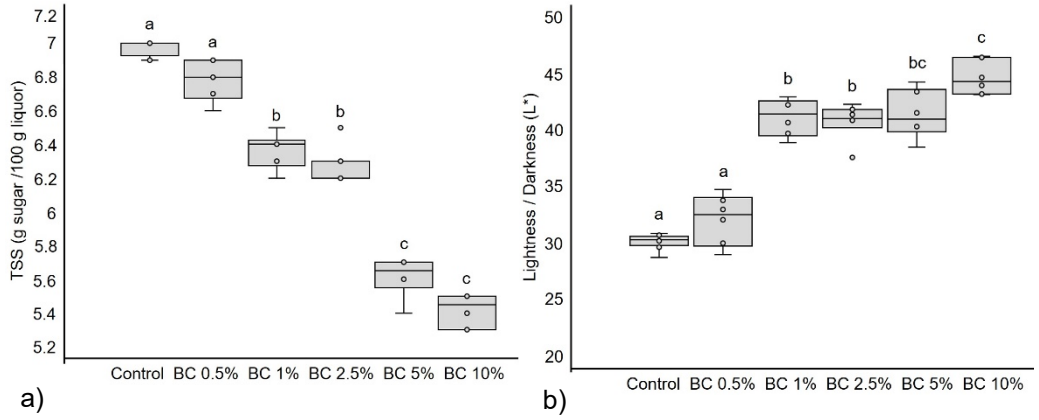


**Figure 3.** a) Total Soluble Solids (TSS) content-, b) Lightness attributes (L*) coloration of the mashed juice of tomato fruits, grown in slightly humous sandy soil with increasing biochar doses (0-, 0.5-, 1-, 2.5-, 5-, 10%) ($n$ = 16/ treatment, $P < 0.05$).

During the experiment, the measured yield per plant significantly increased while the TSS content of the tomato fruits decreased concomitantly with the concentration of applied biochar. In summary, it is possible to increase the yield of tomatoes by increasing the available water content through the appropriate biochar addition. However, the synthesis of TSS might be a more complex process, resulting in higher yields with lower dry matter content. This negative correlation in the non-irrigated field experiment indicates the biochar's adequate water retention capacity, which becomes efficient and determinative for plant growth.

In general, the average pH levels of crushed tomato fruits ranged from pH = 4.27 to pH = 4.40 (within deviation) values. The color of the tomato fruit extracts was a continuously changing parameter along with the vegetation period and the ripening of

the tomato fruits. At the end of the maturation process, the colour of the samples became more intense and darker with maturity progression (Fig. 3, b).

**Nutrient uptake of plants from biochar treated soils**

Regarding the mineral trace elements of plants, the optimal biochar dose significantly increased the nitrogen, phosphorus, and potassium content. The optimum concentration of these elements in plant shoots was recorded at the 1% dose (Table 3).

**Table 3.** Average nutrient content of the fresh biomass (leaves and stem residues) of tomato, grown in slightly humous sandy soil at increasing doses (0, 0.5, 1, 2.5, 5, and 10%) of biochar. (n = 4/treatment). Numbers are mean ± Standard error. Means within a line followed by a common letter do not differ significantly ($P < 0.05$, Games-Howell test)

| | Control | BC 0.5% | BC 1% | BC 2.5% | BC 5% | BC 10% |
|---|---|---|---|---|---|---|
| N (g kg$^{-1}$) | **20.72$^{a}$** ± 0.98 | **26.04$^{b}$** ± 0.29 | **37.66$^{c}$** ± 0.69 | **32.06$^{d}$** ± 1.18 | **30.66$^{de}$** ± 0.59 | **28.98$^{e}$** ± 1.97 |
| P (g kg$^{-1}$) | **0.26$^{a}$** ± 0.011 | **0.27$^{a}$** ± 0.014 | **0.34$^{b}$** ± 0.014 | **0.29$^{a}$** ± 0.011 | **0.27$^{a}$** ± 0.024 | **0.26$^{a}$** ± 0.021 |
| K (g kg$^{-1}$) | **1.30$^{bc}$** ± 0.016 | **1.36$^{d}$** ± 0.024 | **1.56$^{e}$** ± 0.015 | **1.35$^{cd}$** ± 0.018 | **1.23$^{a}$** ± 0.031 | **1.27$^{ab}$** ± 0.017 |
| Ca (g kg$^{-1}$) | **103.81$^{ab}$** ± 0.311 | **105.86$^{b}$** ± 0.363 | **91.39$^{c}$** ± 1.890 | **101.06$^{b}$** ± 0.803 | **89.62$^{bd}$** ± 1.400 | **87.32$^{d}$** ± 1.776 |
| Mg (g kg$^{-1}$) | **9.65$^{a}$** ± 0.387 | **10.51$^{bc}$** ± 0.091 | **10.05$^{ab}$** ± 0.149 | **10.01$^{ab}$** ± 0.175 | **10.50$^{bc}$** ± 0.285 | **10.75$^{c}$** ± 0.247 |
| Mn (mg kg$^{-1}$) | **85.34$^{a}$** ± 2.616 | **90.04$^{a}$** ± 2.375 | **116.00$^{b}$** ± 1.598 | **54.58$^{c}$** ± 3.478 | **49.66$^{c}$** ± 3.408 | **31.24$^{d}$** ± 1.527 |
| Zn (mg kg$^{-1}$) | **97.52$^{a}$** ±. 739 | **129.28$^{b}$** ± 2.13 | **121.12$^{c}$** ± 1.32 | **126.26$^{b}$** ± 1.92 | **104.48$^{d}$** ± 1.767 | **47.70$^{e}$** ± 1.569 |

In the case of N (+55%), P (+76%), and K (+83%), the 1% dose resulted in the highest concentrations, but only for nitrogen did it yield significantly higher results than the control. One of the BC's beneficial effects is that due to its highly porous surface, the cations from water solutes can adsorb on it. Considering this mechanism, it is also advantageous that fewer nutrients are lost and leached into the subsoil water layers in biochar-rich soils. This binding effect was observed after the application of nitrogen-rich organic fertilizer. Biochar may retain nutrients directly through the negative charge that develops on its surface, and this negative charge offers a buffer in the soil. In this case, the relatively high biochar concentration could result in the unavailability of the bound nutrients, thus shifting the environmental conditions out of the plant tolerance limit (see in the column of BC10% dose). The increase in soil pH after the application of biochar due to its liming effects has been widely documented (Sheng & Zhu, 2018). Van Zwieten et al. (2021) observed an increase in soil pH after the application of biochar. On the other hand, the high soil pH value induced by biochar is coupled with its high carbonate content. It adversely affects plant growth at high application rates, which can be explained by nutrient deficiencies. Therefore, the application of the BC amendment must be based on the specific properties (especially the texture, water-holding capacity, CEC) of the soil, with particular attention to its effects on nutrient availability to plants and microorganisms.

**Soil microbial activity under increasing doses of biochar amendments**

The MPN and DHA assessment methods were used to study microbial abundance and activities affected by BC addition. The hypothesis is that higher microbiological diversity and activity of the rhizosphere might result in an increased nutrient supply to the plants. There is also an optimum level of biochar dosage in terms of soil enzyme activity (Fig. 4).

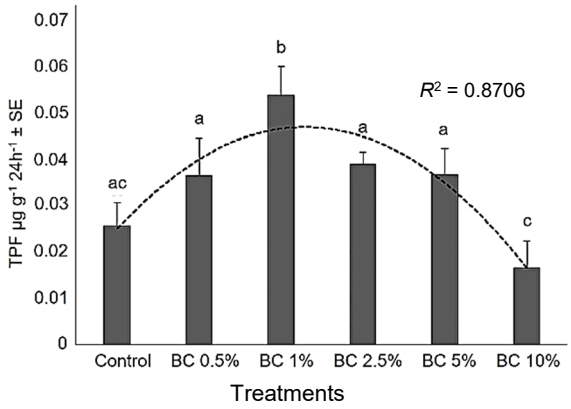


**Figure 4.** Dehydrogenase Enzyme Activity (DHA) of soils treated with increasing doses (0-, 0.5-, 1-, 2.5-, 5-, 10%) of biochar (BC). Significant differences are presented with the letters a, b, c, over the corresponding column of the graph. ($P < 0.05$, Tukey HSD test, $n = 4$/treatment).

The estimated highest activity occurred at 1% of biochar application, while a rate of 10% has reduced the activities below the actual rate in the studied soil. At the same time, the number of aerobic and anaerobic soil bacteria did not show such a trend. On the other hand, the fungal counts showed an increased abundance parallel with the increasing biochar concentration. The highest microbial counts of fungi were measured at the two highest biochar doses, 5% and 10% (Fig. 5).

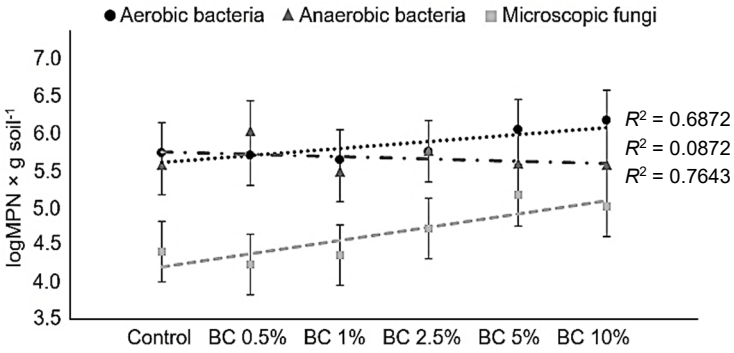


**Figure 5.** Most probable number (MPN) of aerobic/anaerobic bacteria and microscopic fungi in soils, treated with increasing doses (0-, 0.5-, 1-, 2.5-, 5-, 10%) of biochar (BC) ($n = 5$/treatment; $P < 0.05$).

Comparing the response of MPN and DHA assay to the biochar application, there was no statistical interrelation between the two measured parameters in the tested soil samples. Similar results were obtained in a mulching experiment by Kader et al. (2017). In the low-quality soil, reduced soil enzyme activities were frequently found because if any microbe is present, it is often in a dormant stage (waiting for a better soil-environmental condition). Regarding the used low humus sandy soil in our plots,

the surface increased by BC seems to be a critical issue of prospering soil functions. It can be assumed that biochar generally has a large sorption surface, which is vital for protecting microorganisms and preserving their activity in soil-plant systems. Still, attention must also be paid to other environmental stressors (SOM, texture, etc.). Extra high doses, for instance, can result in a negative trend in the measured parameters (yield of tomato; TSS content; nutrient content of the biomass; DHA activity). This can be justified because the large surfaces can bound the soil nutrients and, therefore, might reduce their availability for microorganisms and plants.

**Overall assessment of treatment effects**

Biochar treatment has highlighted the system's complexity that leads to successful crop production; studying the correlations between persistent biochar and crop production variables is therefore essential. Pearson product-moment correlation coefficient (PPMCC) was used to assess the correlation between the measured traits. The analysis showed significant relationships between tomato fruit parameters as well as the soil enzymatic activity and the nutrient uptake of plants. (Table 4).

**Table 4.** Correlations among the different variables in the study

| | | 1 | 2 | 3 | 4 | 5 | 6 | 7 | 8 | 9 | 10 | 11 | 12 | 13 | 14 |
|---|---|---|---|---|---|---|---|---|---|---|---|---|---|---|---|
| 1 | TSS | 1 | | | | | | | | | | | | | |
| 2 | Lightness | -.95** | 1 | | | | | | | | | | | | |
| 3 | Yield | -.93** | .90** | 1 | | | | | | | | | | | |
| 4 | Aerob | -.88* | .94** | .75* | 1 | | | | | | | | | | |
| 5 | Anerob | .40 | -.28 | -.33 | -.28 | 1 | | | | | | | | | |
| 6 | Fungi | -.88** | .78* | .81* | .79* | -.65 | 1 | | | | | | | | |
| 7 | DHA | .27 | -.48 | -.07 | -.67 | .01 | -.18 | 1 | | | | | | | |
| 8 | Nitrogen | -.42 | .19 | .49 | -.06 | -.31 | .35 | .70 | 1 | | | | | | |
| 9 | Phosphorus | .11 | -.36 | -.05 | -.56 | -.30 | -.04 | .88* | .83* | 1 | | | | | |
| 10 | Potassium | .38 | -.60 | -.39 | -.72 | -.11 | -.32 | .78* | .61 | .92* | 1 | | | | |
| 11 | Ca | .88** | -.73 | -.77* | -.68 | .70 | -.94* | .05 | -.57 | -.20 | .05 | 1 | | | |
| 12 | Mg | -.71 | .67 | .57 | .70 | .23 | .53 | -.28 | .18 | -.28 | -.33 | -.51 | 1 | | |
| 13 | Mn | .74* | -.91** | -.71 | -.87* | .05 | -.49 | .69 | .14 | .64 | .81* | .39 | -.53 | 1 | |
| 14 | Zn | .62 | -.67 | -.34 | -.81* | .47 | -.60 | .80* | .23 | .48 | .49 | .59 | -.42 | .63 | 1 |

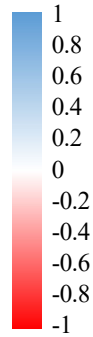


Variables included were: N, P, K, Ca, Mn, Zn content of stem and leaf residues, L*, TSS content of the fruits, and aerobic-, anaerobic-. microscopic fungi count, DHA activity in case of soil. (N = 86. *$p < .05$; **$p < .01$).

Table 4 shows the correlation results between the plants and the corresponding soil parameters. It was observed that the TSS content of the fruits was negatively significantly correlated with its water content (L*) ($p < 0.01$) and total fruit yield ($p < 0.01$). A well-marked correlation was found between the anabolic soil processes (DHA) (caused by microbial activity and plant roots) and plant nutrient uptake. Phosphorus, potassium, and zinc concentrations of plant shoots were significantly correlated ($p < 0.01$) with changes in DHA activity. Although significant correlations were found between the microbial values that could be counted and some plant parameters, the MPN method is not accurate enough to determine these correlations. In the case of the nitrogen uptake, no significant correlation was detected, which may reflect the abundant nitrogen application. Masood et al. (2020) reported that in tomatoes if the available nutrient content (local nitrogen and phosphorus) is adequate for the plant,

it does not promote rhizosphere colonization by the plant growth-promoting rhizobacteria (PGPR). The graphical summary of the scientific results and the potential tendencies of the used biochar doses is shown in Fig. 6.

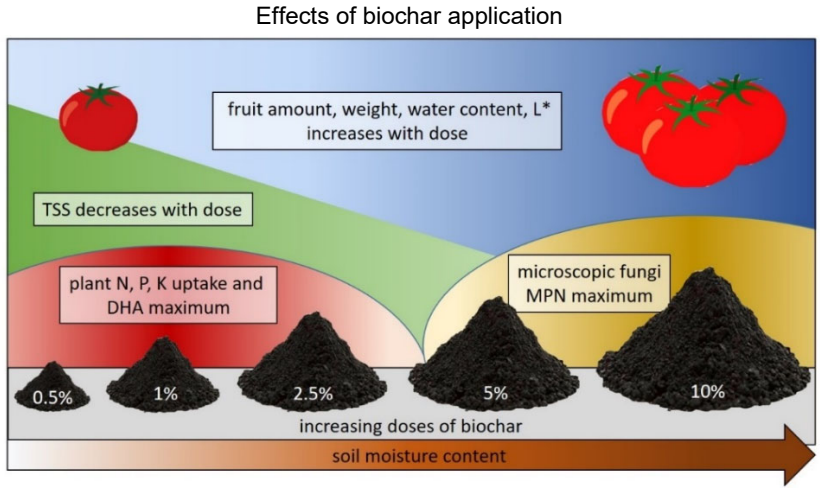


**Figure 6.** The applied increasing biochar doses affected as tendencies on tomato food production and on some soil health parameters in a slightly humous sandy soil (Arenosol).

## CONCLUSIONS

The results highlight that biochar amendments, in general, can improve the growth of tomatoes, due to the improved adsorbing surface characteristics in the studied soil-plant system. Such characteristics of biochar can be beneficial for both plant nutrition and the assessed soil-biological activities. On one hand, the microbial activity in the soil was stimulated by the added biochar, on the other hand, negative effects were observed in some cases in sandy soils at extra high doses. It has been shown that the optimal dose of biochar may differ for crop production and soil ecosystem services. In favourable soil solubility conditions (improved by biochar), the nutrient elements would become 'diluted' in the bigger tomato berry, thus, total suspended solids (TSS) content in tomato will be decreased. High doses of biochar may result in a shift in the soil-environmental conditions due to their high alkaline chemistry, thus affecting the functionality of the microbial groups, investigated. Under arid environmental conditions, the balance between the nutrient absorption capacity and the water- and nutrient availability in the soil might be optimized by applying the right quantity of biochar. Such optimization experiments seems to be necessary to select the most appropriate type and dose of biochar for a certain soil-plant-microbe system.

ACKNOWLEDGEMENTS. The authors are especially grateful to **Arijit Nath** for proofreading in English.

FUNDING: This research was supported by the European Union and co-financed by the European Social Fund (grant agreement no. EFOP-3.6.3-VEKOP-16-2017-00005) and by the European Union and co-financed by the European Regional Development Fund and the Hungarian Government (grant agreement no. GINOP-2.2.1-18-2020-00025).

CONFLICTS OF INTEREST: The authors declare no conflict of interest. The funders had no role in the design of the study; in the collection, analyses, or interpretation of data; in the writing of the manuscript, or in the decision to publish the results.

## REFERENCES

Abd El-Rahim, M.G., Sen, D.O.U., Liu, X.I.N., Shuai, X.I.E., Sharaf, A., Alio Moussa, A. & Hamed, M.H. 2021. Effect of biochar addition method on ammonia volatilization and quality of chicken manure compost. *Zemdirbyste-Agriculture* **108**, 331–338.

Abrol, V., Ben-Hur, M. & Verheijen, F.G.A. 2016. Biochar effects on soil water infiltration and erosion under seal formation conditions: rainfall simulation experiment. *Journal of Soils Sediments* **16**, 2709–2719.

Ahmad, M., Rajapaksha, A.U., Lim, J.E., Zhang, M., Bolan, N., Mohan, D. & Ok, Y.S. 2014. Biochar as a sorbent for contaminant management in soil and water: a review. *Chemosphere* **99**, 19–33.

Ali, Q., Ashraf, S., Kamran, M., Ijaz, M., Rehman, A., Tahir, M. & Ahmad, S. 2019. Organic Manuring for Agronomic Crops. In: Hasanuzzaman M. (eds) A*gronomic Crops. Springer, Singapore.* https://doi.org/10.1007/978-981-32-9783-8 10

Atik, A. 2013. Effects of planting density and treatment with vermicompost on the morphological characteristics of oriental beech (Fagus orientalis Lipsky). *Compost Science & Utilization* **21**, 87–98.

Belák, Á., Héher, B., Füstös, Z., Kovács, M. & Maráz, A. 2014. Endophytic bacteria from *Capsicum annuum* var. Grossum cultivars and their inhibitory effects on *Listeria monocytogenes*. Acta Alimentaria, *International Journal of Food Science* **43**, Suppl. 9–20.

Branthôme, François-Xavier. 2020. WPTC preliminary 2020 global crop estimate. (https://www.tomatonews.com/en/background_47.html)

Cavalcanti, A.L., de Oliveira, K.F., Xavier, A.F., Pinto, D.S. & Vieira, F.F. 2013. Evaluation of total soluble solids (TSS) content and endogenous pH in antimicrobials of pediatric use. *Indian Journal of Dental Research* **24**, 498–501.

Cochran, W.G. 1950. Estimation of bacterial densities by means of the Most Probable Number. *Biometrics* **6**, 105–116.

Dencső, M., Tóth, E., Gelybó, G., Kása, I., Horel, Á., Rékási, M. & Uzinger, N. 2017. Changes in the moisture content and respiration of a calcareous sandy soil after combined treatment with biochar and compost or mineral fertilizer. *Agrochemistry and Soil Science* **66**, 79–93.

Downes, F.P. & Ito, K. 2001. Compendium of methods for the microbiological examination of foods (4th edn.) *American Public Health Association*, Washington, DC 473–481.

Dudás, A., Szalai, Z.M., Vidéki, E., Wass-Matics, H., Kocsis, T., Végvári, Gy., Kotroczó, Zs. & Biró, B. 2017. Sporeforming bacillus bioeffectors for healthier fruit quality of tomato in pots and field. *Applied Ecology and Environmental Research* **15**, 1399–1418.

El-Naggar, A., Lee, S.S., Rinklebe, J., Farooq, M., Song, H., Sarmah, A.K. & Ok, Y.S. 2019. Biochar application to low fertility soils: a review of current status, and future prospects. *Geoderma* **337**, 536–554.

Fekete, I., Berki, I., Lajtha, K., Trumbore, S., Francioso, O., Gioacchini, P. & Kotroczó, Z. 2021. How will a drier climate change carbon sequestration in soils of the deciduous forests of Central Europe? *Biogeochemistry* **152**, 13–32.

Gaffar, S., Dattamudi, S., Baboukani, A.R., Chanda, S., Novak, J.M., Watts, D.W. & Jayachandran, K. 2021. Physiochemical characterization of biochars from six feedstocks and their effects on the sorption of atrazine in an organic soil. *Agronomy* **11**, 716.

Gao, S. & DeLuca, T.H. 2018. Wood biochar impacts soil phosphorus dynamics and microbial communities in organically-managed croplands 2018. *Soil Biology and Biochemistry* **126**, 144–150.

Głąb, T., Palmowska, J., Zaleski, T. & Gondek, K. 2016. Effect of biochar application on soil hydrological properties and physical quality of sandy soil. *Geoderma* **281**, 11–20.

Hardie, M., Clothier, B., Bound, S., Oliver, G. & Close, D. 2014. Does biochar influence soil physical properties and soil water availability? *Plant and Soil* **376**, 347–361.

Joseph, S., Cowie, A.L., Van Zwieten, L., Bolan, N., Budai, A., Buss, W. & Lehmann, J. 2021. How biochar works, and when it doesn't: A review of mechanisms controlling soil and plant responses to biochar. *GCB Bioenergy* **13**, 1731–1764.

Kader, M.A., Senge, M., Mojid, M.A. & Ito, K. 2017. Recent advances in mulching materials and methods for modifying soil environment. *Soil and Tillage Research* **168**, 155–166.

Kocsis, T. 2018. *Biochar and bioeffector combinations affected on biological characteristics of sandy soils*. PhD dissertation and thesis, Szent Istvan University, Budapest. 110 pp.

Lehmann, J., Rillig, M.C., Thies, J., Masiello, C.A., Hockaday, W.C. & Crowley, D. 2011. Biochar effects on soil biota–a review. *Soil Biology and Biochemistry* **43**, 1812–1836.

Liao, H., Zheng, C., Long, J. & Guzmán, I. 2021. Effects of biochar amendment on tomato rhizosphere bacterial communities and their utilization of plant-derived carbon in a calcareous soil. *Geoderma* **396**, 115082.

Liu, X., Zhang, A., Ji, C., Joseph, S., Bian, R., Li, L., Pan, G. & Paz-Ferreiro, J. 2013. Biochar's effect on crop productivity and the dependence on experimental conditions a meta-analysis of literature data. *Plant Soil* **373**, 583–594.

Masood, S., Zhao, X. Q. & Shen, R.F. 2020. *Bacillus pumilus* promotes the growth and nitrogen uptake of tomato plants under nitrogen fertilization. *Scientia Horticulturae* **272**, 109581.

MePAR - Agricultural Field Soil Identification System, Institute of Geodesy, Cartography and Remote Sensing, 2013. Budapest (www.mepar.hu)

Mohammad, A. & Flowers, T.H. 2004. Evaluation of Kjeldahl digestion method. J*ournal of Research* (Science), Bahauddin Zakariya University, Multan, Pakistan **15**, 159–179.

Mohan, D., Pittman, C.U. & Stelle, P.H. 2006. Pyrolysis of wood/biomass for bio-oil: a critical review. *Energy & Fuels* **20**, 848–889.

Raave, H., Escuer-Gatius, J., Kauer, K., Shanskiy, M., Tonutare, T. & Astover, A. 2020. Permanent grassland hay-derived biochar increases plant N, P and K uptake on an acidic soil. *Zemdirbyste-Agriculture* **107**, 227–234.

Ragályi, P., Bernhardt, B., Rékási, M., Draskovits, E., Molnár, S., Molnár, M. & Uzinger, N. 2019. Effect of biochar and microbial inoculant on the element compostion and element yield of maize on acidic and on calcareous sandy soils. *Agrokémia és Talajtan* **68**, 115–137.

Ringer, M., Jakab, G., Sipos, P., Szabó, M., Horváth-Szabó, K., Perényi, K. & Szalai, Z. 2021. Vertical differentiation of pedogenic iron forms–a key of hydromorphic soil profile development. *Hungarian Geographical Bulletin* **70**, 369–380.

Sahrawat, K.L., Kumar, G.R. & Murthy, K.V.S. 2002. Sulfuric acid-Selenium digestion for multi-element analysis in a single plant digest. *Communications in Soil Science and Plant Analysis* **33**, 3757–3765.

Sobik-Szołtysek, J., Wystalska, K., Malińska, K. & Meers, E. 2021. Influence of Pyrolysis Temperature on the Heavy Metal Sorption Capacity of Biochar from Poultry Manure. *Materials* **14**, 6566.

Sheng, Y. & Zhu, L. 2018. Biochar alters microbial community and carbon sequestration potential across different soil pH. *Science of the Total Environment* **622**, 1391–1399.

Teixeira, W.G., Verheijen, F. & de Oliveira Marques, J.D. 2021. Water Holding Capacity of Biochar and Biochar-Amended Soils. In Biochar as a Renewable-Based Material: With Applications in Agriculture, the Environment and Energy, 61–83.

Vaccari, F.P., Maienza, A., Miglietta, F., Baronti, S., Di Lonardo, S., Giagnoni, L., Lagomarsino, A., Pozzi, E., Pusceddu, E., Ranieri, R., Valboa G., & Genesio, L. 2015. Biochar stimulates plant growth but not fruit yield of processing tomato in a fertile soil. Agriculture, *Ecosystems and Environment* **207**, 163–170.

Van Zwieten, L., Kimber, S., Morris, S., Chan, K.Y., Downie, A., Rust, J., Joseph, S. & Cowie, A. 2021. Effects of biochar from slow pyrolysis of papermill waste on agronomic performance and soil fertility. *Plant and soil* **327**, 235–246.

Veres, Zs., Kotroczó, Zs., Magyaros, K., Tóth, J.A. & Tóthmérész, B. 2013. Dehydrogenase activity in a litter manipulation experiment in temperate forest soil. *Acta Silvatica Lignaria Hungarica* **9**, 25–33.

Xu, H., Cai, A., Wu, D., Liang, G., Xiao, J., Xu, M. & Zhang, W. 2021. Effects of biochar application on crop productivity, soil carbon sequestration, and global warming potential controlled by biochar C: N ratio and soil pH: A global meta-analysis. *Soil and Tillage Research* **213**, 105125.

Xu, P., Sun, C.X., Ye, X.Z., Xiao, W.D., Zhang, Q. & Wang, Q. 2016. The effect of biochar and crop straws on heavy metal bioavailability and plant accumulation in a Cd and Pb polluted soil. *Ecotoxicology and environmental safety* **132**, 94–100.

*Agronomy Research* **20**(1), 215–228, 2022
https://doi.org/10.15159/AR.22.009

# The impact of crop management regime on oil content and fatty acid composition in hulless and covered spring barley

L. Legzdiņa[1,*], E. Ivdre[2], D. Piliksere[1], A. Vaivode[1], I. Mieriņa[2] and M. Jure[2]

[1]Institute of Agricultural Resources and Economics, Priekuli Research Centre, Zinātnes iela 2, LV-4126 Priekuļi, Latvia
[2]Institute of Technology of Organic Chemistry, Faculty of Materials Science and Applied Chemistry, Riga Technical University, P.Valdena iela 3/7, LV-1048 Rīga, Latvia
[*]Correspondence: linda.legzdina@arei.lv

Received: November 11th, 2021; Accepted: January 30th, 2022; Published: March 17th, 2022

**Abstract.** Lipids are a minor nutritional component of barley (*Hordeum vulgare* L.) grain and have not been as widely explored as the major components. The aim of this study was to investigate the effect of genotype and environment, including conventional farming system with three crop management regimes, differing in agrochemical input, and organic farming system, on oil content and fatty acid composition in grain of two covered and four hulless spring barley genotypes during two growing seasons. Genotype significantly affected oil content and it was on average 4.26% and ranged in individual barley samples from 2.87 to 5.53%. We found linoleic, oleic, palmitic, α-linolenic, stearic and capric fatty acids in average proportions of 55.6; 21.3; 18.6; 3.7; 0.6 and 0.4%, respectively. Higher average oil content and proportion of α-linolenic acid was found in covered barley. Crop management regime did not significantly affect oil content but had some effect on the proportion of linoleic, α-linolenic, oleic and stearic acid. Decrease of chemical inputs was in favour of oil content and proportion of α-linolenic, oleic and stearic acids but did not promote linoleic acid. Waxy hulless barley line with high oil content and a very high proportion of linoleic acid was identified.

**Key words:** conventional farming, different input of agrochemicals, free lipids, organic farming, genotype and environment effects.

## INTRODUCTION

Vegetable oils mainly contain fatty acid triglycerides. Fatty acids (FA) form various lipids which are involved e. g. in cell membranes. All FA are classified as saturated and unsaturated, according to the amount of the double bonds into their structure. A high intake of saturated fats is linked with a negative effect on health, especially, on the blood lipid profile, which may be attributed to cardiovascular disease (Mensink, 2016). A part of unsaturated FA is known as essential, e. g. linoleic and α-linolenic acids which are not synthesized into human body due to the lack of certain desaturases and should be ingested with diet (Tvrzicka et al., 2011). Functional lipids, including polyunsaturated FA, demonstrate a beneficial effect on human health. ω-3 and ω-6 FA and conjugated

linoleic acid may be useful for the reduction of heart disease, obesity, depression, Alzheimer's disease, Parkinson's disease and atopic dermatitis (Alabdulkarim et al., 2012). The essential FA have a significant role in modulation of gene transcription, function as cytokine precursors, serving as energy sources in complex, and interconnected systems (Glick & Fischer, 2013). α-Linolenic acid has demonstrated an anti-inflammatory effect, as well as reduces stroke risk, size, and/or consequences (Blondeau et al., 2015).

**Oil content and FA composition in barley**

Lipids are a minor nutritional component of barley (*Hordeum vulgare* L.) grain and have not been as widely investigated as other components. Most of the authors have reported barley lipid content in a range of 1.9–3.7% and up to 7.3% in specific high-sugar genotypes, however, it is affected by the choice of analytical procedures, differing between the studies (Osman et al., 2000; Newman & Newman, 2008). Seefeldt et al. (2011) found that lipid biosynthesis in barley mutants with increased lipid content happens ten days earlier than in normal barley. Barley was found to have a little higher oil content than that of wheat, similar to that of rice and lower than in sorghum and oat, the latest being the cereal with superior oil content (Liu, 2011).

Similar to other cereals, oilseeds and legumes, also in barley five major FA are palmitic, stearic, oleic, linoleic and α-linolenic acid. Several other FA in much lower concentrations are reported as well (Liu, 2011). Linoleic acid is the dominant one found in a range from 50 to 60%, followed by palmitic acid from 18 to 25%, oleic acid from 11 to 22%, α-linolenic acid from 2 to 8% and stearic acid from 0.3 to 4.6% (De Man, 1985; Osman et al., 2000; Newman & Newman, 2008; Liu, 2011; Ciołek et al., 2012; Gangopadhyay et al., 2017). Qian et al. (2009) found ten FA in hulless barley (HB) bran oil with a 75% proportion for linoleic acid but no α-linolenic acid. Barley oil was found to have higher relative content of linoleic and α-linolenic acids and lower content of oleic acid than that of oats, rice or sorghum (Osman et al., 2000; Liu, 2011).

**Oil and FA distribution in barley grain**

About 18% of total lipids are concentrated in embryo, 77% in endosperm and 5% in the hulls of barley grain (Newman & Newman, 2008). The hull has a much lower oil content than the following grain outer part fractions and also the completely dehulled grain. Oil concentration in grain is decreases in the direction from the outer parts to inner core; the decrease is very rapid for the first few outer layers followed by gradual reduction. The increase of palmitic and stearic acids and the decrease of oleic and α-linolenic acids towards the grain central part are shown proving a higher amount of unsaturated FA in the whole grain products (Liu, 2011). Barley hull fraction is relatively rich in palmitic and stearic acids but low in α-linolenic acid (De Man, 1985). Qian et al. (2009) reported 8.1% crude oil content in HB bran.

**Effects of genotype and environment**

Significant differences between barley varieties in respect to the content of linoleic, palmitic, oleic and stearic acids have been reported (Gangopadhyay et al., 2017). De Man (1985) found that genotype has a larger effect on barley total FA (TFA), linoleic, oleic and stearic acid contents than growing location and the effect of both factors is similar for palmitic and α-linolenic acids. Significant differences in TFA content are found between two-rowed and six-rowed barley but not between winter and spring type barley.

The effect of *meteorological and soil conditions* on oil and FA content has been comparatively widely studied for various field crops. Analysis of large dataset on many species in China indicated an increase in total unsaturated FA content with increasing latitude and a negative correlations between mean annual temperature and precipitation and the ratio of unsaturated FA (Zhang et al., 2015). Wheat experiments in controlled environments showed, that a rise of growing temperature causes increase of palmitic and oleic acids and a decrease of linoleic and α-linolenic acids (Shamloo et al., 2017). Similar results are reported for oilseed crops (Schulte et al., 2013; Gauthier et al., 2017). De Man (1985) found that palmitic acid content in barley correlates positively with the temperature before flowering, oleic acid has a positive connection to the precipitation before flowering and temperature during ripening, linoleic acid correlates positively to temperature before flowering but negatively to temperature after flowering, and α-linolenic acid is positively affected by temperature before flowering and precipitation during grain ripening.

Only a few results are published on the *effect of fertilizers and crop management systems* on oil and FA contents in food crops. Lower crude fat content in organically versus conventionally grown cereals including barley was reported (Mikulioniene & Balezentiene, 2009). De Man & Dondeyne (1985) reported that nitrogen fertilizer slightly lowers TFA content and significantly decreases oleic acid proportion and increases palmitic acid proportion in barley. A more recent report on sunflower showed that nitrogen fertilizer affects proportion of oleic and linoleic acids positively, palmitic and stearic acids negatively (Abd EL-Satar et al., 2017). Another study on wheat did not find significant effects of nitrogen fertilizer on FA content (Wojtkowiak et al., 2018). For durum wheat no significant *effect of organic/conventional farming* system on FA was found, however, the interaction of genotype and farming system was significant for palmitic, linoleic and oleic acids (Beleggia et al., 2013). Ciołek et al. (2012) reported more lipids in cereals grown under conventional farming system if compared to organic system with the exception of hulless barley (HB) genotype, and more unsaturated FA under organic farming in most cases.

The aim of our study was to investigate the effect of genotype and environment, including conventional farming system with three crop management regimes, aimed to achieve different yield levels, and organic farming system, on oil content and FA composition in hulless and covered spring barley grain.

## MATERIALS AND METHODS

### Field trials

Field trials with two covered and four hulless spring barley genotypes were established under four crop management regimes: conventional crop management (C) system with three agrochemical input levels (C1, C2 and C3) and organic crop management (O) system, in years 2011 and 2012 as described in Legzdiņa et al. (2018). The three agrochemical input levels were aimed to obtain potential yield of 4 t $ha^{-1}$ (C1) and 6 t $ha^{-1}$ (C2 and C3). The amount of nitrogen supplied was 90 and 140 kg $ha^{-1}$, respectively. For C3 foliar fertilizer Kristalon white, containing several mineral elements, was applied in addition to the same input of agrochemicals as for C2. Weather conditions were comparatively warmer and drier (especially in June and the beginning of July) in 2011 and a bit cooler with precipitation above the long-term average in 2012.

**Barley genotypes**

The covered barley (CB) genotypes were varieties currently under production 'Jumara' and 'Rubiola', one hulless barley (HB) variety 'Irbe' and three advanced HB breeding lines. The lines were chosen considering their potentially elevated content of health promoting biologically active compounds. Lines PR-4651 and PR-5099 are waxy barley with comparatively high concentrations of β-D-glucans; PR-5099 is derived from cross with waxy variety 'Washonubet' providing high concentration of tocols as reported by Ehrenbergerová et al. (2006). Line PR-3808 contains a source with a very high content of protein and lysine in its pedigree.

**Grain chemical composition analysis**

The grain yield of the complete plots was harvested, dried and cleaned with a 1.7 mm sieve. One representative grain sample was assembled from all replications for analysis. The grain moisture content ranged from 10.2 to 12.5%. For all analysis barley grain was ground to pass through a sieve ($d < 0.065$ mm).

**Oil content.** Standard method ISO 734–1:2001 was applied to determine the free lipid content. Each sample was analysed in three to five replicates. Briefly, the grains were ground, dried at 105–110 °C and extracted with petroleum ether (fraction 40–70 °C) in a Soxhlet apparatus.

**Derivatization of barley oil triglycerides for gas chromatography (GC) analysis.** Barley oil (80 mg) and potassium hydroxide (0.9 mg) was refluxed in methanol (2.8 mL) for 20 min. After cooling the mixture, the solution with petroleum ether was transferred to a test tube, washed with brine (2×2 mL) and water (3×2 mL), dried over $Na_2SO_4$, filtered and evaporated. The sample was purified prior to GC analysis on silica column (eluent petroleum ether: chloroform, 2 : 1).

**FA composition.** Gas chromatograph (Agilent Technologies 6890N Network GC system, USA) with flame ionization detector was used. The sample of fatty acid methyl esters (FAME) of barley oil was dissolved in hexane (concentration of the sample 10–20 mg $mL^{-1}$) and analysed on DB-Wax capillary column (0.32 mm ×30 m, 0.25 μm). The temperature conditions were as follows: the initial oven temperature was 140 °C, then the temperature was increased to 230 °C with a rate of 5 °C $min^{-1}$, followed by holding the temperature for 15 minutes, increasing the temperature to 250 °C with rate 25 °C $min^{-1}$ and holding the same temperature for an additional 5 minutes. FAME were identified by comparing the retention times with standard compounds (Supelco mixture of 14 FAME from C8 to C24). Helium was used as a carrier gas (flow rate 25 mL $min^{-1}$). Each FAME was quantified by calibration curves with acceptable correlation coefficients.

**Other compounds.** Analysis of α-tocopherol and total polyphenol content was performed as described by Legzdiņa et al. (2018). Content of crude protein, starch and (1→3) and (1→4) β-D-glucans in the dry matter were determined using a NIT analyzer, Infratec 1241 (Foss, Denmark). Lysine content in grain was measured using InfraXact NIR Spectroscopy analyser (Foss, Denmark).

**Statistical analysis**

Data were tested for normality by the *Shapiro-Wilk test* and the homogeneity of variances by the *Levene's test*. The means and significant differences by *T-test*, *one-way*

*ANOVA* and *Tukey's HSD post-hoc tests* (for normally distributed data) or *Welch-t test* and *Games-Howell post-hoc tests* (for non-normally distributed data) and *Kendall's correlation* coefficients of the data were evaluated using the *IBM SPSS Statistics 23* software. To estimate the stability of oil concentration and FA distribution *ecovalence (Wi)* was computed as described by Becker & Leon (1988) and expressed in percentage of the total interaction sum of squares. Values close to zero indicate high stability.

## RESULTS

### Oil content

Oil content was on average 4.26%, and it ranged in individual barley samples from 2.87% in high lysine HB line PR-3808 to 5.53% in CB variety 'Rubiola' (Fig. 1. Both samples grown under C1 management regime in 2011). The *effect of genotype* on oil content was highly significant (Table 1). In 2011 and over both years the mean oil content of CB group significantly surpassed that of HB. CB variety 'Jumara' provided the highest mean in 2011, however, oil content of waxy HB line PR-5099 did not significantly differ and was the most superior in 2012. In 2012 both waxy HB lines significantly surpassed CB varieties and the mean value of them over both years did not significantly differ from CB varieties. Commercial HB variety 'Irbe' and high lysine line PR-3808 were the poorest in oil, but line PR-4651 had contradictory results in each year. Oil content was the most stable according to *ecovalence* for HB 'Irbe' with low values and for PR-5099 with high values, for the other genotypes it was similarly unstable (Table 2).

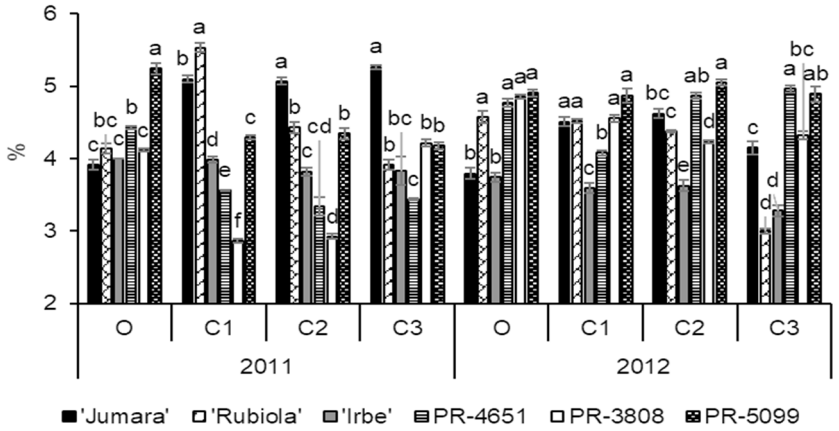


**Figure 1.** Oil content (%) in covered ('Jumara', 'Rubiola') and hulless ('Irbe', PR-4651, PR-3808, PR-5099) barley grain grown under organic (O) and conventional management regimes (C1, C2, C3), 2011–2012 (mean ± SE). Bars with different letters show significant differences within management regimes ($p < 0.05$).

No significant *effect of crop management regime or year* on oil content was found. A trend to increase the average oil content over the genotypes with the decrease of mineral fertilizer amount applied (C3→C2→C1→O) can be seen with a 0.3% difference between O and C3 for average data over both years. The difference between O and C systems was significant (Table 1). However, this trend was not always the case, whilst

looking at the data of individual genotypes (Fig. 1). Mean oil content over the years under O system was always higher than in C system for HB genotypes but not for CB varieties.

**Table 1.** Oil content and saturated fatty acid proportion in hulless and covered barley grain under organic (O) and conventional management regimes (C1, C2, C3), 2011–2012

| Genotype/ crop management | Oil, % | | | Palmitic C16:0, % | | | Stearic C18:0, % | | | Capric C10:0, % |
|---|---|---|---|---|---|---|---|---|---|---|
| | 2011 | 2012 | average | 2011 | 2012 | average | 2011 | 2012 | average | 2011 |
| Jumara | 4.90a | 4.31c | 4.59ab | 23.1 | 21.0 | 22.0a | 0.8 | 0.6 | 0.7 | 0.0 |
| Rubiola | 4.48a | 4.10cd | 4.30abc | 18.7 | 20.6 | 19.6a | 0.6 | 0.8 | 0.7 | 1.3 |
| Irbe | 3.90b | 3.54d | 3.71d | 20.9 | 19.3 | 20.1a | 0.3 | 0.4 | 0.4 | 2.2 |
| PR-4651 | 3.65b | 4.71ab | 4.20bc | 19.4 | 18.7 | 19.0a | 0.4 | 0.4 | 0.4 | 0.9 |
| PR-3808 | 3.63b | 4.47bc | 4.06cd | 19.2 | 20.8 | 20.0a | 1.5 | 0.7 | 1.1 | 0.0 |
| PR-5099 | 4.53a | 4.93a | 4.69a | 11.0 | 9.9 | 10.5b | 0.0 | 0.6 | 0.3 | 0.0 |
| Genotype, *p* | *** | *** | *** | *ns* | *ns* | *** | *ns* | *ns* | *ns* | *ns* |
| O | 4.40 | 4.46 | 4.43 | 18.5 | 16.5 | 17.5 | 0.6 | 1.4a | 1.0 | 0.0 |
| C1 | 4.26 | 4.32 | 4.29 | 19.5 | 20.7 | 20.1 | 0.9 | 0.6ab | 0.7 | 0.7 |
| C2 | 4.01 | 4.39 | 4.18 | 20.1 | 17.2 | 18.6 | 0.6 | 0.2b | 0.4 | 1.2 |
| C3 | 4.18 | 4.08 | 4.13 | 16.7 | 19.1 | 17.9 | 0.3 | 0.2b | 0.2 | 1.0 |
| Management, *p* | ns | *ns* | *ns* | *ns* | *ns* | *ns* | *ns* | *** | *ns* | *ns* |
| Average | 4.20 | 4.30 | 4.25 | 18.7 | 18.4 | 18.6 | 0.6 | 0.6 | 0.6 | 0.7 |
| Year, p | ns | | | ns | | | ns | | | - |
| HB/CB, O/C* | CB>HB *** | | CB>HB ***; O>C ** | | CB>HB ** | | | O>C *** | O>C ** | C>O *** |

** – $p < 0.05$; *** – $p < 0.01$; *ns* – $p > 0.05$; *p – p-value*; a, b, c – different letter indicate significant differences ($p < 0.05$) between genotypes or management regimes. *HB/CB – significant difference between means of hulless and covered barley groups. O/C – significant difference between means in organic and conventional farming systems.

*Oil content correlated* significantly negative with the content of protein, lysine and α-tocopherol in grain (Table 3). There were no significant correlations between oil content and grain yield, 1,000-grain weight and volume weight.

**Fatty acid compositions**

We found in barley grain samples linoleic (C18:2), oleic (C18:1), palmitic (C16:0), α-linolenic (C18:3), stearic (C18:0) and capric (C10:0) acids in average proportions of 55.6, 21.3, 18.6, 3.7, 0.6 and 0.4%, respectively (Tables 1 and 4). Capric acid was found in only seven samples of three genotypes grown in 2011 under C regimes with a proportion 1.3–3.6%. The effect of genotype was significant for linoleic and palmitic acid proportion over both years and for α-linolenic acid proportion in 2012. Significant differences between CB and HB genotype groups were found for palmitic acid proportion in 2012 and for α-linolenic acid proportion in 2012 and over both years with higher means for CB. However, only one HB line was significantly lower than the rest

of the genotypes for palmitic acid and two lines showed a trend to lower α-linolenic acid proportion but the rest were close to CB genotypes.

Waxy HB line PR-5099 was different from the other genotypes for its FA composition, especially under higher input C2 and C3 regimes: it had very high proportion of linoleic acid (up to 88.4% under C3 in 2011) and low proportion of palmitic acid (down to 2.3% under C3 in 2012) if compared to the other genotypes (Fig. 2). PR-5099 also was low in α-linolenic and oleic acid in mo st of the cases. Despite the highest proportion of linoleic acid among the genotypes in all but one environment (C1 in 2011) this line was the most unstable for this FA (Table 2).

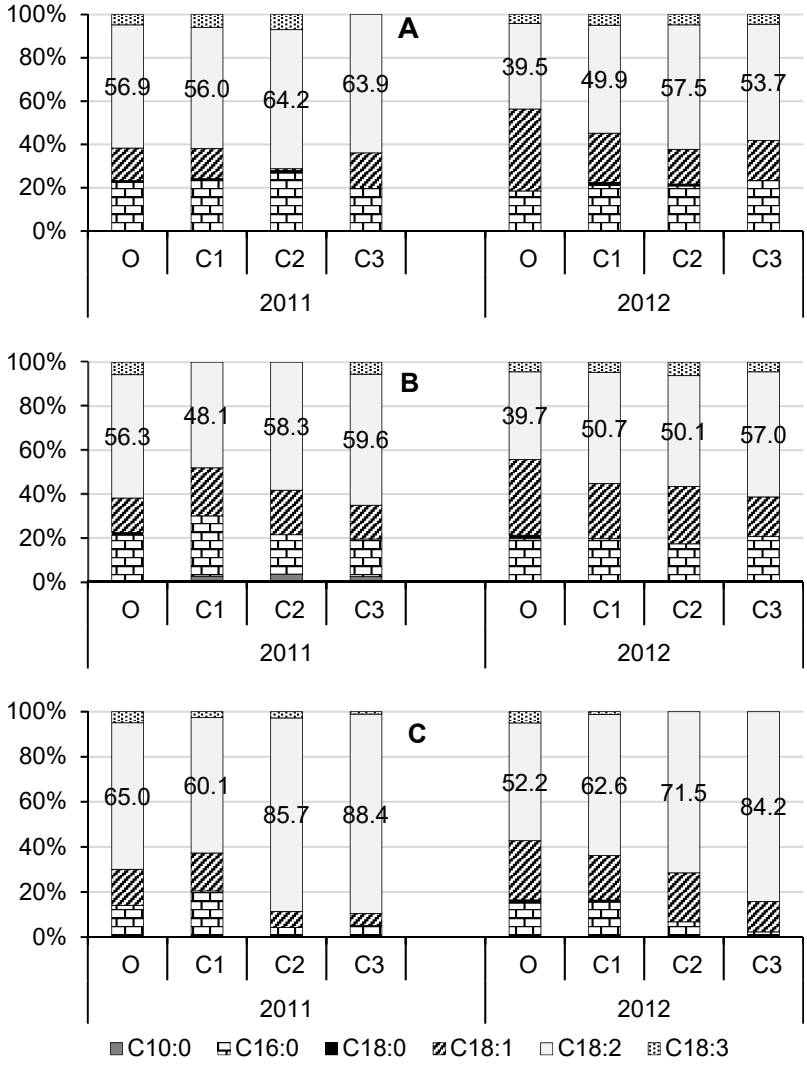


**Figure 2.** Fatty acid composition of covered barley 'Jumara' (A), hulles barley 'Irbe' (B) and hulless waxy barley PR-5099 (C) grown under organic (O) and conventional (C1, C2, C3) management regimes in 2011 and 2012.

CB variety 'Rubiola' was the most unstable for proportions of α-linolenic and palmitic acids. Exceptionally high proportion of α-linolenic acid (14.6%) and the only case with 0.0% palmitic acid was found for the sample of 'Rubiola' with the maximal oil content over the experiment grown under C1 in 2011. In the same year under C2 management regime the proportions were with opposite trends: 0.0% α-linolenic and maximum value for palmitic acid proportion (30.7%) accompanied with low linoleic acid (36.2%).

**Table 2.** Stability of oil content and fatty acid proportion in barley genotypes over four crop management regimes in 2011 and 2012

| Genotype | Ecovalence ($W_i$), % | | | | | |
|---|---|---|---|---|---|---|
| | oil | C 18:1 | C 18:2 | C 18:3 | C 16:0 | C 18:( |
| Jumara | 23.4 | 35.5 | 6.8 | 12.2 | 2.1 | 22.2 |
| Rubiola | 24.8 | 19.5 | 28.7 | 43.2 | 50.2 | 15.7 |
| Irbe | 5.4 | 3.1 | 2.7 | 19.5 | 6.2 | 11.0 |
| PR-4651 | 19.0 | 10.6 | 11.1 | 3.4 | 7.1 | 6.6 |
| PR-3808 | 21.8 | 15.0 | 10.3 | 15.6 | 7.3 | 38.4 |
| PR-5099 | 5.6 | 16.3 | 40.4 | 6.1 | 27.0 | 6.0 |

Linoleic acid proportion correlated significantly negative with oleic, stearic, and palmitic acids and positively with the content of polyphenols, α-tocopherol and starch in grain (Table 3). Proportion of α-linolenic acid was negatively related to protein, lysine and β-glucan content in grain.

**Table 3.** Significant coefficients of Kendall's correlation between barley oil content, FA proportions and some other grain compound content

| Com-pounds | Protein | Lysine | Polyphen ols | α-Toco-pherol | Starch | β-Glucans | C 16:0 | C 18:1 | C 18:0 |
|---|---|---|---|---|---|---|---|---|---|
| oil | -0.233* | -0.214* | | -0.204* | | | | | |
| C 18:2 | | | 0.297** | 0.215* | 0.264** | | -0.291** | -0.638** | -0.327** |
| C 18:3 | -0.262* | -0.285** | | | | -0.256* | | -0.208* | |
| C 18:1 | | | -0.365** | -0.273** | -0.202* | | | | |
| C 16:0 | | | | | -0.268** | | | | |

*$p < 0.05$, ** $p < 0.01$.

*Crop management regimes* significantly influenced the proportion of linoleic, oleic and stearic acid in 2012 and α-linolenic acid over both years (Tables 1 and 4). Significantly higher linoleic acid proportion was in samples grown under conventional farming regimes if compared to organic farming and the average over genotypes increased with mineral fertilizer amount applied in 2012. In 2011 average linoleic acid proportion increased according to management regime sequence C1→C2→C3, however, the mean linoleic acid proportion of organically grown samples surpassed those of C1 and C2. The opposite situation in both years was observed for oleic acid proportion: it was significantly higher under O system in comparison to the C system in 2012 and with a trend to increase with the reduction of mineral fertilization C3→C2→C1 and similar values for O and C3 regimes in 2011. For *α*-linolenic acid proportion the mean genotype values in both years had a slight trend to increase with the decrease of agrochemical input with the highest means under O system. It is proved also by negative correlation between the FA proportion and management regimes in order O→C1→C2→C3 ($r = -0.227$, $p < 0.05$). Mean stearic acid proportion was significantly higher under O system and also had a trend to increase with decreasing mineral fertilization (correlation with management regimes $r = -0.343$, $p < 0.01$).

The conditions of *growing year* affected significantly and conversely the proportions of linoleic and oleic acids (Table 4).

**Table 4.** Unsaturated fatty acid proportion in hulless and covered barley grain under organic (O) and conventional management regimes (C1, C2, C3), 2011–2012

| Genotype/ crop management | Linoleic C18:2, % | | | α-Linolenic C18:3, % | | | Oleic C18:1, % | | |
|---|---|---|---|---|---|---|---|---|---|
| | 2011 | 2012 | average | 2011 | 2012 | average | 2011 | 2012 | average |
| Jumara | 60.3 | 50.2 | 55.2b | 4.4 | 4.6a | 4.5 | 11.5 | 23.7 | 17.6 |
| Rubiola | 51.9 | 49.4 | 50.6b | 5.6 | 4.7a | 5.2 | 22.0 | 24.6 | 23.3 |
| Irbe | 55.6 | 49.4 | 52.5b | 2.8 | 4.8a | 3.8 | 18.3 | 25.9 | 22.1 |
| PR-4651 | 56.4 | 49.5 | 52.9b | 4.0 | 4.0ab | 4.0 | 19.1 | 27.5 | 23.3 |
| PR-3808 | 53.8 | 48.8 | 51.3b | 3.3 | 1.2b | 2.2 | 22.6 | 28.7 | 25.6 |
| PR-5099 | 74.8 | 67.6 | 71.2a | 2.9 | 1.6ab | 2.2 | 11.3 | 20.3 | 15.8 |
| Genotype, *p* | *ns* | *ns* | *** | *ns* | *** | *ns* | *ns* | *ns* | *ns* |
| O | 59.9 | 41.7b | 50.8 | 5.2 | 4.3 | 4.7a | 15.9 | 36.1a | 26.0 |
| C1 | 54.4 | 53.7ab | 54.0 | 4.5 | 3.7 | 4.1ab | 20.1 | 21.4b | 20.7 |
| C2 | 57.1 | 55.9a | 56.5 | 2.8 | 3.3 | 3.0ab | 18.4 | 23.4b | 20.9 |
| C3 | 63.8 | 58.6a | 61.2 | 2.8 | 2.7 | 2.7b | 15.5 | 19.5b | 17.5 |
| Management, *p* | *ns* | ** | *ns* | *ns* | *ns* | ** | *ns* | *** | *ns* |
| Average | 58.8 | 52.5 | 55.6 | 3.8 | 3.5 | 3.7 | 17.5 | 25.1 | 21.3 |
| Year, *p* | ** | | | ns | | | *** | | |
| HB/CB, O/C* | | C>O *** | | | CB>HB *** | CB>HB **; O>C ** | | O>C *** | |

** – $p < 0.05$; *** – $p < 0.01$; *ns* – $p > 0.05$; *p – p-value*; a, b, c – different letter indicate significant differences ($p < 0.05$) between genotypes or management regimes. *HB/CB – significant difference between means of hulless and covered barley groups. O/C – significant difference between means in organic and conventional farming systems.

## DISCUSSION

### Range of oil content and FA distribution

The barley grain *oil content* found by us with an average of 4.25% and maximum 5.65% was relatively high if compared to that reported in other studies (Osman et al., 2000; Newman & Newman, 2008; Liu, 2011; Ciołek et al., 2012). Some reports suggest that genetic factors controlling waxy starch in barley may be linked to genes that increase total lipids (Newman & Newman, 2008); in our study waxy line PR-5099 was superior according to average data and also showed high stability for oil content, whereas the oil content of the other waxy line PR-4651 appeared to be more affected by the environment.

The maximum linoleic acid proportion detected in waxy HB line PR-5099 grown under C crop management regimes with highest agrochemical inputs (71.5–88.4%) noticeably surpassed that reported in barley grain in other studies (De Man, 1985; Osman et al., 2000; Newman & Newman, 2008; Liu, 2011; Ciołek et al., 2012; Gangopadhyay et al., 2017), and this line can be considered to be used for the specific purpose to produce linoleic acid rich oil. Qian et al. (2009) found linoleic acid proportion 75% in HB bran oil, but it cannot be comparable to our results in whole grain because the proportion of unsaturated FA is higher in outer parts of grain (Liu, 2011).

A very high proportion of α-linolenic acid (25%) in combination with low linoleic acid (39%) was found in a HB genotype by Osman et al. (2000). Among our samples, exceptionally high α-linolenic acid proportion (14.6%) was identified in one sample of CB 'Rubiola' also possessing the maximum oil content and complete lack of palmitic acid. We do not have an explanation why this particular sample was so different. α-Linolenic acid was not detected in several HB and CB samples. The range of this FA, found in the majority of samples (0.4–7.0%), is comparable to that reported in other studies (De Man, 1985; Osman et al., 2000; Newman & Newman, 2008; Liu, 2011; Ciołek et al., 2012; Gangopadhyay et al., 2017).

We only found a few published precedents on identification of capric acid in barley grain. Youssef et al. (2012) reported it in comparable amounts to our results (1.5–2.0%).

**Hulless/covered grain type**

The average oil content in CB significantly surpassed that of HB in 2011 and also over both years. However, this difference cannot be explained by covered/hulless grain type, because hulls contain a relatively small amount of oil in accordance with the results of Liu (2011). In addition, higher fat content in naked oat genotypes if compared to husked varieties are reported in oat (Sterna et al., 2014), leading us to think that the most likely differences between genotypes were caused by some other genetic factors, independent from the presence or absence of the hulls. Comparable and even higher oil content to CB varieties in HB PR-5099 also supports this statement. To prove this hypothesis, we would need to repeat the experiment with dehulled CB grain. It must also be taken into account that CB cannot be used for food purposes directly because the hulls are inedible and the grain must be dehulled during production of food.

Our results, combined with those reported by other authors, suggest that differences in *FA composition* are also mostly due to genotype and not due to the grain type. Liu (2011) comparing one HB and one CB variety showed a trend to a higher proportion of oleic acid and a lower proportion of linoleic and α-linolenic acids in HB. According to our results we can point on HB PR-3808 being slightly superior for oleic acid and CB surpassing some but not all HB genotypes for α-linolenic acid, however, HB PR-5099 was exclusively superior for linoleic acid proportion. High palmitic acid proportion in barley hulls if compared to other grain parts reported by De Man (1985) and higher proportion of palmitic acid in CB compared to HB demonstrated by Youssef et al. (2012) are generally in agreement with our results. However, only the HB line PR-5099 had significantly lower palmitic acid proportion than the other CB and HB genotypes.

**Environment and fertilization**

Our data do not support the findings of De Man (1985) that palmitic and α-linolenic acids are affected more by environmental conditions than the other FA. Environmental factors of the particular year were not significant for both previously mentioned FA, but there was some environmental effect due to crop management regime or farming system for the five main barley grain FA.

The negative effect of nitrogen fertilizer on oleic acid proportion reported by De Man & Dondeyne (1985) and Stepien et al. (2019) is in accordance with our work, however, we did not find any increase in palmitic and α-linolenic acid proportions by increasing the fertilizer amount, but a slight opposite trend. There are also some parallels between our data and those presented by Abd EL-Satar et al. (2017) on sunflower in

respect of a positive effect of nitrogen fertilizer on linoleic and negative effect on stearic acid proportions. According to our data, a decrease of chemical input was in favour of oil content and proportions of unsaturated oleic and α-linolenic acids and also saturated stearic acid, but did not favour unsaturated linoleic acid proportion. Particularly important this finding might be in respect of ω-3 α-linolenic acid in relation to health promoting organically grown food products. A significant positive correlation between the amount of Mn fertilizer applied and linoleic acid content found by Stepien et al. (2019) is in agreement with our data, showing the highest average proportion of this FA in C3 management regime, were a number of mineral elements including Mn was applied in form of foliar fertilizer.

In respect to meteorological conditions of the *growing year*, linoleic acid proportion was significantly higher in 2011 with higher mean air temperature, especially before flowering time. It partially agrees with the finding of De Man (1985) in barley but contradicts with more recent results in other field crops, proving negative correlation between unsaturated FA and temperature increase (Schulte et al., 2013; Zhang et al., 2015; Shamloo et al., 2017). We found a significantly higher proportion of oleic acid in comparatively cooler and wetter year 2012 which agrees with positive correlation for this FA with precipitation showed by De Man (1985), but disagrees with the results on the positive effect of temperature on oleic acid in several other crops (Schulte et al., 2013; Gauthier et al., 2017; Shamloo et al., 2017). The strong negative correlation between linoleic and oleic acids can be explained by oleic acid, being a precursor of unsaturated C:18 FA (De Man & Dondeyne, 1985).

**Organic/conventional farming system**

We did not find clear support to the finding of Ciołek et al. (2012) that lipid content tends to be higher in conventionally grown CB grain in comparison to organically grown grain. It was true for variety 'Jumara' in both years, but not for 'Rubiola', which had the lowest oil content under C3 management with the highest application of agrochemicals in both trial years. All HB genotypes had highest mean oil content values under O system if compared to C system, which agrees with the trend in previously mentioned study. The same authors reported a higher proportion of unsaturated FA (especially linoleic acid in wheat and α-linolenic acid in barley) in the oil of organic cereal grain than in conventional grain in most cases. Our results partially support these findings by showing significantly higher mean α-linolenic acid proportion over both years and also oleic acid proportion in one trial year under O system, but contradict by significantly lower linoleic acid proportion under O system (2012).

**Perspective genotypes for oil with health related compounds**

In a study on the content of polyphenols and α-tocopherol in the same material, we found HB genotypes PR-4651 and 'Irbe' being relatively superior (Legzdiņa et al., 2018). In the current study both of them had a moderate oil content with a particularly good stability for 'Irbe'. In addition, PR-4651 provided moderately high proportion and excellent stability of the valuable α-linolenic acid giving additional affirmation for the usefulness for healthy food products. The outstanding line PR-5099 for oil and linoleic acid proportion had a moderately low α-tocopherol content in grain and grain oil, comparatively high polyphenol content in grain and low polyphenol content in grain oil, not contributing to the high antioxidative ability of the oil produced from this genotype.

Barley oil extracted from high oil waxy HB was shown to reduce plasma cholesterol concentration and promote weight gain of chicks if compared to margarine suggesting, that tocotrienol and polyunsaturated FA in barley oil has a hypocholesterolemic effect (Wang et al., 1993). Barley oil cannot be recommended for food directly because the ratio of ω-3 and ω-6 FA does not match up to the optimum, but it can be used as a good source of linoleic acid due to its anticarcinogenic, antiobese, antidiabetic and antihypertensive properties (Qian et al., 2009; Koba & Yanagita, 2014).

The negative relationships between oil content and several compounds (protein, lysine and α-tocopherol) and also between α-linolenic acid proportion and protein, lysine and β-glucan content may indicate difficulties to combine high contents of the respective compounds in the potential varieties during further breeding process. Unlike to our results, a positive relationship between oil and α-tocopherol content was reported in oat (Sterna et al., 2014).

## CONCLUSIONS

The effect of barley genotype was highly significant for the oil content but only in some cases for proportions of linoleic, α-linolenic and palmitic acid. We found higher average oil content and proportion of palmitic and α-linolenic acid in CB than in HB. However, HB line with a high oil content leads to the conclusion, that differences in oil content and FA composition should be explained by other genetic factors and not by hulless and covered grain type.

Crop management regime did not significantly affect oil content in barley grain but had some significant effects on proportions of linoleic, α-linolenic, oleic and stearic acid. A decrease of chemical input was in favour of oil content and proportion of unsaturated α-linolenic and oleic acid and also saturated stearic acid, but did not favour linoleic acid proportion. Organic farming system provided higher oil content and proportions of α-linolenic, oleic and stearic acid.

We identified waxy HB line PR-5099 different from other genotypes with a high oil content, a very high proportion of linoleic acid but low proportion of palmitic acid. We suggest this line for linoleic acid-rich oil production, especially when grown under higher mineral fertilizer input.

ACKNOWLEDGEMENTS. This research was supported by Latvian State Research Program NATRES FOOD (2010–2013).

## REFERENCES

Abd EL-Satar, M.A., Ahmed, A.A.E.H. & Hassan, T.H. A. 2017. Response of seed yield and fatty acid compositions for some sunflower genotypes to plant spacing and nitrogen fertilization. *Information Processing in Agriculture* **4**(3), 241–252. https://doi.org/10.1016/j.inpa.2017.05.003

Alabdulkarim, B., Bakeet, Z.A.N. & Arzoo, S. 2012. Role of some functional lipids in preventing diseases and promoting health. *Journal of King Saud University - Science* **24**(4), 319–329. https://doi.org/10.1016/j.jksus.2012.03.001

Becker, H.C. & Leon, J. 1988. Stability analysis in plant breeding. *Plant Breeding* **101**, 1–23. https://doi.org/10.1111/j.1439-0523.1988.tb00261.x

Beleggia, R., Platani, C., Nigro, F., De Vita, P., Cattivelli, L. & Papa, R. 2013. Effect of genotype, environment and genotype-by-environment interaction on metabolite profiling in durum wheat (Triticum durum Desf.) grain. *Journal of Cereal Science* **57**(2), 183–192. https://doi.org/10.1016/j.jcs.2012.09.004

Blondeau, N., Lipsky, R.H., Bourourou, M., Duncan, M.W., Gorelick, P.B. & Marini, A.M. 2015. Alpha-linolenic acid: an omega-3 fatty acid with neuroprotective properties - ready for use in the stroke clinic? *BioMed Research International* **2015**(1). https://doi.org/10.1155/2015/519830

Ciołek, A., Makarska, E., Wesołowski, M. & Cierpiała, R. 2012. Content of selected nutrients in wheat, barley and oat grain from organic and conventional farming. *Journal of Elemntology* (2/2012), 181–190. https://doi.org/10.5601/jelem.2012.17.2.02

Ehrenbergerová, J., Belcrediová, N., Prýma, J., Vaculová, K. & Newman, C.W. 2006. Effect of cultivar, year grown, and cropping system on the content of tocopherols and tocotrienols in grains of hulled and hulless barley. *Plant Foods for Human Nutrition (Dordrecht, Netherlands)* **61**(3), 145–50. https://doi.org/10.1007/s11130-006-0024-6

Gangopadhyay, N., Rai, D.K., Brunton, N.P., Gallagher, E. & Harrison, S.M. 2017. Fatty acids, sterols and tocols in Irish barley varieties: Profiling and correlation analysis. *European Journal of Lipid Science and Technology* **119**(4), 1–5. https://doi.org/10.1002/ejlt.201600213

Gauthier, M., Pellet, D., Monney, C., Herrera, J.M., Rougier, M. & Baux, A. 2017. Fatty acids composition of oilseed rape genotypes as affected by solar radiation and temperature. *Field Crops Research **212***(August), 165–174. https://doi.org/10.1016/j.fcr.2017.07.013

Glick, N.R. & Fischer, M.H. 2013. The role of essential fatty acids in human health. *Journal of Evidence-Based Complementary and Alternative Medicine* **18**(4), 268–289. https://doi.org/10.1177/2156587213488788

Koba, K. & Yanagita, T. 2014. Health benefits of conjugated linoleic acid (CLA). *Obesity Research & Clinical Practice* **8**(6), e525–e532. https://doi.org/10.1016/j.orcp.2013.10.001

Legzdiņa, L., Ivdre, E., Piliksere, D., Vaivode, A., Mieriņa, I. & Jure, M. 2018. Effect of genotype and crop management systems on the content of antioxidants in hulless and covered spring barley. *Zemdirbyste-Agriculture* **105**(4), 315–322. https://doi.org/10.13080/z-a.2018.105.040

Liu, K. 2011. Comparison of Lipid Content and Fatty Acid Composition and Their Distribution within Seeds of 5 Small Grain Species. *Journal of Food Science* **76**(2), 334–342. https://doi.org/10.1111/j.1750-3841.2010.02038.x

De Man, W. 1985. The effect of genotype and environment on the fatty acid content of barley (Hordeum vulgare L.) grains. *Plant, Cell and Environment* **8**, 571–577.

De Man, W. & Dondeyne, P. 1985. Effect of nitrogen fertilizer on protein content, total fatty acid content and composition of barley (Hordeum vulgare L.) grains. *Journal of the Science of Food and Agriculture* **36**, 186–190.

Mensink, R.P. 2016. Effects of saturated fatty acids on serum lipids and lipoproteins: a systematic review and regression analysis. *World Health Organization,* 1–63.

Mikulioniene, S. & Balezentiene, L. 2009. Responses of cereals grain quality on organical and conventional farming. *Agronomy Research* **7**(II), 677–683.

Newman, R.K. & Newman, C.W. 2008. *BARLEY FOR FOOD AND HEALTH Science, Technology, and Products*. A John Wiley & Sons, Inc., Publication, USA, 245 pp.

Osman, R.O., Abd El Gelil, F.M., El-Noamany, H.M. & Dawood, M.G. 2000. Oil content and Fatty Acid Comp of Barley and Sorghum Grains. *Grasas y Aceites* **51**(3), 157–162.

Qian, J., Jiang, S., Su, W. & Gao, P. 2009. Characteristics of oil from hulless barley (Hordeum vulgare L.) bran from tibet. *JAOCS, Journal of the American Oil Chemists' Society* **86**(12), 1175–1179. https://doi.org/10.1007/s11746-009-1463-7

Schulte, L.R., Ballard, T., Samarakoon, T., Yao, L. Vadlani, P., Staggenborg, S. & Rezac, M. 2013. Increased growing temperature reduces content of polyunsaturated fatty acids in four oilseed crops. *Industrial Crops and Products* **51**, 212–219.

Seefeldt, H.F., Larsen, F.H., Viereck, N., Petersen, M.A. & Engelsen, S.B. 2011. Lipid composition and deposition during grain filling in intact barley (Hordeum vulgare) mutant grains as studied by 1H HR MAS NMR. *Journal of Cereal Science* **54**(3), 442–449. https://doi.org/10.1016/j.jcs.2011.08.009

Shamloo, M., Babawale, E.A., Furtado, A., Henry, R.J., Eck, P.K. & Jones, P.J.H. 2017. Effects of genotype and temperature on accumulation of plant secondary metabolites in Canadian and Australian wheat grown under controlled environments. *Scientific Reports* **7**(1), 1–13. https://doi.org/10.1038/s41598-017-09681-5

Stepien, A., Wojtkowiak, K., Pietrzak-Fiecko, R. & Zalewska, M. 2019. Effect of manganese and nitrogen fertilization on the content of some essential micronutrients and composition of fatty acids in winter wheat grain. *Chilean Journal of Agricultural Research* **79**(December), 616–627. https://doi.org/10.4067/S0718-58392019000400616

Sterna, V., Zute, S., Brunava, L. & Vicupe, Z. 2014. Lipid composition of oat grain grown in Latvia. *9th Baltic Conference on Food Science and Technology "Food for Consumer Well-Being" Foodbalt 2014* 77–80.

Tvrzicka, E., Kremmyda, L.S., Stankova, B. & Zak, A. 2011. Fatty acids as biocompounds: Their role in human metabolism, health and disease - a review. part 1: Classification, dietary sources and biological functions. *Biomedical Papers* **155**(2), 117–130. https://doi.org/10.5507/bp.2011.038

Wang, L., Newman, R.K., Newman, C.W., Jackson, L.L. & Hofer, P.J. 1993. Tocotrienol and fatty acid composition of barley oil and their effects on lipid metabolism. Plant Foods Hum.Hum. Nutr. *Plant Foods for Human Nutrition* **43**, 9–17.

Wojtkowiak, K., Stępień, A., Pietrzak-Fiećko, R. & Warechowska, M. 2018. Effects of nitrogen fertilisation on the yield, micronutrient content and fatty acid profiles of winter wheat (*Triticum aestivum* L.) varieties. *Journal of Elementology* **23**(2), 483–495. https://doi.org/10.5601/jelem.2017.22.3.1524

Youssef, M.K.E., Abd El-Kader El-Fishawy, F., Abd El-Naby Ramadan, E.-S. & MohamedAbd El-Rahman, A. 2012. Assessment of Total Lipid Fractions and Fatty Acids Composition in Raw, Germinated Barleys and Talbina Products. *Food and Public Health* **2**(1), 16–23. https://doi.org/10.5923/j.fph.20120201.04

Zhang, J.-L., Zhang, S.-B., Zhang, Y.-P. & Kitajima, K. 2015. Effects of phylogeny and climate on seed oil fatty acid composition across 747 plant species in China. *Industrial Crops and Products* **63**, 1–8. https://doi.org/10.1016s/j.indcrop.2014.10.045

*Agronomy Research* **20**(1), 229–234, 2022
https://doi.org/10.15159/AR.22.021

# Nutritious lentil and rice meal for sustainable vegan and pescatarian diet

I. Lignicka*, A. Graci (Balgalve) and A.M. Zīdere-Laizāne

Felici LLC, Rigas gatve 8, LV-2164 Adazi, Adazu novads, Latvia
*Correspondence: ilva.lignicka@musli.lv

Received: December 2nd, 2021; Accepted: April 17th, 2022; Published: April 27th, 2022

**Abstract.** Urbanization has been accompanied by changes towards diets that have placed increased pressure on the environment and human health. Shifting diet from beef towards less-impactful proteins is the most important policy goal for dietary sustainability in 2050. Fish can also help to shift to lower emission diets, fish-eaters have nearly the same emissions profile as strict vegetarians. The aim of this study was to develop quick preparation lentil and rice meals that would be suitable for a sustainable vegan and pescatarian diet and to analyse and compare their nutritional values. Sample nutritional values were calculated according to raw material nutritional values. Results show that if most raw materials are plant-based there is no significant difference between vegan and pescatarian quick preparation meal sample nutritional values other than minerals and vitamins. Vegan quick preparation meal sample which contains green lentils has higher iron content comparing to pescatarian quick preparation meal which contains red lentils and freeze-dried salmon powder and has higher vitamin B1, B3 and B6 content.

**Key words:** lentils, pescatarian, rice, sustainable diet, vegan.

## INTRODUCTION

The demand for protein source foods has increased over last few years. As interest for protein is growing it is expected for plant-based protein product market to grow significantly (Ismail et al., 2020). Some of the reasons are expected two or three billion increases in worldwide population, lowering the environmental impact of food production, and providing healthier alternatives for the human diet (Zeece, 2020). Urbanization has been accompanied by changes towards diets that have placed increased pressure on the environment and human health. Urban population growth has been associated with diets based on high consumption of meat, dairy, and processed foods, which contribute to environmental degradation and biodiversity loss and are responsible for around 30% of greenhouse gas (GHG) emissions (Cifuentes et al., 2021). In 2019 World resource institute have published working paper how shifting diets contribute to a sustainable future. Animal based foods are typically more resource-intensive and environmentally impactful to produce than plant-based foods. Shifting diet from beef towards less-impactful proteins is the most important policy goal for dietary sustainability in 2050. Fish can also help to shift to lower emission diets. Fish-eaters

have nearly same emissions profile as strict vegetarians. Vegan diet is the least impactful (Ranganathan et al., 2016). FAO and WHO (2019) also mention that dietary changes towards healthier diets can reduce the environmental impact of the food system, as evidence gathered so far show benefits of shifting towards more plant-based diet, including vegetables, fruits, nuts, pulses, and wholegrains. Due to environmental, ethical and health concerns it is increasingly popular to reduce the consumption of meat. For this reason, the focus on vegan, vegetarian and pescatarian diet in recent years has increased (Wozniak et al., 2020). What is more, life habits due to fast-paced life are changing. Consumers prefer minimum preparation meals, however, it is still important to consume high-quality, nutrient dense meals. Increase in vegan, vegetarian, and flexitarian populations have increased the usage of plant-based proteins (Ismail et al., 2020). Pulses, such as lentil, contain approximately twice the amount of protein as wholegrain cereals like oats, barley, wheat, and rice. About one third of the calories in lentil come from protein, making it the third-highest level of protein by weight of any legume or nut (Samaranayaka, 2017). Hokazono et al. (2009) in their study concluded that organic and sustainable rice production systems have the potential to mitigate global warming and eutrophication. The aim of this study was to develop quick preparation lentil and rice meals that would be suitable for a sustainable vegan and pescatarian diet and to analyse and compare their nutritional values.

## MATERIALS AND METHODS

Quick preparation meal development tests were carried out at the laboratory of Felici LLC. As main ingredients dried lentils (*Lens culinaris*, L.) and rice (*Oryza sativa*, L.) were used. For vegan meal 64% of rice, 26% of green lentils and 10% different additional ingredients (dried carrot pieces, dried parsley, sea salt, dried garlic powder, dried onion pieces, turmeric, and yeast powder) to enrich the taste were used. For pescatarian meal 69% of rice, 20% of red lentil, 2.5% of freeze-dried salmon (*Salmo Salar* and *Oncorhynchus* spp) powder and 8.5% different additional ingredients (black sesame seeds, dried tomato pieces, sea salt, dried spinach flakes, ground ginger and yeast powder) to enrich the taste were used. At first different recipes quick meal samples were prepared, however, according to calculated nutritional value, sensory evaluation, and calculated price one vegan and one pescatarian meal were selected for further analysis. Both quick preparation meal samples can be seen in Fig. 1.


**Figure 1.** Vegan (a) and pescatarian (b) quick preparation meal samples.

Vegan and pescatarian quick preparation meal sample nutritional value, mineral and vitamin content were calculated according to Felici LLC raw material specifications. Calculations were made considering all ingredients used. Daily reference intake was calculated according to regulation (EU) No 1169/2011 of the European Parliament and the council of 25 October 2011. Nutritional claims were calculated according to regulation (EU) No 1924/2006 of the European Parliament.

## RESULTS AND DISCUSSION

As mentioned in studies, depending on the variety, the composition of lentils is approximately 25–28% protein, 60–63% total carbohydrates of which 47% starch and around 1% fat (Faris et al., 2013; Zeece, 2020). According to used raw material specifications red lentils contain 25% protein, 51.7% carbohydrates of which 1.09% sugar, 2.1% fat and 11.4% dietary fibre. Green lentils contain 25.1% protein, 48.3% carbohydrates of which 0.79% sugar, 2.2% fat and 15.1% dietary fibre. A comparison of raw material specifications with literature shows that lentils contain similar protein content like written in other studies, however, they have lower carbohydrate and higher fat content. Depending on the variety, the composition of rice is approximately 6–7% protein, 74–80% carbohydrates of which 67–73% starch and 0.4–3% fat (Zeece, 2020; Carcea, 2021). According to used raw material specification rice contain 7.9% protein, 78.7% carbohydrates of which 0.3% sugar and 0.5% fat. A comparison of raw material specifications with literature shows that rice nutritional value is like data written in other studies. Due to salmon's nutritional profile, flavour, and availability it is one of the most popular fish for many consumers. The major component of fish is water which is a determinant of shelf life (Dawson et al., 2018). According to used raw material specification freeze-dried salmon contains 5% moisture, at least 50% protein and maximum 30% fat. From sustainability perspective freeze-drying is highly energy consuming (Karwacka et al., 2022), but from other hand these products are high quality, longer shelf-life, and less waste. Also, it is possible to decrease energy consumption during freeze-drying. Huang et al. (2009) and Rybak et al. (2021) in their study showed the possible ways to reduce it during freeze-drying process. Still, this practice should be implemented in daily production.

To check nutrient content in selected quick preparation meal samples, nutritional value was calculated according to raw material specifications. The Table 1 illustrates vegan and pescatarian quick meal sample nutritional values and percentage of dietary reference intakes (DRI) for energy, nutrients and iron, vitamin B1, B3 and B6. As it can be seen, both meal samples have similar energy value. As pescatarian meal sample contains sesame seeds and freeze-dried salmon powder, which contain around 30% of fat, it has three times higher fat content than vegan meal sample. Both quick preparation meals contain less than 3 grams of fat per 100 grams of product, they both are still low-fat meals. As mentioned before, lentils and rice have high carbohydrate content, 89 and 90% of rice and lentils mix was used, so prepared samples contain around 70 grams of carbohydrates per 100 grams of each meal sample. Data show that these meals are low sugar. Lower sugar and fibre content in pescatarian meal sample could be explained due to used lentil type and different additional ingredients used for taste enrichment. Meals contain more than 3 grams of fibre per 100 grams of product showing that quick preparation meals are source of fibre. Vegan and pescatarian meal have identical protein

content. Protein makes 14.7% of energy value in vegan meal and 14.1% of energy value in pescatarian meal showing that meals are source of protein.

**Table 1.** Vegan and pescatarian quick meal nutritional value

| Nutritional value | Vegan meal | | Pescatarian meal | |
|---|---|---|---|---|
| | Per 100 g | %, DRI | Per 100 g | %, DRI |
| Energy | 1,502 kJ/354 kcal | 17.7 | 1,566 kJ/370 kcal | 18.5 |
| Fat | 0.8 g | 1.1 | 2.7 g | 3.9 |
| *of which saturates* | 0.1 g | 0.5 | 0.5 g | 2.5 |
| Carbohydrates | 71.0 g | 27.3 | 72.0 g | 27.7 |
| *of which sugars* | 2.1 g | 2.3 | 1.3 g | 1.4 |
| Fibre | 5.9 g | - | 3.4 g | - |
| Protein | 13.0 g | 26.0 | 13.0 g | 26.0 |
| Salt | 2.5 g | 41.7 | 1.6 g | 26.7 |
| Iron | 4.76 mg | 34.0 | 4.40 mg | 31.4 |
| Vitamin B1 (Thiamin) | 0.82 mg | 74.5 | 1.00 mg | 90.9 |
| Vitamin B3 (Niacin) | 5.40 mg | 33.8 | 7.18 mg | 44.9 |
| Vitamin B6 | 0.72 mg | 51.4 | 0.82 mg | 58.6 |

To check additional nutrient content in quick preparation meal samples, vitamin and mineral content were calculated according to raw material specifications, amounts are recorded in Table 1. Both meals samples have significant amount of iron, what is an essential component for almost all biological systems. Humans require iron for energy production, oxygen transport and utilization, cellular proliferation, and pathogen destruction (Lynch et al., 2018). Iron deficiency is the only nutrient deficiency that is significantly widespread in developed and developing countries. This is the reason for the ongoing push for intensified iron fortification of staple diets (Blanco-Rojo & Vaquero, 2019). Lentils are great source of iron, it is present in significant quantity, however, it is known that due to phytochemicals its bioavailability is reduced (Faris & Attlee, 2017). B group vitamins have very important molecular function in human body, they are essential nutrients for adequate brain development, function, and protection (Bonetti et al., 2017). Both meals samples have significant vitamin B1, B3 and B6 content. Also, other studies have shown that lentils are significant dietary source of vitamin B1, B3 and B6 (Faris & Attlee, 2017; Ganesan & Xu, 2017). Different vitamin and mineral content in vegan and pescatarian meals samples are due to lentil types with different nutritional values. Vegan meal sample contains green lentils and pescatarian meal sample contains red lentils. According to EFSA food composition database dried salmon has high vitamin B1, B3, and B6 content. As it has a small percentage in meal it did not play important role in B vitamin content in pescatarian meal. Salmon is rich in vitamin B12, but as it is not base ingredient its content in pescatarian meal is still low and is not mentioned in this study. For more information, iron and B group vitamins bioavailability tests should be performed.

## CONCLUSIONS

This study shows that using rice and lentil as base ingredients it is possible to develop nutritious vegan and pescatarian quick preparation meals according to EFSA nutrition claims. Data show that quick preparation meal samples are low fat, low sugar,

source of fibre and protein, and with high iron and vitamin B1, B2, B3 content. There is only small difference between vegan and pescatarian quick preparation meal sample nutritional values. The freeze-dried salmon powder had an impact on pescatarian meal sample fat content, it was three times higher than vegan meal sample fat content. Used lentil type has no significant impact on quick preparation meal sample nutritional values other than vitamin and minerals. Vegan quick preparation meal sample which contains green lentils has higher iron content. Pescatarian quick preparation meal which contains red lentils and freeze-dried salmon powder has higher vitamin B1, B3 and B6 content. Although both quick preparation meal samples have high iron, vitamin B1, B2 and B3 content there is no data for lentil and rice meal bioavailability. Further element bioavailability tests should be performed. Even though salmon is one of the most popular fish among consumers there are not many freeze-dried salmon producers and descriptive scientific data available.

ACKNOWLEDGEMENTS. In accordance with contract No. 1.2.1.1/18/A/002 between 'Latvian Food Competence Centre' Ltd. And the Central Finance and Contracting Agency, the study is conducted by 'Felici' LLC. With support from the European Regional Development Fund (ERDF) within the framework of the project 'Latvian Food Industry Competence Centre'.

## REFERENCES

Blanco-Rojo, R. & Vaquero, M.P. 2019. Iron bioavailability from food fortification to precision nutrition. A review. *Innovative Food Science & Emerging Technologies* **51**, 126–138.

Bonetti, F., Brombo, G. & Zuliani, G. 2017. Chapter 15 – The role of B group Vitamins and Choline in Cognition and Brain Aging. Watson, R. (eds). *Nutrition and Functional Foods for Healthy Aging*. Academic Press. Cambridge. 139–158.

Carcea, M. 2021. Value of Wholegrain Rice in a healthy Human Nutrition. *Agriculture* **11**(8), 720.

Cifuentes, M.L., Freyer, B., Sonnino, R. & Fiala, V. 2021. Embedding sustainable diets into urban food strategies: A multi-actor approach. *Geoforum* **122**, 1–21.

Dawson, P., Al-Jeddawi, W. & Remington, N. 2018. Effect of Freezing on the Shelf Life of Salmon. *International Journal of Food Science* **2018**, 1686121.

EFSA Food composition database. Atlantic salmon. Available at https://www.efsa.europa.eu/en/microstrategy/food-composition-data

Ganesan, K. & Xu, B. 2017. Polyphenol-Rich lentils and Their Health Promoting Effects. *International Journal of Molecular Sciences* **18**(11), 2390.

Hokazano, S., Hayashi, K. & Sato, M. 2009. Potentialities of organic and sustainable rice production in Japan from a life cycle perspective. *Agronomy Research* **7**(SI), 257–262.

Huang, L., Zhang, M., Mujumdar, A.S., Sun, D., Tan, G. & Tang, S. 2009. Studies on Decreasing Energy Consumption for a Freeze-Drying Process of Apple Slices. *Drying Technology* **27**(9), 938–946.

Faris, M.E., Takruri, H.R. & Issa, A. Y. 2013. Role of lentils (*Lens culinaris* L.) in human health and nutrition: a review. *Mediterranean Journal of Nutrition and Metabolism* **6**, 3–16.

Faris, M.E. & Attlee, A. 2017. Lentils (Lens culinaris, L.): A Novel Functional Food. Shekhar, H. U., Howlader, Z. H., Kabir, Y. (eds) *Exploring the Nutrition and Health Benefits of Functional Foods*. Medical Information Science Reference. USA. 42–72.

FAO and WHO. 2019. Sustainable healthy diets – Guiding principles., FAO and WHO, Rome, p. 37.

Ismail, P., Senaratne-Lenagala, L., Stube, A. & Backenridge, A. 2020. Protein demand: review of plant and animal proteins used in alternative protein product development and production. *Animal Frontiers* **10**(4), 53–63.

Karwacka, M., Ciurzynska, A., Galus, S. & Janowicz, M. 2022. Freeze-dried snacks obtained from frozen vegetable by-products and apple pomace – selected properties, energy consumption and carbon footprint. *Innovative Food Science and Emerging Technologies* **77**, 102949.

Lynch, S., Pfeiffer, C.M., Georgieff, M.K., Brittenham, G., Fairweather-Tait, S., Hurrell, R.F., McArdle, H.J. & Raiten, D.J. 2018. Biomarkers of Nutrition for Development (BOND) – Iron Review. *The Journal of Nutrition* **148**(1), 1001–1067.

Ranganathan, J., Vennard, D., Waite, R., Dumas, P., Lipinski, B. & Searchinger, T., GLOBAGRI-WRR model authors. 2016. Shifting Diets for a Sustainable Food Future. Working paper, Installment 11 of *Creating a Sustainable Food Future*. Washington, DC: World Resources Institute. Accessible at www.worldresourcesreport.org.

Regulation (EU) No 1169/2011 of the European Parliament and the council of 25 October 2011 on the provision of food information to consumers, amending Regulations (EC) No 1924/2006 and (EC) No 1925/2006 of the European Parliament and of the Council, and repealing Commission Directive 87/250/EEC, Council Directive 90/496/EEC, Commission Directive 1999/10/EC, Directive 2000/13/EC of the European Parliament and of the Council, Commission Directives 2002/67/EC and 2008/5/EC and Commission Regulation (EC) No 608/2004.

Regulation (EU) No 1924/2006 of the European Parliament and the council of 20 December 2006 on nutrition and health claims made of foods.

Rybak, K., Parniakov, O., Samborska, K., Wiktor, A., Witrowa-Rajchert, D. & Nowacka, M. 2021. Energy and Quality Aspects of Freeze-Drying Preceded by Traditional and Novel Pre-Treatment Methods as Exemplified by Red Bell Pepper. *Sustainability* **13**, 2035.

Samaranayaka, S. 2017. Chapter 11 – Lentil: Revival of Poor Man`s Meat. In Sustainable protein sources, S.R., Wanasundara, J.P.D., Scalin, L. (eds) *Sustainable Protein Sources*. Academic Press. Cambridge, 185–196.

WHO/FAO/UNU (World Health Organization/Food and Agriculture Organization of the United Nations/United Nations University). 2007. Protein and amino acid requirements in human nutrition. Report of a joint WHO/FAO/UNU Expert Consultation. *WHO Technical Report Series*, No **935**, pp. 284.

Wozniak, H., Larpin, C., Mestral, C., Guessous, I., Reny, J.L. & Stringhini, S. 2020. Vegeterian, pescatarian and flexitarian diets: sociodemographic determinants and association with cardiovascular risk factors in a Swiss urban population. *The British journal of nutrition* **124**(8), 844–852.

Zeece, M. 2020. Food systems and future directions. In Zeece, M. (eds). *Introduction to the Chemistry of Food*. Academic press, Cambridge, 345–397.

## INSTRUCTIONS TO AUTHORS

Papers must be in English (British spelling). A proof-reader will revise English, but authors are strongly urged to have their manuscripts reviewed linguistically prior to submission. Contributions should be sent electronically. Papers are considered by referees before acceptance. The manuscript should follow the instructions below.

**Structure:** Title, Authors (initials & surname; an asterisk indicates the corresponding author), Authors' affiliation with postal address (each on a separate line) and e-mail of the corresponding author, Abstract (up to 250 words), Key words (not repeating words in the title), Introduction, Materials and methods, Results and discussion, Conclusions, Acknowledgements (optional), References.

**Layout, page size and font**

- Use preferably the latest version of **Microsoft Word**, doc., docx. format.
- Set page size to **ISO B5 (17.6×25 cm)**, all **margins at 2 cm**. All text, tables, and figures must fit within the text margins.
- Use single line spacing and **justify the text**. Do not use page numbering. Use **indent 0.8 cm** (do not use tab or spaces instead).
- Use font Times New Roman, point size for the title of article **14 (Bold)**, author's names 12, core text 11; Abstract, Key words, Acknowledgements, References, tables, and figure captions 10.
- Use *italics* for Latin biological names, mathematical variables and statistical terms.
- Use single ('…') instead of double quotation marks ("…").

**Tables**

- All tables must be referred to in the text (Table 1; Tables 1, 3; Tables 2–3).
- Use font Times New Roman, regular, 10 pt. Insert tables by Word's 'Insert' menu.
- Do not use vertical lines as dividers; only horizontal lines (1/2 pt) are allowed. Primary column and row headings should start with an initial capital.

**Figures**

- All figures must be referred to in the text (Fig. 1; Fig. 1 A; Figs 1, 3; Figs 1–3). Avoid 3D charts, background shading, gridlines and excessive symbols. Use font **Arial, 10 pt** within the figures. Make sure that thickness of the lines is greater than 0.3 pt.
- Do not put caption in the frame of the figure.
- The preferred graphic format is Excel object; for diagrams and charts EPS; for half-tones please use TIFF. MS Office files are also acceptable. Please include these files in your submission.
- Check and double-check spelling in figures and graphs. Proof-readers may not be able to change mistakes in a different program.

**References**

- **Within the text**

In case of two authors, use '&', if more than two authors, provide first author 'et al.':

Smith & Jones (2019); (Smith & Jones, 2019);
Brown et al. (2020); (Brown et al., 2020)

When referring to more than one publication, arrange them by following keys: 1. year of publication (ascending), 2. alphabetical order for the same year of publication:

(Smith & Jones, 2019; Brown et al., 2020; Adams, 2021; Smith, 2021)

- **For whole books**

Name(s) and initials of the author(s). Year of publication. *Title of the book* (*in italics*). Publisher, place of publication, number of pages.

Behera, K.B. & Varma, A. 2019. *Bioenergy for Sustainability and Security*. Springer International Publishing, Cham, pp. 1–377.

- **For articles in a journal**

Name(s) and initials of the author(s). Year of publication. Title of the article. *Abbreviated journal title* (*in italic*) volume (in bold), page numbers.
Titles of papers published in languages other than English, should be replaced by an English translation, with an explanatory note at the end, e.g., (in Russian, English abstr.).

Bulgakov, V., Adamchuk, V., Arak, M. & Olt, J. 2018. The theory of cleaning the crowns of standing beet roots with the use of elastic blades. *Agronomy Research* **16**(5), 1931–1949. doi: 10.15159/AR.18.213

Doddapaneni, T.R.K.C., Praveenkumar, R., Tolvanen, H., Rintala, J. & Konttinen, J. 2018. Techno-economic evaluation of integrating torrefaction with anaerobic digestion. *Applied Energy* **213**, 272–284. doi: 10.1016/j.apenergy.2018.01.045

- **For articles in collections:**

Name(s) and initials of the author(s). Year of publication. Title of the article. Name(s) and initials of the editor(s) (preceded by In:) *Title of the collection (in italics)*, publisher, place of publication, page numbers.

Yurtsev, B.A., Tolmachev, A.I. & Rebristaya, O.V. 2019. The floristic delimitation and subdivisions of the Arctic. In: Yurtsev, B.A. (ed.) *The Arctic Floristic Region*. Nauka, Leningrad, pp. 9–104 (in Russian).

- **For conference proceedings:**

Name(s) and initials of the author(s). Year of publication. Name(s) and initials of the editor(s) (preceded by In:) *Proceedings name (in italics)*, publisher, place of publishing, page numbers.

Ritchie, M.E. & Olff, H. 2020. Herbivore diversity and plant dynamics: compensatory and additive effects. In: Olff, H., Brown, V.K. & Drent R.H. (eds) *Herbivores between plants and predators. Proc. Int. Conf. The 38$^{th}$ Symposium of the British Ecological Society*, Blackwell Science, Oxford, UK, pp. 175–204.

**Please note**

- Use '.' ( not ',') for decimal point: 0.6 ± 0.2; Use ',' for thousands – 1,230.4;
- Use '–' (not '-') and without space: pp. 27–36, 1998–2000, 4–6 min, 3–5 kg
- With spaces: 5 h, 5 kg, 5 m, 5 °C, C : D = 0.6 ± 0.2; $p < 0.001$
- Without space: 55°, 5% (not 55 °, 5 %)
- Use 'kg ha$^{-1}$' (not 'kg/ha');
- Use degree sign ' ° ' : 5 °C (not 5 $^{O}$C).